# From Compact Greens to Ascending Stems:

Elucidating the role of ATH1 in regulating internode growth dynamics in *Arabidopsis thaliana*

Shahram Shokrian Hajibehzad

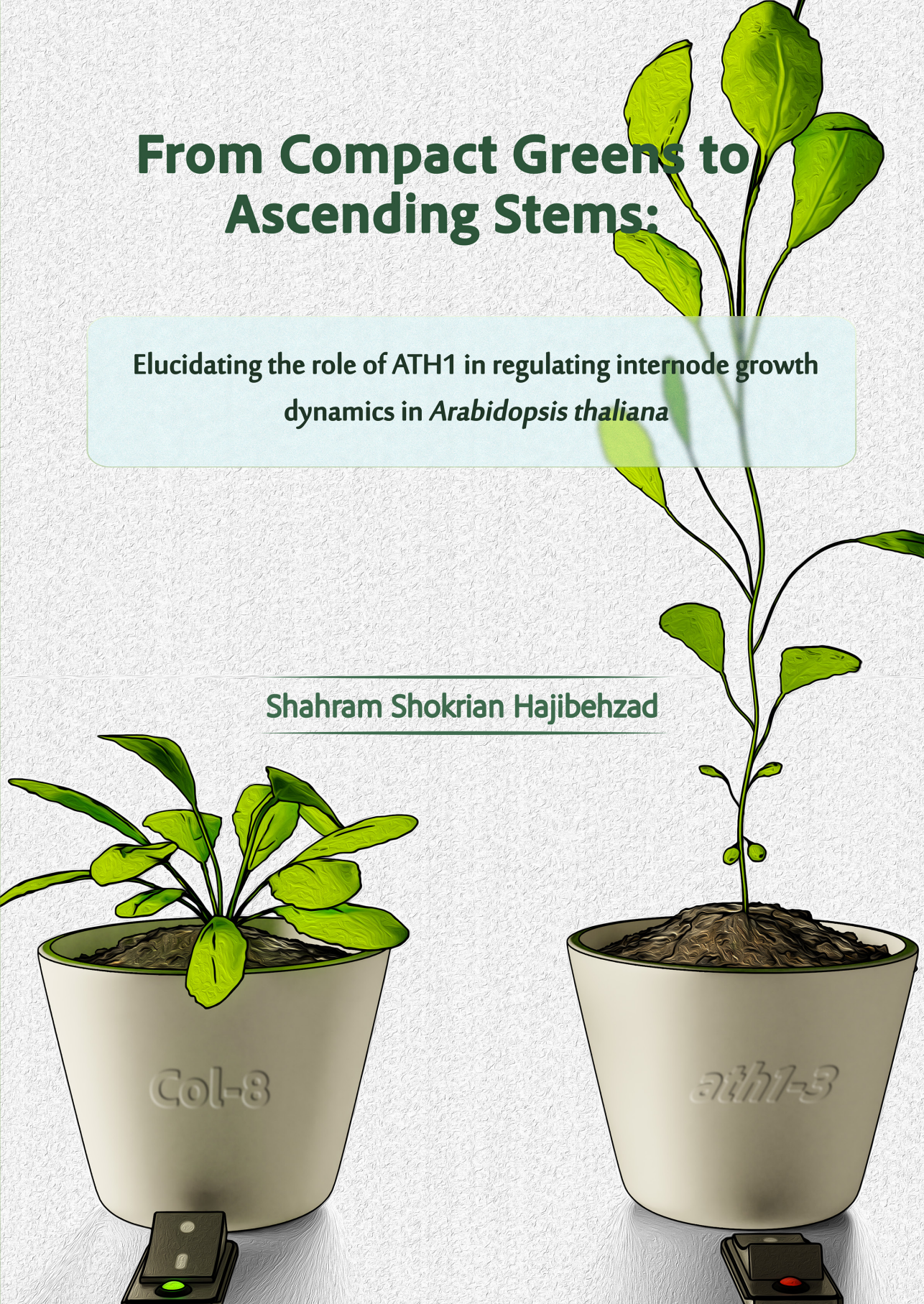

**From compact greens to ascending stems: elucidating the role of ATH1 in regulating internode growth dynamics in *Arabidopsis thaliana***

**PhD thesis**

Shahram Shokrian Hajibehzad

Printed by Proefschriftspecialist | proefschriftspecialist.nl
Layout and design: Erwin Timmerman, persoonlijkproefschrift.nl

# From compact greens to ascending stems

Elucidating the role of ATH1 in regulating internode growth dynamics in *Arabidopsis thaliana*

**Van compacte rozetten tot strekkende stengels**

Het ontrafelen van de rol van ATH1 in de regulatie van internodiëngroei in *Arabidopsis thaliana*

(met een samenvatting in het Nederlands)

**Proefschrift**

ter verkrijging van de graad van doctor aan de
Universiteit Utrecht
op gezag van de
rector magnificus, prof. dr. H.R.B.M. Kummeling,
ingevolge het besluit van het college voor promoties
in het openbaar te verdedigen op

maandag 9 september 2024 des middags te 2.15 uur

door

**Shahram Shokrian Hajibehzad**

geboren op 21 november 1989
te Miandoab, Iran

## Promotor:
Prof. dr. J.C.M. Smeekens

## Copromotor:
Dr. M.C.G. Proveniers

## Beoordelingscommissie:
Dr. E. Baena-Gonzalez
Prof. C. Fankhauser
Prof. dr. ir. R. Immink
Prof. dr. B. Scheres
Prof. dr. A.F.J.M. Van Den Ackerveken

## Contents


Col-8
ath1-3

# Chapter 1

## General Introduction

Shahram Shokrian Hajibehzad[1, 2], Sjef Smeekens[1], Marcel Proveniers[1, 2]

[1] *Molecular Plant Physiology, Department of Biology, Science4Life, Utrecht University, Padualaan 8, Utrecht, 3584 CH, The Netherlands*

[2] *Translational Plant Biology, Department of Biology, Science4Life, Utrecht University, Padualaan 8, Utrecht, 3584 CH, The Netherlands*

## Abstract

As the global population increases, the per capita availability of arable land is approaching critical levels, posing a significant threat to food security. Therefore, it is important to optimize crop yields, particularly in rosette-forming crops such as leafy greens (e.g. lettuce, cabbage) and root vegetables (e.g. carrots, beets). These plants, characterized by their circular cluster of leaves near the ground during the vegetative growth phase, undergo a process called bolting when transitioning to reproductive growth. This results in the formation of an inflorescence stem on top of a compact rosette. Adverse environmental conditions often induce loss of rosette compactness during vegetative growth and premature bolting, significantly impacting yield quantity and quality due to resource reallocation to stem development. Additionally, these conditions can lead to the formation of secondary metabolites that impart a bitter taste to the crops. While the Green Revolution's introduction of semi-dwarf varieties significantly advanced grain yields, a similar enhancement in rosette-forming crop productivity remains to be achieved. This study aims to explore the regulatory mechanisms controlling compact rosette growth and bolting initiation, with a focus on *Arabidopsis thaliana*, a key model organism in plant biology. It will also investigate the influence of environmental factors on these growth stages. The findings could be important in developing methods to improve yields and quality in rosette-forming crops.

## The upward journey: longitudinal elongation during the Arabidopsis life cycle



The life cycle of *Arabidopsis thaliana* is marked by distinct phases of longitudinal growth, primarily influenced by light-regulated developmental mechanisms. This begins shortly after germination when the seedling transitions from a reliance on stored reserves to establishing itself as a photoautotrophic organism. In the absence of light, Arabidopsis seedlings undergo skotomorphogenesis, a specialized growth strategy characterized by rapid hypocotyl elongation while delaying the expansion of cotyledons and root development. Upon reaching light, a dramatic developmental shift occurs, steering the plant into photomorphogenesis. This phase transition is marked by a stark inhibition of hypocotyl elongation, a response orchestrated by a complex interplay of light receptors and signaling pathways. Cotyledons unfold and enlarge, transitioning the plant to a state of photoautotrophy (C1_Fig. 1). The differentiation and maturation of the photosynthetic apparatus are essential during this stage, as they enable effective light capture and energy conversion, supporting subsequent growth phases (Whitelam *et al.*, 1998; Su & Lagarias, 2007; Li *et al.*, 2013, 2017; Pfeiffer *et al.*, 2016; Wang *et al.*, 2021). Following seedling establishment, the Arabidopsis plant enters vegetative growth, defined by the activities at the shoot apical meristem (SAM). With adequate light, the SAM transitions from a dormant state to active development, producing rosette leaves in a spiral pattern characteristic of rosette plants like Arabidopsis. These leaves, while contributing to the overall biomass, show minimal to no elongation at their successive nodes, maintaining a compact plant structure, while focusing energy on expansive leaf development rather than vertical growth (Whitelam *et al.*, 1998; Su & Lagarias, 2007; Li *et al.*, 2013, 2017; Pfeiffer *et al.*, 2016; Wang *et al.*, 2021). As the plant matures, it encounters another major transition: the switch from vegetative growth to flowering. Here, newly formed internodes rapidly elongate, pushing the inflorescence upwards in a process named bolting (Pouteau and Albertini, 2009; Pouteau and Albertini, 2011; Willmann and Poethig, 2011). In many species, the latter is critical for reproductive success, as an elongated inflorescence facilitates both cross-pollination and seed dispersal. Bolting thus represents a second, distinct surge in vertical growth in the life cycle of rosette plants, critical to their reproductive strategy. Finally, the plant enters the terminal phase of its life cycle: the transition from flowering

to senescence. In Arabidopsis, a monocarpic species, flowering culminates in a coordinated cessation of growth at the inflorescence meristems, leading to systemic whole plant senescence. The end of vertical growth at this stage signifies the completion of plant life cycle, with energy and resources diverted to seed maturation and dispersal (Bleecker & Patterson, 1997; Balanzà *et al.*, 2018; Gan, 2018; Martínez-Fernández *et al.*, 2020; Ware *et al.*, 2020). In contrast, polycarpic species maintain vegetative growth after flowering by conserving a supply of meristems in the vegetative state after flower initiation or by reverting back to vegetative development after flowering. This allows them to flower and set seed many times during their lifetime (C1_Fig. 1).

## 1. Seedling establishment: The onset of vertical growth

During skotomorphogenesis or etiolation, Arabidopsis displays a suite of morphological and physiological adaptations for growth in the absence of light. The pronounced elongation of the hypocotyl, closed cotyledons, and the development of an apical hook are characteristic for this phase. These features are the result of a strategic conservation of resources, channeling stored energy towards vertical growth to break through the soil into the light. During this stage, elongation of the hypocotyl is driven by cell expansion rather than cell division, focusing on increasing vacuolar size for growth. This is a survival mechanism that involves a sophisticated balance between conserving energy and rapid elongation, preparing the plant for subsequent photosynthetic activity once it emerges into the light, marking the transition towards photomorphogenesis. The transition from skotomorphogenesis to photomorphogenesis or de-etiolation is underscored by a complex interplay of light perception, signaling, and developmental regulation, where the morphology of plant and physiological state undergo significant changes in response to the first exposure to light (C1_Fig. 1) (Wu, 2014).

### *1.1. Photoreceptor activation and signal transduction*

The commencement of photomorphogenesis is marked by the activation of a series of photoreceptors that detect and respond to various light wavelengths by initiating biochemical signaling pathways that direct plant growth and development. Arabidopsis has evolved an array of photoreceptors capable of discerning

light intensity, direction, duration, and wavelength. These include phytochromes A-E (phyA-E), cryptochromes 1 and 2 (CRY1&2), phototropins 1 and 2 (phot1&2), and the UV-B photoreceptor UV RESISTANCE LOCUS 8 (UVR8), each responding to a specific part of the light spectrum (Kami *et al.*, 2010; Chaves *et al.*, 2011; Suetsugu & Wada, 2013; Burgie & Vierstra, 2014; Jenkins, 2014). While each photoreceptor contributes uniquely to the light perception process, this discussion will focus primarily on phytochromes and cryptochromes, due to their central role in mediating the critical shift from skotomorphogenesis to photomorphogenesis (C1_Fig. 1).



The phytochromes, particularly prominent in sensing red and far-red light, exist in two reversible activity states—an inactive Pr-form and the active Pfr-form. Upon light exposure, they undergo a conformational change, leading to altered gene expression that drives developmental changes (Nagatani, 2004; Jiao *et al.*, 2007; Quail, 2007; Chen & Chory, 2011; Leivar & Monte, 2014; Cheng *et al.*, 2021). Cryptochromes, when activated by blue light, also trigger a cascade of events leading to growth modulation (Bouly *et al.*, 2003). These receptors collectively mediate the developmental transition of seedlings, orchestrating the morphological changes from the elongated hypocotyl and etiolated phenotype associated with skotomorphogenesis to the shorter hypocotyl, expanded cotyledons, and increased chlorophyll accumulation, which are characteristics of the photomorphogenic growth phase.

### *1.2. Integration of light signals by PIFs and COP1-SPA*

The downstream effects of photoreceptor activation are mediated through a complex network of transcription factors and signaling molecules, notably PHYTOCHROME INTERACTING FACTORS (PIFs) and the CONSTITUTIVE PHOTOMORPHOGENIC1/SUPPRESSOR OF PHYA-105 (COP1/SPA) COP1-SPA complex (Ni *et al.*, 1998; Shi *et al.*, 2016). PIFs, in the absence of light, maintain the plant in a skotomorphogenic state, stimulating longitudinal hypocotyl growth. However, upon light exposure, these PIFs are rapidly degraded, thus initiating photomorphogenic development. This degradation, facilitated by the interaction between PIFs and active phytochromes, is a complex process involving phosphorylation, ubiquitination, and proteasome-mediated degradation (Pham *et al.*, 2018a). In addition to degradation, interaction between active phyB and PIFs can also block the DNA-binding capacities of PIF1, PIF3, and PIF4, further facilitating the switch

from skotomorphogenesis to photomorphogenesis (Park *et al.*, 2012, 2018; Qiu *et al.*, 2017; Oh *et al.*, 2019). In a similar vein, cryptochromes regulate PIFs predominantly through the alteration of their transcriptional activities, without inducing their degradation. For instance, it has been shown that CRY1 interacts with PIF4 to suppress its transcriptional activity in response to blue light (Ma *et al.*, 2016; Pedmale *et al.*, 2016).

In addition to PIFs, the COP1-SPA complex serves as a master regulator in response to light signals in Arabidopsis plants, acting predominantly in darkness to maintain skotomorphogenesis. COP1 functions as an E3 ubiquitin ligase and its E3 ligase activity depends on interaction with SPA proteins. By ubiquitinating and thereby promoting the degradation of positive regulators of photomorphogenesis, mostly transcription factors, such as ELONGATED HYPOCOTYL5 (HY5), this E3 ubiquitin ligase complex ensures that the seedling conserves energy and resources until it reaches light, at which point light-activated phytochromes and cryptochromes suppress COP1/SPA activity. This results in the stabilization of COP1/SPA substrates, which now can promote photomorphogenesis (Osterlund *et al.*, 2000; Holm *et al.*, 2002; Saijo *et al.*, 2003). In contrast, in the absence of light, COP1 activity is modulated by PIFs, with PIFs enhancing COP1 activity, to ensure the repression of photomorphogenesis (Xu *et al.*, 2014, 2015, 2017). Together this shapes a tightly controlled feedback mechanism that guarantees finetuning of Arabidopsis development in response to ever changing environmental light conditions, with the COP1-SPA complex at its heart.

### *1.3. Integration of light and hormone signaling pathways*

As Arabidopsis transitions from dark-induced skotomorphogenesis to light-dependent photomorphogenesis, integration of light and hormonal signals regulates the developmental shift of plants. Insights into this process have largely been gained through the study of mutants exhibiting light-grown characteristics in the absence of light, such as shorter hypocotyls, expanded cotyledons, and activation of light-responsive genes. Such phenotypes have been crucial in revealing the roles of key phytohormones—gibberellin, brassinosteroid, and auxin—in modulating plant growth in response to light cues (Chory *et al.*, 1991, 1994; Li *et al.*, 1996; Reed *et al.*, 1998; Cowling & Harberd, 1999).

### *1.3.1. Gibberellins*

Gibberellins (GAs) serve as critical hormonal signals in Arabidopsis, influencing various developmental processes, including seed germination, stem elongation, leaf expansion, floral initiation, and the shift from skotomorphogenesis to photomorphogenesis (Cowling & Harberd, 1999; Alabadí *et al.*, 2004; Fleet & Sun, 2005; Bao *et al.*, 2020). GA20-oxidases and GA3-oxidases, involved in the last two steps of GA biosynthesis, maintain proper GA levels necessary for maintaining growth in darkness (Yamaguchi, 2008). GA deficiency leads to the premature expression of light-regulated genes and developmental patterns associated with photomorphogenesis, such as reduced hypocotyl length and the loss of the apical hook structure (Alabadí *et al.*, 2004, 2008).



GAs exert their effects on plant development through the degradation of DELLA proteins, that act as key repressors of GA signaling (Fu *et al.*, 2002). In the absence of bioactive GAs, nuclear-localized DELLA proteins interact with a wide range of transcription factors, including PIFs, to inhibit GA-mediated growth responses (Sun, 2011; Davière & Achard, 2013). Binding of bioactive GAs by the GA receptor GIBBERELLIN INSENSITIVE DWARF1 (GID1) prompts the ubiquitination and subsequent proteasomal degradation of DELLAs (Ueguchi-Tanaka *et al.*, 2005). In Arabidopsis, DELLA family members, particularly *REPRESSOR OF ga1-3* (*RGA*) and *GA INSENSITIVE* (*GAI)*, are crucial for dark-mediated repression of growth in the absence of bioactive GAs, showing that these DELLA proteins are involved in GA-dependent repression of photomorphogenesis in darkness (Alabadí *et al.*, 2004). The interaction of light with GA signaling is significantly influenced by the role of DELLA proteins. DELLAs are known to inhibit PIFs, such as PIF3 and PIF4, by sequestering their DNA-recognition domains. This sequestration reduces the ability of PIFs to bind to DNA and promote skotomorphogenic growth (Achard *et al.*, 2007; Feng *et al.*, 2008; Lucas *et al.*, 2008). Furthermore, DELLAs can also regulate the abundance of PIF proteins through the ubiquitin-proteasome system, contributing to the coordination of light and GA signals (Lucas *et al.*, 2008). In addition, the blue light receptor CRY1 modulates GA signaling by stabilizing DELLA proteins (Folta *et al.*, 2003; Zhao *et al.*, 2007b,c). By inhibiting the interaction between GA-bound GID1 and DELLAs, CRY1 sustains DELLA levels, thereby limiting GA signaling and contributing to the suppression of hypocotyl elongation that is characteristic of light-grown plants. This multilevel integration of GA signaling with light signaling pathways

highlights the sophisticated regulatory networks that govern plant growth and adaptability to their environment (Xu *et al.*, 2021; Zhong *et al.*, 2021).

### *1.3.2. Brassinosteroids*

In Arabidopsis, brassinosteroids (BRs) are critical for general growth and development, impacting both cell division and differentiation. Like GAs, BRs have been proposed to act as negative regulators of photomorphogenesis, based on the observation that BR-deficient mutants exhibit traits of light-grown plants when grown in darkness, such as short hypocotyls with opened cotyledons, no apical hook, expression of light-inducible genes and development of chloroplasts (Li *et al.*, 1996; Szekeres *et al.*, 1996). BRs and light thus oppositely control the switch from skotomorphogenesis to photomorphogenesis. BRs and light regulate this developmental switch through coordinated interactions, where light represses BR signaling and *vice versa*.

BR perception and signaling is mediated by the BRASSINOSTEROID INSENSITIVE 1 (BRI1) receptor. Upon binding BR, BRASSINOSTEROID-INSENSITIVE 2 (BIN2) kinase, a BR signaling inhibitor, is deactivated. Inhibition of BIN2, subsequently, leads to reduced phosphorylation of BRASSINAZOLE RESISTANT 1 (BZR1) and bri1-EMS-SUPPRESSOR 1 (BES1), the two key transcription factors of BR signaling, causing their activation, and leading to changes in gene expression that, among others, regulate growth (He *et al.*, 2002; Wang *et al.*, 2002; Yin *et al.*, 2002).

Light affects BR signaling to promote photomorphogenesis, among others, through direct photoreceptor interaction with BIN2, BES1, and BZR1. Light-activated CRY1 and phyB, for example, can interact with dephosphorylated BES1 and BZR1, thereby modulating their transcriptional activity and subsequently repressing BR responses (He *et al.*, 2018; Wang *et al.*, 2018; Wu *et al.*, 2018). Moreover, light-activated CRY1 and phyA and phyB can also interact directly with BIN2. In the former case to enhance physical interaction of BIN2 with BZR1, in the latter case most likely to promote its interaction with BES1. For both BZR1 and BES1 this leads to enhanced phosphorylation and thereby inactivation through degradation by the 26S proteasome (He *et al.*, 2018; Zhao *et al.*, 2022). Apart from the photoreceptors mentioned, also HY5, a positive regulator of light signaling, can interact with dephosphorylated BZR1, in this case to repress BZR1 protein stability and its transcriptional activity in regulating target genes related to cotyledon opening (Li & He, 2016). Additionally, HY5 interacts with BIN2 to

enhance its kinase activity, thereby repressing hypocotyl elongation in the light (Li *et al.*, 2020).
The other way around, BR signaling components also modulate light signaling. BIN2, for example, can phosphorylate PIF3, PIF4, and PIF5, causing their degradation via the 26S proteasome pathway, to control hypocotyl growth (Bernardo-García *et al.*, 2014; Ling *et al.*, 2017). In addition, BZR1 interacts with PIF4 to synergistically promote the expression of cell elongation-related target genes and to repress chlorophyll biosynthesis (Bai *et al.*, 2012a; Oh *et al.*, 2012; Wang *et al.*, 2020).

On top of this, recent studies have highlighted the activation of BR biosynthesis by light, vital for processes like apical hook opening and petiole development, suggesting an even more intricate interplay between light and BR signaling than previously understood (He *et al.*, 2002; Kim *et al.*, 2014; Hamasaki *et al.*, 2020).



### *1.3.3. Auxin*

Auxin plays a pivotal role in the regulation of plant growth and development, influencing a wide array of processes from organogenesis and vascular tissue differentiation to cell elongation, division, and differentiation. This phytohormone is central to understanding the dynamics of plant morphology and adaptation, especially in the context of the transition from skotomorphogenesis to photomorphogenesis in Arabidopsis (Iino & Haga, 2005; Teale *et al.*, 2006; Tripathi *et al.*, 2019). Therefore, it is no surprise that light imposes a strong influence on multiple facets of the auxin system, controlling auxin levels, transport, and responsiveness (Liu *et al.*, 2011; Sassi *et al.*, 2012; Willige *et al.*, 2012).

Auxin is synthesized from the amino acid tryptophan in a two-step pathway. First step is the removal of the amino group by the TRYPTOPHAN AMINOTRANSFERASE OF ARABIDOPSIS 1 (TAA1) family of aminotransferases to produce indole-3-pyruvate (IPA). The second step is the oxidative decarboxylation of IPA catalyzed by the YUCCA (YUC) family of flavin monooxygenases to generate indole-3-acetic acid (IAA) (Mashiguchi *et al.*, 2011; Won *et al.*, 2011). Auxin transport is mediated by the combined activities of specialized influx and efflux carriers. In Arabidopsis, the cellular influx of auxin is mediated by the AUXIN RESISTANT1/LIKE AUX1 (AUX1/LAX) family of amino acid permease-like proteins, whereas the efflux from the cells is mainly controlled by members of the PIN-FORMED (PIN) family of transmembrane proteins (Reinhardt *et al.*, 2003; Sassi & Vernoux,

2013). At the core of auxin's action is a complex signaling system that regulates gene transcription. Auxin signaling operates through a de-repression mechanism that regulates gene transcription, involving the interplay of TRANSPORT INHIBITOR RESPONSE1 (TIR1)/AUXIN-SIGNALING F-BOX (AFB) receptors, Auxin/Indole-3-Acetic Acid (Aux/IAA) repressors, and AUXIN RESPONSE FACTOR (ARF) transcription factors (Leyser, 2017). At low auxin levels, Aux/IAA proteins stabilize and repress ARF activity. In contrast, high auxin levels lead to the binding of auxin to TIR1/AFB receptor proteins, causing $SCF^{TIR1/AFB}$-mediated ubiquitination and subsequent degradation of Aux/IAA proteins by the 26S proteasome. This action releases ARFs to modulate the expression of auxin-responsive genes, crucial for various growth and developmental processes (Paciorek & Friml, 2006). Such auxin-responsive genes include members of the *Small Auxin-Upregulated RNA (SAUR*) gene family, a family with 81 members in Arabidopsis, that function in dynamic regulation of adaptive growth in response to developmental as well as environmental cues (Ren & Gray, 2015; Stortenbeker & Bemer, 2018).

Light controls auxin biosynthesis mostly through its effect on PIF stability and activity. For at least three PIFs, PIF 4, 5, and 7, it has been shown that they directly bind to the promoters of YUC8 and YUC9, which encode rate-limiting enzymes in auxin biosynthesis, to activate their expression and driving hypocotyl elongation (Mashiguchi *et al.*, 2011; Won *et al.*, 2011; Hornitschek *et al.*, 2012; Li *et al.*, 2012a; Sun *et al.*, 2012; Wei *et al.*, 2021). Auxin distribution can be modified through light signaling, mediated by HY5, by controlling the intracellular distribution and abundance of PIN proteins (Laxmi *et al.*, 2008). HY5 is further known to suppress auxin signaling by direct activation of the expression of *AUXIN RESISTANT 2* (*AXR2*)/*INDOLE ACETIC ACID 7* (*IAA7*) and *SOLITARY ROOT* (*SLR*)/*IAA14*, both negative regulators of auxin signaling (Cluis *et al.*, 2004). In contrast, PIFs can enhance auxin signaling and thereby promote hypocotyl elongation through their inhibitory effect on expression of *ARF18*, which encodes an auxin signaling repressor (Jia *et al.*, 2020). Light further affects the sensitivity to auxin within the cell through stimulation of protein-protein interactions between photoreceptors and auxin signaling components. Photoactivated phyA, phyB, and CRY1 directly bind Aux/IAAs, thereby competing with TIR1/AFBs. As a result, these AUX/IAAs become stabilized, thereby repressing ARF activity and downstream auxin signaling to regulate hypocotyl elongation (Xu *et al.*, 2018; Yang *et al.*, 2018). Photoactivation further stimulates physical interaction of phyB and CRY1 with ARF6 and ARF8 to

repress their DNA-binding activity and subsequent auxin-responsive gene regulation, resulting in inhibition of hypocotyl elongation under red and blue light (Mao *et al.*, 2020). Differential expression of a subset of SAURs, operating downstream of the core auxin signaling pathway, is a key determinant for the different growth rates of cotyledons and hypocotyls under dark versus light conditions (Sun *et al.*, 2016). Both PIF3 and PIF4, which accumulate in darkness and whose levels rapidly decline upon light exposure, directly bind several of these SAUR encoding genes and differentially regulate their expression in cotyledons and hypocotyls (Sun *et al.*, 2016; Dong *et al.*, 2018).



In conclusion, in Arabidopsis seedlings auxin levels are closely tied to light-regulated growth and development and much of this is achieved by light modulation of the auxin system.

### *1.3.4. BAP/D and HLH/BHLH module: Multi-signal integrators for cell elongation*

Given the complex interplay of light with gibberellins, brassinosteroids, and auxin in plant development, it is recognized that these hormone signals do not function in isolation but rather influence each other across multiple levels from biosynthesis to signaling. In Arabidopsis, a molecular circuit formed by complex protein–DNA and protein–protein interactions among a triad of transcription factors, BZR1, ARF6, and PIF4, and DELLA proteins (BAP/D), and their downstream components, integrates all major growth-regulating signals, including auxin, brassinosteroid, gibberellin, and light (Oh *et al.*, 2014; Bouré *et al.*, 2019; Diao *et al.*, 2023).

The regulation of growth in Arabidopsis through this so-called BAP/D module indicates the ability of plants to coordinate a complex array of signals into a unified regulatory strategy. Acting in opposition to DELLA proteins, BZR1, ARF6, and PIF4 form a regulatory network that modulates gene expression essential for cell elongation (Oh *et al.*, 2014; Bouré *et al.*, 2019). Conversely, DELLA proteins inhibit the DNA-binding and transcriptional activity of all three transcription factors and compete with PIF4 and BZR for binding to ARF6 (Oh *et al.*, 2014; Bouré *et al.*, 2019). Alongside the BAP/D module, antagonistic DNA-binding basic Helix-Loop-Helix (bHLH) and non-DNA-binding bHLH (HLH) transcription factors form a tri-partite regulatory module (HLH/bHLH module) to control cell elongation. Central to this module is the *PACLOBUTRAZOL RESISTANCE* (*PRE*) gene family. This family encodes non-DNA binding transcription inhibitors that

promote cell elongation. They achieve this by sequestering a second set of HLH/bHLH proteins, namely INCREASED LEAF INCLINATION1 BINDING bHLH1 (IBH1), PHYTOCHROME RAPIDLY REGULATED1/2 (PAR1/2), ATBS1 INTERACTING FACTORS (AIFs), and LONG HYPOCOTYL IN FAR-RED1 (HFR1). These factors typically act as brakes on elongation by inhibiting the action of proteins that promote cell elongation. Complementing these are the third-tier proteins of the HLH/BHLH module — HOMOLOG OF BEE2 INTERACTING WITH IBH1 (HBI1), ACTIVATOR FOR CELL ELONGATIONS (ACEs), BR-ENHANCED EXPRESSION2 (BEE2), and CRYPTOCHROME INTERACTING bHLH1 (CIB1), which activate the production of cell wall components and other elements necessary for cell elongation (Zhang *et al.*, 2009; Bai *et al.*, 2012a,b; Wang *et al.*, 2012; Oh *et al.*, 2014; Diao *et al.*, 2023).

The BAP/D and HLH/bHLH modules in Arabidopsis work in concert through a series of feedforward and feedback loops, both positive and negative. For example, the levels of *PRE* mRNA are notably elevated by the presence of hormones such as GA, BR, and auxin. Transcription factors like ARF6, ARF8, BZR1, and PIF4, key components of the BAP/D module, serve to further increase *PRE* expression, demonstrating a positive feedforward mechanism (Oh *et al.*, 2012; Zheng *et al.*, 2017). Similarly, the module boosts the expression of *BEE2*, creating another layer of positive regulation. On the other hand, BAP/D also acts to suppress the expression of *IBH1*, *PAR1*, *PAR2*, and *HFR1*, establishing a negative feedforward control. PREs are vital for enabling PIFs to bind to DNA, forming a positive feedback from HLH/BHLH back to BAP/D. PIFs usually find their DNA-binding ability hindered by IBH1 and PAR1, but PREs effectively neutralize these inhibitors, ensuring the activation of PIFs (Bai *et al.*, 2012a; Ikeda *et al.*, 2012; Oh *et al.*, 2012, 2014). This intricate array of regulatory loops ensures that the BAP/D and HLH/BHLH modules can fine-tune plant growth, allowing for a versatile response across a spectrum of environmental light and dark conditions.

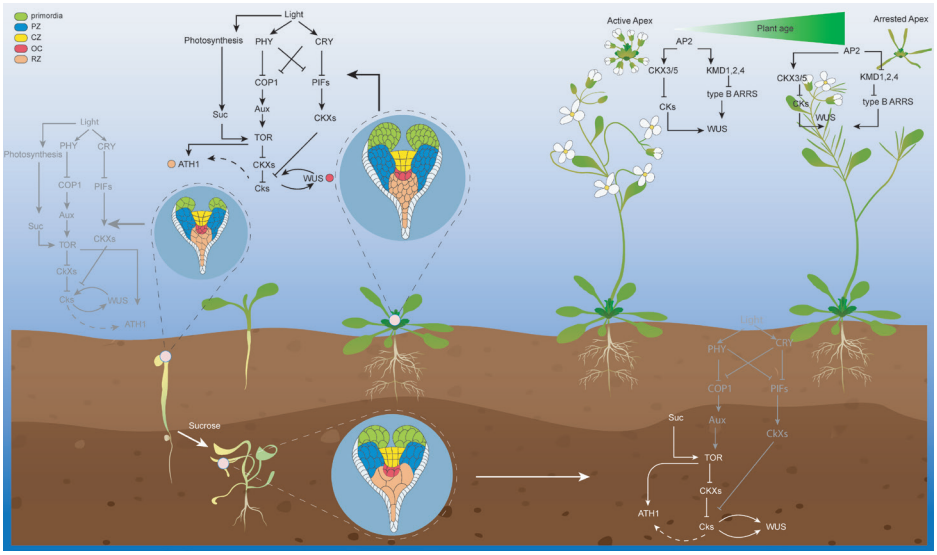


**C1_Fig. 1: Morphological and molecular dynamics in the shoot apical meristem across Arabidopsis developmental phases.**

During germination in darkness, the SAM of plants remains dormant, inhibiting the emergence of aerial parts. Exposure to light activates the SAM, initiating a shift from skotomorphogenesis to photomorphogenesis, which in turn stimulates the development of rosette leaves in the vegetative phase. In the absence of light, dark-grown seedlings are capable of SAM activation if sucrose is available, circumventing the usual light requirement. As the plant matures, it undergoes a reproductive phase change, characterized by the onset of bolting and flowering—this pivotal transition marks the shift from vegetative growth to reproductive development. The lifecycle concludes with a final transition post-flowering, where an orchestrated cessation of floral activity leads to senescence of the plant. Molecularly, SAM activity is modulated by a network where WUSCHEL (WUS) sustains stem cell populations and ARABIDOPSIS THALIANA HOMEOBOX GENE 1 (ATH1) tempers RZ activity during vegetative growth. The Target of Rapamycin (TOR) kinase emerges as a key regulator, influenced by light through photoreceptor-mediated inactivation of COP1 and PIFs. This cascade results in auxin accumulation, promoting TOR kinase activity, which in turn restricts cytokinin (CK) degradation, enhancing CK levels to boost WUS expression. The potential role of CK in ATH1 expression warrants further investigation. Moreover, sucrose can activate TOR independently of light, leading to WUS upregulation and insufficient ATH1 expression to inhibit RZ activity. The cessation of flowering involves similar pathways, with WUS and CK as central players. The decline of WUS in aging plants is hypothesized to result from altered CK oxidase activity or the activation of KMD genes that suppress ARRs necessary for WUS expression.

## 2. Vegetative growth: a temporary cessation in vertical growth

As mentioned before, during skotomorphogenesis, the plant's SAM, which is situated between embryonic leaves, remains dormant. This dormancy allows the plant to direct resources toward longitudinal growth in order to reach the light. Exposure to light induces a transition to photomorphogenesis. At this stage, the plant's hypocotyl growth ceases, the SAM activates, and the vegetative growth phase begins, with leaf production becoming the primary activity. In Arabidopsis, this transition signifies a temporary halt in upward growth, presumably to boost photosynthetic capacity by increasing the rosette leaves' surface area, thus building energy reserves for later growth stages, such as the floral transition. This suppression of vertical growth during the vegetative growth phase is regulated within the meristem itself, where specific genetic and hormonal signals inhibit cell elongation and division, constraining the plant's upward progression (Griffiths & Halliday, 2011; Yoshida *et al.*, 2011; Pfeiffer *et al.*, 2016; Li *et al.*, 2017; Mohammed *et al.*, 2017). The following section explores the SAM's role in regulating growth throughout the vegetative phase (C1_Fig. 1).

### *2.1. The morphology of Shoot Apical Meristem (SAM)*

The SAM of flowering plants (angiosperms) has a distinct structure and function. Morphologically, it consists of three distinct cell layers: L1, L2, and L3. Each layer contributes to specific tissues. Cells in L1 and L2 divide in a specific plane (anticlinally) and give rise to the outer (epidermal) and subepidermal tissues, respectively. L3, through less organized cell divisions, contributes to the plant's internal structure by forming vascular tissue and pith (Kitagawa & Jackson, 2019). Functionally, the SAM can be divided into three zones: the central zone (CZ), the peripheral zone (PZ), and the rib zone (RZ). The CZ harbors a population of slow-dividing, self-renewing stem cells established during embryogenesis. This zone also contains the organizing center (OC) at its base, which is critical for maintaining the stem cell population. Descendants of these stem cells are continuously pushed outward towards the surrounding PZ or downwards into the RZ, located below the OC. Cells within the PZ divide more rapidly and become the source cells for leaf or flower bud formation. In contrast, cells in the RZ differentiate into pith cells and contribute to vascular tissue and stem structures (Han *et al.*, 2020; Zhang *et al.*, 2021). In rosette plants like Arabidopsis, the RZ remains

inactive during vegetative growth, resulting in the compact rosette form (Gómez-Mena & Sablowski, 2008). However, when the plant transitions from vegetative to reproductive growth, the RZ becomes active, leading to rapid elongation of the inflorescence stem, a characteristic feature of bolting (Ruonala *et al.*, 2008). During bolting, the RZ, composed of transverse cell files, undergoes numerous cell divisions followed by elongation, ultimately forming the inflorescence stem (C1_Fig. 1) (Metzger & Dusbabek, 1991; Reddy & Meyerowitz, 2005; Gómez-Mena & Sablowski, 2008; Rutjens *et al.*, 2009; Yadav *et al.*, 2014).



#### *2.1.1. Stem cell initiation and maintenance – WUS-CLV feedback loop*

The pool of embryonic stem cells at the shoot apex is established by WUSCHEL (WUS) (Ikeda *et al.*, 2009). WUS is expressed in the OC of the SAM and induces pluripotency of stem cells by inhibiting differentiation-promoting transcription factors and by integrating hormonal signaling pathways (Busch *et al.*, 2010; Yadav *et al.*, 2013). WUS is a mobile protein that can be transported into adjacent cell layers and induce *CLAVATA3* (*CLV3*) expression. Maintenance of stem cells requires WUS, as well as its movement. Loss of function *wus* mutants or reducing WUS mobility, such as by blocking plasmodesmata, result in stem cell misspecification (Daum *et al.*, 2014). Consequently, the SAM is prematurely terminated, after forming only a few organs. Opposing WUS are the CLV genes, which act as negative regulators of the SAM's stem cell population (Kwon *et al.*, 2022). Mutations in CLV genes cause an overabundance of meristematic cells, either due to excessive cell division or reduced differentiation. This delays the initiation of new organs (Clark *et al.*, 1997; Rojo *et al.*, 2002). Specifically, *CLV3* encodes a peptide signal produced exclusively in the L1 and L2 layers. This peptide diffuses to neighboring cells, where it binds to the CLV1/CLV2 receptor complex, triggering a pathway that inhibits *WUS* expression. In essence, WUS and CLV proteins form a negative feedback loop. This communication between cells (via the WUS-CLV system) allows the OC and CZ to maintain the SAM's stem cell niche (C1_Fig. 1) (Clark *et al.*, 1997; Willmann, 2000).

The WUS-CLV3 feedback loop is deeply connected to cytokinin signaling, a crucial pathway for maintaining the SAM. Cytokinins, known for promoting cell division, directly contribute to SAM maintenance. Mutations that impair cytokinin biosynthesis result in smaller SAMs, while cytokinin catabolic mutations result in larger SAMs – effects similar to those seen when the SAM is treated with exoge-

nous cytokinin (Kurakawa *et al.*, 2007; Wybouw & Rybel, 2018). *WUS* expression is positively regulated by cytokinin through CLV-dependent and -independent pathways. Specifically, Arabidopsis type B response regulators (ARRs) – namely ARR1, ARR10, and ARR12 – bind to the *WUS* promoter, boosting its expression (Xie *et al.*, 2018). Conversely, WUS directly suppresses type-A response regulators (ARR5, 6, 7, and 15), which normally inhibit cytokinin signaling. This action by WUS creates a zone of elevated CK response specifically within the organizing center and central zone (OC/CZ) of the SAM. Intriguingly, ARR1 also stabilizes WUS protein, creating a positive feedback loop that further amplifies the CK signal (Snipes *et al.*, 2018). The positive feedback between WUS and CK is essential for sustaining the stem cell niche within the SAM (Leibfried *et al.*, 2005). Beyond cytokinin, WUS also modulates auxin signaling in the CZ by promoting histone acetylation of genes involved in the auxin pathway (including TRANSPORT INHIBITOR RESPONSE 3 (TIR3), ARF5, and IAA9). This careful regulation ensures basal auxin levels within stem cells, which are crucial for their maintenance (Ma *et al.*, 2019). In summary, WUS acts as a central regulator, finely controlling both cytokinin and auxin output, ultimately determining the size and activity of the stem cell pool within the SAM (C1_Fig. 1).

### *2.1.2. Establishment and maintenance of SAM – class I KNOX transcription factors*

Beyond the WUS-CLV3 feedback loop, the regulatory network within the SAM involves another key player: SHOOTMERISTEMLESS (STM). This KNOTTED1-like homeobox (KNOX1) transcription factor plays a crucial role in both initiating and maintaining the SAM, similar to WUS (Barton & Poethig, 1993; Clark *et al.*, 1996; Endrizzi *et al.*, 1996; Long *et al.*, 1996; Byrne *et al.*, 2002; Su *et al.*, 2020). Interestingly, STM and WUS pathways do not operate independently; they collaborate to fine-tune stem cell regulation. Recent findings by Su et al. (2020) reveal a direct interaction between WUS and STM proteins, significantly influencing the regulation of *CLV3*. STM binds to the *CLV3* promoter, enhancing binding of WUS to this promoter through WUS-STM interaction. This coordinated action between WUS and STM is essential for regulating *CLV3* expression, which is pivotal in maintaining a stable stem cell population. Additionally, the expression of *STM* is dependent on WUS, and WUS-activated expression of *STM* further amplifies WUS-mediated stem cell activity.

*STM* is expressed throughout the shoot meristem, including the stem cells, the organizing center (OC), and the transit-amplifying cells in the PZ before they become incorporated in the organ primordia. In concordance with its role in inhibition of cell differentiation, *STM* is down-regulated in nascent organ primordia (Kim *et al.*, 2003b; Heisler *et al.*, 2005). This down-regulation of *STM* mRNA coincides with auxin accumulation and the activation of organ-specific genes, including the R2R3 MYB transcription factor ASYMMETRIC LEAVES1 (AS1) and the LATERAL ORGAN BOUNDARIES (LOB)-domain protein AS2 (Ori *et al.*, 2000; Byrne *et al.*, 2002)—both known to inhibit KNOX1 gene expression. Additionally, the TEOSINTE BRANCHED1/CYCLOIDEA/PCF (TCP) family of bHLH-type transcriptional regulators represses KNOX1 gene expression in leaf primordia while promoting leaf differentiation. A complex formed by AS1, AS2, and LOB directly targets the promoters of STM and other KNOX class-I genes to suppress their expression (Guo *et al.*, 2008).

Like WUS, the STM protein is a mobile protein. Trafficking of STM within the SAM is a complex process involving several key proteins (Winter *et al.*, 2007; Liu *et al.*, 2018; Kitagawa *et al.*, 2022). Among these, the CHAPERONIN CONTAINING T-COMPLEX POLYPEPTIDE 1 Subunit 8 (CCT8) mediates STM trafficking by facilitating its movement through the plasmodesmata (Kitagawa *et al.*, 2022). STM movement within the SAM is essential for proper SAM function; impediments in its trafficking result in a significant reduction in SAM size and a decrease in *STM*-expressing cells within the SAM (Balkunde *et al.*, 2017). *STM* mRNA, unlike *WUS* mRNA, may also be transported to neighboring cells (Xu *et al.*, 2011; Balkunde *et al.*, 2017). In Arabidopsis, the intercellular transport of mRNA for the maize *STM* ortholog *KNOTTED1* (*Kn1*) involves the plasmodesmata-localized protein ribosomal RNA–processing protein 44A (AtRRP44a). AtRRP44a is required for the developmental functions of STM, suggesting a similar role in *STM* mRNA trafficking in Arabidopsis (Kitagawa *et al.*, 2022). Moreover, there may be a selective mechanism at the plasmodesmata that prevents STM from entering the primordia cells, ensuring precise regulation of SAM activity and organogenesis.

STM contributes to the maintenance of stem cell populations in the SAM by promoting CK biosynthesis, while inhibiting GA biosynthesis (Jasinski *et al.*, 2005). STM specifically inhibits the GA biosynthesis gene *AtGA20ox1*, thereby lowering the level of bioactive GA in the SAM (Hay *et al.*, 2002). Consequently, GA levels are low in all SAM regions, excluding those that lack *STM* expression. STM

induces the production of bioactive CKs by activating the enzyme ISOPENTENYL TRANSFERASE 7 (AtIPT7), which initiates the crucial step in the production of CKs (Yanai *et al.*, 2005). CKs, in turn, enhance *STM* mRNA, resulting in a positive feedback loop (Rupp *et al.*, 1999). *STM* expression in the SAM is therefore associated with decreased GA and increased CK levels. In line with this, reducing CK and increasing GA levels result in phenotypic effects similar to those associated with strong *stm* mutants, showing that the balance between these two hormones as regulated by STM is crucial to maintain SAM (Jasinski *et al.*, 2005).

### *2.1.3. The shoot apical meristem is activated by light*

In Arabidopsis, light is a pivotal factor for post-germination activation of the SAM. Light promotes the maintenance of stem cells and the initiation of lateral organs (Quaedvlieg *et al.*, 1995; Gómez-Mena & Sablowski, 2008; Pfeiffer *et al.*, 2016; Li *et al.*, 2017). The SAM, being shrouded by cotyledons, is not exposed to light and thus cannot directly detect it. It is however suggested that light signals are instead sensed by phytochrome- and cryptochrome-family photoreceptors, leading to the release of mobile signals that travel to the SAM. These signals then reach the SAM and promote the expression of *WUS*, crucial for SAM activity, through CKs (López-Juez *et al.*, 2008; Pfeiffer *et al.*, 2016). CKs, long-distance signaling molecules, ensure coordination between the SAM and distant tissues, crucial for plant growth and organogenesis (Cammarata *et al.*, 2022; Wu *et al.*, 2022). The exact mechanisms by which light modulates cytokinin levels, potentially by degrading CYTOKININ OXIDASES/DEHYDROGENASE (CKX) enzymes or through interaction with PIFs (Janocha *et al.*, 2022) and the TARGET OF RAPAMYCIN (TOR) kinase pathway remain to be fully elucidated (Artins & Caldana, 2022; K *et al.*, 2022; Marash *et al.*, 2022). Light also influences auxin signaling, affecting the localization of auxin transporters like PIN1 (Sassi *et al.*, 2013), which is critical for lateral organ initiation (Yoshida *et al.*, 2011; Sassi *et al.*, 2012; Pfeiffer *et al.*, 2016). In addition, light also controls the rib zone (RZ) activity, with photoreceptor mutants displaying elongated internodes and loss of the rosette structure (Mazzella *et al.*, 2000; Franklin *et al.*, 2003b,a; Franklin & Quail, 2010). The control of the RZ by photoreceptors is linked to the function of a transcription factor known as ARABIDOPSIS THALIANA HOMEOBOX GENE 1 (ATH1). Originally identified as a gene regulated by light, *ATH1* is expressed in various tissues, including the meristem,

where it plays a pivotal role in controlling rib zone activity and thus regulation of internode elongation (C1_Fig. 1) (Quaedvlieg *et al.*, 1995; Hajibehzad *et al.*, 2023).

### *2.1.4. Sugars and SAM activation*

Light not only acts as a signal to steer plant development but also fuels photosynthesis, providing the necessary energy for growth. Therefore, the light-dependent activation of SAM may be directly related to photoreceptor-mediated signaling or indirectly through energy provision, such as sucrose synthesis. In the absence of light, constrained carbon resources lead to SAM inactivity and halted growth. Nevertheless, Arabidopsis can progress through developmental stages in darkness if metabolic sugars are accessible to the shoot apex, indicating that sugars alone can trigger SAM activation. This is supported by findings that Arabidopsis plants, grown in dark conditions with sucrose supplementation, maintain an active stem cell niche, leading to leaf formation during vegetative growth and elongated inflorescences with flowers during the reproductive phase, akin to those in light-grown plants (Araki & Komeda, 1993; Roldán *et al.*, 1999; Pfeiffer *et al.*, 2016; Li *et al.*, 2017; Mohammed *et al.*, 2017; Hajibehzad *et al.*, 2023).

Key for post-germination SAM activation is the induction of *WUS* expression. In line with this, dark-grown seedlings with sugar supplementation exhibit *WUS* expression, implying meristem activation. Similarly, the expression of *STM*, another gene crucial for SAM function, can be triggered by sugar signals in the absence of light (Lopes *et al.*, 2023). The upregulation of *WUS* in the absence of light might be mediated by CKs, as sucrose is known to elevate CK levels in the SAM under dark conditions. This is supported by the observations that in *cytokinin oxidase5* (*ckx5*) *ckx6* double mutants, which have increased CK levels due to disturbed CK catabolism, *WUS* mRNA levels are enhanced in the absence of light and sucrose, and that CK application is able to rescue *WUS* expression when both sugar and light signaling are blocked (Richard *et al.*, 2002; Pfeiffer *et al.*, 2016; Janocha *et al.*, 2022).

While both light and sugar serve as activators of the SAM and promote plant growth, they lead to distinct phenotypic outcomes. Sugar-supplied dark-grown plants characteristically exhibit elongated vegetative internodes, a phenotype absent in light-exposed plants (Roldán *et al.*, 1999). This difference suggests a specific role for light in regulating the RZ. In light-grown plants, the RZ remains inactive, while in the sugar-driven, dark-growth condition, premature RZ activa-

tion seemingly leads to internode elongation (Quaedvlieg *et al.*, 1995; Proveniers *et al.*, 2007; Gómez-Mena & Sablowski, 2008; Rutjens *et al.*, 2009; Ejaz *et al.*, 2021). Therefore, while sugars alone are sufficient to activate the central stem cell population of the SAM and drive differentiation at the meristem periphery, they appear to lack the capacity to repress differentiation within the RZ, the function normally mediated by light signaling pathways.

### *2.1.5. TOR kinase integrates light and sugar signals to activate SAM*

Light signals received by photoreceptors and sucrose derived from photosynthesis are both capable of activating the stem cell population in the SAM, leading to the initiation of new plant organs. The Target of Rapamycin (TOR) protein kinase is essential in this process as it senses nutrient availability and regulates plant growth by regulating metabolism, protein production, and gene expression needed for cell growth (Pfeiffer *et al.*, 2016). As an integrator of light and metabolic signals, TOR kinase activity is essential for SAM activation. It has been established that TOR acts as a convergence point for light and sugar signals, streamlining the regulation of SAM activity. At the molecular level, TOR kinase promotes the expression of *WUS*, which governs stem cell proliferation within the SAM under favorable conditions (Xiong *et al.*, 2013; Pfeiffer *et al.*, 2016; Li *et al.*, 2017; Mohammed *et al.*, 2017; Wu *et al.*, 2019). The precise mechanism through which TOR kinase influences *WUS* expression remains to be fully elucidated. However, it is suggested that TOR kinase reduces the translational efficiency of *CKX* mRNAs when conditions are optimal. This results in lower CKX protein levels, ultimately leading to higher CK concentrations. Conversely, when conditions are unfavorable and TOR kinase activity is inhibited, CKX translation efficiency increases. Therefore, in the presence of light and/or sugar, high TOR kinase activity correlates with elevated CK levels at the SAM. These increased CK levels then trigger a rise in *WUS* expression, ultimately stimulating stem cell activity (C1_Fig. 1) (Pfeiffer *et al.*, 2016; Janocha *et al.*, 2022).

### *2.1.6. Lateral organ initiation – Central role for auxin*

Within the CZ of the SAM, self-renewing stem cells divide, and their progeny migrate to the PZ, where vigorous cell division gives rise to lateral organ primordia. The initiation of organogenesis at the SAM periphery in the PZ is marked by a localized increase in auxin concentration, alongside a shift in the expression

pattern of genes that orchestrate organ-specific development (Reinhardt *et al.*, 2003; Heisler *et al.*, 2005).

The local auxin maxima at the lateral organ primordia are established by active polar transport mediated by auxin efflux carriers from the PIN family of proteins and the AUX1/LAX-family of influx carriers (Reinhardt *et al.*, 2003; Bainbridge *et al.*, 2008). As such, preventing auxin accumulation at the flanks of the SAM prevents the formation of lateral organs, thereby producing pin-shaped structures. (Reinhardt *et al.*, 2000; Guenot *et al.*, 2012). A recent study revealed that the ethylene response factor-type transcription factor *LEAFLESS* (*LFS*) is the sole regulator of leaf initiation in tomato (Capua & Eshed, 2017; Heisler & Byrne, 2020). This gene encodes a protein closely related to the Arabidopsis DORNRÖSCHEN (DRN) and DRN-like (DRNL) proteins (Seeliger *et al.*, 2016). The tomato *LFS* gene is required for leaf initiation and expressed on the flanks of the SAM, where auxin levels are high. In tomato, primordia arising from the periphery of the SAM in *lfs* and *drn/drnl* mutants are unable to initiate cotyledons, leaves, and leaflets, leading to the development of long, *pin-like* shoots (Chandler *et al.*, 2011; Capua & Eshed, 2017). Moreover, Arabidopsis and tobacco plants with overexpression of *DRN* or *DRNL* display abnormal leaf and flower development (Chandler *et al.*, 2007, 2011; Capua & Eshed, 2017). Interestingly, tomato *lfs* mutants eventually develop flowers, suggesting that stem cells are still present in the SAM. Therefore, *LFS* appears to regulate the initiation of lateral leaves independently of the initiation of floral organs. The phenotypic similarity between Arabidopsis *drn drnl* double mutants and the tomato *lfs* mutant suggests that auxin-induced leaf initiation is relayed by an evolutionarily conserved mechanism driven by LFS/DRNL (Chandler *et al.*, 2011; Capua & Eshed, 2017). Nevertheless, recent finding has positioned DRNL as a direct transcriptional target of MP in the PZ, controlling many known MP targets during organ initiation. Consequently, *drn/drnl* mutants mirror the *mp* phenotype, with *pin*-shaped inflorescences, linking auxin signaling to floral organ development (Dai *et al.*, 2023).

### *2.1.7. Rib zone (in)activation – Central role for ATH1*

Similar to the PZ, where stem cell descendants are recruited to form organ primordia, the RZ also undergoes a recruitment process to contribute to stem tissue formation. During the vegetative phase, the SAM maintains a flattened shape. This coincides with a compact and mitotically inactive RZ, while PZ-derived cells

actively transition into leaf primordia. In contrast to the actively dividing PZ, RZ activation is primarily associated with the reproductive phase and contributes to stem elongation, a defining characteristic of this stage. This activation triggers rapid growth of the inflorescence stem (Bencivenga *et al.*, 2016; Serrano-Mislata & Sablowski, 2018; McKim, 2019, 2020). However, if RZ activation occurs abnormally during vegetative development – a deviation from the typical growth pattern of Arabidopsis – the plant adopts a caulescent morphology, characterized by a stem-like structure, rather than the rosette form (Ejaz *et al.*, 2021) (C1_Fig. 1)

The genetic players dictating RZ (in)activity and its regulatory mechanisms are not fully elucidated. However, research has identified a transcription factor called ATH1 as a key player. This BEL1-like homeodomain (BLH) transcription factor is expressed in the vegetative SAM and plays a vital role in RZ regulation. Mutations in *ATH1* lead to elongated internodes during the vegetative phase due to premature activation of the RZ (Ejaz *et al.*, 2021). Conversely, ectopic expression of *ATH1* restricts stem growth after the plant transitions to flowering, resulting in plants that do not develop elongated stems (bolting) but still produce flowers (Cole *et al.*, 2006; Gómez-Mena & Sablowski, 2008; Rutjens *et al.*, 2009).

The connection between light signaling and RZ activity is further supported by the observation of elongated internodes in plants lacking photoreceptors. These light-sensing proteins, such as phytochromes and cryptochromes, appear to play a crucial role in suppressing internode elongation during vegetative growth. For example, plants lacking both phyA and phyB genes lose their characteristic compact rosette form under certain light conditions. This suggests that other photoreceptors might also contribute to controlling internode (Devlin *et al.*, 1996, 1997, 1998; Mazzella *et al.*, 2000; Mazzella & Casal, 2001). Additionally, mutations affecting specific combinations of photoreceptors, such as *phyA phyB* double mutants, and *phyB cry1* double mutants, also result in elongated internodes, particularly at warmer temperatures. In the case of *phyB cry1* mutants, this effect can be even more dramatic, leading to a complete loss of the rosette habit. These findings highlight the significant role of *phyB*, particularly in regulating temperature-dependent internode elongation (Mazzella *et al.*, 2000).

Given the central role of ATH1 in controlling RZ activity and subsequent internode formation and the fact that *ATH1* expression is light-regulated (Quaedvlieg *et al.*, 1995), this raises the question whether ATH1 serves as a critical regulatory

nexus within the SAM, mediating the RZ response to light—a key environmental cue essential for plant growth and development.

## 3. Vegetative to reproductive shift: resuming longitudinal growth



### *3.1. Bolting and transition to reproductive growth*

In Arabidopsis, development begins with hypocotyl elongation. This is followed by a vegetative phase marked by a temporary halt in vertical growth. This pause is essential, likely allowing the plant to prepare for the critical switch to reproductive growth. During this transition a dramatic shift occurs, with the resumption of vertical growth through rapid elongation of the inflorescence stem. Flower development is the most prominent hallmark of this switch, but it encompasses a wider range of morphological changes. These include adjustments in leaf shape (heteroblasty) and alterations in plant architecture. The transition is initiated by the SAM transforming into an Inflorescence Meristem (IM). This transformation reprograms the meristem to produce floral primordia instead of leaf primordia at its periphery. Additionally, previously dormant cells within the RZ become mitotically active. This renewed activity leads to the formation of elongated internodes. This process, known as bolting, signifies a fundamental change in Arabidopsis from an acaulescent to a caulescent growth form (Poethig, 2003, 2013).

### *3.2. Bolting versus flowering: distinctions in developmental processes*

Because in Arabidopsis bolting and flowering occur (almost) simultaneous, many consider bolting to be an essential part of the flowering process. In addition, the terms bolting and flowering are often but wrongly considered synonymous and to exclusively refer to flowering. However, these two terms are not interchangeable for several reasons. First, in several rosette-forming plant species, such as cabbages and radishes, bolting can be induced under suboptimal conditions through gibberellin application, without induction of flowering (Janick & Leopold, 1961; Suge & Rappaport, 1968; Mutasa-Göttgens *et al.*, 2010; Hamano *et al.*, 2015). Second, Arabidopsis and sugar beet plants can be reverted from bolting to vegetative growth under certain conditions, but not from flowering to vegetative growth (Tooke *et al.*, 2005; Reeves *et al.*, 2007). Lastly, flowering can be induced without

bolting. In celery, for example, flowering can be induced after a short vernalization period, without the induction of bolting (Booij & Meurs, 1995).

### *3.3. Agricultural implications of bolting*

The development of an elongated inflorescence stem in plants is believed to be a resource-intensive process, potentially drawing upon the nutrient reserves of leaves and roots. In agricultural contexts, the architectural changes caused by bolting therefore often have undesirable effects with respect to both yield quantity and quality. The timing of this fundamental switch must therefore be tightly controlled. Premature bolting in lettuce and cabbage, for example, reduces marketability by reducing the head density and crop quality (Guttormsen & Moe, 1985). Moreover, in lettuce, as a result of bolting, bitter secondary metabolites are produced and the stem tissue becomes hardened (Sessa *et al.*, 2000). Bolting not only affects the above-ground part of crop plants, but also impacts the quality and weight of below-ground storage organs. In the case of premature bolting in sugar beets and beetroots, the taproots are significantly smaller due to reallocation of nutrients from these harvestable tissues to the developing stems. In addition, beets from bolted sugar beet plants were found to contain 23% less sugar on average than taproots from non-bolted plants of the same age (Wood & Scott, 1975). Moreover, bolted plants often overshadow non-bolted plants, resulting in shade-avoidance responses that cause an extra yield reduction. Although not staple crops, rosette-forming crops are both economically and nutritionally important. Among the ten most widely produced vegetable groups in 2017, five were rosette crops and sugar beets ranked eighth (FAO, 2017). Consequently, small improvements in bolting resistance can have significant impact in the world food supply.

### *3.4. Regulation of stem elongation in Arabidopsis*

Stem elongation in *Arabidopsis thaliana* is regulated by transcription factors of the TALE (three-amino-acid-loop-extension) superfamily, specifically the KNOX and BLH families. Functional heterodimers between BLH and KNOX proteins are required for their nuclear localization and DNA binding activity. Key members include the BLH-family members ATH1, PENNYWISE (PNY), and POUND-FOOLISH (PNF). These form complexes with class I KNOX proteins, such as STM, KNOTTED-LIKE FROM ARABIDOPSIS THALIANA 2(KNAT2), KNAT6, and BREVIPEDICELLUS/KNAT1 (BP/KNAT1). This interplay is essential for controlling stem elongation

associated to the reproductive phase change (Byrne *et al.*, 2002; Bhatt *et al.*, 2004; Kanrar *et al.*, 2006; Gómez-Mena & Sablowski, 2008; Rutjens *et al.*, 2009; Ung *et al.*, 2011; Landrein *et al.*, 2015; Bao *et al.*, 2020).

ATH1 functions as a negative regulator of stem elongation. In mutants lacking *ATH1*, plants undergo premature stem elongation, evident in lengthened rosette internodes, while ectopic expression of *ATH1* represses bolting without affecting flowering. This underscores ATH1's role in maintaining the vegetative state and delaying bolting (Cole *et al.*, 2006; Gómez-Mena & Sablowski, 2008; Rutjens *et al.*, 2009; Ejaz *et al.*, 2021). Conversely, the BLH family members PNY and PNF promote stem elongation. *pny* mutants exhibit a semi-dwarf phenotype with shorter stems due to loss of oriented cell division and growth in the RZ. As a consequence, these mutants display clusters of cauline leaves, flowers, or siliques interspersed with longer internodes. This highlights PNY's role in driving vertical stem growth. While *pnf* single mutants show no obvious phenotype, combined *pny* and *pnf* mutations result in a much stronger effect, with a complete lack of bolting and flowering in double mutants due to the absence of cell division activity in the RZ and the inability to fully induce FMI gene expression. This absence of reproductive development emphasizes the synergistic action of PNY and PNF in triggering the transition from vegetative to reproductive growth. The antagonistic interplay between these transcription factors and ATH1 is evident in their combined effects. For instance, loss of *ATH1* in *pny* mutants restores plant height and clustering. Similarly, the restoration of bolting and flowering in *pny pnf* double mutants by removing *ATH1* demonstrates their opposing roles in regulating stem elongation (Byrne *et al.*, 2003; Bhatt *et al.*, 2004; Smith *et al.*, 2004; Rutjens *et al.*, 2009; Khan *et al.*, 2012; Bencivenga *et al.*, 2016).

The interplay between ATH1, PNY, and PNF extends beyond their interactions, forming an intricate regulatory network with class I KNOX proteins. Overlapping expression patterns during development suggest their coordinated control of internode elongation. In the vegetative state, *ATH1* exhibits high expression throughout the SAM, particularly at the RZ. However, its expression is downregulated as the plant transitions to reproduction. *KNAT2* and *KNAT6* also localize to the vegetative SAM, specifically in the RZ and organ boundaries respectively. Their expression then ceases in the inflorescence meristems, mirroring *ATH1*'s pattern (Byrne *et al.*, 2003; Bhatt *et al.*, 2004; Belles-Boix *et al.*, 2006; Kanrar *et al.*, 2006; Proveniers *et al.*, 2007; Gómez-Mena & Sablowski, 2008; Ragni *et al.*, 2008; Rut-

jens *et al.*, 2009; Hajibehzad *et al.*, 2023). Unlike *ATH1*, *PNY* is expressed throughout the vegetative shoot apex and persists in the generative shoot apex. The precise spatiotemporal expression pattern of *PNF* remains unclear, although transcriptomic data suggests very low expression in the vegetative shoot apex with upregulation during the transition to reproduction. BP, a class I KNOX gene, shares expression domains with *ATH1* in the SAM and RZ, but acts as a positive regulator of stem elongation. Mutations in *BP* result in shorter stems and, significantly, enhance the short stem phenotype of *pny* mutants. PNY and BP antagonize the action of KNAT6 and, to a lesser extent, that of KNAT2. Restoration of bolting and flowering in *pny pnf* double mutants by removing KNAT6 highlights the opposing roles these factors play and further emphasizes the complex genetic control of stem elongation during reproduction (Lincoln *et al.*, 1994; Venglat *et al.*, 2002; Smith & Hake, 2003; Bhatt *et al.*, 2004; Andres *et al.*, 2015; Khan *et al.*, 2015).

## 4. Regenerative to senescence transition (end of flowering)

Following the reproductive phase, Arabidopsis plants eventually enter a less dynamically understood phase—senescence. This phase is equally important as it involves the end of shoot meristem activity, leading to the cessation of growth. This coordinated meristematic arrest is referred to as Global Proliferation Arrest (GPA) (Hensel *et al.*, 1994; Bleecker & Patterson, 1997; Balanzà *et al.*, 2018). Prior studies have revealed that developing seeds and fruits deliver an early signal for GPA by initiating a mechanism that annuls apical meristem activity (Lockhart & Gottschall, 1961; Hensel *et al.*, 1994). Plants with sterile flowers or plants with surgically removed fruits show a delayed GPA (Murneek, 1926; Hensel *et al.*, 1994; Martínez-Fernández *et al.*, 2020). A recent study showed that GPA is controlled in an age-dependent manner, and that auxin is the probable signal emanating from developing seeds (Ware *et al.*, 2020). This study proposes that alterations in auxin transport and signaling at the apical region of the stem is responsible for the effect of fruits on proliferation arrest (C1_Fig. 1) (Ware *et al.*, 2020; Goetz *et al.*, 2021).

Proliferation arrest has enormous ecological and economic implications but only recently molecular insight in this phenomenon has emerged. In an age-dependent manner, a gene regulatory unit consisting of *FRUITFULL* (*FUL*), *APETALA2* (*AP2*) and *WUS* transcription factors was shown to control the timing of the

end of flowering (Balanzà *et al.*, 2018). As plants age, *FUL* expression increases, resulting in reduced expression of *AP2/AP2*-like and *WUS* genes thereby initiating the proliferative arrest (Würschum *et al.*, 2005; Zhao *et al.*, 2007a; Wuest *et al.*, 2016; Balanzà *et al.*, 2018). Interestingly, a novel role for the WUS-CK regulatory feedback loop in proliferation arrest has recently been identified. Merelo et al., 2021 reported that age-dependent elevation of *FUL* leads to a decline in CK signaling, WUS protein levels, and cell division rates (Merelo *et al.*, 2021). CK's role in mediating cell proliferation and maintaining *WUS* expression implies that its down-regulation acts as a downstream regulator of the proliferation arrest (Argueso *et al.*, 2010). *FUL* may affect CK signaling through inhibiting the *KISS ME DEADLY* genes (*KMD1/2/4*), which negatively regulate type B ARRs and thus CK signaling in a process that involves *AP2* (Kim *et al.*, 2013; Balanzà *et al.*, 2018; Martínez-Fernández *et al.*, 2020). Another mechanism by which FUL modulates CK levels in SAM may involve inducing the expression of the CK catabolism genes *CKX3* and *CKX5* (Werner *et al.*, 2003; Werner & Schmülling, 2009). Combined, these results suggest that WUS plays a significant role in the regulation of the end of flowering, as mediated by multiple upstream mechanisms (C1_Fig. 1).



**5. Perspective**

*Arabidopsis thaliana*'s transition from a compact rosette to an elongated stem (bolting) demonstrates remarkable developmental plasticity. While the SAM drives this change, the precise regulatory pathways remain elusive. This adaptability depends on interactions within the meristem's RZ, influenced by cellular processes and environmental cues such as light. Our research addresses several key questions to illuminate this process:

1. **Robustness of the rosette habit**: What molecular pathways ensure the rosette's persistence during the vegetative phase, distinct from other photomorphogenic traits?
2. **Triggering bolting**: What genetic and biochemical changes occur within the SAM to initiate the transition from rosette to stem growth?
3. **ATH1's regulatory role**: How does the TALE transcription factor ATH1, expressed at the shoot apex, contribute to both rosette robustness and bolting control?

## Thesis outline

This thesis investigates the mechanisms underlying rosette initiation and robustness, as well as bolting regulation in Arabidopsis thaliana with an emphasis on ATH1's role.

**Chapter 2**: This chapter investigates the molecular mechanisms governing rosette formation in Arabidopsis. We demonstrate that the TALE transcription factor ATH1, acting downstream of multiple photoreceptors, plays a central role in establishing and maintaining the rosette habit. Our findings reveal that *ATH1* induction is essential for the inactivity of the SAM's rib zone (RZ), thereby preserving the compact rosette form. We show that ATH1 likely achieves this by suppressing photomorphogenesis inhibitors like PIFs, establishing a double negative feedback loop with PIF4 at the SAM. Additionally, we elucidate the interplay between light and sugar signals in ATH1 activation, with TOR kinase serving as a key mediator. This highlights the complex molecular network controlling rosette development in Arabidopsis.

**Chapter 3**: In this chapter, we explore the mechanisms that maintain the compact rosette habit of *Arabidopsis thaliana*. We employ a multi-faceted approach, utilizing confocal imaging, genetic analyses, RNA sequencing, and pharmacological studies. Our investigation reveals the interaction between ATH1 and the BAP/D and HLH/BHLH regulatory modules, which play a crucial role in controlling cell elongation. We demonstrate that ATH1 contributes to the robustness of the rosette by regulating these modules and limiting cell elongation within the deeper layers of the SAM. The chapter concludes by elucidating how ATH1 accomplishes this regulation. We provide evidence that ATH1 suppresses the expression of *PRE* genes locally in the shoot apex, thereby maintaining the compact structure of the rosette.

**Chapter 4**: This chapter delves into the gene regulatory network governed by ATH1 within the SAM during the transition from vegetative to reproductive phase. Utilizing confocal microscopy, we observed a decrease in ATH1 levels at the SAM, which coincided with the floral transition, RZ activation, and the onset of bolting. Subsequently, we employed an inducible ATH1-transgenic line for a transcriptomic

analysis. This analysis enabled us to identify a set of genes expressed in the SAM that could potentially be involved in bolting. These genes have been designated as Bolting-Associated genes Controlled by ATH1 (BACA). Further investigation using gene ontology underscored the significant role of hormonal pathways and cell division regulators downstream of ATH1 during bolting. Notably, ATH1 appears to specifically regulate the biosynthesis and signaling of several hormones, including gibberellin, auxin, brassinosteroid, and ethylene. This regulation influences the dramatic switch from an acaulescent (stemless) to a caulescent (stem-forming) growth pattern.



In the final chapter of this thesis, **Chapter 5**, a summary of the research is presented and discussed in relation to the current understanding within the field. The discussion in this chapter serves as the conclusion of the work and provides insight into the significance of the findings.


Col-8
ath1-3

# Chapter 2

## *Arabidopsis thaliana* rosette habit is controlled by combined light and energy signaling converging on transcriptional control of the TALE homeobox gene *ATH1*

Shahram Shokrian Hajibehzad[1,2], Savani S. Silva[1], Niels Peeters[1], Evelien Stouten[1,3], Guido Buijs[1], Sjef Smeekens[1], and Marcel Proveniers[1,2]

[1] *Molecular Plant Physiology, Department of Biology, Science4Life, Utrecht University, Padualaan 8, Utrecht, 3584 CH, The Netherlands*

[2] *Translational Plant Biology, Department of Biology, Science4Life, Utrecht University, Padualaan 8, Utrecht, 3584 CH, The Netherlands*

[3] *Plant Stress Resilience, Institute of Environmental Biology, Utrecht University, Padualaan 8, 3584 CH Utrecht, The Netherlands*

All data presented in this chapter were previously published in New Phytologist, 239(3): 1051-1067, 2023, by Shokrian Hajibehzad, Shahram, *et al*., titled "*Arabidopsis thaliana* rosette habit is controlled by combined light and energy signaling converging on transcriptional control of the TALE homeobox gene ATH1.

## Abstract

In the absence of light signals, Arabidopsis plants fail to develop the rosette habit typical for this species. Instead, plants display caulescent growth due to elongation of rosette internodes. This aspect of photomorphogenic development has been paid little attention and molecular events involved, downstream of photoreceptor signaling, remain to be identified. Using a combination of genetic and molecular approaches we show that Arabidopsis rosette habit is a photomorphogenic trait controlled by induction of *ARABIDOPSIS THALIANA HOMEOBOX GENE1* (*ATH1*) as downstream target of multiple photoreceptors. *ATH1* induction prevents rosette internode elongation by maintaining the shoot apical meristem (SAM) rib zone area inactive and requires inactivation of photomorphogenesis inhibitors, including PHYTOCHROME INTERACTING FACTOR (PIF) proteins. *ATH1* activity results in tissue-specific inhibition of *PIF* expression, establishing double negative feedback-regulation at the SAM. Light-requirement for *ATH1* expression can be overcome by high sugar availability to the SAM. Both sugar and light signals that induce *ATH1* and, subsequently, rosette habit are mediated by TOR kinase. Collectively, our data reveal a SAM-specific, double-negative ATH1-PIF feedback loop at the basis of rosette habit. Upstream, TOR kinase functions as central hub integrating light and energy signals that control this for Arabidopsis quintessential trait.

## Introduction

Plants are equipped with sophisticated mechanisms to sense the environment and to adapt their growth and development accordingly. Being photoautotrophs, plants are especially attuned to the light environment. This is well illustrated by the dramatic differences in appearance between light- and dark-grown seedlings. In Arabidopsis, dark-grown seedlings have a typical etiolated phenotype, characterized by an elongated hypocotyl, apical hook formation, closed cotyledons, and an arrested shoot apical meristem (SAM). Exposure to light results in inhibition of hypocotyl elongation, apical hook opening, opening and expansion of cotyledons, and SAM activation (Chen & Chory, 2011; Pfeiffer *et al.*, 2016; Mohammed *et al.*, 2017; Janocha *et al.*, 2022). The active SAM gives rise to the aerial plant structures. During the vegetative phase, leaf primordia arise in a spiral phyllotaxy to form a basal rosette in which internode elongation remains arrested. In the absence of light, SAM activity can be induced by exposing the SAM to metabolizable sugar, such as sucrose (Araki & Komeda, 1993; Roldán *et al.*, 1999). Both light- and sugar-mediated SAM activation involve TARGET OF RAPAMYCIN (TOR) kinase, a central component in energy sensing, such that it promotes SAM activity in favorable conditions (Pfeiffer *et al.*, 2016; Li *et al.*, 2017; Mohammed *et al.*, 2017; Janocha *et al.*, 2022). It has been proposed that light, via photoreceptor signaling through CONSTITUTIVE PHOTOMORPHOGENIC1 (COP1), plays a permissive role toward energy signaling in the SAM, possibly by controlling sugar import into the meristem (Mohammed *et al.*, 2017). This might explain why direct access of the SAM to metabolizable sugar can activate the meristem in the absence of light.

Sugar-induced dark morphogenesis in Arabidopsis follows the same developmental phases as in light-grown plants. However, contrary to light-grown plants, in sugar-induced plants stem elongation is not inhibited during vegetative development. Consequently, such plants fail to display a rosette habit and elongated internodes are present between adjacent 'rosette' leaves (Roldán *et al.*, 1999; Mohammed *et al.*, 2017). Similar loss of rosette habit has been observed in light-grown plants lacking several phytochrome (phy) and/or cryptochrome (CRY) photoreceptors (Devlin *et al.*, 1996, 1998, 1999, 2003; Whitelam & Devlin, 1997; Whitelam *et al.*, 1998; Roldán *et al.*, 1999; Mazzella *et al.*, 2000; Franklin *et al.*, 2003b; Hu *et al.*, 2013). In addition, ambient temperature has been reported to modulate light-regulation of rosette habit. At elevated ambient temperature,

phyB and CRY1 redundantly suppress elongation of vegetative internodes (Mazzella *et al.*, 2000). A compact rosette habit thus is a *bona fide* photomorphogenic trait in Arabidopsis. However, despite numerous observations and the economic importance of rosette habit in vegetable crops, this aspect of photomorphogenic development has been paid little attention and molecular events involved downstream of photoreceptor signaling remain to be identified.

In Arabidopsis, internode elongation reflects the activity of the basal part of the SAM, the rib zone (RZ). In light-grown plants, the RZ is compact and mitotically inactive during vegetative growth, resulting in the formation of a compact rosette. At floral transition, the RZ becomes activated to provide cells for rapid elongation of inflorescence internodes of the inflorescence stem (Vaughan, 1955; Sachs *et al.*, 1959a; Peterson & Yeung, 1972; Jacqmard *et al.*, 2003; Bencivenga *et al.*, 2016; Serrano-Mislata *et al.*, 2017). Previously, ectopic expression of *ARABIDOPSIS THALIANA HOMEOBOX GENE1* (*ATH1*) was shown to suppress growth of the inflorescence stem, due to inhibition of internode elongation (Cole *et al.*, 2006; Gómez-Mena & Sablowski, 2008; Rutjens *et al.*, 2009; Ejaz *et al.*, 2021). In wild-type plants, *ATH1* is expressed at the vegetative SAM. At floral transition, when stem growth is initiated, *ATH1* is rapidly downregulated. In plants lacking functional ATH1, the subapical region, where the RZ is located, is enlarged during vegetative development, suggesting that ATH1 restricts growth of this part of the SAM (Proveniers *et al.*, 2007; Gómez-Mena & Sablowski, 2008). In line with this, light-grown *ath1* mutants display slightly elongated rosette internodes, resembling those of higher-order photoreceptor mutants (Li *et al.*, 2012b; Ejaz *et al.*, 2021). *ATH1* was originally identified in a screen for light-regulated genes and its expression is induced by light during seedling de-etiolation (Quaedvlieg *et al.*, 1995). In dark-grown seedlings lacking COP1, *ATH1* transcript levels are elevated as well, suggesting that *ATH1* expression is under the control of this negative regulator of photomorphogenesis (Quaedvlieg *et al.*, 1995; Proveniers *et al.*, 2007). In line with this, *cop1* mutants exhibit a constitutive deetiolated phenotype in darkness, including formation of a compact rosette (Deng & Quail, 1992). Together with SUPPRESSOR OF PHYA-105 (SPA) proteins, COP1 forms an E3 ubiquitin ligase complex, which acts by regulating the stability of photomorphogenesis-promoting transcription factors. In addition, COP1/SPA stabilizes proteins of the PHYTOCHROME INTERACTING FACTOR (PIF) family in darkness to promote etiolation (Ponnu & Hoecker, 2021). Upon exposure to light, phyto-

chromes physically interact with PIF proteins and promote their turnover, resulting in de-etiolation (Pham *et al.*, 2018b; Ponnu & Hoecker, 2021).

Here we show that ATH1 confers rosette habit in light-grown, vegetative Arabidopsis plants by integration of signals from multiple photoreceptors. *ATH1* is induced by blue, red, and far-red light requiring both PHY- and CRY-family photoreceptors. Dark-grown wildtype plants, and higher-order photoreceptor mutants display strongly reduced levels of *ATH1* in the SAM. In both cases, increased expression of *ATH1* is sufficient to restore compact rosette internodes. Finally, we introduce a regulatory feedback loop whereby multiple PIFs and ATH1 repress each other's expression in a tissue-specific manner, contributing to the maintenance of rosette habit.



Furthermore, in the absence of light, *ATH1* can be induced by the direct availability of metabolic sugars to the SAM. We show that increasing amounts of sucrose result in a corresponding increase of *ATH1* expression and associated increased inhibition of vegetative internode elongation. Both light- and metabolic signal-mediated induction of *ATH1* at the SAM requires activation of TOR kinase.

## Results

### ATH1 restores rosette habit in dark-grown plants

When germinated and grown in darkness stem cells remain dormant in Arabidopsis (Pfeiffer *et al.*, 2016; Mohammed *et al.*, 2017). This morphogenetic arrest can be overcome by availability of sucrose to the aerial part of the plant. Sugar-induced, dark-morphogenesis of Arabidopsis plants follows the same developmental phases as light-grown plants. However, such plants fail to develop a compact rosette (C2_Fig. 1a, b). The compact rosette habit of light-grown Arabidopsis plants is conferred by ATH1 (Li *et al.*, 2012b; Ejaz *et al.*, 2021). We tested whether *ATH1* expression is sufficient for development of a compact rosette in dark-grown plants. For this, dexamethasone (Dex)-inducible *35Spro:ATH1-HBD* seedlings were grown in continuous darkness in the presence of sucrose (C2_Fig. 1a, b). Induction of nuclear expression of ATH1 resulted in strong repression of rosette internode elongation and, consequently, restoration of rosette habit, while Col-8 control plants and mock-treated *35Spro:ATH1-HBD* plants displayed elongated vegetative internodes, resulting in loss of rosette habit (C2_Fig. 1a, b). Under these condi-

tions, vegetative internodes of *ath1* mutants were slightly more elongated than those of control plants (C2_Fig. 1a, b; C2_Fig. S1), suggesting that *ATH1* might still be expressed to some extent in the absence of light, despite previous findings showing otherwise (Quaedvlieg *et al.*, 1995). Possibly, sucrose addition to induce dark morphogenesis resulted in *ATH1* induction. Indeed, in the absence of both sucrose and light *ATH1* was not expressed, whereas in the presence of one percent sucrose *ATH1* transcript levels reached up to 20% of those in light-grown plants (C2_Fig. 1c, d). Thus, sucrose can substitute for light to induce *ATH1* expression at the shoot apex. Furthermore, the relationship between sucrose and *ATH1* levels seems dose-dependent (C2_Fig. 1e; C2_Fig. S2).

Importantly, these observations suggest a close correlation between *ATH1* transcript levels at the shoot apex and the extent to which rosette internode elongation is suppressed. We, therefore, analyzed elongation of vegetative internodes in dark-grown *35Spro:ATH1-HBD* plants exposed to increasing concentrations of Dex (C2_Fig. 1f). Increased Dex-concentrations are expected to result in increased ATH1 levels in the nucleus and, hence, stronger inhibition of internode elongation. This was indeed observed, with a maximum inhibitory effect on internode elongation in plants exposed to 100 nM Dex (C2_Fig. 1f). In line with this, dark-grown Col-8 plants displayed increasing inhibition of rosette internode elongation when exposed to increasing concentrations of sucrose, with complete restoration of internode compactness characteristic for rosette habit at 2.5% sucrose (C2_Fig. 1f, g). As expected, in *ath1* mutants internode elongation remained unaffected at all sucrose concentrations tested (C2_Fig. 1g). This strongly suggests that sucrose-induced repression of rosette internode elongation in dark-grown plants is *ATH1*-dependent. These findings further show that loss of compact rosette habit, generally observed in sucrose-stimulated, dark-grown Arabidopsis plants, can be attributed to suboptimal *ATH1* expression at the shoot apex.

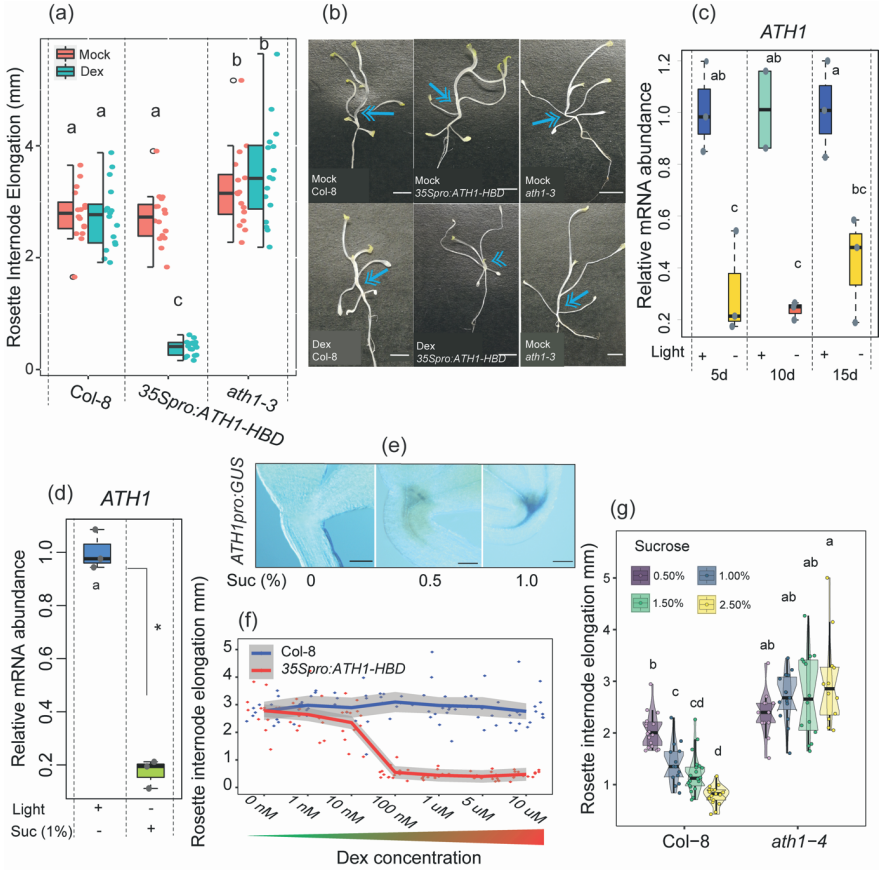


**C2_Fig. 1: *ATH1* expression is sufficient to restore compact rosette growth in dark-grown Arabidopsis plants.**

(**a**) Average rosette internode elongation in dark-grown Col-8, *ath1-3*, and *35Spro:ATH1-HBD* plants treated with 0.1% ethanol (mock) or 10 µM dexamethasone (Dex). Sucrose was added three days after the start of the experiment. (**b**) Representative three-week-old, dark-grown plants used in A. Arrows indicate elongated rosette internodes, the arrowhead indicates suppression of internode elongation. Scale bars denote 2 mm. (**c**) Relative expression of *ATH1* in Col-8 plants grown for either five, ten, or fifteen days (d) in continuous light or continuous darkness at 22°C. Sucrose was present at a one percent final concentration from the beginning of the experiment. Transcript levels were normalized to *MUSE3* (AT5G15400). The average of three biological replicates is shown. Error bars represent standard deviation of the ΔCT mean. (**d**) Relative expression of *ATH1* in seven-day-old seedlings grown in continuous light (+) or continuous darkness (-) in the presence (+) or absence (-) of one percent sucrose. Transcript levels were normalized to *GAPC2* (AT1G13440). The average of three biological replicates is shown. The asterisk (*) in the figure represents a p-value of 0.04953 for the observed difference, determined using the non-parametric Kruskal-Wallis rank sum test. (**e**) GUS-stained seven-day-old, dark-grown *ATH1pro:GUS* seedlings in the absence (0%) or presence (0.5% and 1%) of

sucrose. GUS activity is visible as a blue precipitate. Scale bars represent 0.01 mm. (**f**) Average rosette internode elongation in three-week-old dark-grown Col-8 and *35Spro:ATH1-HBD* plants treated with increasing concentrations of Dex (0 nM to 10 µM). (**g**) Average rosette internode elongation of three-week-old dark-grown Col-8 and *ath1-4* seedlings treated with increasing concentrations of sucrose (0.5 to 2.5%). In (a, c, g) differing letters signify statistically significant differences ($P < 0.05$) as determined by a one-way analysis of variance with Tukey›s honest significant difference post hoc test for (a and b), and a multiple comparison analysis using the Dunn Test with the Benjamini-Hochberg method for (g). In (a,f,g) colored dots indicate rosette internode elongation scores of individual seedlings.

## SAM morphology of sucrose-stimulated, dark-grown seedlings resembles that of light-grown *ath1* mutants

In light-grown *ath1* mutants elongation of vegetative internodes results from premature RZ activity (Roldán *et al.*, 1999; Rutjens *et al.*, 2009; Ejaz *et al.*, 2021). To confirm that the elongated internode phenotype observed in dark-grown Arabidopsis plants also results from premature activation of stem development, we compared shoot apices of light- and dark-grown Col-8 seedlings with those of light-grown *ath1-4* seedlings (C2_Fig. 2a-c). When grown for five days in continuous light, *ath1-4* mutants displayed elongated vegetative internodes, whereas those of Col-8 plants remained compact (C2_Fig. S3a, c, f). Comparing both genotypes showed the four most apical cells of a central cell file running from the L1 layer into the subapical RZ region of the SAM to be of similar length. In contrast, more basal RZ cells were significantly more elongated in *ath1-4* mutants (C2_Fig. 2a, c, f). A similar morphology was observed in dark-grown, sucrose-supplied Col-8 seedlings, where compact rosette habit is no longer maintained (C2_Fig. S3b). Compared to light-grown seedlings, basal cells were significantly more elongated in dark-grown Col-8 seedlings, resembling the elongated RZ cells of light-grown *ath1-4* mutants. The four apical cells were of similar length in light- and dark-grown Col-8 seedlings (C2_Fig. 2a-c, f).

Since ectopic expression of *ATH1* restored a compact rosette habit in dark-grown seedlings (C2_Fig. 2.1a, b; C2_Fig. S3d, e, f), we examined whether this is caused by inhibition of RZ activity. Indeed, induction of *ATH1* specifically repressed cell elongation in the basal RZ cells (C2_Fig. 2b, d-f). Taken together, these findings indicate that loss of rosette habit as a result of rosette internode elongation in the absence of light results from premature RZ activation due to significantly reduced *ATH1* expression at the shoot apex.

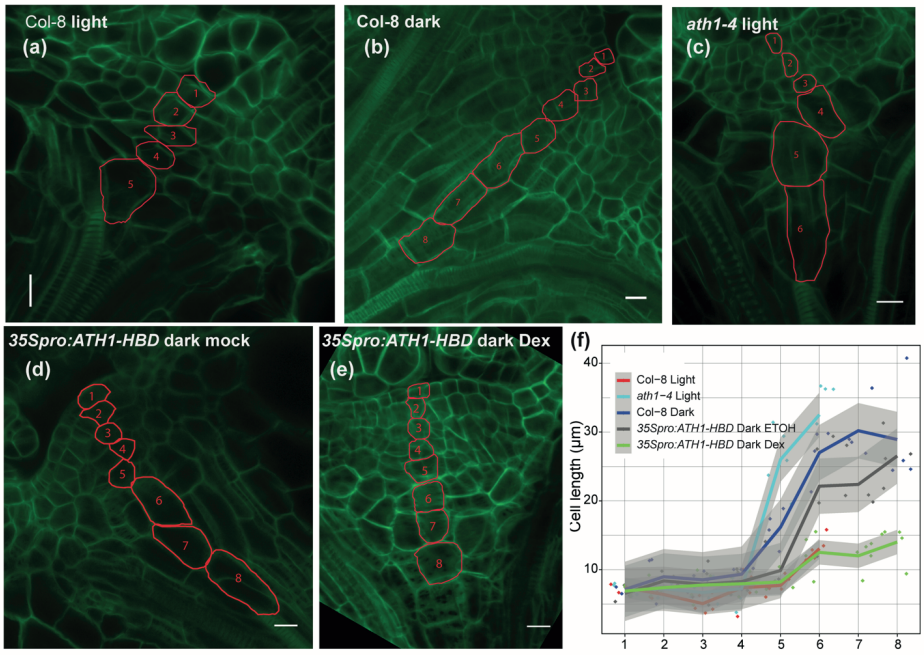


**C2_Fig. 2: Sugar-induced dark-grown seedlings display a SAM morphology similar to light-grown *ath1* mutants.**

Median longitudinal optical sections through the shoot apical meristems of (**a, b**) five-day-old Col-8, (**c**) *ath1-4*, and (**d, e**) *35Spro:ATH1-HBD* seedlings grown at 27°C in the presence (a, c) or absence (b, d, e) of light. Mock treatment (d) is 0.1% ethanol, Dex treatment (e) is 10 µM dexamethasone. Cells marked in red form a central cell file extending from the epidermis into the subapical region that forms the rib zone. Scale bars represent 10 µm. (**f**) Quantification of cell lengths as illustrated in (a-e). Individual cell lengths were measured per position in apical-basal direction. Per genotype and condition four or five individual apices were analyzed. The numbers on the x-axis correspond to the cell position as depicted in (a-e).

## ATH1 functions downstream of multiple photoreceptors to maintain a compact rosette

Rosette internode elongation can also be observed in light-grown photoreceptor mutants, such as higher order phytochrome mutants and *phyB cry1* mutants (Devlin *et al.*, 1996, 1998, 1999, 2003; Whitelam & Devlin, 1997; Whitelam *et al.*, 1998; Roldán *et al.*, 1999; Mazzella *et al.*, 2000; Franklin *et al.*, 2003b; Hu *et al.*, 2013). *ATH1* expression is strongly light-dependent (C2_Fig. 2.1c, d), raising the question of whether light-mediated expression of *ATH1* depends on these photo-

receptors. Analysis of *ATH1* mRNA levels in seedlings grown under different wavelengths of light revealed that apart from white light, monochromatic blue, red, and far-red light induce *ATH1* to significant levels, suggesting that *ATH1* is under control of multiple photoreceptors (C2_Fig. 3a). We next determined *ATH1*-promoter activity and mRNA levels in a series of phytochrome and/or cryptochrome photoreceptor mutants grown under various light quality conditions (C2_Fig. 3c; C2_Fig. S4a-d). In white light *ATH1* levels were somewhat decreased in *phyB* and *cry1* single mutants, whereas combination of both mutations significantly affected *ATH1* expression (C2_Fig. 3c; C2_Fig. S4a). Similarly, introduction of additional *phy* mutations in a *phyB* background or combination of the phytochrome chromophore biosynthesis mutant *hy1* with *cry1* and/or *cry2* mutations resulted in moderate to severe reduction in *ATH1* levels in white light, confirming that light-mediated *ATH1* expression is controlled by multiple photoreceptors (C2_Fig. 3c; C2_Fig. S4a). Repeating experiments under monochromatic light conditions revealed that red-light-mediated induction of *ATH1* is mostly the result of phyB function, in cooperation with phyD and phyE, whereas phyA is largely responsible for *ATH1* induction in far-red light (C2_Fig. 3c; C2_Fig. S4b, d). Under blue light, CRY1 and CRY2 redundantly contribute to *ATH1* activity, with CRY1 being the predominant cryptochrome under the conditions tested (C2_Fig. 3c; C2_Fig. S4c). Moreover, all photoreceptor mutants previously reported to display loss of rosette habit due to elongation of vegetative internodes, including *phyBDE* and *phyB cry1* (Devlin *et al.*, 1998; Mazzella *et al.*, 2000), had severely reduced *ATH1* levels (C2_Fig. 3c; C2_Fig. S4a-d ).

Internode elongation reflects activity of the basal part of the SAM and is controlled by ATH1. Therefore, we compared the spatial activity of the *ATH1* promoter in *phyBDE* and *phyB cry1* with that in L*er* control plants and a *phyB* mutant. High levels of GUS activity were present in the SAM and emerging leaf primordia of L*er ATH1pro:GUS* seedlings grown in white light. Corroborating our qPCR data, GUS activity was significantly reduced in *phyB cry1 ATH1pro:GUS* and *phyBDE ATH-1pro:GUS* plants, whereas in a *phyB* background GUS activity was only moderately affected (C2_Fig. 3b). The most prominent effect of reduced photoreceptor signaling on *ATH1*-promoter activity was in the SAM. In both *phyB cry1* and *phyBDE* GUS activity could hardly be detected in the SAM, including the RZ, whereas in leaf primordia a more modest reduction was observed (C2_Fig. 3b).

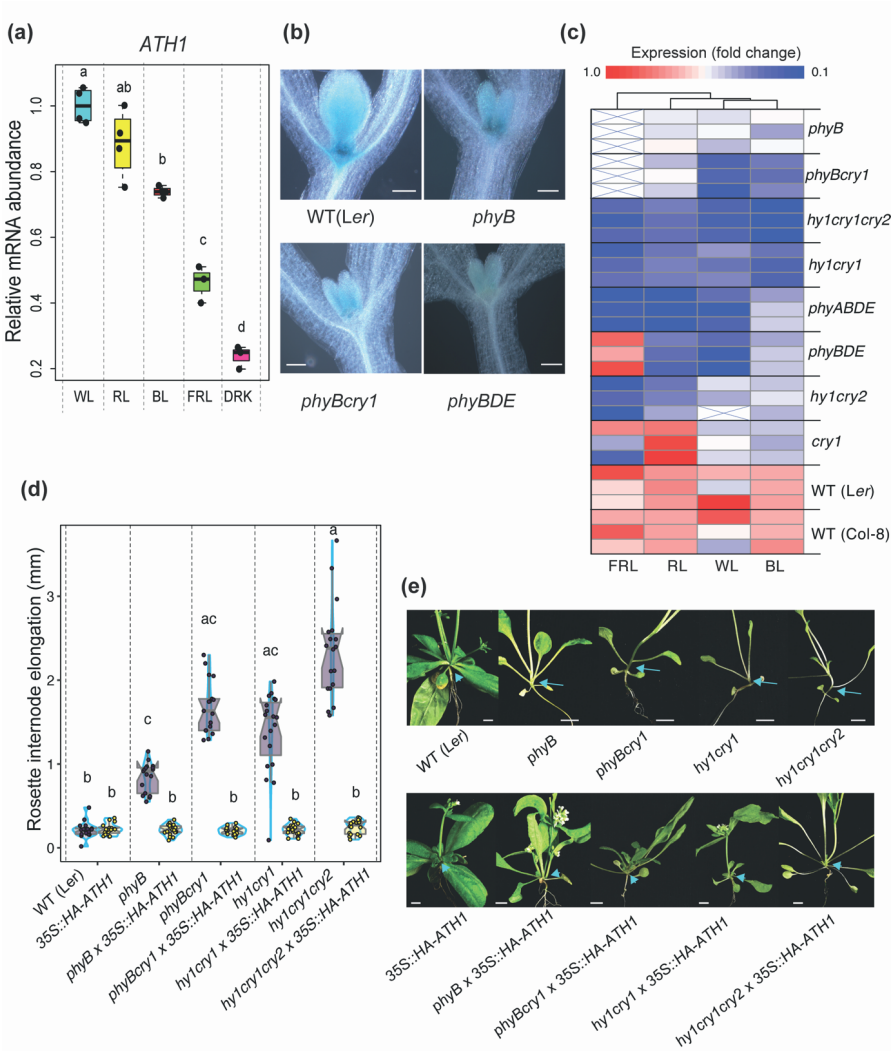


**C2_Fig. 3: Significant reduction in *ATH1* expression levels underlies loss of compact rosette habit in photoreceptor mutants.**

(**a**) Expression of *ATH1* in seven-day-old seedlings (L*er*) grown in SD white light (WL), red (RL), blue (BL), far-red light (FRL) or continuous darkness (DRK). Transcript levels were normalized to *GAPC2* (AT1G13440). Dots indicate the average values of four biological replicates per light treatment, each consisting of 40-50 seedlings. (**b**) Shoot apices of GUS-stained, seven-day-old ATH1$_{pro}$:GUS seedlings in different genetic backgrounds (Col-8, *phyB*, *phyBcry1*, and *phyBDE*). Plants were grown in white light under short-day conditions. Scale bars represent 0.01 mm. (**c**) Heat map generated from qPCR data on relative *ATH1* expression in indicated photoreceptor mutants (see **C2_Fig. S1**), when compared to wild-type control plants (L*er* and Col-8). Transcript levels were normalized to *GAPC2* (AT1G13440; BL) or *MUSE3* (AT5G15400; RL,

FRL and WL). The average of three biological replicates is shown, each replicate consisting of 40-50 seedlings. Red corresponds to high relative expression and dark blue corresponds to low relative expression. A linear fold change scale is displayed on top. (**d**) Average rosette internode elongation in WT (L*er*), *phyB*, *phyBcry1*, *hy1cry1*, and *hy1cry1cry2* in the absence or presence of a $Pro_{35S}$*:HA-ATH1* transgene. Plants were grown under LD conditions. In (a and d) different letters denote statistically significant differences between groups ($P < 0.05$) as determined by a one-way analysis of variance with Tukey's honest significant difference post hoc test (a) or a multiple comparison analysis using the Dunn Test with the Benjamini-Hochberg method (d). Colored dots indicate the average rosette internode length per individual ($n \geq 16$ individual plants per genotype). (**e**) Representative plants from (d). Arrows indicate elongated rosette internodes; arrowheads indicate complete suppression of internode elongation. Scale bars represent 5 mm.

Taken together, these findings suggest that phytochrome and cryptochrome photoreceptor families contribute to compact rosette habit in Arabidopsis through induction of *ATH1* expression in the SAM.

This was further tested by constitutively expressing *ATH1* in a number of photoreceptor mutants that display elongation of vegetative internodes when grown under standard, long-day conditions. Under these conditions, L*er* control plants never display detectable elongation of rosette internodes. In contrast, internodes of *phyB*, *phyBcry1*, *hy1cry1*, and *hy1cry1cry2* mutants were visibly elongated, and the extent to which rosette internode elongation was affected correlated with *ATH1* levels in respective mutants (C2_Fig. 3c-e; C2_Fig. S4a). As expected, constitutive expression of *ATH1* completely suppressed internode elongation in these mutants (C2_Fig. 3d, e). Thus, establishing high levels of *ATH1* is sufficient to restore internode compactness of rosette habit in higher order photoreceptor mutants.

In conclusion, compact rosette habit, quintessential for light-grown Arabidopsis plants, is imposed by *ATH1* activity in the shoot apex under control of multiple blue and red/far-red light photoreceptors.

### Light-mediated *ATH1* expression is controlled by central light-signaling components

*ATH1* was first identified as a light-regulated gene that is derepressed in dark-grown *cop1* mutants (Quaedvlieg *et al.*, 1995). COP1, in conjunction with SPA proteins, functions as a repressor of light signaling in darkness. In light, activated phytochrome and cryptochrome family members suppress the activity of the COP1/SPA complex to promote photomorphogenesis (Ponnu & Hoecker, 2021). Light-mediated *ATH1* expression involves both phytochrome and cryptochrome

family members. Since COP1 is a downstream signaling component of these photoreceptor families, we analyzed the role of COP1 in the regulation of *ATH1* expression and compactness of vegetative internodes. First, we compared *ATH1* expression levels between dark-grown Col-8 and *cop1-4* seedlings, with and without added sucrose (C2_Fig. 4a). In line with Quaedvlieg et al. (1995), in dark-grown *cop1-4* mutants, carrying a mild loss-of-function allele of *COP1*, *ATH1* expression was clearly derepressed. Already in the absence of sucrose, *ATH1* accumulated to higher levels than observed in sucrose-supplied Col-8 plants. In the presence of sucrose, *cop1-4 ATH1* transcript levels increased even further (C2_Fig. 4a), indicating that light and sucrose signaling contribute, at least partially, independently to induce *ATH1* expression.



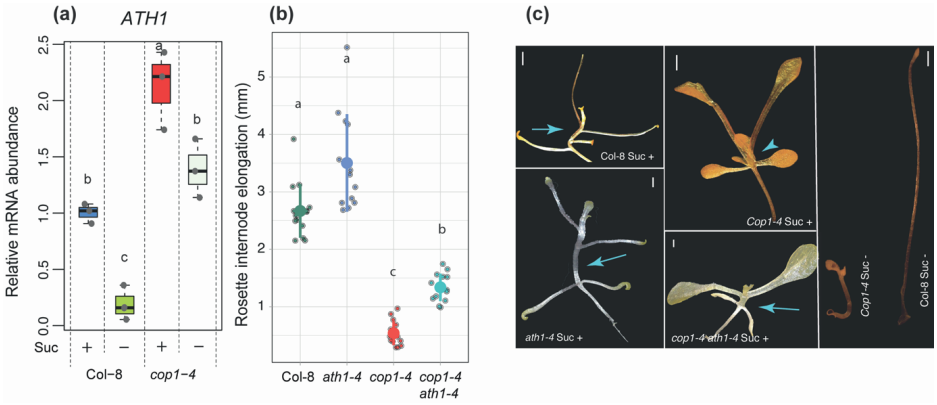


**C2_Fig. 4: Derepression of *ATH1* contributes to a compact rosette habit in dark-grown *cop1* mutants.**

(**a**) Relative mRNA abundance of *ATH1* in shoot apices of two-week-old dark-grown seedlings. The average of three biological replicates is shown. At least 20 shoot apices were used for each biological replicate. (**b**) Average rosette internode lengths of 3-week-old Col-8, *ath1-4*, *cop1-4,* and *cop-1 ath1-4* plants (n ≥13) grown in continuous darkness for three weeks at 22°C, in the presence of one percent sucrose. In (a and b) different letters denote statistically significant differences between groups ($P < 0.05$) as determined by a one-way analysis of variance with Tukey's honest significant difference post hoc test for (a) and a multiple comparison analysis using the Dunn Test with the Benjamini-Hochberg method for (b). (**c**) Representative plants from (b). Arrows indicate elongated rosette internodes, arrowheads indicate complete suppression of internode elongation. Scale bars represent 0.5 mm. Sucrose (Suc +) or sorbitol (Suc -), both to a final concentration of one percent, were added three days after start of the experiment (a, c).

Accordingly, vegetative internodes of sucrose-supplied, dark-grown *cop1-4* mutants did not elongate, contrasting to those of Col-8 plants (C2_Fig. 4b, c). A compact growth habit in darkness is lost in *cop1-4 ath1-4* double mutants, indicating that this phenotype requires ATH1 (Fig 4c). However, compared to *ath1-4*, internode elongation in *cop1 ath1* double mutants is still much reduced, suggesting the involvement of other loci apart from *ATH1* (C2_Fig. 4b, c).

Like COP1, PIFs also function as downstream components in both phytochrome and cryptochrome light signaling (Ma *et al.*, 2016; Pedmale *et al.*, 2016; Pham *et al.*, 2018a). PIF proteins function as partially redundant, negative regulators of light responses to maintain skotomorphogenesis in dark-grown seedlings. Upon exposure to light, phytochromes promote the turnover of PIFs, whereas photoactivated CRY1 interacts with PIF4, resulting in suppression of PIF4 transcriptional activity (Ma *et al.*, 2016). As a consequence, plants switch from skotomorphogenesis to photomorphogenesis. In line with this, quadruple *pif1pif3pif4pif5* (*pifq*) mutants display a constitutively photomorphogenic phenotype in darkness (Leivar *et al.*, 2009). In addition, PIFs can directly interact with COP1, thereby enhancing substrate recognition and ubiquitination activity of the COP1 E3 ligase complex (Xu *et al.*, 2014; Kathare *et al.*, 2020). Therefore, we tested whether PIF proteins might function upstream of *ATH1* in the regulation of compact rosette habit. To this end, we analyzed rosette internode compactness in a series of sucrose-supplied, dark-grown single, double, triple, and quadruple *pif* mutant combinations. In *pifq* mutants complete repression of rosette internode elongation was observed, resulting in the formation of a compact rosette in darkness (C2_Fig. 5a). None of the double or triple mutants tested were as compact as the quadruple *pifq* mutant, whereas of the single mutants tested, only *pif4* displayed a significant reduction in rosette internode length when compared to control plants (C2_Fig. 5a). This indicates that PIF1, PIF3, PIF4, and PIF5 redundantly contribute to rosette internode elongation in etiolated plants. Of these, PIF4 contributes the most, as can be inferred from its mutant phenotype and the significant inhibition of internode elongation in higher order mutants carrying a *pif4* allele, while inhibition of internode elongation is absent in *pif1pif3* and only subtly enhanced by *pif5* mutation in *pif4pif5* and *pif3pif4pif5* (C2_Fig. 5a).

Next, we compared *ATH1* transcript levels between shoot apices of dark-grown Col-8, *pif4* and *pifq* plants (C2_Fig. 5b). In line with the observed rosette internode lengths, a significant increase in *ATH1* was seen in both *pif4* (1.7x) and *pifq* (3x) mu-

tants when compared to control plants. To examine whether ATH1 is responsible for the inhibition of rosette internode elongation in dark-grown *pifq* mutants, we combined *ath1-3* and *pifq* mutations. Surprisingly, vegetative internodes of sucrose-supplied, dark-grown *pifq ath1* plants were only mildly elongated, resulting in partial loss of a compact rosette habit. Compared to *ath1* plants, *pifq ath1* internodes were on average 70% shorter (C2_Fig. 5c). This might suggest that PIFs control rosette internode elongation mostly independent of ATH1. Alternatively, the relationship between PIFs and ATH1 could be more complex. ATH1-PIF feedback regulation would explain for the *pifq ath1* internode phenotype. Recently, *PIF4* was identified as binding target of ATH1, but no significant differences in *PIF4* expression could be detected between *ath1* and WT plants on whole-seedling basis (Ejaz *et al.*, 2021). This does not rule out a tissue-specific, regulatory feedback loop between ATH1 and PIFs. To explore the presence of such regulatory interaction between ATH1 and PIFs, we quantified *PIF* transcript levels in shoot apices of genotypes with altered *ATH1* expression (C2_Fig. 5d, e). ATH1 is expected to have an inhibitory effect on *PIF* expression and in sucrose-supplied, dark-grown plants *ATH1* levels are low (C2_Fig. 2.1c, d). Therefore, *35Spro:ATH1-HBD* plants were used to examine the effect of ATH1 on *PIF1*, *PIF3*, *PIF4* and *PIF5* mRNA levels in dark conditions (C2_Fig. 5d). In light-grown vegetative plants, *ATH1* levels at the shoot apex are relatively high. Therefore, in light conditions the effect of ATH1 on these *PIFs* was analyzed using *ath1-3* plants (C2_Fig. 5e). In both conditions, a clear effect of ATH1 on *PIF* expression was observed. In dark-grown plants, induction of ATH1 resulted in significant down-regulation of *PIF1*, *PIF3* and *PIF4*, and, to a lesser extent, *PIF5* (C2_Fig. 5d). In light-grown plants, *PIF1*, *PIF3*, *PIF4*, and *PIF5* levels were significantly up-regulated in the absence of *ATH1* (C2_Fig. 5e). Thus, ATH1 acts as a negative regulator of *PIF1*, *PIF3*, *PIF4*, and *PIF5* in the shoot apex. Together, our data support the presence of a double-negative transcriptional feedback loop between ATH1 and PIF family members. Such ATH1-PIF interdependence for suppression of rosette internode elongation explains the observed incomplete loss of rosette habit compactness in *cop1-4 ath1-4* mutants (C2_Fig. 4b, c), since PIF1, PIF3, PIF4 and PIF5 are required for dark-mediated rosette internode elongation in the absence of ATH1 (C2_Fig. 5c) and these PIFs are degraded in darkness in the presence of a *cop1-4* mutation (Pham *et al.*, 2018c,b).

Overall our data show that loss of internode compactness and thereby loss of rosette habit in dark-grown Arabidopsis plants is part of a skotomorphogenesis program, achieved through active repression of *ATH1*, mediated by COP1 and PIF proteins.

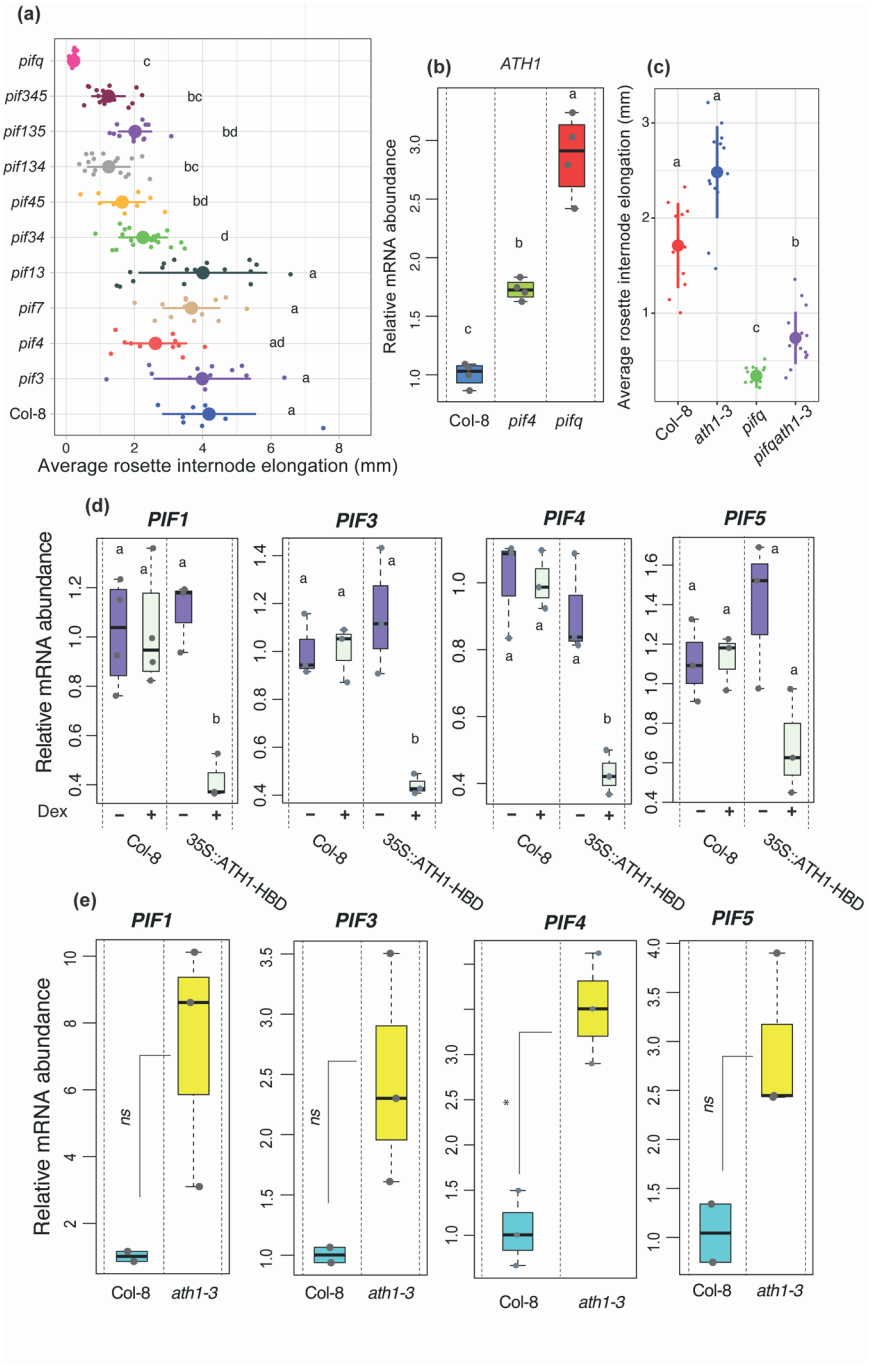
(a)
pifq
pif345
pif135
pif134
pif45
pif34
pif13
pif7
pif4
pif3
Col-8
Average rosette internode elongation (mm)
(b)
ATH1
Relative mRNA abundance
Col-8
pif4
pifq
(c)
Average rosette internode elongation (mm)
Col-8
ath1-3
pifq
pifqath1-3
(d)
PIF1
PIF3
PIF4
PIF5
Relative mRNA abundance
Dex
Col-8
35S::ATH1-HBD
(e)
PIF1
PIF3
PIF4
PIF5
Relative mRNA abundance
ns
*
Col-8
ath1-3

**C2_Fig. 5: A double-negative feedback loop between ATH1 and PIFs is required for initiation and maintenance of rosette growth habit.**

(**a**) Average internode lengths of 3-week-old Col-8, *pif3*, *pif4*, *pif7*, *pif1pif3*, *pif3pif4*, *pif4pif5*, *pif1pif3pif4*, *pif1pif3pif5*, *pif3pif4pif5*, and *pifq* (*pif1pif3pif4pif5*) plants grown in continuous darkness at 22°C. Sucrose was added to the medium to a final concentration of one percent three days after the start of the experiment. Colored dots indicate average rosette internode elongation scores of individual seedlings (n ≥9). (**b**) Relative mRNA abundance of *ATH1* in SAM-enriched tissue of 14-day-old, dark-grown Col-8, *pif4*, and *pifq* seedlings (n≥20 per biological replicate; four biological replicates). Transcript levels were normalized to *GAPC2* (AT1G13440). Sucrose was present at a one percent final concentration from the start of the experiment. (**c**) Average internode lengths of three-week-old Col-8, *pif4*, *pifq*, and *pifq ath1-3* plants grown in continuous darkness at 22°C. Sucrose was added to the medium to a final concentration of one percent three days after the start of the experiment. Colored dots indicate average rosette internode elongation scores of individual seedlings (n ≥11). (**d, e**) Relative mRNA abundance of indicated *PIF* genes in SAM-enriched tissue of 14-day-old, dark-grown Col-8 and *35Spro:ATH1-HBD* (n ≥3) (d), or 39-day-old, light-grown (SD conditions) Col-8 and *ath1-3* seedlings (n ≥2) (e). For (d) seedlings were treated with a mock (0.1% ethanol, Dex -) or 10 μM dexamethasone (Dex +) at day three, and in total, 30-40 shoot apices were used for each biological replicate. For light-grown plants (e), three shoot apices were used per biological replicate. Transcript levels were normalized to *GAPC2* (AT1G13440). Seedlings were treated with a mock (0.1% ethanol, Dex -) or 10 μM dexamethasone (Dex +) (d). In (a-d) different letters denote statistically significant differences between groups ($P < 0.05$) as determined by a one-way analysis of variance with Tukey's honest significant difference post hoc test for (b and d) and a multiple comparison analysis using the Dunn Test with the Benjamini-Hochberg method for (a and c). In (c) the Kruskal-Wallis test utilized to distinguish significant differences between groups, with results of p values depicted as "ns" for non-significant and an asterisk (*) for a p-value of 0.04953.

## Photosynthesis-derived sugars are no prerequisite for light-induced *ATH1* expression

*ATH1* expression in the shoot apex can be induced by light and sucrose (C2_Fig. 2.1d, e; C2_Fig. 3a). Since light acts as both a developmental signal, and an energy source through photosynthesis, we investigated the exact role of light in induction of *ATH1* expression. Therefore, we examined *ATH1*-promoter activity in plants where photosynthesis was inhibited. To this end, *ATH1pro:GUS* seedlings were grown in darkness for five days, without sucrose to deplete plant metabolizable sugar. Five hours before light treatment, plants were put in a $CO_2$-deficient environment, after which plants were grown for two days in continuous light (C2_Fig. 6a). $CO_2$ removal inhibits photosynthetic carbon assimilation and, thereby, accumulation of sugars. Compared to mock treatment, *ATH1*-promoter activity was

decreased, but GUS staining was still clearly visible (C2_Fig. 6b; C2_Fig. S5a). Similarly, chemical inhibition of photosynthesis by adding norflurazon or lincomycin resulted in slightly reduced *ATH1* expression (C2_Fig. S5a; C2_Fig. S6). This indicates that *ATH1* is affected by light acting as both a developmental trigger and an energy source through photosynthesis. It further shows that photosynthesis-derived sucrose contributes to, but is not a prerequisite for light-induced *ATH1* expression. This is in line with the observation that *ATH1* is derepressed in dark-grown *cop1* seedlings even in the absence of sucrose (C2_Fig. 4a).

Sugars function as energy resource and as signaling molecules (Li & Sheen, 2016). To distinguish between these functions in the induction of *ATH1*, *ATH1* expression and *ATH1*-promoter activity were determined in dark-grown Col-8 plants supplied with either sorbitol, sucrose, glucose, fructose, or palatinose (C2_Fig. 6c; C2_Fig. S5c).

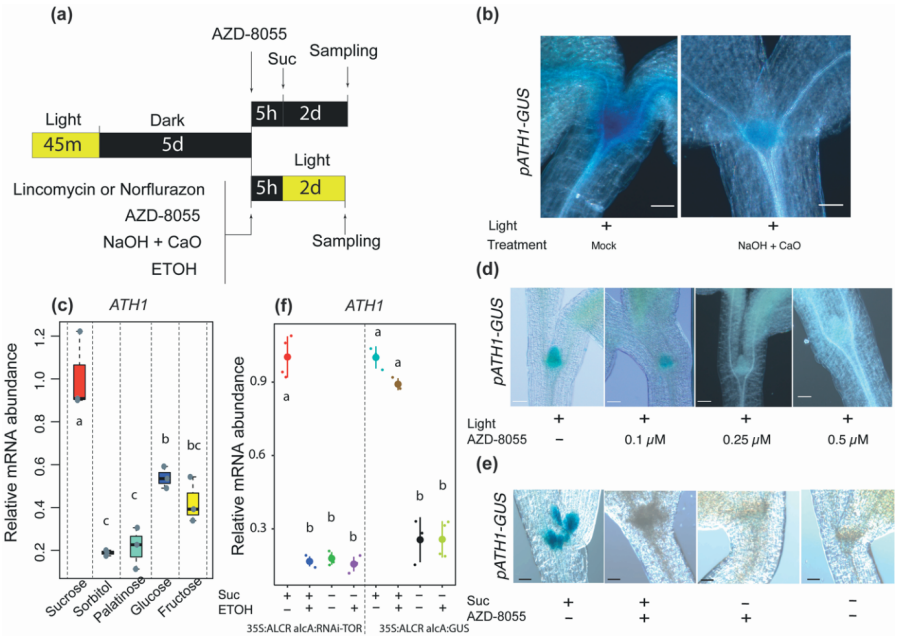


**C2_Fig. 6: *ATH1* expression is independently regulated by light and sucrose.**

(**a**) Schematic representation of the experimental setup. $ATH1_{pro}$*:GUS* seeds were light-treated for 45 minutes to stimulate germination, before growth in continuous darkness for five days. AZD-8055, lincomycin, norflurazon were then added or $CO_2$ was removed (NaOH + CaO) and seedings were grown for an additional five hours in darkness before switching to *ATH1*-inducing conditions (continuous light or continued growth in darkness in the presence of sucrose (Suc))

for two more days. (**b**) Shoot apices of GUS-stained *ATH1*$_{pro}$*:GUS* seedlings grown in $CO_2$-free air (NaOH + CaO), according to the scheme depicted in (a). Mock-treatment was without NaOH + CaO. Scale bars represent 0.05 mm. (**c**) Relative expression of *ATH1* in seven-day-old, dark-grown seedlings, grown in the presence of either sucrose, glucose, fructose, palatinose, or sorbitol, all at a final concentration of one percent in the growth medium. Sugars were added at the start of the experiment. Transcript levels were normalized to *MUSE3* (At5g15400). The average of three biological replicates is shown. At least 30 seedlings were used for each biological replicate. (**d, e**) Shoot apices of GUS-stained *ATH1*$_{pro}$*:GUS* seedlings treated with the TOR kinase inhibitor AZD-8055 before switching to ATH1-inducing conditions (continuous light (d) or darkness in the presence of one percent sucrose (e)) according to the scheme depicted in (a). Scale bars represent 0.01 mm. (**f**) Relative expression of *ATH1* in seven-day-old, dark-grown *35S::ALCR alcA:RNAi-TOR* and *35S:ALCR alcA:GUS* (control line) seedlings in the presence or absence of ethanol (ETOH; 0.1%) and/or sucrose (Suc; 1%), as depicted in (a). ETOH was added after five days of growth in darkness. After an additional five hours in darkness sucrose was added and plants were sampled after two more days in darkness. Transcript levels were normalized to *GAPC2* (AT1G13440). The average of three biological replicates is shown. At least 30 seedlings were used for each biological replicate. In (c and f) different letters denote statistically significant differences between groups ($P < 0.05$) as determined by 1-way ANOVA followed by Tukey's post hoc test.



Glucose, fructose and sucrose are metabolizable sugars also known to function as signaling molecules (Rabot *et al.*, 2012). Sorbitol and palatinose are non-metabolizable sugars, but where palatinose can function as signaling molecule, sorbitol is neither metabolized nor signaling molecule (Ramon *et al.*, 2008). Neither sorbitol nor palatinose had a significant effect on *ATH1* expression, whereas a clear increase in *ATH1* could be observed when either sucrose, glucose or fructose was present (C2_Fig. 6c). This strongly suggests that sugars as energy source induce *ATH1* expression.

**Sucrose and light independently regulate *ATH1* expression via TOR kinase**

TOR kinase, a critical sensor of resource availability, is required for the activation of shoot and root apical meristems (Xiong *et al.*, 2013; Pfeiffer *et al.*, 2016; Li *et al.*, 2017). It integrates, among others, energy and environmental cues, including light signals to direct growth and development. The fundamental role of TOR kinase downstream of light and energy signals, led us to investigate whether TOR activity is needed for sugar-dependent, dark morphogenesis in general and *ATH1* induction in particular. Employing a similar experimental setup as mentioned in the previous section (C2_Fig. 6a), the effect of the TOR kinase inhibitor AZD-8055 (Montané & Menand, 2013; Dong *et al.*, 2015) on light- and sucrose-induced

*ATH1*-promoter activity was studied. Light-mediated induction was efficiently suppressed by AZD-8055, resulting in complete inhibition of promoter activity at a concentration 0.5 μM (C2_Fig. 6d). Similarly, AZD-8055 fully inhibited the positive effect of sucrose on *ATH1* (C2_Fig. 6e; C2_Fig. S5b, S7). In line with these findings, conditional silencing of *AtTOR* in *35S:ALCR alcA:RNAi-TOR* seedlings (Deprost *et al.*, 2007) led to complete inhibition of sucrose-mediated induction of *ATH1* (C2_Fig. 6f). When applied for an extended period, in the presence of sucrose, AZD-8055 inhibited dark-morphogenesis in a dose-dependent manner (C2_Fig. S8a, b), indicating that, next to *ATH1* induction, TOR activity is necessary for sucrose-dependent, dark morphogenesis in general.

TOR kinase has been reported to contribute to seedling de-etiolation and COP1 represses TOR activity during skotomorphogenesis (Chen *et al.*, 2018). We therefore tested whether COP1-mediated regulation of *ATH1* is TOR-dependent. This is indeed the case, as in the presence of AZD-8055 *ATH1* is no longer derepressed in dark-grown *cop1-4* plants (C2_Fig. S9).

TOR kinase, thus, integrates light and sucrose signals leading to activation of *ATH1* gene expression at the shoot apex. Upstream of TOR kinase, a PHY-COP1 regulatory pathway functions as negative regulator of TOR activity. In darkness, COP1 inhibits TOR, resulting in repression of *ATH1*. As a consequence, in dark-grown plants a compact rosette habit is lost due to activation of stem development. In light, COP1 activity is inhibited allowing for TOR kinase to induce *ATH1* as part of the de-etiolation process, resulting in a compact rosette characteristic for *A. thaliana* (C2_Fig. 7). TOR was recently reported to control cytokinin homeostasis at the SAM by translational repression of several mRNAs encoding cytokinin catabolic enzymes, including the RZ-expressed CYTOKININ OXIDASE/DEHYDROGENASE5 (CKX5) (Janocha *et al.*, 2022). Adding cytokinin to dark-grown Arabidopsis seedlings results in strong induction of *ATH1*-promoter activity, even in the absence of metabolizable sugar (C2_Fig. S10), suggesting that TOR-mediated regulation of *ATH1* might be indirect through cytokinin.

## Discussion

In plants most of the adult body is formed post-embryonically by the continuous activity of the shoot and root apical meristems. At the completion of embryogenesis these meristems are quiescent, but become reactivated after germination. In Arabidopsis, light is crucial for SAM reactivation (López-Juez *et al.*, 2008; Pfeiffer *et al.*, 2016; Mohammed *et al.*, 2017). A direct outcome of this is the production of leaves. In rosette plants, like Arabidopsis, these leaves give rise to a basal rosette: a whorl of leaves without elongation between successive nodes. The rosette habit is widespread amongst flowering plants and provides several advantages compared to taller, less compact plants, such as protection from (a)biotic stresses (Schaffer & Schaffer, 1979; Bello *et al.*, 2005; Larcher *et al.*, 2010; Thomson *et al.*, 2011; Fujita & Koda, 2015). In Arabidopsis, light requirement for SAM activation can be overcome by availability of metabolizable sugars to the meristem (Araki & Komeda, 1993; Roldán *et al.*, 1999). However, under such conditions plants fail to establish a compact rosette. Instead, they display a caulescent growth habit due to elongation of rosette internodes. Here we show that this dramatic change in growth habit in the absence of light is caused by premature RZ activation due to insufficient expression of the light-induced *ATH1* gene at the SAM. Our observations confirm a fundamental role for ATH1 in Arabidopsis rosette habit and support a role for TOR kinase as central hub for integration of energy and light signaling in controlling cell differentiation and organ initiation at the SAM.

Previously, activation of the SAM following germination, via induction of *WUSCHEL* (*WUS*), and subsequent initiation of leaf primordia were shown to be synergistically controlled by light-signaling pathways and photosynthesis-derived sugars, both conveyed by TOR kinase (Pfeiffer *et al.*, 2016; Li *et al.*, 2017). In line with this, we show that TOR activity is necessary for sugar-induced, dark morphogenesis in Arabidopsis. Furthermore, we show that *ATH1* expression at the SAM, required to inhibit RZ activation during vegetative development, is additively induced by sugar and light-signaling and that TOR kinase activity is essential for both. Thus, TOR kinase not only integrates light and energy signals to activate the central stem cell population and subsequent differentiation processes at the meristem periphery, but also to repress differentiation processes at the basal part of the meristem by inhibiting RZ activity. Potentially, induction of *ATH1* through light and energy signals might result from SAM activation.

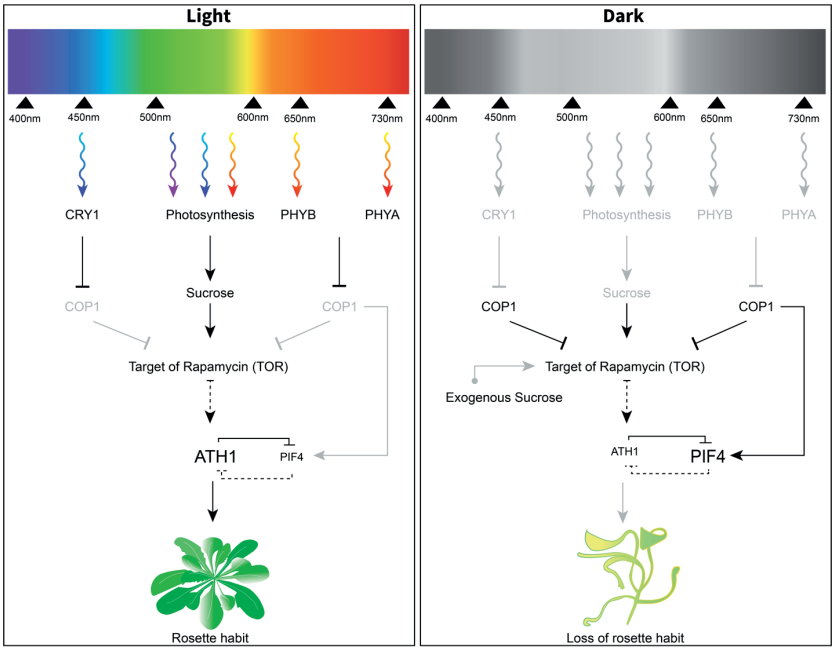


**C2_Fig. 7: Light and sucrose signaling pathways converge at TOR kinase to control *ATH1* expression and subsequent rosette growth habit in *Arabidopsis thaliana*.**

(**left panel**) Expression of *ATH1* is mediated by the activity of TOR kinase in response to both sugar and light. In response to light, photoreceptor signaling inhibits the activity of a COP1-containing protein complex that acts as a central repressor of light signaling in darkness. This releases the inhibitory effect of COP1 on TOR kinase. Activation of TOR kinase then leads to both activation of the SAM and induction of *ATH1* expression in the SAM. As a consequence of *ATH1* expression in the SAM, *PIF* gene expression, including *PIF4*, is locally inhibited. This contributes to inhibition of rib zone activity and, consequently, suppression of rosette internode elongation with the for Arabidopsis typical rosette growth habit as a result. As TOR kinase is a major regulator of mRNA translation, the effect on *ATH1* expression is most likely indirect (dotted arrow; see Discussion). (**right panel**) In the absence of light, the COP1-complex is stabilized and inhibits TOR kinase activity and subsequent SAM activation. In addition, the COP1-complex stabilizes PIF proteins in darkness to positively regulate skotomorphogenesis. As a combined effect, *ATH1* is not expressed under these conditions. As discussed, the PIF inhibitory effect on *ATH1* expression, including that of PIF4, is most likely indirect (dotted inhibitory arrow). Sucrose-availability to the SAM can substitute for light both in the case of SAM activation and for *ATH1* induction. Although both processes are mediated through TOR kinase, sucrose levels sufficient to activate the SAM only result in weak expression of *ATH1*, probably as the result of still active COP1-PIF signaling. Resulting ATH1 levels are insufficient to suppress rib zone activity. As a consequence, in most circumstances sugar-induced dark-grown seedlings display a caulescent growth habit due to premature rib zone activation resulting in elongation of vegetative internodes.

This appears unlikely, as in the absence of sucrose the SAM of dark-grown *cop1* mutants remains dormant, while *ATH1* is expressed to relatively high levels. In addition, SAM activation and *ATH1* induction responses differ in their sensitivity to sucrose. Concentrations adequate to activate the SAM and initiate organogenesis, fail to induce significant levels of *ATH1*.

How TOR kinase controls *ATH1*-promoter activity is currently unknown. TOR is a major regulator of translation (Schepetilnikov & Ryabova, 2017). Active TOR promotes translation of mRNAs harboring uORFs within their leaders, by triggering reinitiation after uORF translation (Schepetilnikov *et al.*, 2011, 2013). *ATH1* carries a 1279-nt leader sequence, containing seven AUG-containing uORFs. However, for ATH1 we do not expect TOR-mediated translational control to be a major type of regulation. First, none of the seven *ATH1* uORFs seems to be translated (Hu *et al.*, 2016). Second, a close correlation can be observed between *GUS* mRNA levels and GUS activity in our *ATH1pro:GUS* line, a translational fusion that contains the entire *ATH1* leader sequence (compare C2_Fig. 2.1e and C2_Fig. S8; C2_Fig. S7). Together, this argues against strong uORF-mediated translational control of ATH1. Therefore, the effect of TOR kinase on *ATH1* is, most likely, indirect, possibly through TOR-mediated regulation of cytokinin homeostasis, as was previously reported for *WUS* (Janocha *et al.*, 2022).

In the absence of light, *ATH1* is repressed by negative regulators of photomorphogenesis, including COP1, fitting with previous finding that in darkness COP1 represses TOR kinase (Chen *et al.*, 2018). Here we report that, in darkness, sucrose can substitute for light to induce *ATH1* and this also requires TOR kinase (C2_Fig. 7). Most likely, sucrose affects TOR kinase activity independently of COP1 since sucrose-mediated induction of *ATH1* can still be observed in a *cop1* background. Light signaling inactivates COP1, resulting in induction of auxin biosynthesis. Auxin then activates the small Rho-like GTPase ROP2, which in turn activates TOR (Cai *et al.*, 2017; Li *et al.*, 2017; Schepetilnikov *et al.*, 2017). Constitutive expression of activated ROP2 stimulates TOR in the shoot apex and is sufficient to promote organogenesis in the absence of light (Li *et al.*, 2017). Sugars are known to trigger the accumulation of auxin, along with its biosynthetic precursors and such sucrose-induced auxin might activate TOR kinase in darkness, in the presence of COP1 (Chourey *et al.*, 2010; LeClere *et al.*, 2010; Sairanen *et al.*, 2012; Mohammed *et al.*, 2017). Worth mentioning in this respect is that the

same PIF proteins identified here as repressors of *ATH1*, repress sugar-induced auxin biosynthesis (Sairanen *et al.*, 2012).

Similar to the peripheral zone, where lateral organs are generated, the RZ, where differentiation into stem tissue occurs, is continuously replenished by a population of dividing stem cells in the central zone of the SAM. An active central stem cell population is therefore a prerequisite for RZ activity. When TOR kinase is inactive, quiescence of the shoot stem cell population (C2_Fig. S8) prevents the RZ being activated, even though ATH1-mediated inhibition of RZ activity is absent (C2_Fig. S7). In light-grown or sucrose-supplemented dark-grown Arabidopsis seedlings, activated TOR kinase allows for stem cell activation. However, subsequent activation of the RZ is prevented via TOR-kinase-mediated ATH1 induction. In the presence of light, *ATH1* expression is induced in a functionally redundant manner by multiple photoreceptors operating in response to broad wavelengths of light (C2_Fig. 7). This ensures presence of *ATH1* in the SAM under all light conditions, inhibiting RZ activity, with the characteristic compact rosette of Arabidopsis as result. In line with this, loss of rosette compactness has been observed in light-grown Arabidopsis plants lacking multiple functional phytochrome and/or cryptochrome photoreceptors. Control of vegetative internode elongation in response to changes in light quality and/or ambient temperature was shown to be mediated by concerted action of phyA, phyB, phyD, phyE, and/or CRY1, all of which we identified as having a role in light-mediated induction of *ATH1* (Devlin *et al.*, 1996, 1998, 1999, 2003; Whitelam & Devlin, 1997; Whitelam *et al.*, 1998; Mazzella *et al.*, 2000; Franklin *et al.*, 2003b; Kanyuka *et al.*, 2003; Strasser *et al.*, 2010; Zhang *et al.*, 2017). Often not appreciated in literature, compact rosette habit is thus a genuine photomorphogenic trait in Arabidopsis. Remarkably, rosette internode compactness is a non-plastic trait, unlike other photoreceptor-driven developmental responses in Arabidopsis, such as elongation of hypocotyl, petiole, and inflorescence stem. Compact rosette growth is not affected in wildtype plants even under light quality and/or temperature regimes that cause rapid elongation of aerial plant organs. Plasticity of growth and development is often considered adaptive, enabling sessile plants to adjust rapidly to a changing environment (Schlichting, 1986; Schlichting & Levin, 1986). However, as mentioned, rosette growth provides several advantages compared to caulescent growth. Loss of a compact rosette in response to environmental cues, therefore, might be detrimental to plant fitness and viability. Compact rosette habit is not constitutively

expressed in all rosette species (our unpublished observations) and this trait, as a result of selection, may have become fixed in Arabidopsis through genetic assimilation (Ehrenreich & Pfennig, 2016). Important contributors to genetic assimilation are genetic variants that alter gene regulation. Plausible ways in which gene regulation might facilitate loss of phenotypic plasticity are i) decoupling of the regulation of genes that control a plastic trait from environmental cues or ii) the evolution of additional regulatory pathways that makes their expression insensitive to the environment (Ehrenreich & Pfennig, 2016). The latter might be the case for Arabidopsis rosette internodes, given that *ATH1* expression is induced in response to broad wavelengths involving multiple photoreceptors. Moreover, it has been proposed that ATH1 controls internode elongation by antagonizing a large number of genes that promote internode growth, mostly independent of each other (Ejaz *et al.*, 2021). This assumption fits with the observation that *pifq* not completely reduced internode elongation in *ath1-3*. Such multitarget control by ATH1 of genes that affect internode elongation would further contribute to the robustness of compact rosette habit in Arabidopsis. Therefore, it is of interest to investigate whether ATH1 has a similar role in other rosette species and, if so, whether differences in plasticity of rosette compactness can be linked to differences in light-signaling control of *ATH1* and/or decoupling internode elongation genes from ATH1 regulation.



In this study, we identified *PIF1*, *PIF3*, *PIF4*, and *PIF5* as transcriptional targets of ATH1. *PIF4* and PIF signaling components were previously identified as binding target of ATH1 (Ejaz *et al.*, 2021). Therefore, ATH1 might affect the expression of these four *PIF* genes through direct transcriptional repression. Our finding that PIF4, and at least one of the other PIF proteins, PIF1, PIF3, or PIF5, in turn function as negative regulators of *ATH1* suggest the presence of a double-negative feedback loop between ATH1 and PIF family members (C2_Fig. 7). Whether these PIFs also directly target *ATH1* is currently unknown, but, given the fact that the rib-zone expressed cytokinin catabolism gene *CKX5* is a direct transcriptional target of these PIFs (Hornitschek *et al.*, 2012; Zhang *et al.*, 2013; Pfeiffer *et al.*, 2016) and *ATH1*-promoter activity is strongly induced by cytokinin, we hypothesize that the PIF inhibitory effect on *ATH1* is indirect, via local reduction in cytokinin levels.

Signaling systems that contain double-negative feedback loops can, in principle, convert graded inputs into switch-like, irreversible responses (Ferrell, 2002). Such a genetic toggle switch is a bistable dynamical system, possessing two

stable equilibria, each associated to a fully expressed protein. ATH1 has a fundamental role in maintaining internode compactness in Arabidopsis during vegetative growth. In light-grown plants, *ATH1* is expressed throughout the shoot meristem, including the subapical region where it represses stem growth. Plant switching to reproductive growth rapidly downregulate *ATH1* at the shoot meristem, marking the onset of bolting and emergence of an elongated inflorescence (Proveniers *et al.*, 2007; Gómez-Mena & Sablowski, 2008; Ejaz *et al.*, 2021). Such stem elongation is absent in plants constitutively expressing *ATH1,* without affecting flower formation (Cole *et al.*, 2006; Gómez-Mena & Sablowski, 2008; Rutjens *et al.*, 2009). Present study shows that both absence of ATH1 and induced *ATH1* expression leads to pronounced changes in *PIF* gene expression at the SAM associated with significant elongation or complete suppression of rosette internodes, respectively. PIF proteins have been associated with bolting time and/or stem internode elongation (Brock *et al.*, 2010; Todaka *et al.*, 2012; Galvão *et al.*, 2019; Arya *et al.*, 2021; Jenkitkonchai *et al.*, 2021). Moreover, elongated rosette internodes can be observed in *35S::PIF4* plants (Figure 1d in Kumar *et al*. (2012)). It is therefore proposed that an ATH1-PIF toggle switch underlies the rapid and distinctive switch in Arabidopsis growth habit that marks floral transition.

## Materials and Methods

### Plant materials and growth conditions

*Arabidopsis thaliana* (L.) Heynh. seeds were obtained from the Nottingham Arabidopsis Stock Center (http://arabidopsis.info/) or were kind gifts. For genotypes used, see C2_Table S1.

*ATH1pro:GUS*-containing lines were obtained through crosses. Offspring was backcrossed at least four times to parental acceptor genotypes. *Pro$_{35S}$:HA-ATH1*-containing lines were obtained through genetic transformation as described previously (Proveniers *et al.*, 2007). Per genotype over ten independent, homozygous single insert lines were used for further analysis. To obtain *cop1-4 ath1-4* and *pifq ath1-3* plants, F2 offspring from respective crosses was first phenotype-selected (*cop1-4*: short hypocotyl in darkness; *pifq*: short-petiole phenotype). Plants were then genotyped using primers listed in C2_Table S2.

For plant growth, seeds were chlorine-gas sterilized for 4h using a 4 ml 37% HCl/100 ml commercial bleach (4.5% active chlorine) mixture and put on soil (Primasta) or sterile 0.8% plant agar (Duchefa Biochemie) with full-strength Murashige-Skoog medium (MS salts including MES (pH 5.8) and vitamins; Duchefa Biochemie) in square Petri dishes (120x120 mm). After stratification (2-3 days, 4°C), plants were grown in climate-controlled growth cabinets (Snijders, Microclima 1000) in short-day (SD; 8 hours light/16 hours dark) or long-day (LD; 16 hours light/8 hours dark) photoperiods, under 120 µmol/$m^2$/s fluorescent white-light conditions (Sylvania, Luxline Plus Cool White) and 70% relative humidity. For monochromatic light conditions, a Snijders Microclima cabinet equipped with Philips GreenPower LEDs (red light: 124.35 µmol/$m^2$/s, blue light: 6.14 µmol/$m^2$/s, far-red light: 77.57 µmol/$m^2$/s) was used.



For liquid culture, ten to twenty seeds were added to 20 ml half-strength MS medium (MS salts including MES Buffer (pH 5.8) and vitamins; Duchefa Biochemie) in 100 ml bottles on a rotary shaker (185 rpm, 22 °C). Bottles were sealed with Steristoppers® (Heinz Herenz, Hamburg). After stratification, seeds were exposed to fluorescent light (1-1.5 hours, 120 µmol/$m^2$/s) to stimulate germination. Bottles were then wrapped in aluminum foil. Sucrose (50% w/v) or sorbitol (50% w/v) was added at the start or day three of the experiment. To prevent seedling exposure to light, sugars were added by injection through the aluminum foil-covered bottle stopper using a syringe with long needle.

Ethanol-induction of TOR RNAi lines was previously described (Deprost *et al.*, 2007). Instead of growing plants on soil and using ethanol vapor for induction of the ethanol switch, plants were grown in liquid medium and, using syringe and needle, ethanol was added directly to the growth medium to a final concentration of 0.1% (v/v) after five days of dark cultivation. After an additional five hours in darkness sucrose was added. Plants were sampled after two more days of growth in darkness.

Growth in a $CO_2$-deficient environment was accomplished as in Pfeiffer *et al*. (2016).

**Phenotypic analyses**

For light-grown plants, total rosette internode length was measured using a caliper. For dark-grown seedlings, plants were photographed after three weeks of growth and ImageJ (Schneider *et al.*, 2012) was used to measure total rosette

internode length. Average rosette internode length was determined by dividing total rosette internode length by the total number of rosette leaves.
Meristem cell size was determined using confocal laser scanning microscopy. In median, longitudinal optical sections through shoot apices a central cell file extending from the epidermis into the subapical region where the hypocotyl vascular strands converge was identified. Using ImageJ, per position individual cell lengths were then measured in apical-basal direction.

**Gene expression analysis**
Samples were snap-frozen in liquid nitrogen and stored at -80°C before RNA extraction. For each experiment three or four biological replicates and two technical replicates were included. RNA was isolated using a RNeasy mini or micro kit (Qiagen). Genomic DNA was removed using DNaseI (Thermo Scientific) and cDNA was synthesized from 500 ng - 1 µg RNA using RevertAid H Minus Reverse Transcriptase and Ribolock RNAse inhibitor (Thermo Scientific) and a mix of anchored odT(20) primers (Jena Bioscience) and random hexamers (IDT). qPCR reactions were performed using qPCRBIO SyGreen Blue mix (PCRBIO) on a ViiA7 Real Time PCR system. ViiA7 software was used to analyze the data. Relative expression levels were calculated using the ΔΔCt method (Livak & Schmittgen, 2001), normalized to *GAPC2* (AT1G13440) and/or *MUSE3* (AT5G15400) expression. For primer sequences used, see C2_Table S3.

**β-Glucuronidase Staining and Microscopy**
Seedlings were harvested and vacuum-infiltrated in β-glucuronidase (GUS) staining buffer (50 mM sodium phosphate buffer (pH=7.2), supplemented with 0.1% Triton X-100, 100 mM, potassium ferrocyanide, 100 mM, potassium ferricyanide, 2 mM 5-bromo-4-chloro-3-indolyl glucuronide). Samples were incubated o/n at room temperature and subsequently cleared in ethanol. Images were taken with a Nikon DXMI200 camera attached to a Zeiss Stemi SV11 stereo microscope. GUS staining area was measured and quantified using Image J.

**Confocal microscopy**
Seedlings were cleared using the ClearSee method (Kurihara *et al.*, 2015) and imaged at a resolution of 0.25 x 0.25 x 0.5 µm using a Carl Zeiss LSM880 Fast AiryScan microscope with a Plan-Apochromat 63x/1,2 Imm Korr DIC objective

(numerical aperture 1.40, oil immersion) and ZEN software (blue edition, Carl Zeiss). Calcofluor White Stain (Sigma-Aldrich) staining was performed as described before (Ursache *et al.*, 2018). Excitation was at 405 nm and emission filters were set between 425 nm and 475 nm. All replicate images were acquired using identical microscopy parameters for each experiment. Images were processed with Fiji (version 1.52, Fiji) and Adobe Illustrator.

**Statistical analysis**

Data plotting and statistical analysis were performed using RSTUDIO.1.0.143 (www.rstudio.com) with R v.3.6.2 (https://cran.r-project.org/). To compare differences between experimental groups, one-way ANOVA and Fisher's Least Significant Difference test were applied. Prior to conducting ANOVA, the normality and homogeneity of variance assumptions were verified using histograms, ggnorm, and Shapiro tests for normality and the Levene and Bartlett tests for homogeneity. In cases where ANOVA assumptions were not met, the Dunn Test with the Benjamini-Hochberg method was used for multiple comparisons. T-tests were applied only if the assumptions were met for comparing two groups, otherwise the Kruskal-Wallis test was used. Results were corrected using the Bonferroni correction with an alpha level of 0.05, and all analyses were performed using the agricolae package (Mendiburu, 2020). Figures were compiled using Adobe Illustrator and ImageJ software.



## Acknowledgements

*phyA cry1*, *phyB cry1* and *phyA phyB cry1* seeds were a kind gift of Jorge Casal. *hy1, cry1, cry2, cry1 cry2, hy1 cry1, hy1 cry2, and hy1 cry1 cry2* seeds were a kind gift of Enrique Lopez-Juez and *cop1-4* seeds were kind gift of Jan Lohmann.

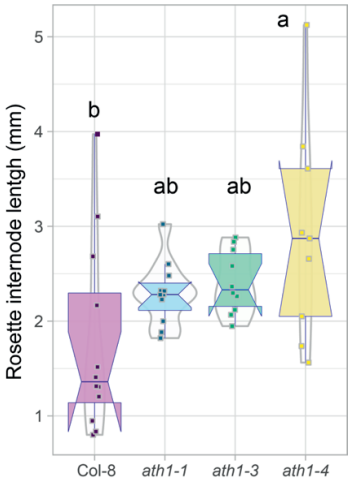


**C2_Fig. S1: Different *ath1* alleles display highly comparable rosette internode phenotypes.**

Average rosette internode elongation in three-week-old, dark-grown *ath1-1*, *ath1-3*, and *ath1-4* mutants. Plants were grown in liquid medium for three weeks and treated with 1% sucrose from day three after germination. Data were analyzed using 1-way ANOVA and Tukey's post hoc test. Statistically significant differences between groups are denoted by different letters ($P < 0.05$).

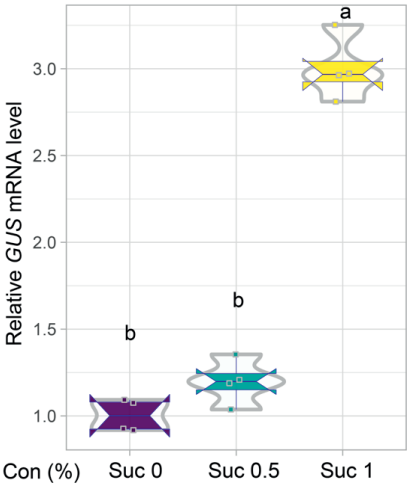


**C2_Fig. S2: *GUS* mRNA levels in sucrose-induced *ATH1*$_{pro}$*:GUS* seedlings.**

Relative *GUS* mRNA levels in seven-day-old, dark-grown *ATH1*$_{pro}$*:GUS* seedlings in the absence (0%) or presence (0.5% and 1%) of sucrose (n≥20 per biological replicate; four biological replicates). Transcript levels were normalized to *MUSE3* (At5g15400). Different letters denote statistically significant differences between groups ($P < 0.05$) as determined by 1-way ANOVA and Tukey's post hoc test.

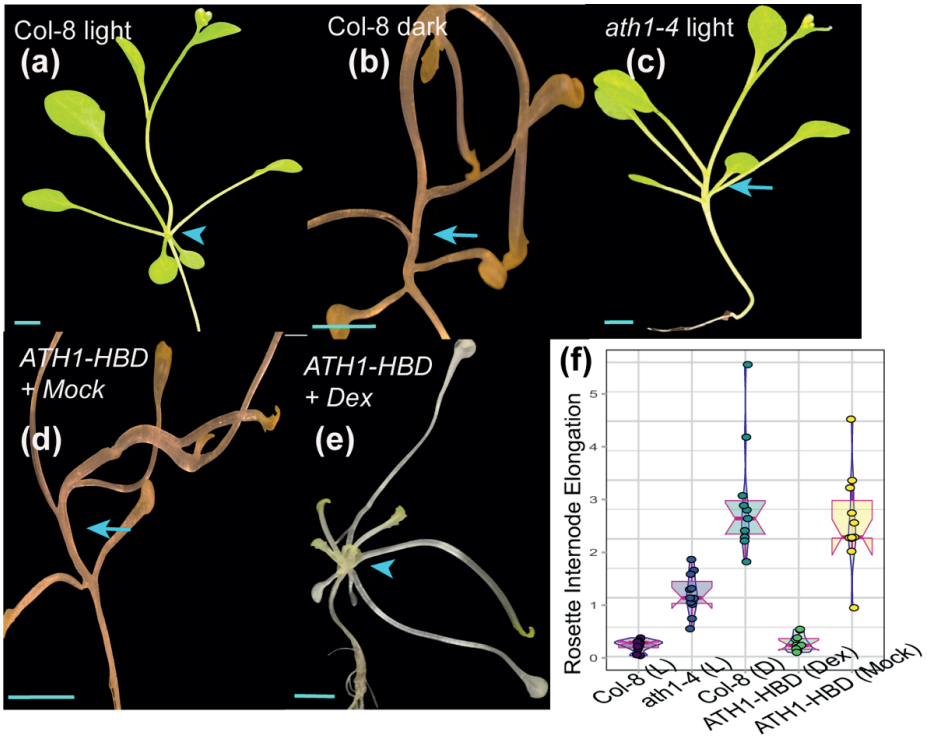


**C2_Fig. S3: Sugar-induced, dark-grown seedlings phenocopy light-grown *ath1*mutants.**

(**a, b**) Rosette elongation phenotypes of wild-type Col-8, (**c**) *ath1-4*, and (**d, e**) *35Spro:ATH1-HBD* (*ATH1-HBD*) plants grown in the presence (a, c) or absence (b, d, e) of light at 27°C. *35Spro:ATH1-HBD* plants were treated either with (d) a mock (0.1% ethanol) or (e) 10 µM dexamethasone (Dex). Dark-grown plants (b, d, e) were supplemented with sucrose to a final concentration of one percent three days after the start of the experiment. Arrows indicate elongated rosette internodes, arrowheads indicate complete suppression of internode elongation. (**f**) Average rosette internode lengths of plants depicted in (a-e). Per genotype and treatment 10 individual plants were analyzed. Scale bars represent 5 mm.

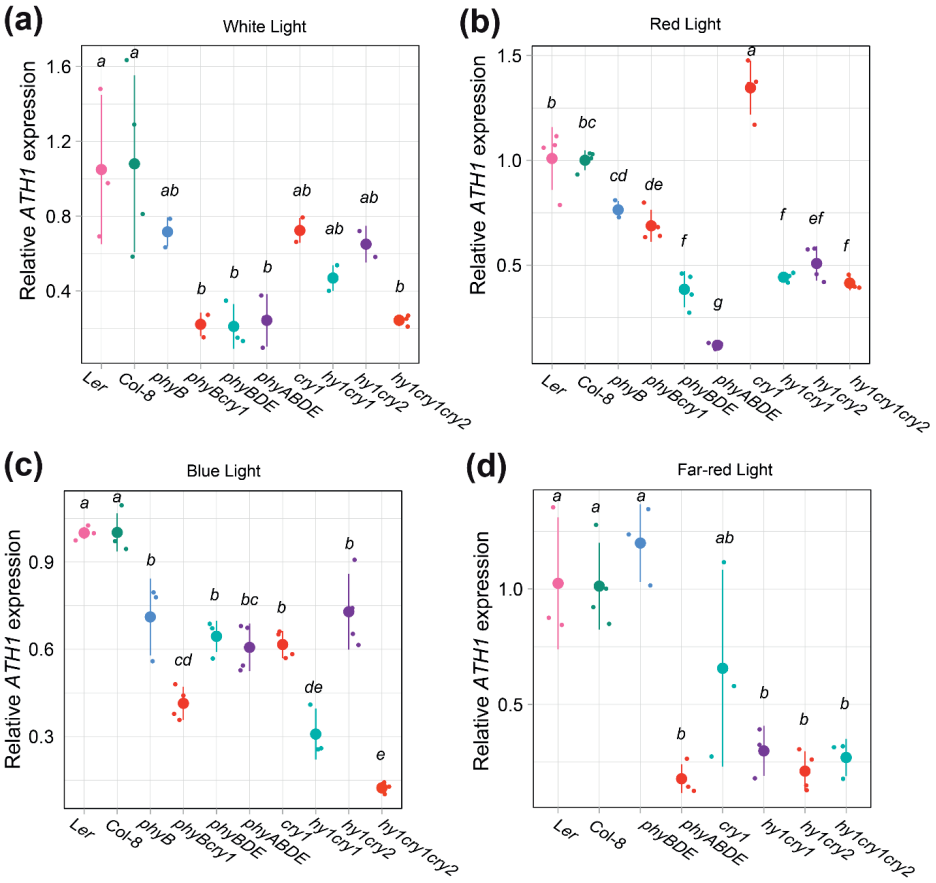


**C2_Fig. S4: Relative *ATH1* mRNA abundance in different photoreceptor mutants.**

Relative expression of *ATH1* in seven-day-old wild type (*Ler* and Col-8) and indicated photoreceptor mutants grown under SD conditions in the presence of (**a**) white light (WL), (**b**) red light (RL), (**c**) blue light (BL) or (**d**) far-red light (FRL). Transcript levels were normalized to *GAPC2* (*AT1G13440;* BL) or *MUSE3* (*AT5G15400*; WL, RL, and FRL). Data shown are the average of three biological replicates. At least 30 seedlings were used for each biological replicate. Different letters denote statistically significant differences between groups ($p < 0.05$) as determined by 1-way ANOVA followed by Tukey's post hoc test.

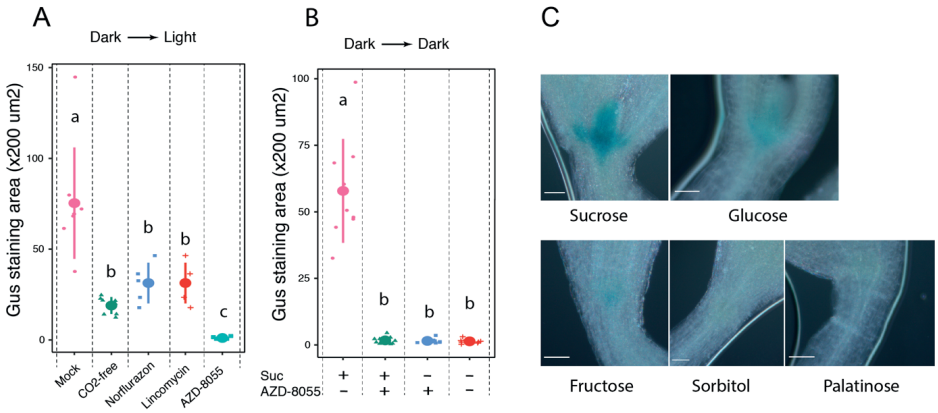


**C2_Fig. S5: *ATH1*$_{pro}$*:GUS* activity in seven-day-old seedlings grown in darkness in the presence of different sugars.**

(**a, b**) Quantification of GUS-staining intensity in *ATH1*$_{pro}$*:GUS* shoot apices from **C2_Fig. 5b, e**. Different letters denote statistically significant differences between groups ($p < 0.05$) as determined by 1-way ANOVA followed by Tukey's post hoc test. (**c**) Shoot apices of GUS-stained *ATH1*$_{pro}$*:GUS* seedlings grown in continuous darkness for seven days. Plants were grown in the presence of either sucrose, glucose, fructose, palatinose, or sorbitol, all added to the growth medium to a final concentration of one percent at the start of the experiment. Scale bars represent 0.05 mm.

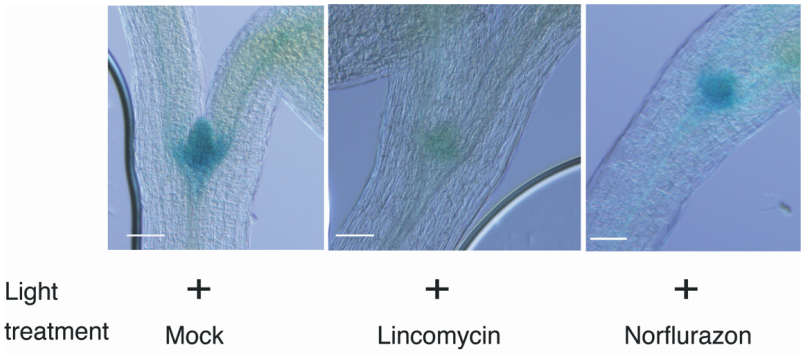


**C2_Fig. S6: Chemical inhibition of photosynthesis negatively impacts *ATH1*-promoter activity.**

Shoot apices of GUS-stained *ATH1*$_{pro}$*:GUS* seedlings grown in the presence of either 0.5 mM lincomycin or 5 µM norflurazon according to the experimental setup as in **C2_Fig. 6a**. Mock-treatment was with DMSO to a final concentration of 0.1%. Scale bars represent 0.05 mm.

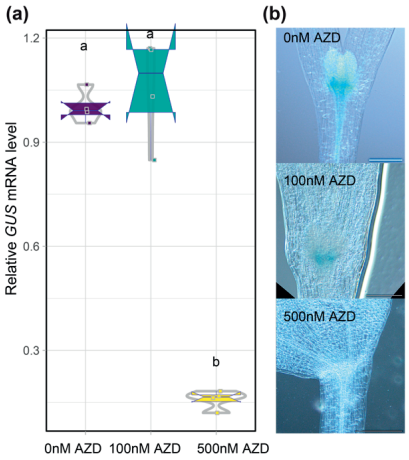


**C2_Fig. S7: Effect of TOR kinase activity on ATH1-promoter activity.**

**(a)** Relative *GUS* mRNA levels in seven-day-old *ATH1*$_{pro}$*:GUS* seedlings grown in the absence (0 nM) or presence (100 nM or 500 nM) of AZD-8055 (n≥30 per biological replicate; four biological replicates). Experimental setup was as depicted in **C2_Fig. 6a**. Transcript levels were normalized to *MUSE3* (At5g15400). Different letters denote statistically significant differences between groups (P < 0.05) as determined by 1-way ANOVA and Tukey's post hoc test. **(b)** Shoot apices of GUS-stained, seven-day-old *ATH1*$_{pro}$*:GUS* seedlings grown under the same conditions as in (a). Scale bars represent 200 µm.

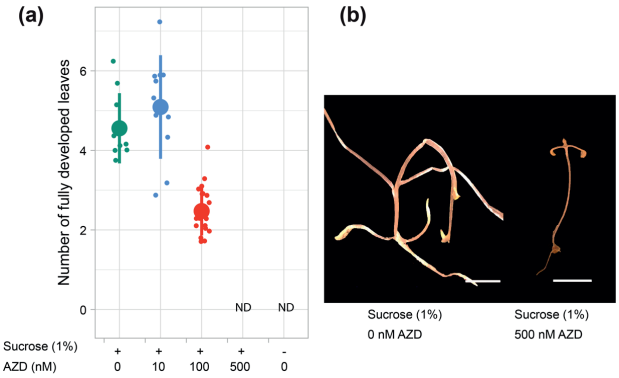


**C2_Fig. S8: Sugar-mediated dark morphogenesis requires TOR kinase activity.**

**(a)** Leaf outgrowth in 3-week-old, dark-grown Col-8 plants treated with different concentrations of AZD-8055 (AZD; 0, 10, 100, 500 nM) in the presence of sucrose (+). Control treatment was 1% sorbitol (-) in the absence of AZD-8055. Sucrose, sorbitol and AZD-8055 were added three days after germination. Like control-treated plants, sucrose-supplemented plants treated with a high concentration of AZD-855 (500 nM) did not grow out any leaves (ND; none detected). **(b)** Representative plants as scored in (a). Scale bar denotes 4 mm.

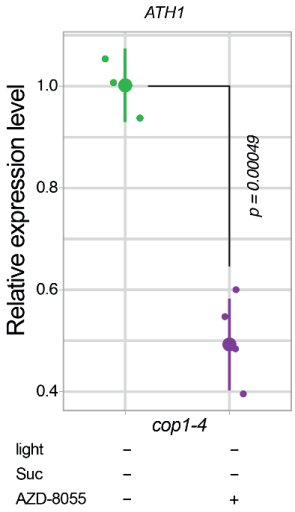


**C2_Fig. S9: Effect of TOR inhibition on *ATH1* expression in *cop1-4* mutant seedlings.**

Relative expression of *ATH1* in seven-day-old *cop1-4* mutants grown according to the experimental setup indicated in Fig. **5a**. Seeds were light-treated for 45 minutes to stimulate germination and then grown in continuous darkness for five days. Following the addition of AZD-8055, the seedlings were grown for two more days in darkness before samples were taken. Transcript levels were normalized to *MUSE3* (AT5G15400). The average of three (AZD-8055 -) or four (AZD-8055 +) biological replicates is shown. At least 30 seedlings were used for each biological replicate. The *p-value* of significant difference, as determined by the two-tailed Student's t-test, is indicated in the figure.

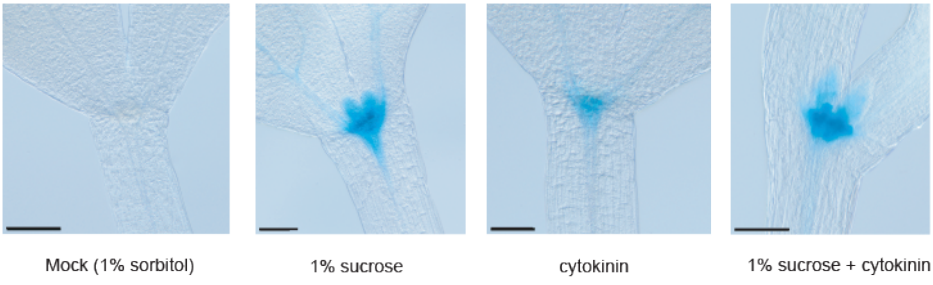


**C2_Fig. S10: Cytokinin potently induces ATH1-promoter activity in the absence of both light and metabolizable sugar.**

Shoot apices of seven-day-old, GUS-stained $ATH1_{pro}$*:GUS* seedlings grown in the presence of 1% sorbitol (Mock), 1% sucrose, 75 µM benzyladenine (cytokinin), or a combination of sucrose (1%) and cytokinin (75 µM benzyladenine). Scale bars represent 100 µm.

**C2_Table S1. Plant genotypes used in chapter 2.**

| Genotypes | Reference | NASC ID/kind gift of |
|---|---|---|
| Col-8 accession | | N60000 |
| Ler accession | | NW20 |
| *ath1-1* (Col-8) | (Proveniers *et al.*, 2007) | |
| *ath1-3* (Col-8) | (Proveniers *et al.*, 2007) | |
| *ath1-4* (Col-8) | (Li *et al.*, 2012b) | Lin Xu |
| *cop1-4* (Col-8) | (McNellis *et al.*, 1994) | Jan U. Lohmann |
| *cry1-1* (Col-8) | (Ahmad & Cashmore, 1993) | N70 |
| *hy1-1* (Ler) | (Muramoto *et al.*, 1999) | NW67 |
| *hy1cry1* (Ler) | (López-Juez *et al.*, 2008) | N9855 |
| *hy1cry2* (Ler) | (López-Juez *et al.*, 2008) | N9856 |
| *hy1cry1cry2* (Ler) | (López-Juez *et al.*, 2008) | N9854 |
| *pif3-1* (Col-8) | (Kim *et al.*, 2003a) | N530753 |
| *pif4-1* (Col-8) | (Huai *et al.*, 2018) | N667486 |
| *pif4pif5* (Col-8) | (Leivar *et al.*, 2012) | N68096 |
| *pif7-1* (Col-8) | | N68809 |
| *pif3pif4* (Col-8) | | N66046 |
| *pif1pif3* (Col-8) | | N66045 |
| *pif1pif3pif4* (Col-8) | | N66500 |
| *pif1pif3pif5* (Col-8) | | N66047 |
| *pif3pif4pif5* (Col-8) | | N66048 |
| *pif1pif3pif4pif5* (*pifq)* (Col-8) | (Leivar *et al.*, 2008b) | N66049 |
| *phyB-5* (Ler) | (Reed *et al.*, 1993) | N6213 |
| *phyBDE* (Ler) | (Shalitin *et al.*, 2002) | Jorge J. Casal |
| *phyABDE* (Ler) | (Franklin *et al.*, 2003a) | |
| *phyBcry1*(Ler) | (Mazzella *et al.*, 2000) | Jorge J. Casal |
| *ATH1pro:GUS* (Col-8) | (Proveniers *et al.*, 2007) | |
| $35S_{pro}$*:ATH1-HBD* (Col-8) | (Proveniers *et al.*, 2007) | |
| $Pro_{35S}$*:HA-ATH1* (Col-8) | (Proveniers *et al.*, 2007) | |
| *35S::ALCR alcA:RNAi-TOR* (Ler) | (Deprost *et al.*, 2007) | Christian Meyer |
| *35S:ALCR alcA:GUS* (Ler) | (Deprost *et al.*, 2007) | Christian Meyer |

**C2_Table S2: Primers used for genotyping in chapter 2.**

| Gene | Left primer (LP) | Right primer (RP) | Ref., & notes |
|---|---|---|---|
| *pif1-1* (SAIL_256_G07) | LP: AAGGAAGGAGGAGGAATAGGC | RP: CATGAATTTCTCGAGGCTGAG | (Sparks *et al.*, 2016) |
| | LB: GCTTCCTATTATATCTTCCCAAATTACCAATACA | | |
| *pif3-7* | A: GGTCACCATGCTCCAACTCT | B: CCTGAGAAAGTAGGCGGAGA | 1 |
| | C: TCTCCGCCTACTTTCTCAGG | D: TGTTGCGTTTTACAGAAACAATC | |
| *pif3-1* (SALK_030753) | LP: AGTCTGTTGCTTCTGCTACGC | RP: TTGCATAAGGCATTCCCATAC | |
| | LB: ATTTTGCCGATTTCGGAAC | | |
| *pif4-2* (SAIL_1288_E07) | LP: ACCTCCTCAAGTCATGGTTAAGCCTAAGCC | RP: TCCAAACGAGAACCGTCGGT | (Leivar *et al.*, 2008a) |
| | LB: TAGCATCTGAATTTCATAACCAATCTCGATACAC | | |
| *pif5-3* (SALK_087012) | LP: CGATTTGTTACCCATGGTTTG | RP: CCTTGCTCGATTTTTGTTACG | (Sparks *et al.*, 2016) |
| | LB: ATTTTGCCGATTTCGGAAC | | |
| *pif7-1* | LP: CCGTTCATGGTCTAGGCG | RP: CATCCTCTGGTTTATCCTATCACGCCG | (Leivar *et al.*, 2008a) |
| | LB: TGATAGTGACCTTAGGCGACTTTTGAACGC | | |
| *ah1-3* (SALK_113353) | LP: CGCTCGATTATTCATCTCGAG | RP: CACTCTATATCATTTGCCCGC | |
| | LB: ATTTTGCCGATTTCGGAAC | | |
| *ath1-4* | ATH1int-F: CCGAGTTAGATCCACAGTTACA | ATH1int-R: CATTTCCGCATACATCTCTTC | 2 |

1: WT (A + B = 248bp, A + D = 784bp, C + D = 132bp); *pif3-7* (A + B = no band, A + D = no band, C + D = 132bp)

2: *ath1-4* is an EMS mutant (TGG-> TGA, CDS nt1170). The ATH1int-F and ATH1int-R primers generate PCR amplicons of 905 bp containing the *ath1-4* SNP. In wild-type plants, BseGI results in two fragments (259 and 648 bp) of the amplicon while the *ath1-4* mutant remains uncut.

**C2_Table S3: Primers used for qPCR in chapter 2.**

| Gene | Sequence Fw | Sequence Rv | Ref,. |
|---|---|---|---|
| *ATH1* (AT4G32980) | CAACGAGGTTTGCCTGAGAAA | TTCGGGTAAGGGTGAAGGAA | |
| *PIF1* (AT2G20180) | TGAATCCCGTAGCGAGGAAACAA | TTCCACATCCCATTGACATCATCTG | (Xu *et al.*, 2017) |
| *PIF3* (AT1G09530) | CTGAAAGGAGACGGCGTGATAG | CAGATAGTAACCAGACGCCATTGAC | (Zhong *et al.*, 2012) |
| *PIF4* (AT2G43010) | CAGCTTCAAGTGATGTGGATG | CATAACCGGAAATCGAGGTAA | (Qi *et al.*, 2020) |
| *PIF5* (AT3G59060) | CAACTCCAAGTGATGTGGATG | CAATTGCATCTGACTTTGCAT | (Qi *et al.*, 2020) |
| MUSE3 (AT5G15400) | GGGCACTCAAGTATCTTGTTAGC | TGCTGCCCAACATCAGGTT | (Pei *et al.*, 2007) |
| GAPC2 (AT1G13440) | TTGGTGACAACAGGTCAAGCA | AAACTTGTCGCTCAATGCAATC | (Czechowski *et al.*, 2005) |


Col-8
ath1-3

# Chapter 3

## Multi-level control of a general elongation program confers robust rosette habit in *Arabidopsis thaliana*

Shahram Shokrian Hajibehzad[1, 2, 6], Savani S Silva[1, 6], Evelien Stouten[1, 3], Yoëlle Hilbers[1], Sandi Paulisic[5], Christian Fankhauser[5], Basten Snoek[4], Sjef Smeekens[1], Marcel Proveniers[1, 2]

[1] *Molecular Plant Physiology, Department of Biology, Science4Life, Utrecht University, Padualaan 8, 3584CH, Utrecht, The Netherlands*

[2] *Translational Plant Biology, Department of Biology, Science4Life, Utrecht University, Padualaan 8, 3584CH, Utrecht, The Netherlands*

[3] *Plant Stress Resilience, Institute of Environmental Biology, Utrecht University, Padualaan 8, 3584 CH Utrecht, The Netherlands*

[4] *Theoretical Biology and Bioinformatics, dept. Biology, Utrecht University, Padualaan 8, 3584 CH Utrecht, the Netherlands*

[5] *Faculty of Biology and Medicine, Centre for Integrative Genomics, University of Lausanne, Génopode Building, Lausanne CH-1015, Switzerland*

[6] *These authors contributed equally*

## Abstract

This study examines the role of ARABIDOPSIS THALIANA HOMEOBOX1 (ATH1) in maintaining the developmental robustness of *Arabidopsis thaliana*'s rosette structure under various hormonal and environmental conditions. Employing methods such as hormonal treatments, genetic crossings, and the analysis of suppressor mutants, the research highlights ATH1's essential role in preserving the compact nature of the rosette habit by specifically inhibiting internode elongation. It also confirms that ATH1 selectively targets aspects of growth, notably without affecting the elongation of hypocotyls and petioles, thereby pinpointing its unique contribution to the plant's rosette habit robust development. Through RNA sequencing, the study expands our understanding of ATH1's wide-reaching effects on gene expression related to hormonal signaling and environmental adaptation, providing significant molecular insights. This research further uncovers how ATH1 modulates key growth-regulatory modules—BAP/D and HLH/BHLH—through the direct suppression of *PIF4* and *PRE6/KDR* expression within the meristem, revealing a complex regulatory network crucial to ATH1's role in plant growth and adaptation. This mechanism, achieved by inhibiting numerous genes involved in cell elongation, grants a robust rosette habit. In contrast, the removal of *ATH1* leads to increased sensitivity to external factors in *ath1* mutants, resulting in a range of rosette phenotypes that highlights the gene's vital role in ensuring plant form stability against environmental and hormonal changes. This detailed investigation of ATH1's function emphasizes its importance in the interplay between genetic regulation and environmental adaptation, suggesting pathways for improving plant resilience through genetic engineering.

## Introduction

Plants, due to their sessile nature, are constantly exposed to fluctuating environmental conditions throughout their lifecycle. Unlike animals, plant development primarily occurs post-embryonically and is characterized by continuous growth. To overcome their immobility and to successfully adapt to a rapidly changing environment, plants have evolved extensive developmental plasticity. This allows plants of the same genotype to display different phenotypes depending on post-embryonic development in response to environmental variations. Such developmental plasticity enables plants to maximize fitness under suboptimal growth conditions and relies on cellular machinery that integrates diverse internal and external signals, coordinating downstream growth responses (Palmer *et al.*, 2012).



In Arabidopsis, the BAP/D regulatory module coordinates growth through cell elongation regulation in response to multiple cues. This module includes the transcription factors BRASSINAZOLE RESISTANT 1 (BZR1), AUXIN RESPONSE FACTOR 6 (ARF6), and PHYTOCHROME INTERACTING FACTOR 4 (PIF4), alongside DELLA proteins that function as principal suppressors of gibberellin (GA) signaling (Bai *et al.*, 2012a,b; Gallego-Bartolomé *et al.*, 2012; Oh *et al.*, 2012, 2014; Küpers *et al.*, 2023). The complex regulation of its components allows the BAP/D module to receive and process information from both hormonal and environmental cues to regulate adaptive growth (Bouré *et al.*, 2019; Favero *et al.*, 2020). BAP/D-module transcription factors, either individually or collectively, modulate hormonal signaling to promote growth. BZR and ARF proteins positively regulate elongation growth in response to signals from the brassinosteroid (BR) and auxin hormone pathways, respectively. GA de-represses the BAP transcription factors by promoting the degradation of DELLA proteins, which are key negative regulators of GA signaling. Specifically, the DELLA proteins REPRESSOR OF GA (RGA) and GIBBERELLIC ACID INSENSITIVE (GAI) play major roles in repressing hypocotyl elongation by inhibiting PIF4, BZR1, and ARF6 function through physical interactions with these transcription factors. Environmental cues affecting hypocotyl elongation, such as light quality and temperature, are integrated with hormonal cues through PIFs. Light activates phytochromes, which in turn repress PIFs. When phytochromes are inactivated, for example by low red/far-red light ratios, PIFs become stabilized, and downstream elongation responses are activated (Bouré *et al.*, 2019; Favero *et al.*, 2020). At elevated temperatures, PIF4

promotes hypocotyl elongation by transcriptionally inducing auxin biosynthesis genes. Auxin-dependent hypocotyl elongation depends on BR accumulation and subsequent activation of BZR1. BZR1 then promotes PIF transcription, creating an amplifying positive feedforward loop that controls temperature-responsive hypocotyl elongation (Ibañez *et al.*, 2018). Promotion of cell elongation by the BAP module requires a tripartite helix-loop-helix/basic-helix-loop-helix (HLH/bHLH) module, which is formed through antagonistic interactions among DNA-binding bHLH factors, such as members of the PACLOBUTRAZOL RESISTANCE (PRE) family, which promote growth, and non-DNA-binding HLH factors, including ILI1-binding bHLH1 (IBH1), which inhibit plant growth (Hao *et al.*, 2012; Ikeda *et al.*, 2012; Zhiponova *et al.*, 2014).

Although plant development is remarkably plastic, some phenotypes remain largely constant, even across different environments. The ability of an organism to produce a consistent or invariant phenotype under environmental perturbations is referred to as robustness. Developmental robustness is a fundamental characteristic of multicellular organisms and is thought to be selectively advantageous (Visser *et al.*, 2003). The Arabidopsis rosette habit, that characterizes the vegetative growth phase, is remarkably insensitive to environmental and genetic perturbations and, thus, provides an excellent example of developmental robustness. Rosette habit offers several advantages over caulescent growth and is widespread among flowering plants, both dicots and monocots, and in plants with different life history strategies alike (Martorell & Ezcurra, 2002; Bello *et al.*, 2005; Larcher *et al.*, 2010; Cohen, 2011; Marks *et al.*, 2011; Fujita & Koda, 2015; Hao *et al.*, 2017). Hence, the loss of the rosette habit in response to perturbations is likely detrimental to plant fitness and viability.

Rosette habit is characterized by a basal whorl of leaves without internode development between successive nodes. Internode development and subsequent stem formation require the activity of the sub-apical region of the shoot apical meristem (SAM), known as the rib zone (RZ) (Serrano-Mislata & Sablowski, 2018; McKim, 2019, 2020). During the vegetative growth phase, the RZ is inhibited and remains mitotically inactive, leading to a compact rosette (Sachs *et al.*, 1959b,a; Metzger & Dusbabek, 1991; Bencivenga *et al.*, 2016). It has been recently demonstrated that the homeodomain transcription factor *ARABIDOPSIS THALIANA HOMEOBOX1 (ATH1)* is a key regulator of RZ activity in Arabidopsis (Ejaz *et al.*, 2021; Hajibehzad *et al.*, 2023). In seedlings, *ATH1* is first expressed two days after ger-

mination in the SAM and leaf primordia, where it remains highly expressed during vegetative growth (Proveniers *et al.*, 2007; Gómez-Mena & Sablowski, 2008). As a result, RZ activity is inhibited, resulting in the characteristic rosette growth habit. At floral transition, *ATH1* expression at the SAM is downregulated, leading to RZ activation and bolting, marked by rapid elongation of newly formed internodes that give rise to the inflorescence stem, is initiated. In loss-of-function *ath1* mutants, RZ activity is no longer restricted to the generative growth phase (Gómez-Mena & Sablowski, 2008; Rutjens *et al.*, 2009). Consequently, *ath1* mutants exhibit slightly elongated vegetative internodes (Li *et al.*, 2012a), a phenotype that is significantly enhanced by the absence of light, shade avoidance syndrome-inducing end-of-day FR light treatment, or GA application, such that this results in a shift toward caulescent growth (Ejaz *et al.*, 2021; Hajibehzad *et al.*, 2023). Loss-of-function mutations in *ATH1* thus result in a loss of developmental robustness.



Developmental robustness emerges from the intricate interplay among genes within gene regulatory networks and environmental cues, frequently encompassing multiple feedback loops that enable the system to adapt and compensate for disturbances (Broeck *et al.*, 2020). We previously identified a SAM-specific, double-negative *ATH1-PHYTOCHROME-INTERACTING FACTOR 4* (*PIF4*) feedback loop at the core of Arabidopsis rosette habit, with TOR kinase acting upstream as a central hub integrating light and energy signals (Hajibehzad *et al.*, 2023). Here, we show that downstream, ATH1 controls internode elongation by antagonizing BAP/D and HLH/bHLH modules, as well as their inputs, at multiple levels. Through inhibition of a large number of genes that promote cell elongation, mostly independent of each other, ATH1 confers robustness to the rosette growth habit of *Arabidopsis thaliana*. In line with this, in *ath1* mutants, elongation of rosette internodes becomes highly sensitive to hormonal, environmental, and genetic changes, transitioning the Arabidopsis rosette habit into a phenotypically plastic trait with vegetative plant phenotypes ranging from compact rosette habit to complete loss of rosette habit. Conversely, under- or overexpression of *ATH1* targets that operate downstream of the BAP/D module in the regulation of cell elongation, thereby uncoupling them from hormonal and environmental input, results in the stable expression of, respectively, rosette or caulescent growth habits.

## Results

**Arabidopsis rosette habit becomes a plastic trait in the absence of ATH1**

In Arabidopsis, the growth rates of aerial organs, including the hypocotyl, petioles, and inflorescence stem display a high degree of plasticity and adapt in response to environmental stimuli such as variations in light quality, temperature, and photoperiod (Favero *et al.*, 2020; Pierik *et al.*, 2021; Krahmer & Fankhauser, 2024). In contrast, growth of vegetative internodes is not affected by environmental fluctuations, not even by conditions of altered light quality or temperature that typically induce rapid elongation in other aerial plant organs (C3_Fig. 1a-d). As a result, rosette growth habit, which is a defining feature of Arabidopsis, remains consistent across all environmental conditions.

The compact rosette growth pattern in Arabidopsis is sustained through the activity of ATH1 at the SAM. By maintaining the RZ area inactive, ATH1 prevents elongation of rosette internodes (Ejaz *et al.*, 2021; Hajibehzad *et al.*, 2023). Correspondingly, *ath1* mutants exhibit slightly elongated rosette internodes under control conditions (LD, 22°C) (C3_Fig. 1a, b) (Li *et al.*, 2012b; Ejaz *et al.*, 2021). Previous findings indicate that under end-of-day far-red (EOD-FR) conditions, the elongation of *ath1* rosette internodes significantly increases (Ejaz *et al.*, 2021). This implies that the elongation of vegetative internodes becomes plastic in the absence of ATH1. To further investigate this, *ath1* mutants were cultivated under elevated temperature, low red/far-red (R/FR), or short-day photoperiod conditions. While control plants (Col-8) exhibited a compact rosette morphology across all conditions examined, *ath1* mutants consistently displayed evident elongation of rosette internodes (C3_Fig. 1a, b). Furthermore, when subjected to modified light (quality) or temperature conditions, known to typically induce rapid elongation in hypocotyls, compared to control conditions (LD, 22°C) *ath1* mutants demonstrated even more pronounced internode elongation (C3_Fig. 1a-d) (Gómez-Mena & Sablowski, 2008; Ejaz *et al.*, 2021; Hajibehzad *et al.*, 2023). Unlike its pronounced effect on vegetative internodes, loss of ATH1 did not impact hypocotyl elongation responses (C3_Fig. 1c, d).

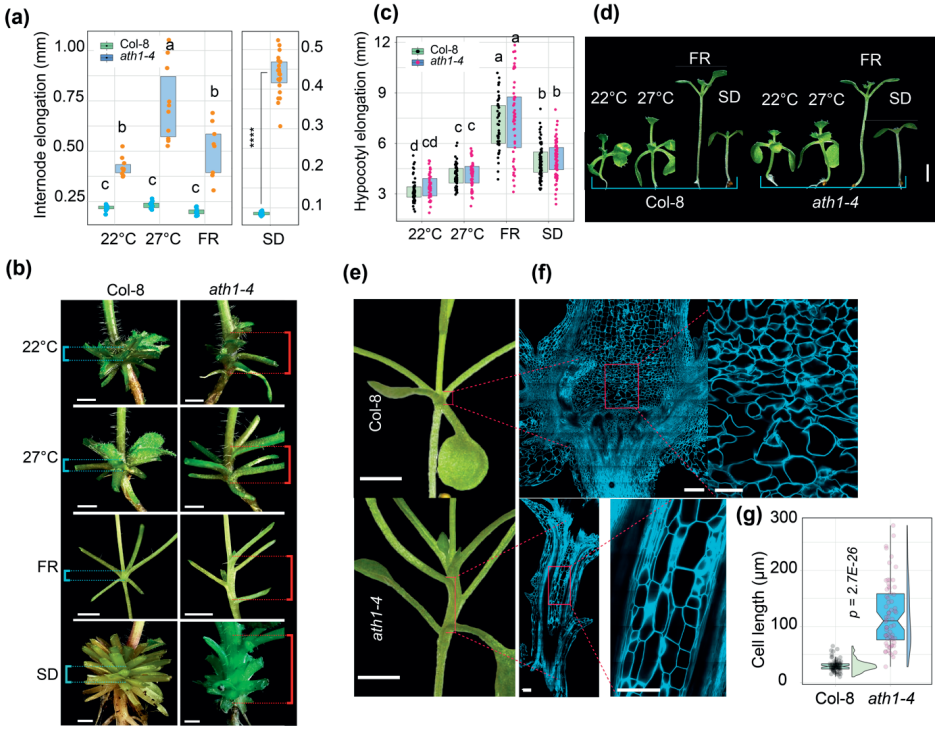


**C3_Fig. 1: Comparative analysis of morphological and cellular responses in Col-8 and *ath1-4* *Arabidopsis thaliana* under variable growth conditions.**

**(a)** Box plot showing relative internode elongation in Col-8 and *ath1-4* plants at 22°C, 27°C, under far-red light (FR), and short day (SD) conditions. Letters indicate statistically homogeneous subsets according to a one-way ANOVA, followed by Fisher's least significant difference (LSD) test with Bonferroni correction (α = 0.05) from the agricolae package, and asterisks denote significant differences determined by unpaired two-tailed Student's t-test (*P-value* < 0.0001). **(b)** Representative images of Col-8 and *ath1-4* plants demonstrating phenotypic differences in internode development at 22°C, 27°C, FR, and SD conditions. Scale bars = 10 mm. **(c)** Box plot displaying hypocotyl elongation in 7-day-old Col-8 and *ath1-4* under the same conditions as in (a). Statistical subsets are indicated by letters. **(d)** Side-by-side comparison of Col-8 and *ath1-4* seedlings showing overall plant morphology and hypocotyl elongation under 22°C, 27°C, FR, and SD conditions. **(e)** Close-up view of Col-8 and *ath1-4* internodes, highlighting the differences in architecture. **(f)** Confocal microscopy images of internode cross-sections from Col-8 and *ath1-4*, with a focus on cellular organization and elongation. Scale bars in the left images = 100 µm, and in the right images (zoomed-in areas) = 20 µm. **(h)** Violin plot with embedded box plot summarizing the cell length measurements from internode cross-sections, showing a significant difference between Col-8 and *ath1-4* (p-value indicated above the plots).

Likewise, when *ATH1* was ectopically expressed in higher-order photoreceptor mutants, which normally exhibit elongated hypocotyls and petioles alongside a loss of compact rosette structure, the elongation of hypocotyls and petioles remained unaffected (C3_Fig. S1a), whereas a compact rosette habit was restored (Hajibehzad *et al.*, 2023). ATH1, thus, specifically influences the phenotypic plasticity of vegetative internodes, where its presence endows robustness to the development of a compact rosette growth habit.

The plastic responses of hypocotyls and petioles to environmental changes are primarily driven by cell elongation or a combination of cell division and elongation, respectively (Favero *et al.*, 2020). To investigate the cellular basis of rosette internode plasticity, internodes of *ath1* plants grown under low R/FR-light conditions were imaged and compared to those of control plants grown under the same conditions. Reflecting the pronounced elongation of internodes in *ath1* mutants under low R/FR light, organized files of longitudinally elongated cells were evident between successive nodes. This stands in contrast to control plants, where smaller isodiametric cells lacking clear organization occupy the region at the base of the rosette from which all leaves originate (C3_Fig. 1e, f). Due to the absence of clear organization, coupled with a compact rosette structure, it is impractical to quantify cell numbers between successive nodes in control plants. Nonetheless, considering that cells within internodes of *ath1* plants are approximately three to four times more elongated compared to cells in the corresponding region of control plants (C3_Fig. 1g) and the relative internode elongation in *ath1* plants is three to four times higher than in control plants under the specified conditions, it suggests that ATH1 primarily restrains internode elongation by impeding cell elongation.

**Suppression of auxin, BR or GA signaling restores compact rosette habit in *ath1* mutants**

In Arabidopsis, cell elongation driven by light and temperature plays a substantial role in plant growth and morphogenesis. These environmental cues are integrated into a sophisticated hormonal signaling network, prominently featuring gibberellins (GA), brassinosteroids (BR), and auxin (Bai *et al.*, 2012a; Gallego-Bartolomé *et al.*, 2012; Oh *et al.*, 2014). Previous work by Ejaz et al. (2021) identified genes involved in the regulation of GA and auxin plant hormone homeostasis among the binding targets of ATH1. Moreover, these authors noted that elongation of

vegetative internodes was significantly enhanced in *ath1* mutants that lacked all five DELLA proteins, which act as repressors of GA signaling, or when continuously treated with GA (Ejaz *et al.*, 2021). ATH1, thus, potentially modulates internode cell elongation through local regulation of plant hormone homeostasis. To further test this, we applied auxin, GA, or BR to shoot apices of *ath1* mutants and Col-8 control plants and monitored rosette internode elongation. In control plants, the application of these hormones did not significantly affect the compact internode architecture, preserving the characteristic rosette growth habit and further highlighting the robustness of this trait in Arabidopsis (C3_Fig. 2a-d). In contrast, *ath1* mutants displayed a marked increase in internode length following hormone application, particularly in case of GA, which induced a shift towards a more stem-like (caulescent) growth habit (C3_Fig. 2a-d). In alignment with this observation, treating *ath1* mutants with hormone biosynthesis inhibitors like paclobutrazol (PAC) or brassinazole (BRZ), which specifically inhibit GA and BR biosynthesis respectively, restored a compact rosette habit. Meanwhile, control plants showed no change (C3_Fig. 2e-f). To support these pharmacological analyses, we crossed *ath1* mutants with *pCLV3::rgaΔ17* plants and *bzr1-D* mutants. *pCLV3::rgaΔ17* plants express a GA-insensitive form of the DELLA repressor protein RGA in the shoot apex, resulting in GA-insensitivity in this tissue (Galvão *et al.*, 2012). The dominant *bzr1-1D* mutation causes a constitutive BR response (Wang *et al.*, 2002). Consistent with earlier findings, *ath1* plants regained a compact rosette structure when GA signaling was inhibited in the shoot apex (C3_Fig. 2g), while continuous BR signaling resulted in increased internode elongation in plants lacking *ATH1* (Wang *et al.*, 2002) (C3_Fig. 2h, i).

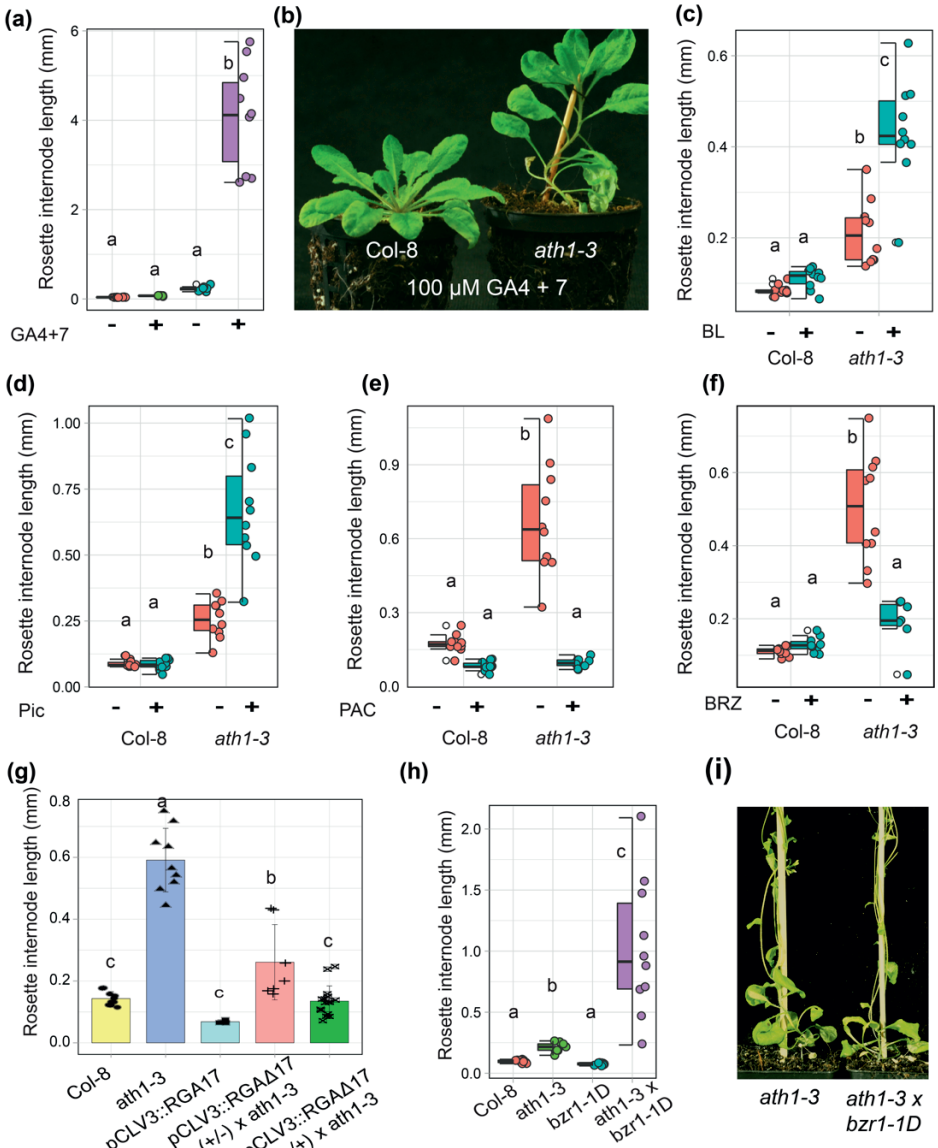


**C3_Fig. 2: Effect of growth regulators and mutations on rosette internode elongation in *Arabidopsis thaliana*.**

**(a)** Box plot depicting the relative internode length in Col-8 and *ath1-3* genotypes when grown under short day (SD) conditions and treated with either 0.1% DMSO or 100 µM gibberellic acid (GA4+7). **(b)** Visual comparison of Col-8 and *ath1-3* phenotypes following GA4+7 treatment. **(c)** Quantitative analysis of rosette internode elongation in Col-8 and *ath1-3* under standard long day (LD) conditions, with treatments of 0.1% DMSO (-) or 1 µM brassinolide (BL; (+)). **(d)**

Average internode elongation of LD-grown Col-8 and *ath1-3* plants treated with 0.1% DMSO (-) and 5 µM picloram (+). **(e)** Average length of rosette internodes of 0.1% DMSO (-) or 120 µM paclobutrazol (PAC; (+))-treated Col-8 and *ath1-3* grown under FR conditions. **(f)** Average rosette internode elongation of Col-8 and *ath1-3* mutants grown under LD conditions at 27°C and treated with 0.1% DMSO (-) or 1 µM BRZ (+). **(g)** Average rosette internode length of Col-8, *ath1-3*, *pCLV3::RGAΔ17*, and *ath1-3 pCLV3::RGAΔ17* (homozygous and heterozygous) plants grown under FR conditions. **(h)** Average internode elongation of LD-grown Col-8, *ath1-3*, *bzr1-1D* and *ath1-3 bzr1-1D*. **(i)** Representative phenotypes of *ath1-3* and *ath1-3 bzr1-1D* mutants in (h). Letters above the graphs indicate subsets of data that are statistically homogenous according to a one-way ANOVA, followed by a Fisher's least significant difference (LSD) test with Bonferroni correction (α = 0.05) from the agricolae package



Dependence on a normally functioning auxin and BR system for internode elongation was further emphasized by the identification of second-site mutations that reinstate a compact rosette growth habit in *ath1* mutants, even when subjected to low R/FR conditions or increased ambient temperature. In an EMS mutagenesis screen on *ath1* mutants to identify genetic components that suppress internode elongation, nine *suppressor of ath1-3 rosette internodes* (*sri*) mutants were obtained (C3_Fig. S2a). Two of these, *ath1 sri113* and *ath1 sri93*, could be linked to mutations affecting BR and auxin homeostasis, respectively. Apart from restoration of a compact rosette habit, both suppressor mutants exhibited general growth inhibition, resulting in smaller leaves, short petioles and/or shorter inflorescence stems. The *sri113* mutant was mapped to a G to A substitution in exon 4 of the BR biosynthesis gene DWF1 gene, causing an Gly-167 to Glu amino acid change. Gly-167 is a semi-conserved residue in the DWF1 FAD-binding domain that is believed to be critical for DWF1 function (Choe *et al.*, 1999). DWF1 catalyzes the conversion of 24-methylene cholesterol to 24-campesterol. Therefore, application of exogenous BL can rescue *dwf1* mutants (Klahre *et al.*, 1998; Choe *et al.*, 1999; Youn *et al.*, 2018). Similarly, BL-treatment rescued the observed general growth defects, as well as restored rosette internode elongation treating in *ath1-3 sri113* plants (C3_Fig. S2b, c). This strongly suggest that *DWF1* mutation is responsible for the repression of rosette internode elongation in *ath1-3* mutants. Remarkably, neither application of auxin or GA could induce rosette internode elongation in *ath1-3 sri113*, while these hormones are sufficient to do so in *ath1-3* plants (C3_Fig. S2d, e). When plants were treated with a mixture of GA and BL or picloram and BL, *ath1-3 sri113* mutants responded the same as *ath1-3* single mutants (data not shown). These results suggest that a complex, cooperative,

and interdependent relationship exists between GA, auxin and BR in inducing internode elongation in the absence of ATH1.

In the *ath1 sri93* mutant, we identified a SNP that changed the proline amino acid at position 70 in the conserved region of domain II of the SHORT HYPOCOTYL 2/INDOLE-3-ACETIC ACID INDUCIBLE 3 (SHY2/IAA3) protein to a serine. This same Pro70 → Ser70 mutation had previously been identified as *shy2-101* and was found to inhibit auxin-mediated degradation of SHY2/IAA3, making the mutant auxin-insensitive (Goh *et al.*, 2012). As expected, *ath1 sri93* plants were not responsive to treatment with both auxin and BL combined (C3_Fig. S2f). To confirm that this mutation was responsible for the observed phenotype, we sequenced individuals of a segregating population of *ath1-3 sri93* plants for the region containing this SNP. Plants homozygous for the SNP showed severe dwarfism, while heterozygous plants had an intermediate dwarfism phenotype in comparison to a normal growth and development in plants homozygous for the wild-type allele (data not shown).

To summarize, both pharmacological and genetic analyses show that the Arabidopsis rosette habit possesses remarkable stability and resilience due to the presence and activity of ATH1. This robustness is contrasted by the notable plasticity in elongation of vegetative internodes that can be observed in response to both environmental and hormonal cues when *ATH1* is absent. While our findings have so far illuminated the crucial roles of auxin, BR, and GA signaling in this developmental process, the exact molecular interactions and pathways by which ATH1 and these hormones coordinate internode elongation processes are yet to be fully understood.

**ATH1-mediated suppression of internode cell elongation involves local control of hormone homeostasis and light signaling pathways at the shoot apex**

To better understand the role of ATH1 in regulating RZ activity and subsequent internode elongation, RNA-seq analysis was used to compare shoot apex gene expression levels between *ath1* mutants and Col-8 control plants. To ensure the absence of RZ activity in control plants, this analysis was conducted under conditions non-inductive for bolting and flowering. This revealed 3,730 genes that were differentially expressed between the two genotypes ($p\text{-value} < 0.05$), of which 1,688 genes (45%) were upregulated and 2,042 genes (55%) were downregulated

in plants lacking *ATH1* (C3_Fig. 3a). The upregulated genes in the *ath1* mutants are primarily related to intracellular transport, transport, and localization, which might reflect the increased growth of internodes in these plants (C3_Fig. 3b). In addition, genes involved in hormone biosynthesis and response were overrepresented among the genes that were differentially higher expressed in *ath1* shoot apices (C3_Fig. 3b). Among these are *AMIDASE1* (*AMI1*) and *NITRILASE2* (*NIT2*), the products of which are involved in the production of the most common type of auxin in plants, indole-3-acetic acid (IAA), through the indole-3-acetaldoxime (IAOx) and indole-3-acetamide (IAM) pathways, respectively (Rosquete *et al.*, 2012). Apart from auxin biosynthesis, also BR and GA biosynthesis are likely to be targeted by ATH1, as BR biosynthesis genes *DWARF1 (DWF1)*, *DWF3*, and *DWF5* (Choe *et al.*, 1999), as well as the GA biosynthesis gene *ARABIDOPSIS THALIANA GIBBERELLIN 20-OXIDASE1* (*AtGA20OX1*) were significantly upregulated in *ath1* mutants. Collectively, and consistent with our observations that auxin, BR, and GA significantly promote internode elongation in absence of ATH1, this suggests that ATH1 regulates internode elongation by locally inhibiting accumulation of these hormones at the shoot apex.

The genes exhibiting downregulation in *ath1* mutants are predominantly linked to environmental responses and processes related to immunity and defense (C3_Fig. 3c), the latter of which could suggest that not only a compact rosette morphology itself, but also the regulatory mechanism underlying it, contributes to biotic stress resilience. Notably, the down-regulated genes associated to environmental responses are mostly involved in light (quality)- and temperature-mediated responses (C3_Fig. 3c). Again, this aligns well with our observations that low R/FR light quality ratios and warm temperatures promote internode elongation in *ath1* mutants (C3_Fig. 1a, b). Worth mentioning in this context are *ELONGATED HYPOCOTYL5* (*HY5)* and *HY5 HOMOLOGUE* (*HYH*), whose proteins acts as master regulators of a light-mediated transcriptional regulatory hub that, among others, negatively regulates hypocotyl and petiole elongation in light (Xiao *et al.*, 2022). At the same time, *PIF1* and *PIF4*, which also encode central regulators of light signaling and that, as key positive regulators of elongation growth, antagonize the effects of HY5 and HYH, showed a significant increase in expression in the shoot apices of *ath1* mutants (Hedden & Proebsting, 1999; Kim *et al.*, 2005a; Plackett *et al.*, 2012; Rosquete *et al.*, 2012).

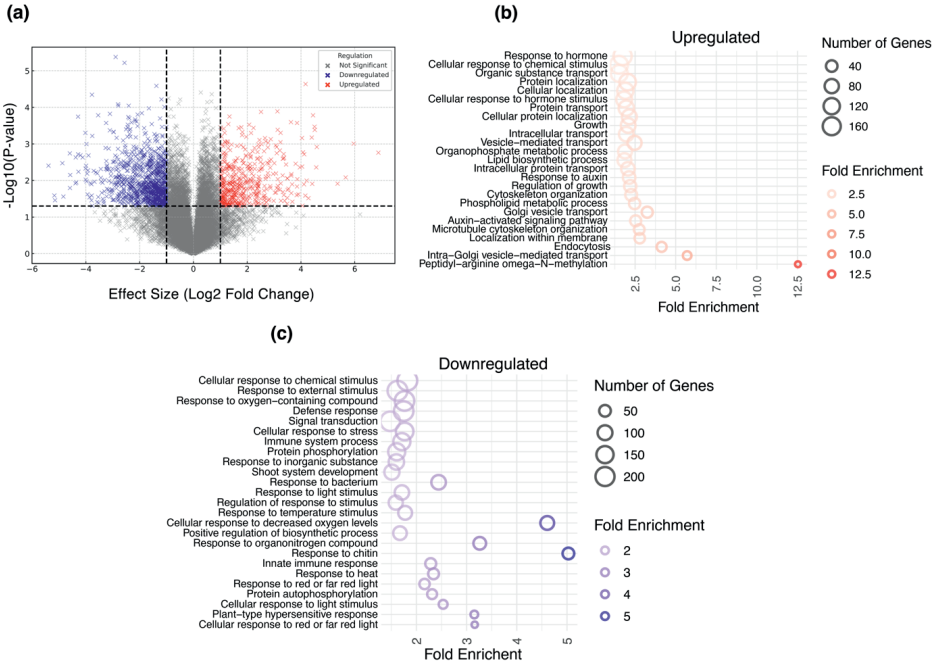


**C3_Fig. 3: Transcriptomic analysis and functional categorization of DEGs between the shoot apices of Col-8 and *ath1-3* mutants.**

**(a)** Volcano plot displaying the statistical significance (-log10 P-value) against the magnitude of change (log2 fold change) in gene expression between Col-8 (wild-type) and *ath1-3* mutants grown under SD conditions. Upregulated genes in *ath1-3* mutants (vs. Col-8) are shown in red, downregulated genes in blue, and genes with non-significant changes in gray. The dashed lines represent the threshold for statistical significance. **(b)** Bubble chart representing the biological processes enriched among the upregulated genes. The size of the bubble indicates the number of genes involved, and the color intensity represents the fold enrichment of the process. **(c)** Bubble chart representing the biological processes enriched among the downregulated genes, with bubble size and color intensity denoting the same as in **(b)**.

While our RNA-seq data suggest that ATH1 suppresses elongation of rosette internodes, thereby establishing a compact rosette habit, through local control of light signaling and hormone biosynthesis, such mechanism is not sufficient to explain the role of ATH1 in maintaining rosette habit a robust trait. The insensitivity of control plants to auxin, BR or GA application with respect to internode growth (C3_Fig. 2a-d), implies that the mechanism by which ATH1 confers robustness to this trait goes beyond simple regulation of hormone levels. It likely entails more

intricate regulation, such as modulation of hormone signaling pathways and their integration with environmental cues.

**Elongation of rosette internodes in *ath1* mutants is mediated by a central growth-regulatory circuit controlling cell expansion**

Our morphological observations have so far demonstrated that, in the absence of ATH1, elongation of rosette internodes has become plastic, and is influenced strongly by factors that regulate cell elongation such as light, hormones, and temperature (C3_Fig. 1a, b). As such, the plasticity of these internodes bears a striking resemblance to the phenotypic plasticity observed in hypocotyls (C3_Fig. 1c, d) (Krahmer & Fankhauser, 2024). Moreover, elongation of vegetative internodes in *ath1* mutants can be primarily attributed to cell expansion (C3_Fig. 1e-g), mirroring the mechanism driving hypocotyl elongation (Ma & Li, 2019). In Arabidopsis, hypocotyl cell elongation is regulated by complex crosstalk among hormonal and environmental signals, including particularly light, temperature, auxin, BR, and GA (Bai *et al.*, 2012a,b; Oh *et al.*, 2014). Overrepresentation of genes specifically involved in these hormonal pathways and/or light signaling among genes differentially expressed in shoot apices of *ath1* mutants (C3_Fig. 3b, c) underscores the striking similarity between hypocotyl growth plasticity and the observed rosette internode plasticity in *ath1* mutants. Collectively, this strongly indicates that a molecular mechanism similar to the one governing cell elongation in hypocotyls underlies the induced elongation responses in *ath1* rosette internodes. To better understand the role of ATH1 in regulating vegetative internode development, we, therefore, compared our gene expression dataset with a publicly available dataset from Kohnen et al. (2016), that resulted from a study investigating how hypocotyls respond transcriptionally to growth-stimulating conditions with low red/far-red light (C3_Fig. 4a, b). This study revealed a common gene expression pattern associated with promoting growth across various organ-specific growth processes under controlled environmental conditions (Kohnen *et al.*, 2016).

As expected, this comparison identified a significant number of differentially expressed genes (DEGs) shared between the two datasets (C3_Fig. 4c). Specifically, 269 genes upregulated in *ath1* shoot apices were also found to be upregulated in hypocotyls under low R/FR light conditions (*p-value of 4.4e-16*; hypergeometric test). These genes account for 8% of the total upregulated DEGs identified in both the shoot apex and hypocotyl datasets (C3_Fig. 4c).

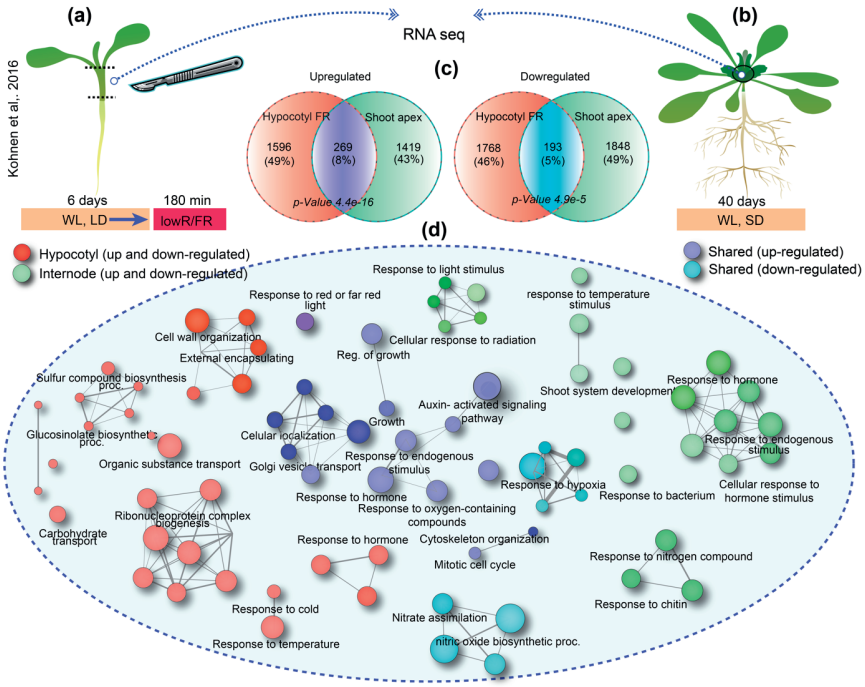


**C3_Fig. 4: Comparison of *ath1-3* shoot apex gene expression with Col-0 hypocotyl gene expression under low red/far-red light (Kohnen et al., 2016) reveals overlapping cell elongation related genes.**

**(a)** Schematic representation of the experimental design used by Kohen et al. (2016), where Arabidopsis seedlings were initially grown under standard light/dark cycles for six days, followed by exposure to low red/far-red (lowR/FR) light conditions for 180 minutes prior to harvesting for hypocotyl transcriptome analysis. **(b)** Diagram of the experimental conditions we used in this study for investigating the transcriptomes of internodes in *ath1-3* mutants and wild type (Col-8) plants. These plants were grown under short-day conditions with standard SD conditions for a duration of 40 days. Subsequently, RNA extractions were performed on tissues from their shoot apical meristems to assess differential gene expression. **(c)** Venn diagrams display the count of differentially expressed genes (DEGs) identified as upregulated or downregulated in Col-0 hypocotyls after treatment with lowR/FR light and in the internodes of *ath1-3* mutants. The p-values indicating statistical significance were derived using a hypergeometric test, underscoring the non-random association between the gene expression changes observed and the experimental treatments applied. **(d)** The ShinyGO Venn diagram network illustrates the interrelations among the top 20 enriched Gene Ontology (GO) terms for both upregulated and downregulated genes, in addition to those genes found in common between the two conditions. Node sizes correspond to the number of genes within each GO term, while edge thickness reflects the extent of gene overlap between connected terms. Nodes are interconnected if they share a substantial gene subset, defined as more than 20% commonality.

In addition, 193 genes were commonly downregulated (*p-value of 4.9e-5*), making up 5% of the combined downregulated DEGs (C3_Fig. 4c). GO term analysis of the shared upregulated and downregulated genes provided an overview of the biological processes and pathways commonly affected in these tissues (C3_Fig. 4d). Interestingly, GO terms for the upregulated shared genes included those related to light signaling, hormone response, and cellular growth processes, which suggests involvement of a conserved response mechanism to elongation-promoting environmental cues. Downregulated shared genes were associated with GO terms related to nitrogen assimilation and nitric oxide (NO) biosynthesis, as well as hypoxia response. NO is a key signaling molecule in several plant processes, including regulation of hypocotyl growth, and is a product of nitrate assimilation (Chamizo-Ampudia *et al.*, 2017). NO inhibits hypocotyl elongation, among others, through regulation of BR signaling components at the transcript level (Castillo *et al.*, 2018). Downregulation of associated genes, thus, fits well with the induced growth responses studied here. How to interpret the enrichment of hypoxia-response related genes is not clear. Hypoxia itself, does not directly influence hypocotyl elongation (Abbas *et al.*, 2015). Submergence stress, however, which results in hypoxia, does induce hypocotyl elongation in Arabidopsis (Wang *et al.*, 2019).

In essence, the significant overlap in DEGs between *ath1* shoot apices and hypocotyls exposed to low R/FR light indicates that ATH1 controls vegetative internode elongation by targeting a general mechanism that integrates multiple signaling pathways to govern cell elongation.

In Arabidopsis, the BAP/D module acts as a central nexus for cell elongation, coordinating environmental light signals with internal hormonal cues such as auxin, BR, and GA to regulate growth. Key to the BAP/D module are the transcription factors BZR1, ARF6, and PIF4, whose activity is inhibited by DELLA proteins. Upon deactivation by GA, DELLA proteins release these factors, promoting growth (Bai *et al.*, 2012a,b; Oh *et al.*, 2014). Considering these insights, we hypothesized that ATH1 might locally suppress cell elongation in the basal part of the shoot apex by modulating the activity of the BAP/D module. To test this hypothesis, we investigated the overlap between genes regulated by ATH1 and those targeted by the BAP/D module, focusing on cell elongation. We compared genes upregulated in the *ath1* mutant shoot apex with datasets detailing gene expression changes in hypocotyls in response to BR, auxin (Nemhauser *et al.*, 2004), and

low R/FR light conditions (Kohnen *et al.*, 2016). These conditions are known to induce hypocotyl elongation via modulation of the BAP/D module activity. We specifically selected genes that were upregulated in the *ath1* shoot apex dataset and present in at least one of the three BAP/D-related datasets (auxin, BR, low R/FR light). This analysis identified 95 genes upregulated in *ath1* shoot apices that were also responsive to cell elongation-promoting signals in hypocotyls (C3_Fig. 5a). In wild-type plants, the local inhibition of these genes by ATH1 might play a role in suppressing cell elongation in the basal area of the shoot apex, known as the RZ, thus maintaining a compact rosette habit. Consequently, we have termed these genes Rib Zone-repressed Genes implicated in Cell Elongation (RGCE). To further investigate the relationship between RGCE genes and growth, we analyzed their expression in seedlings shifted from growth-promoting dark conditions to growth-inhibiting light conditions (C3_Fig. 5b). Remarkably, 79 of the RGCE genes were significantly differentially expressed between these conditions. Importantly, a majority of them (82%; 65 genes) displayed opposite expression patterns between growth-inhibiting versus growth-promoting conditions (C3_Fig. 5b), underscoring a pivotal role of RGCE genes in regulating growth.

To investigate whether the RGCE genes can be directly regulated by components of the BAP/D module, using publicly available ChIP-seq datasets, we examined which of these 95 genes serve as binding targets of BZR1, ARF6, and/or PIF4 (Oh *et al.*, 2012). This revealed that 78% of these genes can be directly bound by at least one of these transcription factors, and that approximately 70% of the RGCE genes can be bound by at least two out of these three transcription factors (C3_Fig. 5c). Direct binding by LEAFY (LFY), a transcription factor known not to be involved in cell elongation processes, was included as a control (Moyroud *et al.*, 2011). LFY was found to be associated with only 12% of RGCE genes, showing a clear overrepresentation of BAP/D module transcription factor binding targets among the RGCE genes. Intriguingly, only a minor portion of the RGCE genes (7%) appeared as direct targets of ATH1 (Ejaz *et al.*, 2021). Interestingly, this includes PIF4, one of the members of the BAP/D module (C3_Fig. 5c). This indicates that ATH1 regulates the elongation of vegetative internodes by targeting the downstream effects of the BAP/D module, largely through indirect mechanisms, such as modulating signal inputs. This inference aligns with findings from our RNA-seq data. Additionally, ATH1 potentially exerts its influence by directly modulating key components of the central BAP/D module, including *PIF4*.

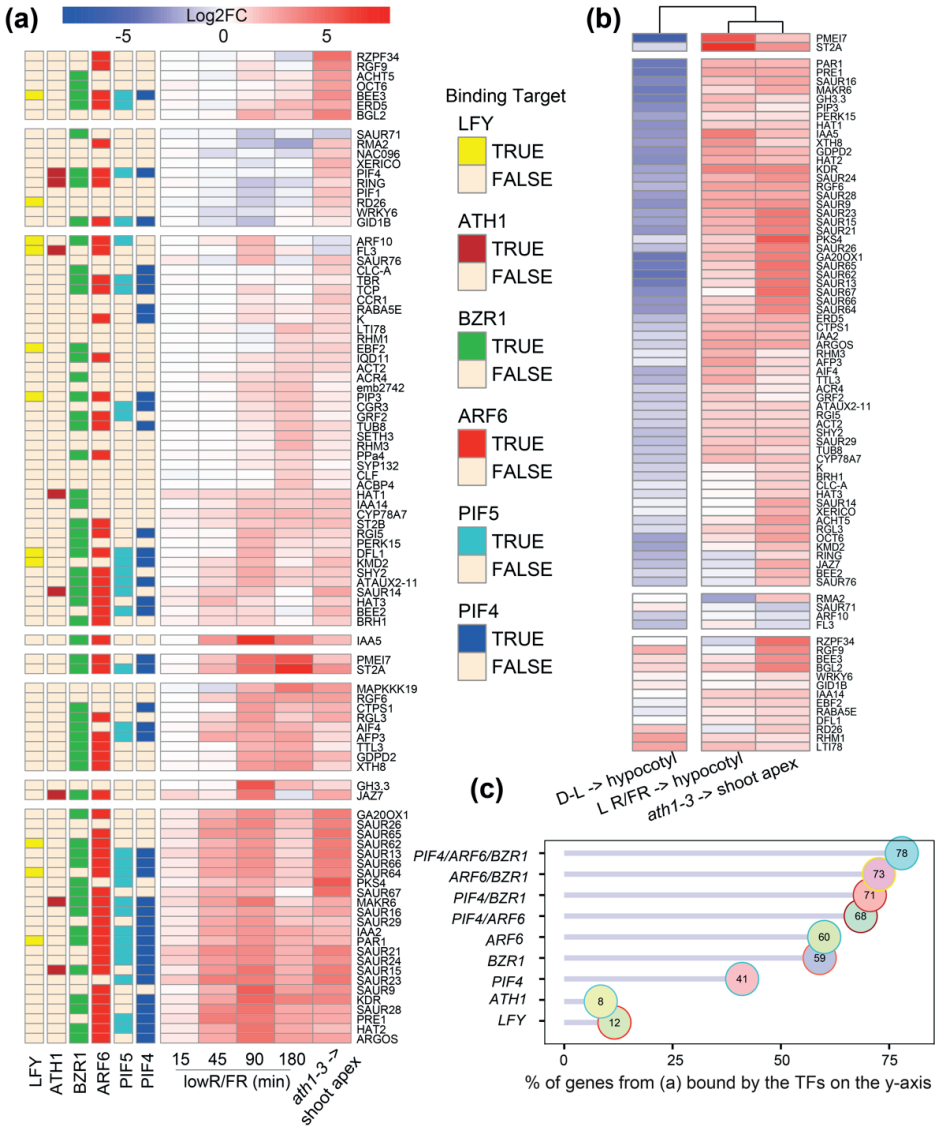


**C3_Fig. 5: Comparative analysis of gene expression in *ath1-3* mutant meristems and hypocotyls under light and hormonal treatments.**

**(a)** Heatmap comparing upregulated genes in *ath1-3* mutant shoot apices with those responsive to low red/far-red (R/FR) light, BR, and auxin in hypocotyls. The dataset from Nemhauser et al. (2004) was used to identify BR and auxin-responsive genes, whereas the dataset from Kohnen et al. (2016) was used to identify genes responsive to FR in the hypocotyl. This subset of genes was selected as being upregulated in *ath1-3* shoot apices and also showed increased expression in response to at least one of the other stimuli. For the heatmap we depicted the expression of these genes for Kohnen et al. (2016) data set in response to various treatments of light

alongside the *ath1-3* shoot apex gene expression. The annotated panel provides information on whether these genes are known direct transcriptional targets ('TRUE') of the transcription factors PIF4 (blue), PIF5 (cyan), ARF6 (red), BZR1 (green), ATH1 (tomato), and LFY (yellow), or not bound by these factors ('FALSE'). **(b)** Heatmap showing the expression values of a selection of genes from panel (a) that were found to be differentially enriched in a dataset of seedlings undergoing transformation from dark (growth-inducing) to light (growth-restricting) conditions. The expression of these genes in the hypocotyl was compared in response to FR (180 min; Kohnen et al. (2016)), internode (*ath1-3* dataset), and dark-to-light conditions (Sun et al. 2016). **(c)** Proportional analysis of transcription factor binding reveals complex regulatory interactions. This chart illustrates the percentage of genes from panel (a) that are direct transcriptional targets of the indicated transcription factors, either individually or in specific combinations. Individual factor percentages represent genes bound exclusively by that factor. Dual combination percentages represent genes bound by at least one of the two factors, while the trio percentage represents genes bound by at least one of the three factors.

**Local inhibition of PIF4 by ATH1 does not entirely account for rosette habit robustness**

The hypothesis that ATH1 directly targets the BAP/D member PIF4 to suppress cell elongation within the RZ is supported by several observations. As a central component of the BAP/D module, PIF4 is crucial for cell elongation in Arabidopsis (Bai *et al.*, 2012b,a; Oh *et al.*, 2014). Previously, ATH1 was shown to directly target *PIF4* at the transcriptional level (Ejaz *et al.*, 2021). Current work shows that *PIF4* expression is derepressed in *ath1* mutant shoot apices (C3_Fig. 5a), and our recent work shows that modulation of *PIF4* by ATH1 is meristem specific (Hajibehzad *et al.*, 2023). Moreover, 40% of RGCE genes are transcriptional targets of PIF4 (C3_Fig. 5c).

To examine the specific role of PIF4 in *ath1* rosette internode elongation, we crossed the *pif4-2* loss-of-function mutation into the *ath1-3* background. We then evaluated internode elongation in their offspring under growth-promoting conditions. In *ath1-3 pif4-2* mutants, internode elongation was significantly reduced at elevated temperatures and, to a lesser extent, under low R/FR light conditions (C3_Fig. S3a, b). Under low R/FR conditions, but not at warm temperatures, PIF4 is redundant to PIF7, which is essential for hypocotyl elongation in FR (Leivar *et al.*, 2008a). We therefore also generated *ath1-3 pif7-1* double mutants and grew them at 27°C or in low R/FR conditions. In low R/FR conditions, *pif7-1* completely suppressed internode elongation of *ath1-3*, whereas *ath1-3 pif7-1* mutants grown at 27°C elongated similarly to *ath1-3* single mutants (C3_Fig. S3c, d). Likewise,

when treated with GA and auxin *ath1-3 pif7-1* mutants responded as *ath1-3* single mutants (C3_Fig. S3e, f). Taken together, this suggests that induction of internode elongation in *ath1* mutants requires multiple PIFs, with PIF7 playing a dominant role in low R/FR conditions and PIF4 playing a more redundant role in both low R/FR conditions and at increased ambient temperature.

Consistently, in *ath1-3 pifq* mutants, which lack PIF1, PIF3, PIF4 and PIF5, elongation of vegetative internodes is completely eliminated in *ath1* plants when grown under normal light conditions (Ejaz *et al.*, 2021), as well as under elevated temperatures (C3_Fig. 6a, b). Nevertheless, *ath1-3 pifq* mutants exhibited internode elongation responses to external application of auxin and BR treatments similar to *ath1-3* mutants, while GA application had minimal effect (C3_Fig. 6c, d). The latter might be explained by the role of GA in promoting elongation responses through the alleviation of DELLA repression on PIFs.



While ATH1 affects the expression of several *PIFs* (C3_Fig. 5a; Hajibehzad *et al.*, (2023)), particularly *PIF4*, within the SAM, the simultaneous loss of multiple PIFs thus only conditionally restores a compact rosette habit in the absence of ATH1. Collectively, this suggests that while ATH1 inhibits elongation of rosette internodes by locally regulating the PIF pathway, the resilience of the rosette growth habit to growth-promoting signals cannot be solely attributed to this level of regulation by ATH1. Consistent with this notion, overexpression of *PIF4* alone did not lead to internode elongation in plants with functional ATH1 (C3_Fig. 7a, c, e).

The observation that the absence of PIF7 alone can fully restore the rosette habit in *ath1-3* mutants under low R/FR light conditions, while combined deficiencies in PIF1, PIF3, PIF4 and PIF5 still lead to partial elongation under similar conditions (C3_Fig. 6c, d), suggests that ATH1-mediated control of PIF7, in conjunction with its regulation of these other PIFs, might comprehensively account for the robustness of Arabidopsis rosette habit. However, *PIF7* expression seems unaffected by ATH1 (C3_Fig. 5a). This, and the resilience of vegetative internodes to diverse growth-inducing conditions, suggests the mechanism by which ATH1 controls this trait may be more complex.

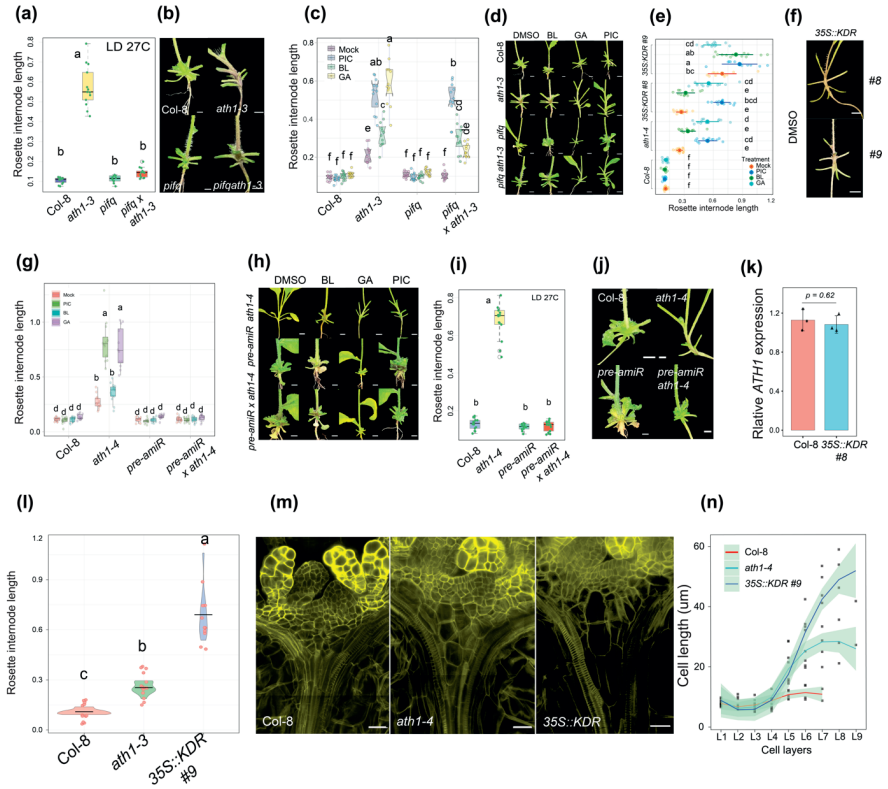


**C3_Fig. 6: Investigating the effects of light and growth regulators on rosette internode elongation.**

**(a)** Boxplot showing the average length of rosette internodes in Col-8, *ath1-3*, *pifq*, and *pifq ath1-3* genotypes grown under long-day (LD) conditions at 27°C. **(b)** Visual representation of Arabidopsis plants corresponding to data in (a). Scale bars = 2 mm. **(c)** Boxplot of average rosette internode lengths for Col-8, *ath1-3*, *pifq*, and *pifq ath1-3* grown under LD with treatments of 0.1% DMSO (mock), 5 µM Epi-brassinolide (BL), 1 µM auxin, and 100 µM gibberellin GA4+7. **(d)** Representative plant phenotypes from (c), detailing treatment responses. Scale bars = 3 mm. **(e)** Boxplot comparison of rosette internode lengths in Col-8 and *ath1-4*, alongside two lines overexpressing *KDR/PRE6* (*35S::KDR* #8 and #9), under LD conditions with various growth regulator treatments (0.1% DMSO (mock), 5 µM BL, 1 µM auxin, and 100 µM GA4+7). **(f)** Representative phenotypes for the data presented in (e). Scale bars = 3 mm. **(g)** Boxplot depicting the average length of rosette internodes for Col-8, *ath1-4*, *pre-amiR*, and *pre-amiR ath1-4* genotypes grown under LD at 22°C treated with 0.1% DMSO (mock), 5 µM BL, 1 µM auxin, and 100 µM GA4+7. **(h)** Illustrative phenotypes for genotypes and treatments shown in (g). Scale bars = 3 mm. **(i)** Boxplot analysis of rosette internode lengths for Col-8, *ath1-4*, *pre-amiR*, and *pre-amiR ath1-4* genotypes grown under LD at 27°C. **(j)** Photographs of representative plant phenotypes from (i). Scale bars = 2 mm. **(k)** Relative *ATH1* gene expression levels in 1-week-old Col-8 and *35S::KDR #8* seedlings grown under LD conditions, as determined by

quantitative PCR (qPCR). Data represent the mean of three to four biological replicates, with statistical significance assessed by Student's t-test (*p-values* indicated). **(l)** Boxplot illustrating the average length of rosette internodes in Col-8, *ath1-3*, and *35S::KDR #8* grown in LD at 22°C. **(m)** Confocal microscopy images of median longitudinal sections of shoot apical meristems in 7-day-old Col-8, *ath1-4*, and *35S::KDR #8* seedlings grown at 22°C. Scale bars represent 10 µm (**n**) Graphical quantification of cell lengths from meristem sections in (m), measured along the apical-basal axis. Four to five individual apices were analyzed per genotype and condition. Statistical groupings indicated by letter annotations are derived from a one-way ANOVA, followed by Fisher's least significant difference (LSD) test with Bonferroni correction (α = 0.05), utilizing the agricolae package.



**Local inhibition of *PRE6/KDR* within the shoot apex is of paramount importance for the robustness of the rosette habit in Arabidopsis**

The BAP/D module exhibits a complex interplay with the downstream HLH/bHLH module, which is a critical determinant in the regulation of cell elongation. Within this intricate framework, *PRE* genes, which encode a suite of non-DNA-binding HLH factors, play a proactive role in promoting cell elongation. PRE proteins engage in dynamic interactions with other members of the HLH and bHLH protein families, effectively serving as modulatory bridges within the growth-promoting signaling cascade. By binding to and sequestering HLH factors that act as negative regulators of cell elongation, PREs create an environment that is conducive to cell growth (Bai *et al.*, 2012b,a; Wang *et al.*, 2012; Oh *et al.*, 2014).

Our RGCE gene set includes two *PRE* genes, *PRE1* and *PRE6/KIDARI* (*PRE6/KDR*) (C3_Fig. 5a). Both genes are direct transcriptional targets of BAP/D module transcription factors and are significantly upregulated in *ath1* shoot apices (C3_Fig. 5a). They are, thus, integral to cell elongation processes downstream of the BAP/D module (Bai *et al.*, 2012b,a; Wang *et al.*, 2012; Oh *et al.*, 2014). This suggests that local suppression of these *PRE* genes within the meristem could be key to the maintenance of a compact rosette habit by ATH1.

To test this, we crossed the *ath1-4* mutant with a transgenic line expressing a *pre-amiR* construct, which was designed to suppress the expression of four *PRE*-gene members (*PRE1*, *PRE2*, *PRE5*, and *PRE6*/*KDR*) via artificial microRNA technology (Oh *et al.*, 2014). The resulting *ath1-3 pre-amiR* plants maintained a compact rosette habit across a range of environmental and hormonal conditions, including elevated temperatures and exogenous application of auxin, BR, or GA (C3_Fig. 6g-j). Furthermore, *PRE6/KDR* overexpression significantly elongated

rosette internodes in wild-type plants and in plants with Dex-induced constitutive *ATH1* expression (C3_Fig. 7b).

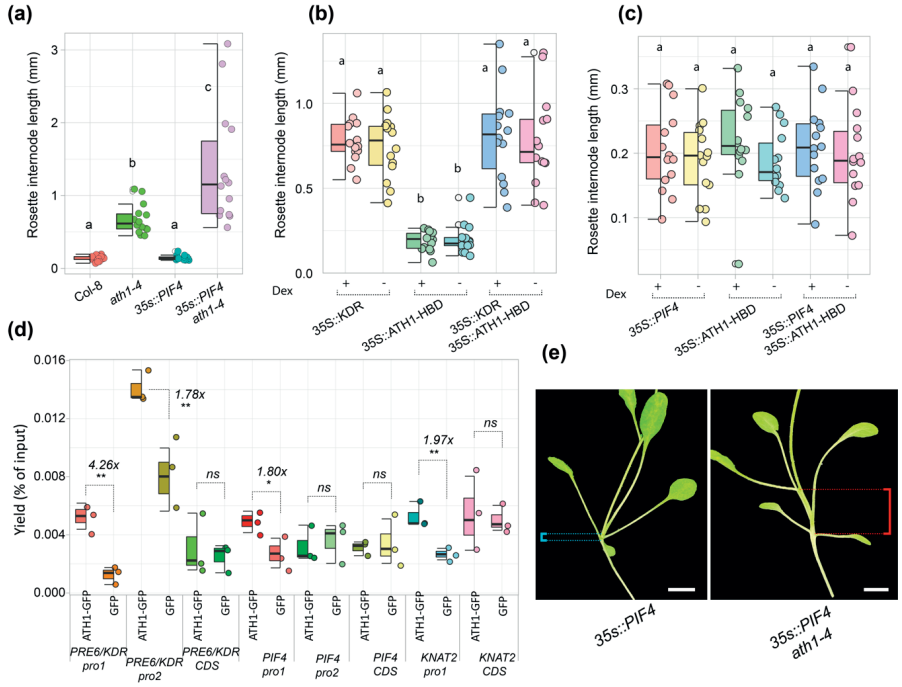


**C3_Fig. 7: Analysis of ATH1 binding to promoters of *KNAT2*, *PRE6/KDR* and *PIF4* as revealed by ChIP-qPCR.**

**(a)** Average length of rosette internodes (mm) in Col-0, *ath1-4*, *35S::PIF4*, and *35S::PIF4 ath1-4* plants grown under long-day (LD) conditions at 22°C, showing significant differences among genotypes as indicated by different letters (a, b, c). **(b)** The average length of rosette internodes in *35S::KDR* (#8), *35S::ATH1-HBD*, and *35S::KDR; 35S::ATH1-HBD* plants grown under standard LD conditions at 22°C in the presence (+) and absence (-) of dexamethasone (Dex), showing significant differences among genotypes as indicated by different letters (a, b). **(c)** The average length of rosette internodes in *35S::PIF4*, *35S::ATH1-HBD*, and *35S::PIF4 35S::ATH1-HBD* plants grown under standard LD conditions at 22°C in the presence (+) and absence (-) of dexamethasone (Dex), with differences among treatments denoted by different letters. **(C)** The average length of rosette internodes in *35S::PIF4*, *35S::ATH1-HBD*, and *35S::PIF4; 35S::ATH1-HBD* plants grown under standard LD conditions at 22°C in the presence (+) and absence (-) of dexamethasone (Dex). **(d)** ChIP-qPCR analysis of the interaction between ATH1 and ATH1 binding motifs containing GATTGA boxes in the promoters and coding sequences of the *PRE6/KDR*, *PIF4*, and *KNAT2* genes. Fold enrichment over the control is shown, with statistical significances indicated (n.s. not significant, *p<0.05, **p<0.01). KNAT2 was used as

a positive control because it has been demonstrated to be a direct and strong transcriptional target of ATH1. The results of the ChIP assay, obtained from three independent biological replicates, are shown as a percentage of the input (yield; % of input) with fold changes indicated above the bars. **(e)** Representative plants from (a). Scale bars represent 10 mm, with the *35S::PIF4 ath1-4* genotype showing a noticeable increase in internode length compared to *35S::PIF4*. One-way analysis of variance (ANOVA) and Fisher's LSD test with Bonferroni correction ($\alpha = 0.05$) were used to determine the statistical homogeneity of the data subsets indicated by letters above the graphs. The analysis was performed using the agricolae package in R.

On top of this, *PRE6/KDR*-mediated internode elongation was only minimally affected by the addition of exogenous auxin or BR, and remained unaffected by GA application (C3_Fig. 6e, f). Elongation of rosette internodes can also be observed in *35S::PRE1* plants (see Figure 1A in (Lee *et al.*, 2006)). Crucially, elongation of rosette internodes in *PRE6/KDR* overexpression lines occurred independently of changes in *ATH1* expression (C3_Fig. 6k), supporting the hypothesis that ATH1's governance of compact rosette formation relies on downstream inhibition of *PRE* genes. Importantly, seedlings overexpressing *PRE6/KDR* exhibited a more pronounced cell elongation in the RZ and longer internodes compared to the *ath1-4* mutants (C3_Fig. 6l-n). This emphasizes the significance of PRE6/KDR in regulating cell elongation in the RZ and, consequently, maintenance of rosette habit downstream of ATH1.

To further dissect the mechanism by which *ATH1* regulates the expression of *PRE6/KDR* to promote compact rosette growth, we employed Chromatin Immunoprecipitation quantitative real-time PCR (ChIP-qPCR) assays on SAM-enriched material from rosette-stage *ath1-3* plants complemented with an *pATH1::ATH1-GFP* reporter construct (*ath1-3 pATH1:ATH1-GFP;* (Ejaz *et al.*, 2021)). Plants expressing nuclear-localized Green Fluorescent Protein from the ATH1 promoter (*pATH1:GFP-nls*) were used as an experimental control. Promoters of *PIF4* and *KNOTTED-LIKE FROM ARABIDOPSIS THALIANA 2* (*KNAT2*) served as positive controls for ATH1 binding targets, given previous evidence of ATH1 binding to GATTGA-motif containing regions in these promoters (Ejaz *et al.*, 2021). To examine whether ATH1 directly regulates *PRE6/KDR*, we searched for ATH1-binding motifs in the *PRE6/KDR* promoter. This identified two GATTGA-motifs in a 2kb-region upstream of the *PRE6/KDR* transcription start site. A ChIP-qPCR assay using vegetative *ath1-3 pATH1:ATH1-GFP* plants confirmed previous observation of ATH1 binding to the promoters of PIF4 and KNAT2 and revealed that ATH1 can bind to both regions of the *PRE6/KDR* promoter containing the GATTGA-motif (C3_Fig.

7d), indicating that in vegetative shoot apices *PRE6/KDR* is a direct transcriptional target of ATH1. By local suppression of *PRE6/KDR*, and possibly also of *PRE1*, in the RZ, ATH1 prevents RZ activation. This inhibition results in the lack of internode elongation observed during vegetative growth, contributing to the distinctive compact rosette form commonly seen in Arabidopsis plants during this developmental stage. Overall, ATH1 thus inhibits the elongation of vegetative internodes by locally targeting the BAP/D module core, through direct regulation of *PIF4*, as well as by modulating BAP/D signal inputs. Additionally, also at the transcriptional level, ATH1 directly regulates members of the PRE-IBH1-HBI1 tripartite HLH/bHLH module, which are pivotal in growth regulation downstream of the BAP/D module.

Establishing redundant and interconnected mechanisms that ensure stability in response to environmental fluctuations, the localized, multilevel regulation facilitated by ATH1 probably plays a crucial role in providing robustness to a compact rosette growth habit in Arabidopsis.

## Discussion

While plant development displays notable adaptability, certain traits maintain consistency, regardless of varying environmental conditions. The capacity of an organism to maintain a stable phenotype amidst environmental changes is known as robustness. Arabidopsis rosette habit, a distinctive feature of its vegetative growth phase, demonstrates exceptional resilience to both environmental and genetic variations. Here, we show that this robustness lies in the regulatory network orchestrated by the transcription factor ATH1. While other plant structures, such as hypocotyls, petioles, and inflorescence stems exhibit strong plasticity in elongation responses to such cues, compact rosette habit is maintained due to local suppression of a central growth-promoting network by ATH1, thereby preventing RZ activation and subsequent elongation of vegetative internodes.

This growth-promoting network, comprising the BAP/D module and its downstream HLH/bHLH module, integrates signals from endogenous auxin, BR, and GA hormones, as well as environmental stimuli like light and temperature, to stimulate cell expansion.

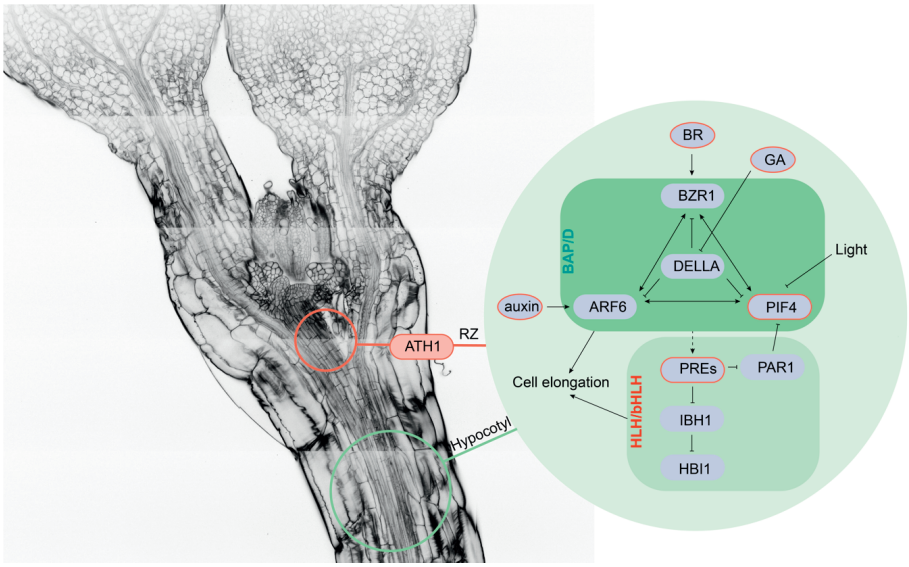


**C3_Fig. 8: ATH1 exerts local, multilevel control over a general cell elongation network in the RZ to promote a compact rosette habit.**

This figure highlights the multi-level regulatory influence of the ATH1 gene on cell elongation processes within the RZ, contrasting this mechanism with established cell elongation pathways in the hypocotyl. ATH1 modulates a core cell elongation program, comprised of the BAP/D module (dark green) and HLH/bHLH module (light green), at input level by modulating auxin, BR, and GA hormone homeostasis – hormones important for cell elongation. Additionally, ATH1 directly affects the core of the BAP/D module, by directly binding to the PIF4 promoter, thereby inhibiting its expression alongside that of other PIFs within the shoot apex. Crucially, ATH1 also (directly) affects BAP/D signaling output by repressing multiple PREs, major components of the HLH/bHLH module. This localized, multilevel suppression of a general cell elongation network is key for the ATH1-mediated robustness of rosette habit in Arabidopsis. Red circles emphasize ATH1's regulatory impact on the core cell elongation modules, as identified in this work.

This coordinated regulation facilitates high levels of developmental plasticity, particularly in structures such as hypocotyls and petioles. Developmental plasticity and robustness exist as opposite ends of a spectrum, sharing mechanistic connections where the presence of one inherently excludes the other (Schwab *et al.*, 2019). Our research indicates that within the shoot apex ATH1 plays an active role in suppressing signaling within this plasticity-promoting network during the vegetative growth phase, thereby conferring robustness to compact rosette growth habit (C3_Fig. 8). This suppression occurs at multiple levels, further contributing to the robustness of this trait. First, ATH1 presumably regulates

hormone balance, thus constraining the impact of growth-promoting hormones on RZ activity. Secondly, ATH1 directly represses expression of key components within the BAP/D module, including PIF4. Lastly, and of crucial importance, ATH1 directly inhibits expression of *PRE* transcriptional regulators that are central to the HLH/bHLH module (C3_Fig. 8). This specific suppression presumably leads to the indirect silencing of numerous downstream genes crucial for cell elongation, as highlighted by our RNA-seq findings. This multifaceted regulation underscores ATH1's significance as a central regulator of internode growth and development and plays a vital role in maintaining the robustness of Arabidopsis rosette habit.

Our findings suggest that ATH1 primarily inhibits internode elongation by regulating cell elongation. Three key hormones influencing cell elongation are auxin, BR, and GA (Oh *et al.*, 2014). Our transcriptome analysis indicates that ATH1 regulates the levels and activity of these hormones within the shoot apex. However, this regulation alone appears inadequate to account for the resilience of rosette habit, as external hormone treatments do not promote internode elongation in plants with functional ATH1. Hence, ATH1 likely targets primarily the core cell elongation network downstream of these hormones.

Robustness is commonly attributed to gene network topology, including feedback or feedforward regulatory loops (Lempe *et al.*, 2012; Boukhibar & Barkoulas, 2016). Our previous work identified a SAM-specific, double-negative ATH1-PIF feedback loop at the basis of rosette habit (Hajibehzad *et al.*, 2023; Chapter 2). However, while this ATH1-PIF feedback loop plays a crucial role in maintaining the rosette habit, it alone cannot fully account for the robustness of this trait. Our current findings indicate that even when multiple PIFs (PIF1, 3, 4, 5) are disrupted in a background lacking functional ATH1, elongation of rosette internodes remains plastic under certain conditions. Moreover, overexpression of *PIF4* leads to elongation of rosette internodes solely in the absence of ATH1. In contrast, when multiple PREs are suppressed, robust rosette habit is restored in an *ath1* mutant background. Furthermore, overexpression of *PRE6/KDR* alone is sufficient to induce elongation of rosette internodes, even in the presence of ATH1. Since ATH1 directly inhibits *PRE6/KDR* accumulation within the shoot apex, and potentially also *PRE1*, ATH1 likely enhances the robustness of the rosette growth habit by concurrently targeting multiple *PREs*, both directly and indirectly. The latter in-

volves the regulation of BAP/D module activity, achieved through hormonal input modulation and direct transcriptional regulation of BAP/D core components.

PREs play a crucial role in in facilitating growth by promoting cell elongation throughout various stages of plant development. They likely interact with both inhibitory bHLH factors (like IBH1) and PIFs to achieve this. PREs may stimulate growth by counteracting inhibitory bHLHs and potentially by facilitating PIF activity. The latter may occur through the inhibition of PHYTOCHROME RAPIDLY REGULATED1 (PAR1) and PAR2, which in turn inhibit PIF4 (Lee *et al.*, 2006; Zhang *et al.*, 2009). Alternatively, PREs might directly inhibit IBH1, which typically sequesters the growth-promoting HBI1. Inhibiting IBH1 could activate HBI1 alongside ARF6, promoting cell growth (Oh *et al.*, 2012). Hormones such as auxin, BR, and GA, known for their involvement in cell elongation-based growth, regulate PRE activity. They maintain elevated *PRE* levels in actively growing organs, while decreased hormone levels in mature organs may result in reduced *PRE* expression, allowing inhibitory bHLHs to predominate and impede growth. *ATH1*, during the vegetative growth phase stably expressed in the RZ of the SAM, thus most likely promotes robust rosette habit by locally repressing *PRE*s, including *PRE1* and *PRE6/KDR* (C3_Fig. 8). This suppression likely tips the balance towards IBH1 activity (and potentially indirectly reduces PIF4 activity), thereby inhibiting cell elongation and maintaining the compact rosette form. Interestingly, in the SAM *ATH1* is downregulated upon the reproductive phase change, which coincides with the onset of rapid stem elongation (bolting). This suggests that downregulation of ATH1 in the SAM could potentially shift the balance towards PRE dominance, which may lead to cell elongation and the initiation of bolting. However, the exact mechanisms by which ATH1 and hormones regulate this balance, along with the precise roles of PREs and IBH1, require further investigation. Future studies exploring these mechanisms and the relationship between *ATH1* expression, hormone signaling, and PRE/IBH1 activity within the SAM will offer a deeper understanding of the molecular mechanisms underlying internode elongation.

As mentioned, developmental robustness arises from the structure of gene networks, which includes factors such as redundant gene activity, gene interconnectivity, and regulatory framework (Lachowiec *et al.*, 2016). Here, we trace developmental robustness of compact rosette growth habit to a specific member of the BLH-type TALE homeobox transcription factor gene family, *ATH1*. Rosette growth habit represents an adaptive strategy that enables plants to thrive in

various environmental conditions while efficiently utilizing available resources. Having just a single key regulator in place, streamlining the genetic architecture required for the rosette habit, offers efficiency and potential adaptability. However, it also introduces risks, as mutations in *ATH1* could have significant phenotypic impact. This trade-off between efficiency and vulnerability is a fascinating aspect of streamlined regulatory systems. Remarkably, *ATH1* expression itself remains robust across a wide range of environmental cues, including light quality and metabolic signals (C3_Fig. S1b; Hajibehzad *et al.*, 2023). This consistent expression under diverse conditions is likely fundamental to the resilience observed in the rosette habit.

While our discoveries may diverge from prevalent assumptions regarding the molecular basis of robustness, there is precedent for trait robustness being upheld by the activity of a single member within a gene family. Specifically, the *BES1/BZR1 HOMOLOG* (*BEH*) transcription factor *BEH4* has previously been identified as maintaining the robustness of dark-grown hypocotyl length (Lachowiec *et al.*, 2018). In case of *BEH4*, it was hypothesized that its role in developmental robustness arises through the topology of its connections with other family members. BEH4 likely facilitates developmental robustness by ensuring appropriate cross-talk among members of the BZR/BEH family. ATH1 is known to form functional heterodimers with other members of the TALE homeodomain (HD) family of transcription factors (Bellaoui *et al.*, 2001; Rutjens *et al.*, 2009). At the same time, members of the TALE HD family are (potential) transcriptional targets of ATH1 (Ejaz *et al.*, 2021). Future work will show if ATH1, in a similar vein to BEH4, promotes developmental robustness by integrating regulatory cross-talk among these gene family members. Furthermore, this example highlights the diverse strategies employed by biological systems to achieve robustness, thereby enhancing our comprehension of adaptation and survival.

## Materials and Methods

### Plant materials, growth conditions and phenotyping

All *Arabidopsis thaliana* genotypes employed in this study, including the wild-type Columbia-8 (Col-8; NASC ID: N60000), Landsberg *erecta* (L*er*; NASC ID: NW20), and various mutants and transgenic lines were sourced from the Not-

tingham Arabidopsis Stock Center, unless otherwise specified. The specific genotypes used were as follows: *ath1-3* (Proveniers *et al.*, 2007), *ath1-4* (Li *et al.*, 2012b), *pif4-2*, *pif7-1, pif1pif3pif4pif5 (pifq)* (Leivar *et al.*, 2008b)*, CLV3::rgaΔ17* (Galvão *et al.*, 2012), *bzr1-D* (Wang *et al.*, 2002), *pre-amiR* line (Oh *et al.*, 2012), *35Spro:ATH1-HBD*, *Pro35S:HA-ATH1* (Proveniers *et al.*, 2007), *phyB-5* (Reed *et al.*, 1993), *phyBcry1* (Mazzella *et al.*, 2000), *hy1cry1*, *hy1cry1cry2* (López-Juez *et al.*, 2008), and *35S:KDR* (lines 8 and 9) (Buti *et al.*, 2020). The *ath1 sri113* and *ath1 sri93* suppressor mutants were derived from an in-house ethyl methane sulfonate (EMS) mutagenesis screen (see below for details).

Seeds were sterilized using chlorine gas for 4 hours, employing a mixture of 4 ml 37% HCl and 100 ml commercial bleach (4.5% active chlorine), and then sown on either soil (Primasta B.V., Asten, The Netherlands) or sterile 0.8% plant agar (Duchefa Biochemie B.V., Haarlem, The Netherlands) supplemented with full-strength Murashige–Skoog medium (including MES, pH 5.8, and vitamins). Stratification was carried out for 2–3 days at 4°C. Plants were grown in climate-controlled growth cabinets (Microclima 1000; Snijders Labs, Tilburg, The Netherlands) under short-day (SD; 8 h light/16 h dark) or long-day (LD; 16 h light/8 h dark) photoperiods, at a light intensity of 120 µmol $m^{-2}$ $s^{-1}$ (Luxline Plus Cool White, Sylvania, OH, USA), and 70% relative humidity. For specific light conditions, a Snijders Microclima cabinet equipped with Philips GreenPower LEDs was utilized, providing red, blue, and far-red light at specified intensities.

Measurements of average internode length and hypocotyl elongation were standardized across samples. Internode length was calculated by measuring the height from the cotyledons to the last rosette leaf with a digital caliper and dividing by the number of rosette leaves. Hypocotyl lengths were obtained using a flatbed scanner and analyzed with ImageJ software, ensuring consistent scale and measurement settings across all samples. RZ cell length (C3_Fig. 6m) was assessed via confocal laser scanning microscopy. Median, longitudinal optical sections through shoot apices identified a central cell file extending from the epidermis to the subapical region where hypocotyl vascular strands converge. Individual cell lengths in this file were measured in the apical-basal direction using ImageJ.

**Hormone treatments**

Plants were initially grown for one week on MS plates containing a 0.1% mock solution (either ethanol or DMSO, depending on hormone compatibility). Treat-

ments with 1 µM Picloram (Auxin; Sigma-Aldrich), 100µM GA4+7 (GA; Duchefa), or 5µM epi-brassinolide (BR; Sigma-Aldrich) were applied directly to the plates. Following this initial week, the seedlings were transferred to soil. These hormone applications were continued thrice weekly, utilizing a precise method (e.g., spray bottle) to apply the hormone solutions, which were enhanced with 0.01% Silwet-L77 to ensure effective adherence to the shoot apex. This regimen was maintained until the opening of the first flower, employing a mock solution as a control for comparison. Paclobutrazol (PAC) treatments commenced with seeds germinated on a nylon membrane (Sefar Nitex 03-100/44) atop MS agar plates, facilitating easier handling. After germination, seedlings were moved to MS agar plates enriched with a PAC solution of specified concentration (120 µL PAC, 5µM final concentration) or a 0.1% DMSO mock solution. On the seventh day, seedlings were transplanted to soil and received either mock or PAC treatments, supplemented with 0.01% Silwet L-77 to enhance application efficacy, applied by spraying three times a week. Following the onset of flowering, the elongation of the rosette internodes was measured to evaluate the impact of the treatments on plant growth, using a digital caliper for precision.

**EMS treatment of *ath1-3* seeds and mutant selection**

EMS-induced mutant plants of the *ath1-3* genotype were generated by initially soaking approximately 50,000 seeds in water at 4°C overnight to synchronize germination. These seeds were then divided into three groups and treated with 0.3%, 0.4%, or 0.6% v/v ethyl methane sulfonate (EMS; Sigma-Aldrich), ensuring even exposure by incubating overnight at room temperature with gentle shaking, under safe handling conditions to mitigate EMS's mutagenic risks. Post-treatment, the seeds (M1) underwent several washes to thoroughly remove any residual EMS and were then sown under long-day (LD) conditions for growth. The resulting M1 plants were organized into 40 pools for harvesting M2 seeds. M2 seeds, specifically those from the 0.3% EMS treatment, were suspended in 0.1% agarose solution and densely planted on soil. After three weeks of growth at 27°C under LD conditions, plants not exhibiting rosette internode elongation (identified as *sri* mutants) were selected and subjected to low red to far-red (R/FR) light conditions. Any *ath1-3 sri* mutants showing internode elongation under these conditions were discarded. M3 seeds were collected from the remaining plants. For identification of true suppressor mutants within the M3 generation

of *ath1-3 sri* mutants, we replicated the initial M2 screening process. Selected mutants were back-crossed with *ath1-3* to produce BC1F1, followed by selfing to generate BC1F2 seeds. These seeds were grown under LD conditions at 27°C for 15 days at a medium density, then under short-day (SD) conditions for an additional 15 days to promote biomass accumulation. From each of the BC1F2 *ath1-3 sri* lines, leaf material was collected from at least 50 individuals showing the suppressor phenotype and from 50 parental *ath1-3* mutants for comparison. Genomic DNA was then extracted from these samples using the DNeasy Plant Mini Kit (QIAGEN), ensuring a rigorous approach to identifying genetic suppressors of the *ath1-3* phenotype. At the Utrecht Sequencing Facility (USEQ; www.useq.nl), 500 ng of genomic DNA was used to generate libraries, which were then sequenced on Illumina NextSeq500 sequencers using the TruSeq DNA Nano LT kit (Illumina). The reads were 2x150 bp in length and had a coverage of more than 50x. The quality of the raw reads was assessed using FastQC version 0.11.8, and reads with a Phred score lower than 20 were trimmed using Trim Galore! version 0.6.0. The SIMPLE version 1.8.1 bioinformatic pipeline (Wachsman *et al.*, 2017) was employed to align the reads to the Arabidopsis TAIR10 reference genome, identify SNPs, and discover potential causal mutations.



**RNA-sequencing data analysis**

RNA sequencing was performed on wild type (Col-8) and *ath1-3* mutant *Arabidopsis thaliana* plants grown under the short-day conditions (8 h light, 16 h dark; 21°C; %70 humidity) for 40 days. Three shoot apical meristems were carefully collected from each biological replicate of the plants, snap frozen in liquid nitrogen and stored at -80°C. RNA was extracted from these meristems using the Qiagen RNAeasy micro-kit and sent to the Utrecht Sequencing Facility (USEQ; www.useq.nl) for sequencing. Sequence reads from raw FASTQ files underwent quality control using FastQC (v0.11.8). TrimGalore (v0.6.5) trimmed reads based on quality and adapter presence, followed by another FastQC check. rRNA reads were filtered using SortMeRNA (v4.3.3), and the remaining reads were aligned to the reference genome fasta using STAR (v2.7.3a). QC on mapped files was performed using Sambamba (v0.7.0), RSeQC (v3.0.1), and PreSeq (v2.0.3). Readcounts were generated using Subread FeatureCounts module (v2.0.0) with Arabidopsis_thaliana.TAIR10.51.gtf as annotation, and normalized using edgeR (v3.28). Differential expression analysis was performed using an in-house R-script with DESeq2 (v1.28)

and raw readcounts as input. Genes with an average of less than 1 annotated read per sample were removed. For the remaining genes, mean read count, log2FC, and p-value between genotypes were calculated.

**Cloning and assembly of the *pATH1::GFP-nls* transcriptional fusion construct**
The ATH1 promoter (Proveniers *et al.*, 2007) was PCR-amplified with Gateway-compatible attB sites and cloned into *pDONR-pATH1*. The *nlsGFP* sequence was cloned from *pGREEN:GW:NLS-GFP* (Horstman et al., 2015) and integrated into *pGEMT221-nlsGFP*. *pDONR-pATH1* and *pEN-R2-6-L3* (containing NOS-terminator; (Karimi *et al.*, 2007)) were linearized with PvuI to facilitate Multisite Gateway reaction, which assembled the *ATH1* promoter, *nlsGFP*, *pEN-R2-6-L3* NOS-terminator, and the final *pATH1::GFP-nls* construct within the *pGrnII0125-R4R3* binary vector. Following transformation into *E. coli* and selection on kanamycin, positive clones were verified by colony PCR, restriction analysis, and sequencing. Subsequently, the *pATH1::GFP-nls* construct was introduced into Arabidopsis wild type plants (Col-8) using floral dip transformation method. Homozygous plants harboring the integrated construct were selected through antibiotic resistance and PCR analysis, and these plants were used for ChIP-qPCR experiments.

**ChIP-qPCR and qPCR-based gene expression analysis**
For ChIP-qPCR, approximately 1,500 *ath1-3 pATH1-ATH-GFP* and *pATH1::GFP-nls* plants were grown for 40 days under standard SD conditions (SD; 8 h light/16 h dark) to make sure all plants were in the vegetative growth phase. SAM-enriched material was carefully isolated by first removing all leaves from the vegetative shoot apices and then any remaining tissue until the SAM was visible under a binocular microscope. Samples were then promptly frozen on dry ice. A modified version of the previously described ChIP assay protocol was used for this experiment (Gendrel *et al.*, 2005; Payá-Milans *et al.*, 2019). SAM tissue crosslinked with formaldehyde (1% final concentration) in a vacuum pump-connected desiccator for 15 minutes. Crosslinking was terminated by the addition of 125mM glycine followed by a 5-minute application of vacuum. The pellets were resuspended in microcentrifuge tubes and sonicated for 15 minutes at 4°C using a Bioruptor on the HIGH setting, with 30-second on/off intervals. ChromoTek GFP-Trap® Magnetic Agarose beads were added to the chromatin lysate and incubated overnight at 4°C. The ChIP DNA was purified using the Qiagen QIAquick PCR Purification

Kit according to the standard protocol. qPCR was performed to analyze the immunoprecipitated DNA, and the amount of DNA fragment co-precipitated with the beads was calculated and compared to the amount of the same genomic fragment in the total input DNA, resulting in a percentage of input. To investigate potential ATH1 regulation, we searched for its DNA-binding motif (GATTGA, as identified by Ejaz et al., (2021)) within the promoter regions of *PRE6/KDR*, *PIF4*, and *KNAT2*. As a control, the same motif search was conducted within the coding sequences of these genes. Primers were designed to encompass these target regions and subsequently used for qPCR analysis. For reference, the specific ChIP-qPCR primers are listed in C3_Table S1.

Samples were frozen in liquid nitrogen and stored at -80°C until ready for RNA extraction for qPCR experiments. Each experiment used three to four biological replicates and two technical replicates. RNA was isolated using a Qiagen RNAeasy mini- or micro-kit. Genomic DNA was then removed from the samples using Thermo Scientific DNase I. cDNA was synthesized from 500 ng of RNA using RevertAid H Minus Reverse Transcriptase, Thermo Scientific Ribolock RNAse inhibitor, and a mix of anchored odT(20) primers from Jena Bioscience and random hexamers from IDT. The qPCR reactions were performed using PCRBIO qPCRBIO SyGreen Blue mix in 384-well plates with a total volume of 5 µL on a Thermo Fisher ViiA7 Real-Time PCR system. The CT values were obtained using ViiA7 software. To determine the relative expression levels of the target gene, the ΔΔCt method was used and the expression levels were normalized to those of the housekeeping genes GAPC2 (*AT1G13440*) and MUSE3 (*AT5G15400*). Statistical analysis of the differences in ΔΔCt values between different experimental conditions or groups was performed using either an independent sample t-test or ANOVA test ($p < 0.05$) in Rstudio version 1.2.5033. The primer sequences used in the qPCR reactions can be found in C3_Table S2.

**Gene set enrichment analysis**

Gene Set Enrichment Analyses (GSEA) were conducted using ShinyGO v0.61, tailored for Gene Ontology (GO) Enrichment Analysis in Arabidopsis thaliana (available at http://bioinformatics.sdstate.edu/go/), with a stringent false discovery rate (FDR) threshold of 0.05. The network of enriched GO categories was visualized via ShinyGO, applying a cutoff of 0.3 and default settings for other parameters. A two-tiered computational approach was utilized to refine the list

of GO terms linked to differentially expressed genes. Initially, GO terms meeting an FDR threshold of <0.001 were selected to ensure statistical significance. Redundancy was minimized by calculating the Jaccard index to assess gene set overlaps, retaining terms with unique gene sets (overlap <80%) and the highest FDR within their categories. The foremost 25 GO terms were illustrated in Fig. 3a and 3b. This approach was similarly applied to analyze common up- , down-regulated and the unique genes between the *ath1-3* dataset and the hypocotyl dataset in response to low red/far-red light, as reported by Kohnen et al., (2016). Visualization focused on the top 20 most significant GO terms using ShinyGO, with selected GO terms refined and tailored in Illustrator and shown in Figure 4d. Node sizes indicate the number of genes per GO term, and edge thickness reflects the extent of gene overlap between terms. Connections between nodes signify a significant gene subset share, defined as more than 20% overlap. This visual representation underscores the complex interplay of biological pathways, offering profound insights into the molecular responses at play.

**Confocal Microscopy**

For the confocal microscopy study, we focused on Col-8 and *ath1-4* mutants that were grown under conditions of low red to far-red (R/FR) light. The procedure involved imaging longitudinal cross-sections of vegetative internodes. To prepare the samples, we first removed the rosette leaves and excised the internode regions, which were then promptly fixed using a 4% paraformaldehyde solution in phosphate-buffered saline (PBS). This was followed by a 30-minute vacuum incubation to enhance penetration of the fixative. Subsequently, the internodes were rinsed three times with PBS to remove excess fixative and then submerged in ClearSee solution for a duration of two weeks for clearing. After the clearing process, the internodes were dried and embedded in warm 4% agarose. This mixture was then quickly solidified by cooling on ice to create agarose plugs. These plugs were sectioned into 200 µm slices using a Leica VT1000S vibratome. The slices were then stained with 50% calcofluor white solution (Sigma-Aldrich) for one hour to enhance the tissue's fluorescence properties. For imaging, we employed a Carl Zeiss LSM880 Fast AiryScan microscope, equipped with a Plan-Apochromat 63x/1.2 Imm Korr DIC objective and operated using ZEN software (blue edition, Carl Zeiss). The imaging parameters were set with an excitation wavelength of

405 nm and emission filters ranging from 425 nm to 475 nm to optimize the fluorescence detection.
Post-imaging, Adobe Illustrator and Fiji (version 1.52, Fiji) software were utilized for image processing, ensuring that the obtained confocal images were of high quality. To further explore RZ in Col-8, *ath1-4*, and *35S::KDR #8* lines (C3_Fig. 6), these plants were grown at a controlled temperature of 22°C for seven days. Following the growth period, they were fixed in PFA, cleared in ClearSee solution for two weeks, and finally imaged using the same confocal microscopy technique. This approach ensured the acquisition of high-resolution images, facilitating an in-depth examination of the cellular and structural details within the internode regions of the plants studied.



**Statistical analysis and data visualization**
The legends accompanying the figures detail the statistical analyses conducted. For analyses involving multiple comparisons, we utilized Fisher's Least Significant Difference (LSD) test alongside a one-way Analysis of Variance (ANOVA) procedure, incorporating a Bonferroni correction to maintain an alpha level of 0.05. These analyses were conducted using the agricolae package in R. For additional statistical assessments not covered by the aforementioned methods, we applied a two-sided t-test, setting the significance threshold at a p-value of 0.05. To visualize our data, we generated heatmaps and various graphs utilizing the R programming environment. Subsequent enhancements and polishing of these visual representations were performed using Adobe Illustrator.

## Acknowledgements

*pCLV3::rgaΔ17* seeds were a kind gift of the Detlef Weigel lab (Max Planck Institute for Biology Tübingen). The pre-amiR line was a kind gift of Zhiyong Wang (Stanford University). The *35S:KDR* lines were a kind gift of the Ronald Pierik lab (Wageningen University & Research). The *ath1-3 pATH1-ATH-GFP* line was a kind gift of Robert Sablowski (John Innes Centre, UK).

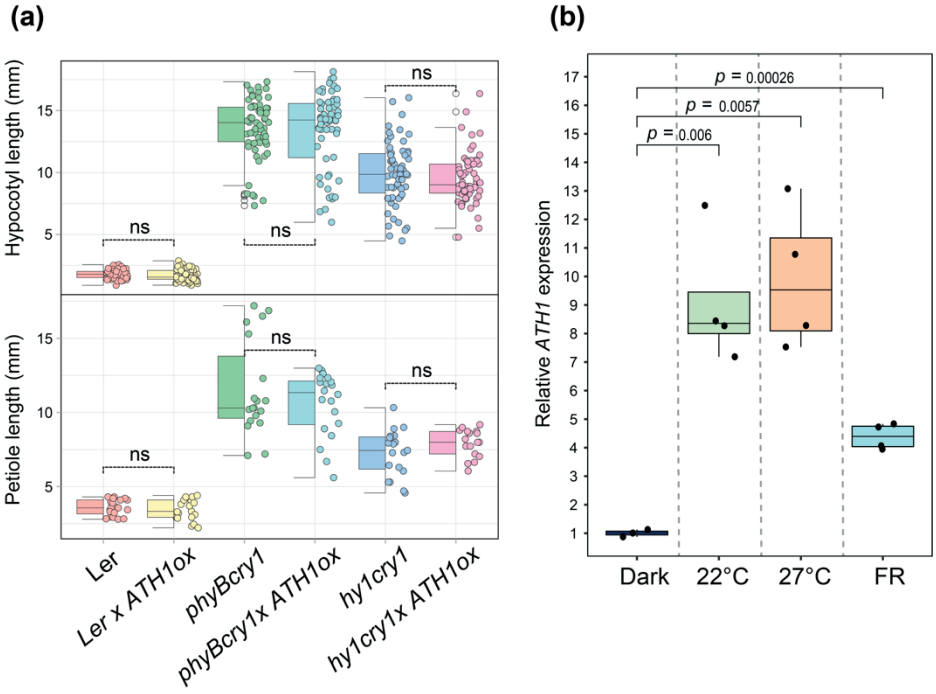


**C3_Fig. S1: Analysis of *ATH1* overexpression on Arabidopsis plant morphology and its expression under various conditions.**

**(a)** Quantitative assessment of petiole and hypocotyl lengths in wild-type (Ler), *phyBcry1*, and *hy1cry1 Arabidopsis thaliana* genotypes, with and without the *pro35S:HA-ATH1* transgene. Petiole lengths were measured on the third leaf of plants grown under long-day (LD) conditions using a caliper, while hypocotyl lengths were determined on 7-day old seedlings grown under the same conditions using ImageJ software. Statistical significance was assessed using Student's t-test, with no significant differences denoted by "ns." **(b)** Expression levels of *ATH1* in Col-8 seedlings after one week of growth under long-day (LD) conditions at varying temperatures (22°C, 27°C) and low red/far-red light (FR), compared to seedlings grown in the dark. Quantitative PCR (qPCR) was utilized to measure *ATH1* expression, with the data representing the mean of three to four biological replicates. Statistical significance was evaluated using Student's t-test, and the corresponding *p-values* are indicated for each comparison.

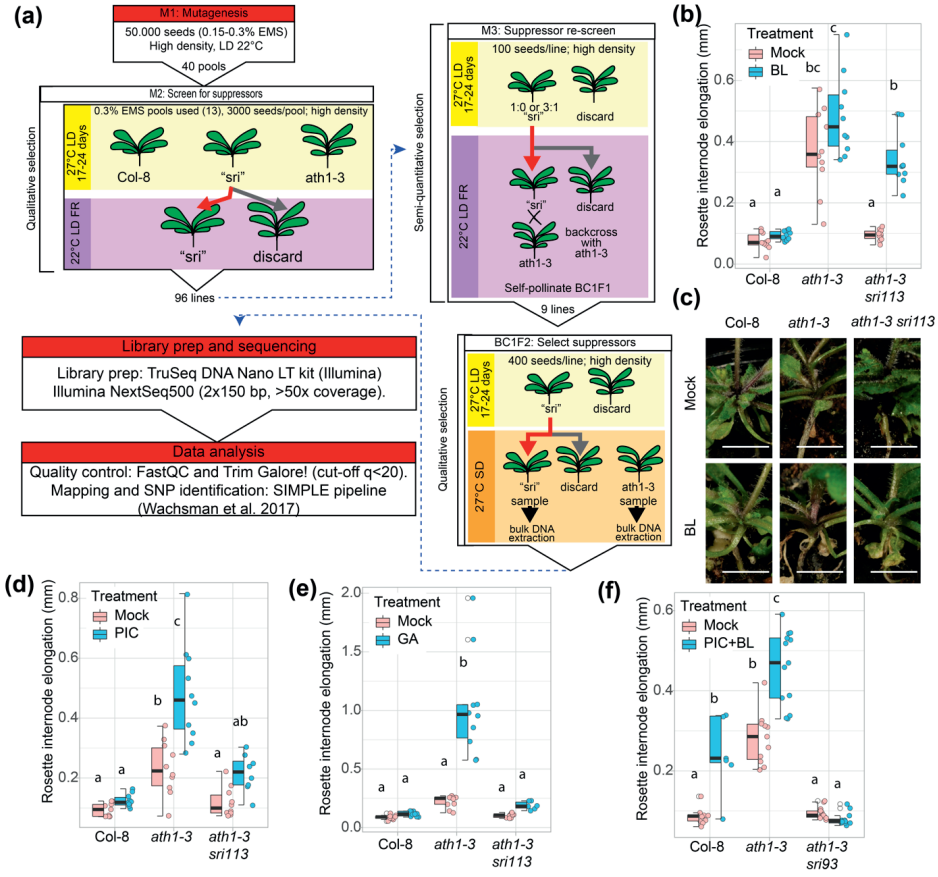


**C3_Fig. S2: Characterization of *ath1-3 suppressor mutants* and modulation of rosette internode elongation.**

**(a)** Schematic representation of the EMS mutagenesis and subsequent screening process to isolate *ath1-3 suppressor mutants* (*sri*) with reduced rosette internode elongation phenotype in the *ath1-3* background. The M1 generation was subjected to EMS mutagenesis, followed by a qualitative selection in the M2 generation under long-day (LD) conditions at 22°C with a subsequent environmental shift to low red/far-red (FR) light to enhance the rosette elongation phenotype. M3 generation was screened for *sri* suppressors with a 1:0 or 3:1 segregation ratio and backcrossed with *ath1-3* to establish BCF1 populations. In the BCF1:2 generation, the *sri* phenotype was reconfirmed under similar conditions followed by bulk DNA extraction for suppressor identification. **(b)** Quantitative analysis of rosette internode elongation in Col-8, *ath1-3*, and *ath1-3 sri113* mutants under LD conditions at 27°C, treated with either a mock solution of 0.1% DMSO or 5 µM Epi-brassinolide (BL). **(c) (C)** Visual depiction of the phenotypic differences corresponding to the quantitative data in (b), displaying 28-day old plants treated with mock or BL. Scale bars indicate 5 mm. **(d)** Measurement of rosette internode elongation in Col-8, *ath1-3*, and *ath1-3 sri113* mutants under LD conditions at 22°C, following treatment

with either 0.1% DMSO (mock) or 1 µM picloram (PIC). **(e)** Assessment of rosette internode length in Col-8, *ath1-3*, and *ath1-3 sri113* mutants under the same LD conditions at 22°C, with treatments of 0.1% ethanol (EtOH, mock) or 100 µM gibberellic acid (GA4+7). **(f)** Comparative analysis of rosette internode elongation in Col-8, *ath1-3*, and *ath1-3 sri93* mutants grown under LD conditions at 22°C, treated with a mock solution of 0.1% DMSO or a combined treatment of 1 µM picloram and 5 µM brassinolide (PIC+BL).
Statistical analysis was conducted using one-way ANOVA and Fisher's LSD test with Bonferroni correction ($\alpha = 0.05$) to determine significance among the groups. Different letters above the data points denote statistically significant differences, as determined by the agricolae package in R.

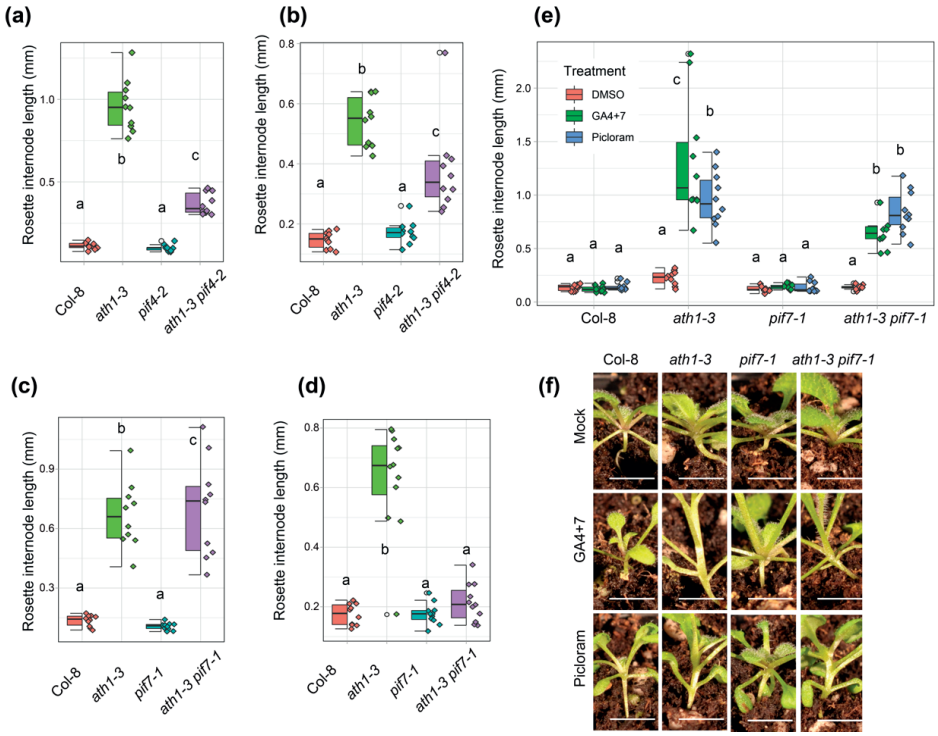


**C3_Fig. S3: Elucidating the role of *PIFs* in modulating rosette internode elongation in Arabidopsis.**

**(a, b)** Quantitative comparison of rosette internode lengths among Col-8 (wild-type), *ath1-3*, *pif4-2*, and *ath1-3 pif4-2* mutant Arabidopsis lines. Measurements were conducted on plants grown under long-day (LD) conditions with (a) low red/far-red light (lowR/FR) and (b) at elevated temperature (27°C). (**c, d**) Comparative analysis of internode lengths in rosettes from Arabidopsis lines: Col-8 (wild type), *ath1-3*, *pif7-1*, and the double mutant *ath1-3 pif7-1*. These measurements were taken under long-day conditions with (c) high temperature (27°C) and (d) low R/FR ratio. **(e)** Rosette internode length analysis of Col-8, *ath1-3*, *pif7-1*, and *ath1-3 pif7-1* mutants under standard LD conditions with treatments of 0.1% DMSO (control), 100 µM gibberellic acid (GA4+7), and 5 µM picloram. **(f)** Representative photographs of 22-day-old plants corresponding to the treatments in (e), illustrating the morphological effects of the treatments on rosette internode elongation. Each image serves as a visual reference for the quantitative data presented. Statistical significance across different genotypes and treatments was determined using one-way analysis of variance (ANOVA) followed by Fisher's LSD test with a Bonferroni correction applied to maintain an alpha level of 0.05. Data subsets with different letters are statistically distinct. Analysis was performed utilizing the agricolae package in R, and the letters above the graphed data points indicate the groups among which significant differences were identified.

**C3_Table S1: Primers used of ChIP-qPCR in chapter 3.**

| Gene | Sequence Fw | Sequence Rv | Motif |
|---|---|---|---|
| ***KDR/PRE6* (AT1G26945) pro1** | AGTCAAGTCACTCGGTTCGA | AGCTTTGTGGACTGACTTTGA | GATTGA |
| ***KDR/PRE6* (AT1G26945) Pro2** | TGTGTGTATTTTAACTTCTGAATACT | TGAATAAATAGATCAATCTTGTCCT | GATTGA |
| ***KDR/PRE6* (AT1G26945) CDS** | CATCAGGAACTTACACAGAGAGG | TCCTAATGATGGCTGCTTCG | no |
| ***PIF4* (AT2G43010) pro1** | TCAGTAATTACATACACCGTAACAC | GTTGTCAGTCAATCATACCTATACTC | GATTGA |
| ***PIF4* (AT2G43010) pro2** | ACGCTATAGATGATTGTGATTTGAC | AGAGGTGGTTTCTTATCTGTACC | GATTTGA |
| ***PIF4* (AT2G43010) CDS** | TTTAGTTCACCGGCGGGACAGC | AGTGGTCCAAACGAGAACCGTCG | no |
| ***KNAT2* (AT1G70510) pro1** | AGAAGTGCGATAAGTGGAGTG | GGTAGCTAGGTGCTCATTATCAA | GATTGA |
| ***KNAT2* (AT4G32980) CDS** | CGCCTATGGAAATAGCGTGTATA | GGATCAGCTCCAAAGCAAGA | no |

**C3_Table S1: Primers used of qPCR in chapter 3.**

| Gene | Sequence Fw | Sequence Rv | Ref,. |
|---|---|---|---|
| ***ATH1* (AT4G32980)** | CAACGAGGTTTGCCTGAGAAA | TTCGGGTAAGGGTGAAGGAA | |
| **MUSE3 (AT5G15400)** | GGGCACTCAAGTATCTTGTTAGC | TGCTGCCCAACATCAGGTT | (Li *et al.*, 2022a) |
| **GAPC2 (AT1G13440)** | TTGGTGACAACAGGTCAAGCA | AAACTTGTCGCTCAATGCAATC | (Czechowski *et al.*, 2005) |


Col-8
ath1-3

# Chapter 4

## From rosette to stem elongation: Investigating the ATH1-mediated molecular mechanisms governing bolting in *Arabidopsis thaliana*

Shahram Shokrian Hajibehzad[1, 2], Savani S Silva[1], Evelien Stouten[1,3], Bram van Eijnatten[4], Basten Snoek[4], Sjef Smeekens[1], Marcel Proveniers[1, 2]

[1] *Molecular Plant Physiology, Department of Biology, Science4Life, Utrecht University, Padualaan 8, 3584CH, Utrecht, The Netherlands*

[2] *Translational Plant Biology, Department of Biology, Science4Life, Utrecht University, Padualaan 8, 3584CH, Utrecht, The Netherlands*

[3] *Plant Stress Resilience, Institute of Environmental Biology, Utrecht University, Padualaan 8, 3584 CH Utrecht, The Netherlands*

[4] *Theoretical Biology and Bioinformatics, dept. Biology, Utrecht University, Padualaan 8, 3584 CH Utrecht, the Netherlands*

## Abstract

In the life stages of rosette plants, the vegetative phase is distinguished by tightly packed leaves at the ground level, lacking upward stem development. Upon transitioning to the reproductive stage, these plants undergo 'bolting'—a rapid vertical growth of the stem that aids in seed dispersal. However, premature bolting can detract from the crop's yield and quality, for instance, by causing bitterness. The ARABIDOPSIS THALIANA HOMEODOMAIN1 (ATH1) transcription factor from the BEL1-LIKE HOMEODOMAIN family is pivotal in controlling stem elongation. Its activity within the shoot meristem is essential for maintaining a compact rosette structure by delaying bolting. A decline in *ATH1* expression within the meristem is instrumental for initiating bolting as the plant enters the reproductive phase. However, the specific mechanisms through which ATH1 controls bolting remain elusive. This study ventures into the molecular landscape downstream of ATH1 amidst this vital phase transition. Employing a time-series transcriptome sequencing approach, we analyzed plants under controlled bolting-inductive conditions, while sustaining ATH1 activity to observe downstream gene expression dynamics. This enabled us to discern a suite of genes that respond to ATH1's regulatory role during bolting. Our investigations reveal that ATH1 coordinates a gene network crucial for cell cycle processes, including cell division, DNA replication, and cytokinesis. ATH1 also modulates key hormonal pathways, such as those involving auxins, gibberellins, and brassinosteroids. Our data strongly suggest ATH1's specific impact on GA degradation, BR biosynthesis, and auxin equilibrium in the meristem, potentially influencing localized suppression of stem elongation. In summary, our findings illuminate ATH1's regulatory domain and suggest potential strategies to manage bolting and stem growth by targeting hormone regulation and cell division-related genes within the meristem. This could have implications for preserving the overall growth integrity of crop plants.

## Introduction

Most rosette plants exhibit contrasting growth habits during vegetative and reproductive development, with internode elongation being a critical determinant in shaping these growth habits. During vegetative growth, rosette plants form a compact rosette close to the ground, consisting of a whorl of tightly packed leaves with no visible stem due to the absence of internode elongation. Upon transitioning to the reproductive phase, these plants typically undergo a dramatic architectural change through a process known as bolting, which is characterized by the rapid elongation of the inflorescence stem as a consequence of excessive internode growth. In nature, rosette habit (or acaulescence) provides several advantages over a caulescent growth habit, including protection against various biotic and abiotic stressors. The switch from acaulescent to caulescent growth is thought to facilitate seed dispersal (Schaffer & Schaffer, 1979; Martorell & Ezcurra, 2002; Soons *et al.*, 2004; Bello *et al.*, 2005; Fujita & Koda, 2015). The timing of bolting is a crucial agronomic trait, especially in crops such as those in the *Brassicaceae* family, lettuce, and sugar beet. Premature bolting can divert resources from valuable vegetative parts (such as leaves, tubers, and roots), reducing crop yield and crop quality. For example, in lettuce, premature bolting leads to the accumulation of secondary metabolites that contribute to bitterness (Mutasa-Göttgens *et al.*, 2010; Hoffmann & Kluge-Severin, 2011; Dally *et al.*, 2018; Assefa *et al.*, 2019; Abolghasemi *et al.*, 2021; Han *et al.*, 2021; Li *et al.*, 2022b).

The onset of bolting in rosette plants is governed by mitotic changes in the rib meristem/rib zone (RM/RZ), which is located in the subapical region of the shoot apical meristem (SAM) (Sachs, 1965; Reddy & Meyerowitz, 2005; Bencivenga *et al.*, 2016). During vegetative growth, the RM/RZ is characterized by a tightly packed arrangement of cells with dense cytoplasm, which remains quiescent in terms of mitotic activity, contributing to the maintenance of a compact rosette habit (Sachs *et al.*, 1959a; Sachs, 1965; Hempel & Feldman, 1994; Jacqmard *et al.*, 2003; Gómez-Mena & Sablowski, 2008; Kwiatkowska, 2008; Bencivenga *et al.*, 2016). During the transition to reproductive growth, this zone undergoes a surge in mitotic activity, predominantly via periclinal divisions. This results in the reorganization of these cells into transverse files (ribs) that leads to elongated internodes between successive nodes, facilitating the transition from rosette growth to stem growth (Sachs *et al.*, 1959b,a; Peterson & Yeung, 1972; Metzger

& Dusbabek, 1991; Jacqmard *et al.*, 2003; Kwiatkowska, 2008; Bencivenga *et al.*, 2016; Serrano-Mislata *et al.*, 2017). Initial internode growth based on cell proliferation near the shoot apex is gradually replaced by growth based on cell elongation and cell differentiation further down the developing stem (Jacqmard *et al.*, 2003). Recent advances in imaging techniques have further elucidated the cellular dynamics within the RM/RZ, revealing a division into a rapidly dividing peripheral RZ that contributes cells for stem epidermis and a more slowly dividing central RZ that forms the core structures of the stem (Bencivenga *et al.*, 2016). As the RM/RZ region appears to lack a true meristematic identity, with the cells making up the central and peripheral RZ being supplied from the overlying central and peripheral zones of the SAM, respectively, we will consider the RM/RZ region a single entity further referred to as the RZ (Hall & Ellis, 2012; Bencivenga *et al.*, 2016).

In *Arabidopsis thaliana*, local control of internode elongation is provided by the BEL1-LIKE HOMEODOMAIN (BLH)-family transcription factor protein ARABIDOPSIS THALIANA HOMEOBOX1 (ATH1) (Ejaz *et al.*, 2021; 2023). During vegetative development, *ATH1* is expressed throughout the SAM, including the subapical region, and at the base of leaf primordia. Expression of *ATH1* in the vegetative shoot apex is particularly significant for maintaining a rosette growth habit. In plants lacking functional *ATH1*, premature RZ activation results in the formation of elongated rosette internodes and, depending on growth conditions, (partial) loss of rosette habit (Proveniers *et al.*, 2007; Gómez-Mena & Sablowski, 2008; Rutjens *et al.*, 2009; Li *et al.*, 2012b; Ejaz *et al.*, 2021; Hajibehzad *et al.*, 2023). As plants transition to reproductive growth, *ATH1* expression in the SAM is downregulated by an as-yet-unknown mechanism that likely facilitates the development of an elongated inflorescence stem (Proveniers *et al.*, 2007; Gómez-Mena & Sablowski, 2008). Consistent with this, constitutive expression of *ATH1* at the SAM inhibits elongation of the inflorescence stem at floral transition by impeding internode growth, without affecting flowering (Cole *et al.*, 2006; Sablowski, 2007; Gómez-Mena & Sablowski, 2008; Rutjens *et al.*, 2009). This suggests that ATH1 promotes rosette habit during vegetative growth by repressing bolting. Previously, it has been suggested that ATH1 inhibits inflorescence stem growth, mostly by limiting cell proliferation (Sablowski, 2007; Gómez-Mena & Sablowski, 2008). Our recent findings showed that ATH1 specifically maintains the rosette growth habit in Arabidopsis during the vegetative phase mainly by inhibiting RZ cell elongation. This is achieved through direct regulation of key cell elongation

modules, including the BAP/D and HLH/BHLH modules (Hajibehzad *et al.*, 2023; Chapter 3).

In this chapter, we aim to delineate the molecular mechanisms governed by ATH1 that steer internode elongation upon floral transition, a fundamental aspect of bolting. Using RNA sequencing, we monitored the dynamics of shoot apex gene expression in a synchronized population of bolting-induced plants. Comparing genome-wide expression levels over time between control plants, where *ATH1* becomes down-regulated upon bolting induction, and transgenic plants that continuously express ATH1, enabled the identification of a specific cluster of genes under control of ATH1 and involved in the bolting process. A detailed analysis of this gene set suggests that ATH1 represses bolting through local control of both plant hormone homeostasis, especially that of auxin, gibberellin, and brassinosteroids, and cell proliferation These findings open up new avenues for manipulating bolting and stem elongation in crops through strategic regulation of hormone levels and/or signaling and control of cell division processes at the SAM, without impairing overall growth and development.



## Results

### Downregulation of *ATH1* at the shoot apical meristem coincides with RZ activation and the onset of bolting

Previous studies have demonstrated that, unlike in wild-type plants, the RZ of Arabidopsis plants lacking functional *ATH1* exhibits an active state already in the vegetative growth phase. Depending on growth conditions, this allows for elongation of vegetative internodes (Ejaz *et al.*, 2021; Hajibehzad *et al.*, 2022). In wild-type Arabidopsis plants, enhanced activity of the RZ is only observed during the reproductive growth phase, driving the rapid internode elongation that results in the formation of an elongated inflorescence stem (Vaughan, 1955).

To compare the RZ of vegetative *ath1* mutant plants with that of both vegetative and bolting wild-type plants, *ath1-3* and Col-8 (wild-type) plants were grown in conditions that are non-inductive to bolting and subsequently transferred to bolting-inductive conditions. Under these conditions, bolting is induced synchronously at the population level, with the first macroscopic signs, such as a 0.5 cm stem extension, visible 7 days after transfer. Using confocal microscopy, shoot

apices were imaged at 0, 1, and 4 days post-shift. Plants kept in non-inductive conditions served as a control. Changes in cell elongation were determined by measuring the heights of individual cells in the central zone (CZ) and RZ areas. Based on morphological landmarks defined previously (Bencivenga *et al.*, 2016), the CZ and underlying RZ were defined as areas at respectively 0-45 µm and 45-90 µm from the apex tip, within 15 µm in both directions from the main axis of the apex.

At all timepoints, both Col-8 and *ath1-3* plants retained in non-inductive conditions, exhibited a weakly curved apex, from which blade-shaped leaf primordia initiated at the flanks (C4_Fig. 1a), characteristic for vegetative development (Sarojam *et al.*, 2010). Under these conditions, the RZ of the control plants was compact and RZ cells showed a random organization (C4_Fig. 1a), reflecting an inactive state, again typical of vegetative development in Arabidopsis. In contrast, and consistent with previous observations (Ejaz *et al.*, 2021; Hajibehzad *et al.*, 2022), in *ath1* mutants, elongated, transverse cell files, indicative of RZ activity, were present in the subapical region of the SAM at all timepoints under non-inductive conditions (C4_Fig. 1a). In Col-8 plants, a highly similar RZ morphology and, thus, RZ activity was only observed four days after transfer to bolting-inductive conditions. At the same time, the SAM had taken on a domed shape with rounded floral primordia developing at its flanks, indicating that the developmental identity of the SAM had changed to an inflorescence meristem (IM) and flowering had been initiated (Kwiatkowska, 2008). In *ath1* mutants, shifting plants to inductive conditions also led to IM determination and floral induction, but no additional changes in RZ morphology could be observed (C4_Fig. 1a). These observations are supported by cell height analysis of individual cells in the CZ and RZ areas. Bolting induction increased cell height of Col-8 RZ cells, but not those of *ath1-3*. Until day four of induction, when Col-8 elongation caught up to *ath1-3*, RZ cells were shorter in Col-8, further confirming that the *ath1-3* RZ is already active during vegetative development (C4_Fig. 1d). Unlike the RZ, the CZ of *ath1* mutants was still responsive to inductive conditions, as, associated with doming of the SAM, CZ cells in both control and mutant plants increased in height after transfer (C4_Fig. 1a, c).

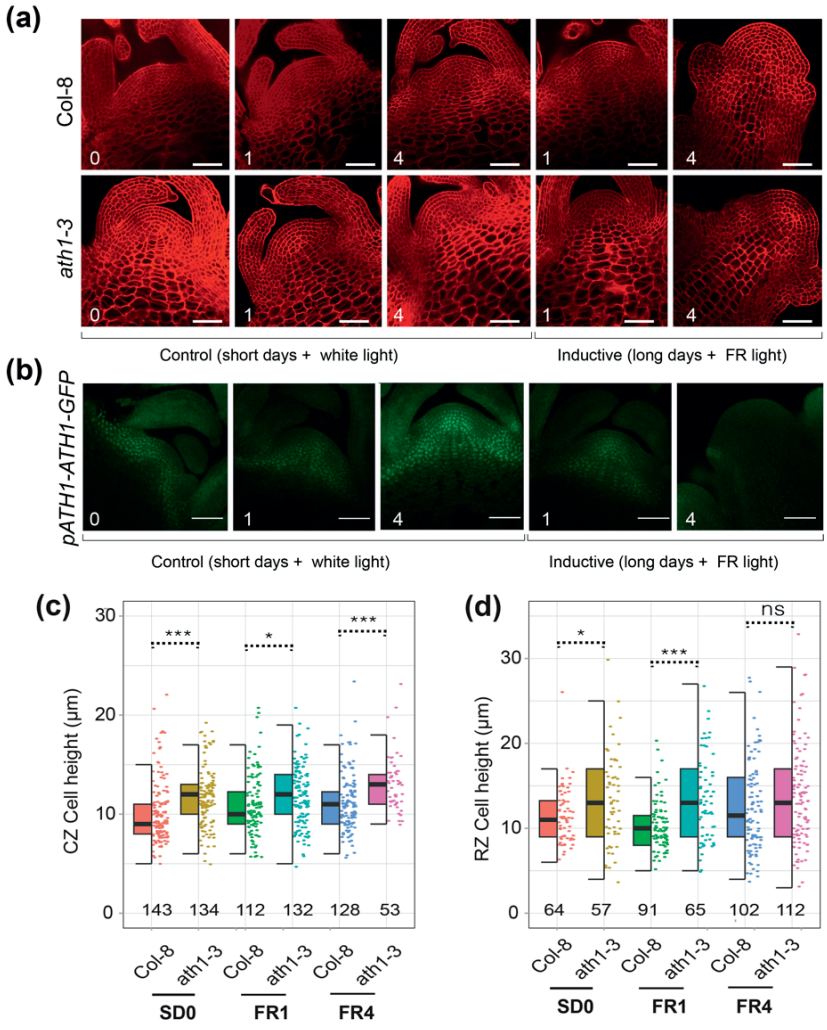


**C4_Fig. 1: RZ activation during bolting coincides with *ATH1* downregulation in the shoot apex.**

**(a)** Confocal micrographs of shoot apices from wild type (Col-8) and *ath1-3* plants stained with mPS-PI. The plants were grown under control conditions for five weeks with short-day (white light) and subsequently exposed to either control or bolting inductive conditions with long-days (white light + FR light). Images taken at 0, 1, and 4 days after the shift are representative of the experimental conditions. The scale bar represents 50 µm. **(b)** Confocal micrographs depicting the spatiotemporal expression of 5-week old *ATH1:ATH1-GFP* plants grown under short day conditions (white light) and transferred to bolting induction (white light + FR light) or kept under control conditions. Samples were collected from four apices at 0, 1, and 4 days after transfer to bolting inductive condition. The scale bar represents 50 µm. **(c-d)** The sizes of the CZ (c) and RZ (d) for the apices shown in (a) were determined by calculating the average

areas of the medial sections from four separate apices per genotype, time point, and condition. The statistical significance of the differences is denoted using asterisks, where *, ***, and ns represent $p<0.05$, $p<0.001$, and $p>0.05$, respectively. The CZ region was defined as the top 0-45 µm from the apex, and the RZ region was defined as 45-90 µm from the top of the apex. The analysis focused on cells located within 15 µm of the main axis. The numbers displayed above the x-axis represent the number of measured cell heights. Differences in cell height were statistically analyzed using Mann-Whitney U tests with a significance level of $\alpha=0.05$.

In Arabidopsis, reproductive phase change, when bolting and flowering are induced, coincides with downregulation of *ATH1* at the shoot apex (Proveniers *et al.*, 2007; Gómez-Mena & Sablowski, 2008). Constitutive expression of *ATH1* inhibits growth of the inflorescence stem, with no obvious effect on flowering, suggesting that down-regulation of *ATH1* allows for the bolting transition to occur. We analyzed the spatiotemporal dynamics of ATH1 protein localization during bolting induction by imaging *ath1-3* shoot apices complemented with an *pATH1::ATH1-GFP* reporter construct. In non-inductive conditions, ATH1-GFP was visible throughout the SAM, predominantly in the RZ and lateral boundaries of the meristem (C4_Fig. 1b). Following bolting induction, ATH1-GFP was still present 1-day post transfer, but could no longer be detected in the SAM after 4 days of induction. This loss of expression coincides with the initiation of elongation of the RZ in Col-8 plants, marking the onset of bolting. Notably, at 4 days of induction, ATH1-GFP reappears at the flank of the meristem in floral primordia from stage 1 onwards, which is in line with *ATH1* mRNA expression data (C4_Fig. 1a, b) (Khan *et al.*, 2015).

Thus, loss of *ATH1* expression from the SAM coincides with activation of the RZ regardless of timing. This supports the critical role of *ATH1* suppression as a prerequisite for RZ activation and subsequent internode elongation during both vegetative and reproductive growth. Downregulation of *ATH1* at the shoot apex as part of the reproductive phase change, therefore, allows for the bolting transition to occur through de-repression of an internode elongation program.

**Induction of bolting is a reversible process that solely depends on ATH1 activity in the SAM**

Bolting is often recognized as a critical component of the flowering response, occurring concomitantly with the reproductive phase change — a developmental transition that shifts plant from vegetative to reproductive growth. This phase

transition, once triggered, is usually irreversible (Müller-Xing *et al.*, 2014). To test if this is also the case for bolting, we used *35Spro:ATH1-HBD* plants that allow for controllable activation of ATH1. These plants constitutively express ATH1 fused to the hormone binding domain (HBD) of the rat glucocorticoid receptor (Rutjens *et al.*, 2009). In the absence of the glucocorticoid hormone dexamethasone (Dex), ATH1-HBD fusion protein is held in an inactive state, due to its cytoplasmic localization. Dex application facilitates nuclear translocation, enabling immediate gene regulation by ATH1.

The *35Spro:ATH1-HBD* plants were grown under non-bolting conditions for five weeks before being shifted to bolting-inductive conditions, with ATH1 activation at various successive time points. Subsequently, the development of the inflorescence stem was assessed. Control experiments with mock-treated *35Spro:ATH1-HBD* and Dex-treated wild-type plants (Col-8) exhibited typical growth patterns. However, continuous Dex treatment from the onset of bolting-inductive conditions till the end of the life cycle (timepoint 0 till end) caused significant growth suppression in both the inflorescence stem and pedicels (C4_Fig. 2a, c), corroborating earlier findings of plants with constant *ATH1* expression (Cole *et al.*, 2006; Gómez-Mena & Sablowski, 2008; Rutjens *et al.*, 2009). Also, in line with previous observations, this effect was primarily attributed to the inhibition of internode elongation (C4_Fig. 2b). ATH1 activation either two- or five-days post condition shift (timepoint 2 or 5 till end) presented similar growth inhibition (C4_Fig. 2a-c). Endogenous *ATH1* is no longer expressed at the SAM four days after switching the plants to bolting-inductive conditions and *ATH1* down-regulation coincides with the onset of bolting (C4_Fig. 1a, b), indicating that induction of bolting is a reversible process that solely depends on ATH1 activity in the SAM, contrasting to floral induction.

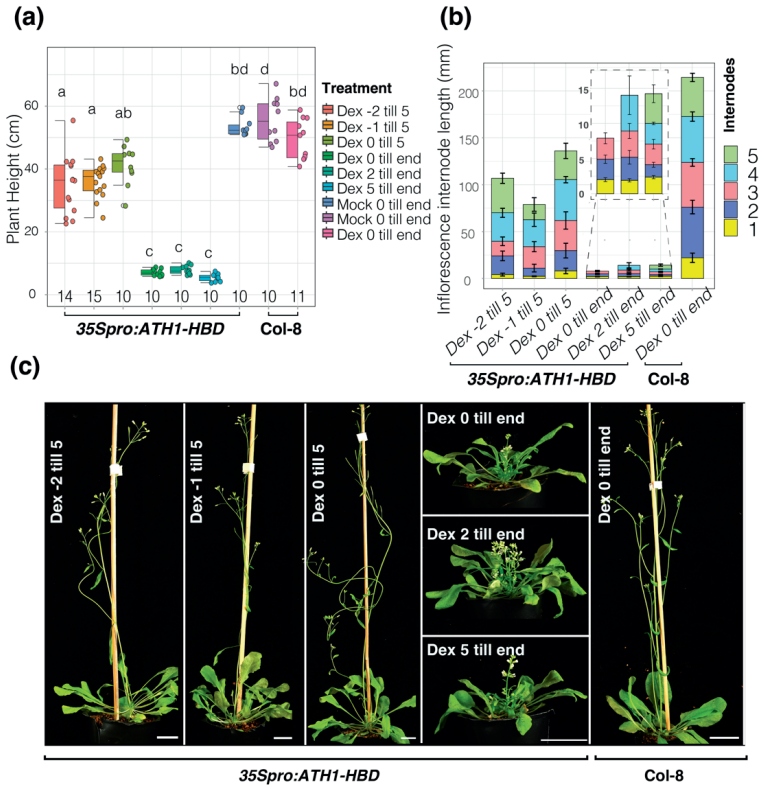


**C4_Fig. 2: ATH1 downregulation in meristem does not lead to a permanent developmental switch.**

**(a)** The average plant height (cm) of two different genotypes – wild type (Col-8) and 35Spro:ATH1-HBD grown under short day (white light) conditions for 35 days before transferring to bolting-induced long days (white light + FR light). Dexamethasone (Dex) or Mock (0.01% ETOH) treatments were applied at various time points and durations. Dex and Mock treatments started either 2 or 1 day(s) prior to the switch and continued until day 5 after the switch (Dex -2 and -1 till 5), or started on the day of the switch and continued until day 5 (Dex 0 till 5). Alternatively, treatments began on the day of the switch, or 2 or 5 days after the switch, and continued until the end of flowering (Dex 0, 2, 5, till end). The number of plants used for each treatment and genotype is indicated on the graph. Statistically significant differences between groups ($P < 0.05$) are denoted by different letters, as determined by 1-way ANOVA followed by Tukey's post hoc test. **(b)** Average inflorescence internode length (mm) of the plants shown in (a), calculated based on the presence of cauline leaves along the stem. Internodes were defined as the portion of the stem between two adjacent cauline leaves. A magnified view of the internode length for selected treatments that resulted in relatively short elongation compared to others is presented in the middle section of the graph. The y-axis scale of the magnified plot is in mm. Error bars indicate the standard deviation of the mean (n >10). **(c)** Representative plants from (b) are displayed.

This is substantiated by the observation that when ATH1 activation is terminated before completion of reproductive growth, bolting was still initiated, despite it initially being inhibited at reproductive phase transition. Plants in which ATH1 was induced during the first five days after transfer to inductive conditions (timepoint 0 till 5) did grow an elongated inflorescence stem, although with a shorter overall height compared to control(-treated) plants (C4_Fig. 2a, c). This was mostly due to reduced elongation of internodes 1 and 2 (C4_Fig. 2b). As these internodes were still significantly more elongated than in plants where ATH1 was activated during the entire reproductive growth phase, this also indicates that, once ATH1 is no longer active, internode elongation, within a limited developmental window, can still be initiated some period after internode formation.

Similar observations were made for plants where ATH1 was induced one or two days prior to switching conditions, up till day 5 in bolting-inductive conditions (timepoints -1 or -2 till 5) (C4_Fig. 2b). However, in these plants the first internode was on average shorter than in plants that were treated with Dex starting from the moment of transfer. This indicates that to maintain high levels of ATH1 activity at the SAM in order to maximally prevent internode elongation it is desirable to induce *ATH1* at least one day before switching plants to bolting-inductive conditions.

Overall, it can be concluded that ATH1 functions as a key repressor of internode elongation and that down-regulation of *ATH1* at the SAM during reproductive phase change suffices for the bolting transition to occur. Since re-establishing ATH1 activity at the SAM is sufficient to inhibit internode elongation and loss of functional *ATH1* during vegetative development results in RZ activation, one could argue that internode elongation/bolting is the default state in Arabidopsis. Suppression of the default state at any time only requires ATH1 activity at the shoot meristem.

**Identification of bolting-associated genes controlled by ATH1**

To elucidate the molecular mechanisms driving bolting and to identify the targets of ATH1 in this process, a time-series transcriptomic analysis was employed. For this, Col-8 and *35Spro:ATH1-HBD* plants were grown under non-inductive conditions and then transferred to bolting-inductive conditions while being treated with Dex or a mock solution (Ethanol). SAM-enriched tissue was collected at multiple time points (0, 2, 4, 6 days after switching) and subjected to RNA-seq analysis (C4_Fig. 3a). Over the selected period of time endogenous *ATH1* expression at

the SAM becomes down-regulated, RZ activity is induced, and floral primordia are formed (C4_Fig. 1a, b; C4_Fig. S1). In line with this, in Col-8 plants subjected to Ethanol (CE) or Dex (CD) treatment, and in Ethanol-treated *35Spro:ATH1-HBD* plants (AE), the shift to inductive conditions results in visual bolting and flowering and, eventually, similar overall plant heights at the end of flowering (C4_Fig. 2a, c). In contrast, Dex-treated *35Spro:ATH1-HBD* plants (AD) exhibited a significant inhibition of inflorescence elongation, leading to a non-bolting phenotype (C4_Fig. 2a, c). Despite the absence of internode elongation due to sustained ATH1 activity at the SAM, the timing of flowering and flower morphogenesis paralleled that of control (-treated) plants. This indicates that ATH1 predominantly affects the bolting transition without altering other aspects of the vegetative-to-reproductive phase change.

To identify genes associated with bolting and regulated by ATH1, but excluding those associated with flowering, we first identified genes that are linked to the vegetative-to-reproductive-phase transition in general. These genes exhibited differential expression at 2-, 4-, or 6-day time points relative to the initial day (day 0) in CE, CD, and AE plants. Only genes that overlap between CE, CD, and AE conditions were selected, to exclude potential effects from transgene insertion and chemical treatments. This approach identified 946 differentially expressed genes (DEGs) at time point 2, 591 DEGs at time point 4, and 2594 DEGs at time point 6 after transfer to bolting-inductive conditions (C4_Fig. 3b; C4_Fig. S2).

Gene ontology (GO) enrichment analysis of these DEGs revealed significant enrichment of genes involved in key biological processes, such as hormone-mediated signaling pathways, response to external stimuli, regulation of plant growth, and cell cycle processes (C4_Fig. 3c). Further, at the 2-day time point, genes involved in secondary metabolite biosynthesis, mostly that of glucosinolates, were strongly enriched. This is in line with previous observations that glucosinolates accumulate in the Arabidopsis inflorescence upon bolting and probably reflects a need of the plant to protect plant reproductive parts, which have a high fitness value, from biotic stressors (Andersen & Halkier, 2014). At later time points, a clear switch towards flowering and floral organ development was observed (C4_Fig. 3c), matching our previous observation that 4 days after transferring plants to bolting-inducing conditions the SAM had taken on IM identity and floral primordia had been initiated (C4_Fig. 1a). Our transcript profile of bolting-induced shoot apices, thus, reflects both major transitions that characterize reproduc-

tive phase change, the bolting transition and floral transition. Given that ATH1 down-regulation and RZ activation were not observed one day after transfer of plants to inductive conditions (C4_Fig. 1a, b), and floral pathway integrator (FPI) genes and floral meristem identity (FMI) genes were already significantly induced at the 2-day time point (C4_Fig. S4), this further illuminates the concurrent nature of these transitions.

Next, we determined which of the identified DEGs associated with the vegetative-to-reproductive phase transition are under ATH1 regulation. Given the broader role of ATH1 in plant development beyond bolting (Cao *et al.*, 2020; Crick *et al.*, 2021), this approach refined our focus to genes controlled by ATH1 specifically during this developmental phase transition. In CE, CD, and AE plants endogenous *ATH1* expression at the SAM becomes down-regulated upon switching the plants to bolting-inductive conditions (C4_Fig. S1), allowing for the bolting transition to occur. Therefore, the expression of ATH1-controlled genes is expected to either follow a similar pattern as *ATH1*, or an inverse one, depending on ATH1 functioning as an activator or repressor, respectively. In AD plants, where continuous high ATH1 activity at the SAM persists due to the application of Dex, the expression levels of these genes are anticipated to remain stable over time. Initially, we screened the genes identified in Figure 3b at all time points and selected those that were significant in at least one of the time points (T2, or, T4, or T6) and this yielded a total of 2938 unique genes. We then applied a two-step filtering process to this set of genes. First, we selected genes that showed no significant change in expression over time in AD plants. Second, we compared their expression between AD plants and AE plants and selected those genes that were at any timepoint differentially expressed between AD plants and AE plants. This two-pronged selection process led us to identify 649 unique genes regulated by ATH1 during reproductive phase change (C4_Fig. 4a-d). Since continuous activation of ATH1 in plants grown under bolting-inductive conditions does not visibly impact floral transition and flower formation (C4_Fig. 2c) and, more importantly, expression of FPI and FMI genes and most of the key regulatory genes involved in floral patterning remains unaltered under these conditions (C4_Fig. S4), these genes can be considered specifically associated to the bolting transition. Therefore, these genes will be referred to as Bolting-Associated genes Controlled by ATH1 (BACA) (C4_Fig. 4; C4_Fig. S3).

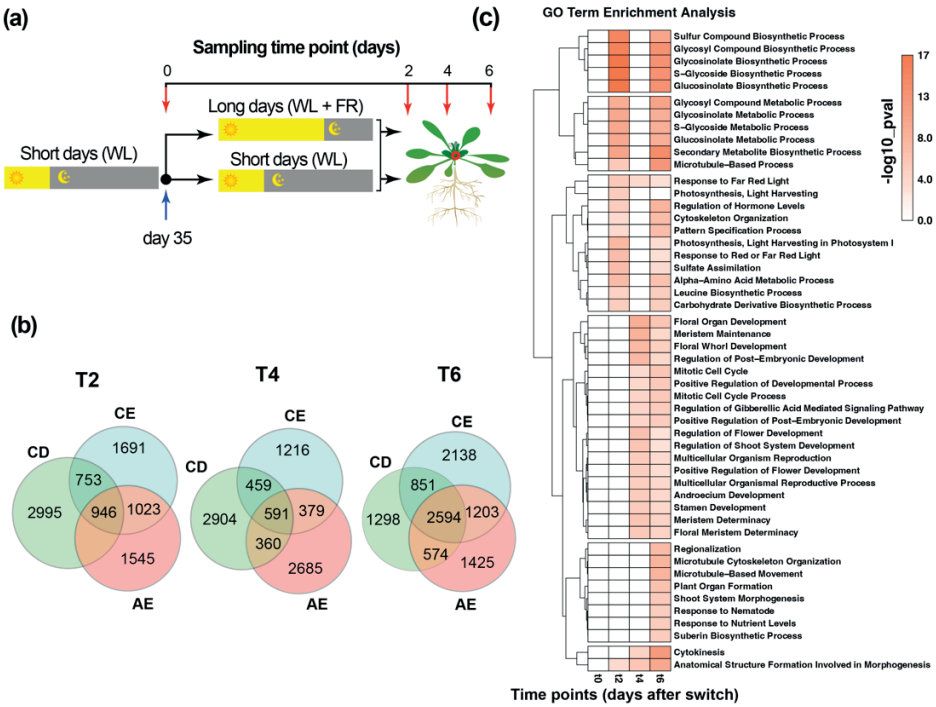


**C4_Fig. 3: Bolting induction leads to transcriptional reprogramming in the shoot apex.**

**(a)** Experimental design for RNA sequencing analysis of wild type (Col-8) and 35Spro:ATH1-HBD plants. Plants were grown under non-inductive short-day conditions (white light (WL)) for 35 days, and RNA samples were collected prior to the switch to inductive long-day conditions (WL + far-red (FR)) at day 0. Subsequently, plants were subjected to inductive conditions and RNA samples were collected at 2, 4, and 6 days post-switch. Each biological replicate consisted of 3 shoot apical meristem samples that were harvested and snap-frozen for RNA extraction. **(b)** Venn diagram of differentially expressed genes (DEGs) between CE (Col-8 treated with ethanol), CD (Col-8 treated with Dex), and AE (35Spro:ATH1-HBD treated with ethanol). The DEGs were identified by comparing the gene expression levels at each of the three time points (T2, T4, and T6) to the T0 time point. **(c)** Heatmap displaying the -Log10 p values of gene ontology terms associated with the set of overlapping genes between CE, CD, and AE identified in (b) for each time point.

**ATH1 inhibits the bolting transition through mediation of plant hormone homeostasis**

The transition from the vegetative phase to the reproductive phase in plants involves notable changes in hormone levels. Gibberellin is widely recognized as a hormone that promotes bolting. However, substantial alterations in other hormones such as auxin, brassinosteroids, cytokinins, and jasmonic acid have also been noted in plants undergoing or sensitive to bolting. In addition, there is evidence to suggest that also ethylene has a role in regulating the timing of bolting and subsequent internode elongation (Frugis *et al.*, 2001; Ogawara *et al.*, 2003; Achard *et al.*, 2007; Yoshida *et al.*, 2010; Hao *et al.*, 2018). Here, our analysis of the BACA gene set revealed a significant enrichment for genes involved in hormone-mediated signaling pathways, notably for gibberellin, brassinosteroids, and auxin (C4_Fig. 5a, 6a-c).



Gibberellin (GA) is pivotal for bolting, but not flowering, in Arabidopsis plants grown under long-day conditions (Blázquez *et al.*, 1998; Regnault *et al.*, 2014). Local GA biosynthesis is largely dependent on the activity of GA20-oxidase (GA20ox) and GA3-oxidase (GA3ox) enzymes that convert the GA precursor GA12 into bioactive GA4 and GA1 (Yamaguchi, 2008). GA, when present, promotes stem elongation by facilitating the degradation of DELLA proteins such as GIBBERELLIC ACID INSENSITIVE (GAI) and REPRESSOR OF GAI (RGA), which otherwise inhibit this process (Dill *et al.*, 2001; King *et al.*, 2001; Serrano-Mislata *et al.*, 2017). Recent findings by Ejaz et al. (2021) have pinpointed the GA biosynthetic gene *ARABIDOPSIS THALIANA GIBBERELLIN 3-BETA-HYDROXYLASE 1* (*ATGA3OX1*), the GA catabolism gene *ARABIDOPSIS THALIANA GIBBERELLIN 2-OXIDASE 6* (*ATGA2OX6*), and the GA signalling gene *RGA* as binding targets of ATH1 during vegetative growth. Yet, these genes did not fulfil the criteria to be classified as BACA genes. Instead, the gibberellin catabolism gene *ARABIDOPSIS THALIANA GIBBERELLIN 2-OXIDASE 4 (ATGA2OX4*) (Thomas *et al.*, 1999; Rieu *et al.*, 2008) was observed to be upregulated in AD plants, while its expression in the SAM decreased progressively in control plants under conditions that induce bolting (C4_Fig. 6a, b). *ATGA2OX4* encodes a functional C19-GA 2-oxidase and is expressed at the base of the SAM, where the RZ is located (Jasinski *et al.*, 2005). This suggests that ATH1-regulated GA deactivation may serve as a protective mechanism to prevent the influx of GA from surrounding tissues. This modulation of GA levels might be important, particularly as GA is known to promote cell

division within the RZ—a key process in the onset of stem growth (Sachs *et al.*, 1959a; Peterson & Yeung, 1972; Mutasa-Göttgens *et al.*, 2010). Therefore, ATH1 might well suppress bolting by reducing GA concentrations within the RZ.

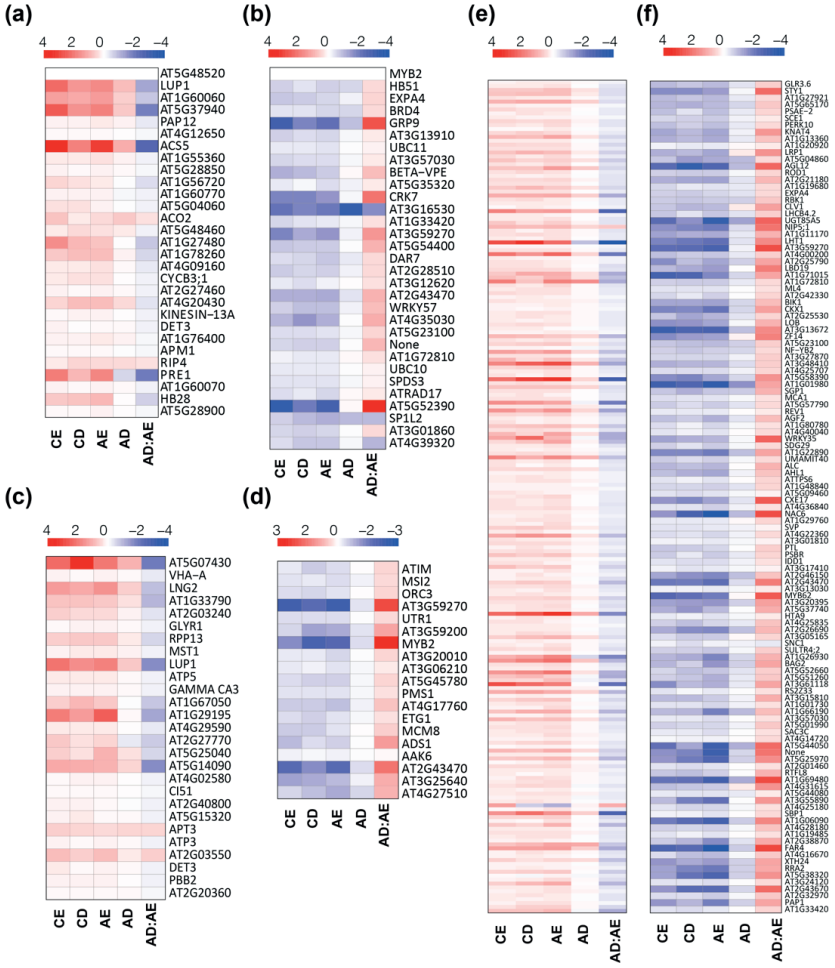


**C4_Fig. 4: Bolting associated genes controlled by ATH1.**

Heatmap displaying the Log2FC values of DEGs identified in Figure 3b, further selected based on their significant expression in AD compared to AE (AD at each time point compared to AE) and their lack of change in ADi compared to AD0. The upregulated DEGs at time point 2 are indicated in **(a)**, time point 4 in **(c)**, and time point 6 in **(e)**. The downregulated DEGs are shown for time point 2 in **(b)**, time point 4 in **(d)**, and time point 6 in **(f)**. The color scheme reflects the Log2FC values, with upregulated DEGs indicated in red and downregulated DEGs indicated in blue. The complete heatmap for **(e)**, which includes gene names, is shown in Supplementary Figure 3.

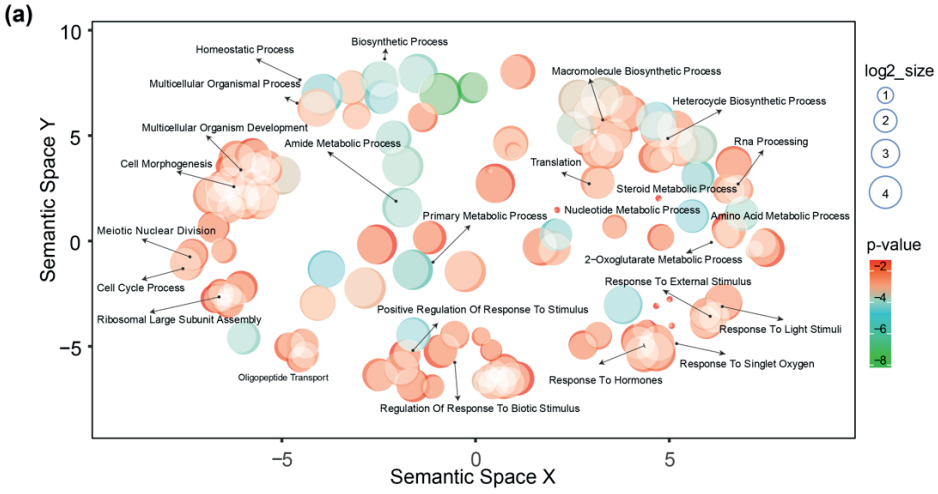


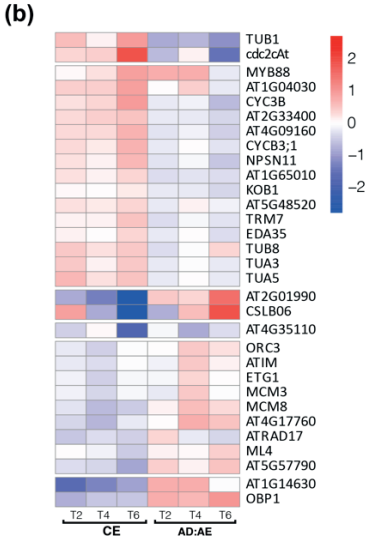


(c)

| Cell division related processes | Genes |
|---|---|
| Cell cycle | TUBB1\| MYB88\| NPSN11\| ETG1\| MCM8\| DOF3.4\| EDA35\| CYC3B \| ORC3\| TUBA3\| TUBB8\| cdc2cAt\| MCM3\| ATIM\| RAD17 |
| Regulation of cell cycle | MYB88\| DOF3.4\| EDA35\| CYCA2- 2\| cdc2cAt\| ATIM\| RAD17 |
| Mitotic cell cycle | TUBB1\| CYC3B \| TUBA3\| TUBB8\| MCM3\| RAD17 |
| Structural constituent of cytoskeleton | TUBB1\| TUBA3\| TUBB8 |
| MCM complex | ETG1\| MCM8\| MCM3 |
| DNA replication | MYB88\| ETG1\| ORC3\| MCM3\| ATIM |
| Regulation of cell cycle phase transition | MYB88\| CYCA2- 2\| ATIM\| RAD17 |
| DNA replication origin binding | MCM8\| ORC3\| MCM3 |
| Organelle organization | TUBB1\| NPSN11\| ETG1\| MCM8\| EDA35\| TUBA3\| TUBB8\| MCM3 |
| Cell cycle phase transition | MYB88\| CYC3B \| ATIM\| RAD17 |
| E2FA -Transcription factor E2FA target gene | MYB88\| MCM8\| ORC3\| MCM3\| ATIM\| RAD17 |
| DNA metabolic process | ETG1\| MCM8\| ORC3\| MCM3\| ATIM\| RAD17 |
| Nucleoside-triphosphatase activity | TUBB1\| MCM8\| TUBA3\| TUBB8\| MCM3 |
| Microtubule cytoskeleton organization | TUBB1\| TUBA3\| TUBB8 |
| Cellular response to DNA damage stimulus | ETG1\| MCM8\| MCM3\| ATIM\| RAD17 |
| Cell division | MYB88\| NPSN11\| ETG1\| EDA35\| CYCA2 - 2 |
| Cell cycle DNA replication | MYB88\| ORC3\| MCM3 |

**C4_Fig. 5: Multifaceted gene expression dynamics in Arabidopsis bolting revealed by transcriptome profiling.**

**(a)** ReviGO representation of Gene Ontology (GO) terms overrepresented in the BACA gene set, with Semantic Space X and Y representing two principal components derived from a multidimensional scaling (MDS) of the semantic similarities between GO terms. This visualization clusters GO terms that are semantically close to each other, allowing for a simplified and meaningful interpretation of complex GO term relationships (Reijnders 2021). The size of the circles indicates the log2 number of genes enriched in the respective GO term, and the color spectrum represents the range of P-values, indicating the significance of enrichment. Only genes with significant expression changes at one or more time points (T2, T4,

or T6) were included. **(b)** Heatmap illustrating the Log2 Fold Change (Log2FC) of genes enriched for the GO term "Cell cycle process". The heatmap depicts the expression values of these genes in CE plants (Col-8 treated with ethanol) and *35Spro:ATH1-HBD* plants treated with Dex (AD) compared to Ethanol (AE). The color scale depicts upregulation in red and downregulation in blue. **(c)** Table providing details of the genes shown in panel **(b)**, including their respective roles in different stages of cell division process.

Furthermore, *MYB DOMAIN PROTEIN 62* (*MYB62*) expression aligned closely with that of *ATGA2OX4*, showing a decrease in control plants under conditions that favour bolting, in contrast to the increased expression in AD plants (C4_Fig. 6a, b). *MYB62*, as a growth regulator, significantly affects stem elongation and the timing of bolting. Overexpression of *MYB62* induces a phenotype indicative of GA deficiency, characterized by stunted stem growth—an effect partially reversible with the application of GA, highlighting MYB62's role in the GA pathway (Devaiah *et al.*, 2009). Noteworthy is the finding that MYB62 directly binds and activates *ARABIDOPSIS THALIANA GIBBERELLIN 2-OXIDASE 7* (*GA2OX7*), thus elevating its expression and contributing to the catabolism of GA, ultimately leading to diminished GA levels (Qi *et al.*, 2021). The concurrent downregulation of *MYB62* and *ATH1* during bolting supports the notion that SAM-localized ATH1 supresses bolting by restricting GA availability to the RZ.

In addition to GA, Brassinosteroids (BRs) are pivotal in controlling diverse plant growth and developmental pathways, including the reproductive transition marked by bolting (Saini *et al.*, 2015). Mutants with impaired BR biosynthesis, such as *dwarf1* (*dwf1*) and *dwf4*, exhibit stunted stem growth. Similarly, the *brassinosteroid insensitive 1* (*bri*) BR receptor mutant shows a complete absence of stem elongation, mirroring the phenotype of plants with disrupted GA biosynthesis (Kauschmann *et al.*, 1996; Zhou *et al.*, 2023). Although these genes are not categorized within the BACA gene set, in our study, bolting correlated with differential expression of several BR biosynthesis genes, including *DWARF5* (*DWF5*), *CONSTITUTIVE PHOTOMORPHOGENIC DWARF* (*CYP90A1/CPD*), and *BRASSINOSTEROID-6-OXIDASE 1* (*CYP85A1/BR6OX1*) (Szekeres *et al.*, 1996; Bishop *et al.*, 1999; Hamasaki *et al.*, 2020). Whereas these genes were upregulated during bolting in control plants, in AD plants their expression was notably reduced, especially in case of *CYP90A1/CPD* and *CYP85A1/BR6OX1*, with a less pronounced decrease observed for *DWF5* (C4_Fig. 6a- c). The enzymes encoded by these genes are essential for specific stages in BR biosynthesis: CYP90A1/

CPD is involved in the C-3 oxidation, and CYP85A1/BR6OX1 carries out C-6 oxidation, essential for transforming 6-deoxoCS into castasterone (Nomura *et al.*, 2005; Ohnishi *et al.*, 2012). *DWF5* contributes to the biosynthesis of a Δ7-sterol reductase, vital for converting 5-dehydroepisterol to 24-methylenecholesterol in the BR pathway (Choe *et al.*, 2000; Zhou *et al.*, 2023). Plants carrying loss-of-function mutations for these genes are characterized by inhibited inflorescence stem elongation, resulting in significantly dwarfed plants, comparable to that observed in *ATH1* overexpression plants (Clouse, 2002; Kim *et al.*, 2005b; Cole *et al.*, 2006; Ohnishi *et al.*, 2012; Hajibehzad *et al.*, 2023). Together this suggests that *ATH1* down-regulation during bolting may be necessary to allow for local activation of BR biosynthetic genes, thereby promoting BR accumulation at the shoot apex, which appears to be indispensable for bolting.



In contrast to GA and BR, which are known to positively influence stem elongation when present in the stem (Azpiroz *et al.*, 1998; Eriksson *et al.*, 2006), the role of auxin in this process is multifaceted, and likely requires a delicate balance in hormone levels for appropriate stem development during bolting. Disruptions in polar auxin transport, as demonstrated by *pin1* mutants and *PIN6* overexpression lines, can lead to an overaccumulation of auxin in the stem and, consequently, inhibition of inflorescence stem elongation (Cazzonelli *et al.*, 2013; Ditengou *et al.*, 2018). In contrast, *pin6* mutants have a higher stem elongation rate than wild type plants, again showing the importance of auxin homeostasis for normal bolting (Ditengou *et al.*, 2018). Analysis of the BACA gene set indicated that in AD plants, where persistent ATH1 activity inhibits bolting, several genes integral to auxin regulation are mis-regulated (C4_Fig. 6a-c). Notably, there is a marked upregulation of the SHORT-INTERNODES/STYLISH (SHI/STY) family genes *SHI* and *STY1* that are known to enhance the activity of auxin biosynthesis genes such as *YUCCA4* (*YUC4*) and *YUC8*, critical for establishing local auxin peaks (Sohlberg *et al.*, 2006; Eklund *et al.*, 2010; Ståldal *et al.*, 2012; Baylis *et al.*, 2013). The pronounced expression of *SHI* and *STY1*, alongside that of *AAO1*—a gene also involved in auxin synthesis (Seo *et al.*, 1998)—in AD plants suggests an elevation in local auxin levels at the meristem to potentially growth inhibiting concentrations (C4_Fig. 6a-b).

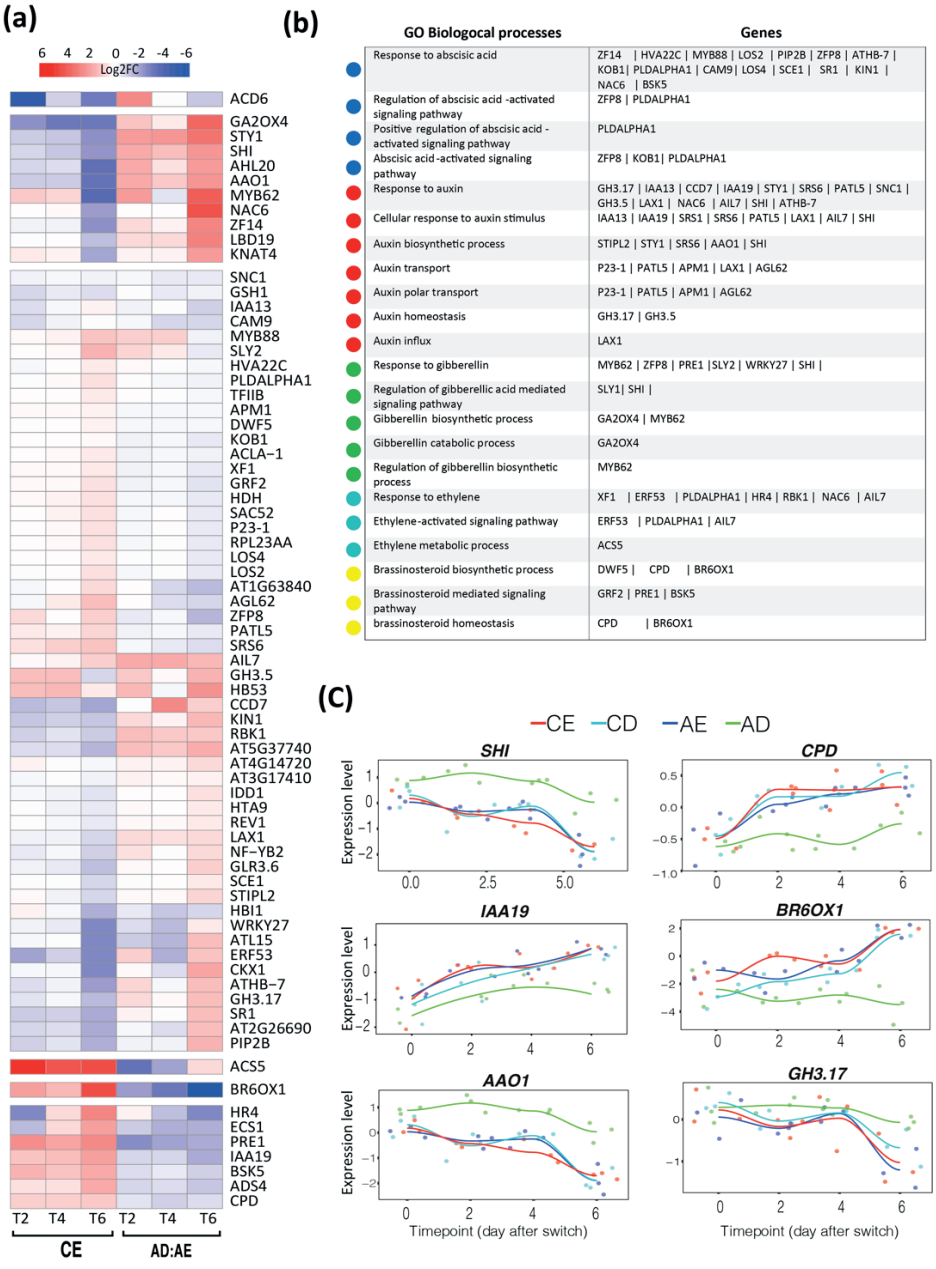


**C4_Fig. 6: Transcriptome analysis reveals the involvement of ATH1 in regulating light and hormone signaling pathways.**

**(a)** Heatmap illustrating the Log2 Fold Change (Log2FC) of genes enriched for the GO terms "response to hormones" key bolting associated gene controlled by ATH1 set identified in Figure 4a. The expression values of these genes are shown in CE plants (Col-8 treated with ethanol)

and *35Spro:ATH1-HBD* plants treated with Dex (AD) compared to Ethanol (AE). The color scale used in the heatmap shows upregulation in red and downregulation in blue. **(b)** Table providing details of the genes shown in panel (a), including their respective roles in hormone and light signaling pathways. **(c)** Graphs depicting the gene expression levels of selected genes from (a), chosen based on their pronounced expression levels or their prominent roles in hormone signaling pathways, across all time points in CE, CD, AE, and AD plants.

The lack of stem elongation in plants that overexpress *SHI* or *SHI-RELATED SEQUENCE* (*SRS*) genes (Fridborg *et al.*, 1999; Kuusk *et al.*, 2002; Eklund *et al.*, 2010; Hong *et al.*, 2012), which mimics the non-bolting phenotype observed in plants that ectopically express *ATH1* (Cole *et al.*, 2006; Gómez-Mena & Sablowski, 2008; Hajibehzad *et al.*, 2022), further supports this conclusion. Additionally, we observed a sharp downregulation in the auxin signaling component *IAA19* in AD plants (C4_Fig. 6a, c), suggesting an influence of ATH1 on the auxin signaling pathway as well. In AD plants BR levels are supposed to be reduced at the SAM, so lower *IAA19* could be the result of decreased BR levels (Nakamura *et al.*, 2003). Moreover, an observed moderate increase in *LIKE-AUX1* (*LAX1*) expression in AD plants, encoding an auxin influx carrier (Swarup & Bhosale, 2019), suggests a potentially active auxin uptake system during the bolting phase regulated by ATH1 (C4_Fig. 6a). The elevated expression of *GRETCHEN HAGEN3.5* (*GH3.5*) and *GH3.17* in AD plants, involved in auxin inactivation through auxin conjugation (Staswick *et al.*, 2005; Aoi *et al.*, 2019), further suggests that local deactivation of auxin also contributes to maintaining auxin homeostasis in relation to ATH1-mediated bolting (C4_Fig. 6a-c). Collectively, these findings point to ATH1 exerting a complex influence on the auxin pathway, affecting local biosynthesis, transport, signalling and overall homeostasis during the transition from the vegetative to reproductive phase.

As mentioned, apart from GA, BRs, and auxin, cytokinin and ethylene plant hormones have been implicated before in the regulation of bolting. In line with this, ethylene and cytokinin-related genes are present in the BACA set (C4_Fig. 6a, b). *1-AMINOCYCLOPROPANE-1-CARBOXYLATE SYNTHASE5* (*ACS5*), essential for ethylene biosynthesis, fails to become upregulated in AD plants grown under bolting-inductive conditions, whereas *CYTOKININ OXIDASE/DEHYDROGENASE1* (*CKX1*), implicated in cytokinin degradation (Schaller *et al.*, 2014), is no longer down-regulated in AD plants under these conditions (C4_Fig. 6a). This suggests

that the mechanism by which ATH1 controls bolting includes local modulation of ethylene and cytokinin levels at the shoot apex.

Although not commonly associated with bolting, a significant number of BACA genes can be associated to abscisic acid (ABA) signalling (C4_Fig. 6a). Worth mentioning in this context is *KOBITO1* (*KOB1*), a light-regulated gene involved in ABA response and cell elongation through regulating cellulose biosynthesis (Pagant *et al.*, 2002; Kong *et al.*, 2012). *KOB1* is slightly upregulated during bolting in control plants, but shows a substantial decrease in AD plants grown in inductive conditions (C4_Fig. 6a). In line with this observation, loss-of-function *kob1* plants display short inflorescence stems due to impaired internode elongation, a phenotype that is consistent with that seen of *ATH1*-overexpressing plants (Pagant *et al.*, 2002; Cole *et al.*, 2006; Gómez-Mena & Sablowski, 2008; Hajibehzad *et al.*, 2023). In summary, our transcriptome analyses highlight ATH1 as a central factor in the coordination of complex hormonal cues at the shoot apex necessary to inhibit the bolting transition

**ATH1 impacts cell division processes during bolting**

In Arabidopsis, the shift from vegetative to reproductive development is characterized by a surge in cell division, particularly in the RZ of the shoot apex, which is crucial for stem elongation (Jacqmard *et al.*, 2003; Kwiatkowska, 2008). This developmental transition has been previously highlighted for its dramatic increase in number of differentially expressed cell cycle-related genes (Klepikova *et al.*, 2015). Our transcriptomic data confirm this previous observation, revealing a substantial representation of genes within the BACA cluster that are implicated in cell cycle progression, DNA replication, and cytokinesis (C4_Fig. 5a-c).

The transition through various stages of the cell cycle is governed by serine-threonine protein kinase complexes, each consisting of a cyclin-dependent kinase (CDK) and a regulatory cyclin (CYC) unit. These complexes are integral in managing key cell cycle checkpoints. Analysis of the BACA gene set, points to the role of ATH1 in regulating the expression of certain CDK-cyclin complex genes, such as *cdc2cAt/CDC2C*, *CYC3B*, and *CYCB3;1* (C4_Fig. 5b, c). Notably, the *cdc2cAt/CDC2C* gene is distinct due to its exclusive expression in floral tissues and its unique expression pattern and gene structure, suggesting it has a specialized role in the cell cycle during floral development (Hemerly *et al.*, 1995; Fobert *et al.*, 1996; Lessard *et al.*, 1999). The expression of this gene, along with

*CYC3B* and *CYCB3;1*—both of which are cyclin genes in Arabidopsis (Wang *et al.*, 2004; Motta *et al.*, 2021)— is reduced in plants with constitutively active nuclear ATH1 (C4_Fig. 5b), implying that ATH1 controls RZ activity and, hence, bolting by influencing the expression of CDK-cyclin complex genes.

Additionally, the presence of the DNA-binding-with-one-finger (DOF) transcription factor *AtDOF3.4/OBP1* within the BACA gene cluster is noteworthy. *OBP1* is known to regulate cell cycle progression by targeting the expression of essential cell cycle and replication machinery genes in a developmentally specific manner (Skirycz *et al.*, 2008). Interestingly, *OBP1* expression is diminished in control plants undergoing bolting, but increased in AD plants with persistent *ATH1* activity (C4_Fig. 5b). This contrasting pattern of *OBP1* expression, along with the suppressed inflorescence stem elongation observed in Arabidopsis plants overexpressing *OBP1* (Skirycz *et al.*, 2008), aligns with OBP1 as an early target in the regulation of bolting.



DNA replication, a vital step in cell division, is regulated by a complex network of proteins. Among these, the BACA gene set contains several key players: *ORIGIN RECOGNITION COMPLEX3* (*ORC3*), *MINI-CHROMOSOME MAINTENANCE 3* and 8 (*MCM3* and *MCM8*), and *E2F TARGET GENE1* (*ETG1*), which are central to initiating and executing DNA replication (C4_Fig. 5c). ORC3 is a component of the ORC complex responsible for binding to replication origins at the onset of S phase, which is crucial for initiating DNA replication (Collinge *et al.*, 2004). The ORC complex also recruits the MCM complex, consisting of a hexamer of MCM proteins that all share a well conserved helicase domain important for unwinding DNA helices, allowing replication forks to form and DNA synthesis to proceed. ETG1, as an associated component of the MCM complex, acts as a regulator of DNA replication (Takahashi *et al.*, 2008). Our data shows downregulation of these DNA replication-associated genes in the absence of ATH1 activity, suggesting ATH1 impacts on DNA replication to delay bolting (C4_Fig. 5b).

Cytokinesis marks the final stage of cell division and requires tubulin proteins. The BACA gene set, contains several tubulin genes, including *TUBULIN BETA-1 CHAIN* (*TUB1*), *TUBULIN ALPHA-3* (*TUA3*), and *TUA5*. In AD plants with continued ATH1 activity after switching to bolting-inducing conditions, the expression of these tubulin genes is markedly reduced, with *TUB1* being absent (C4_Fig. 5b). These findings point to ATH1, to control internode development, exerts a regulatory effect on tubulin gene expression, thereby impacting the cytokinesis process.

In summary, internode development is based on a combination of cell proliferation and cell elongation, followed by cell differentiation further down the developing stem (Jacqmard *et al.*, 2003). A large representation of cell proliferation-associated genes within the BACA cluster, encompassing cell cycle, DNA replication, and cytokinesis components, suggest that limiting cell proliferation forms a significant part of the mechanism by which ATH1 inhibits inflorescence stem growth.

## Discussion

In Arabidopsis, the phenomenon of bolting emerges as a pivotal developmental stage, marking the transition from vegetative growth to reproductive maturity. It is within the SAM's CZ where the foundational activity begins, hosting pluripotent stem cells destined to differentiate and give rise to the plant's aerial architecture. These stem cells typically undergo division at a conservative rate, yet they are the progenitors of daughter cells that have two distinct fates: contributing to the formation of new organ primordia along the SAM's periphery or fueling the production of an inflorescence stem at bolting (Soyars *et al.*, 2016; Kean-Galeno *et al.*, 2024). Bolting in Arabidopsis is defined by a pronounced surge in cell proliferation within the uppermost region of the RZ, an area teeming with nascent cells destined for rapid elongation and subsequent differentiation as they descend (Sachs *et al.*, 1959a; Sachs, 1965; Gómez-Mena & Sablowski, 2008). This crucial phase of development not only shapes the plant's structural integrity but also has far-reaching implications for its reproductive capabilities and, consequently, the efficiency of agricultural production systems reliant on such processes.

**ATH1's regulatory influence in the RZ: A cloak over cell division**

Our transcriptome analysis has cast light on ATH1's regulatory role in modulating cell cycle genes in the shoot meristem, presumably at the RZ apex. By exerting regulatory control over a host of genes critical for cell cycle progression, DNA replication, and cytokinesis, ATH1 controls the bolting transition (C4_Fig. 5a-c). The genes within the BACA cluster, such as *cdc2cAt/CDC2C*, *CYC3B*, and *CYCB3;1*, highlight the influence of ATH1 on the cell division machinery. For instance, the upregulation of *cdc2cAt/CDC2C*, a cyclin-dependent kinase, in wild-type plants during bolting underscores its role in advancing the cell cycle. However, in the

presence of *ATH1*, its expression is markedly subdued, suggesting a repression of cell division. Arabidopsis has three *cdc2* kinases: *cdc2a*, *cdc2b*, and *cdc2c*. The *cdc2c* is active during both DNA synthesis (S phase) and the transition from the second growth phase (G2) to mitosis in plant cells (Fobert *et al.*, 1996). In dormant human cells, levels of *cdc2* are low, but increase when cells re-enter the cycle (Lee *et al.*, 1988; Furukawa *et al.*, 1990). The observed increase in *cdc2cAt* in the SAM of plants beginning to bolt suggests the initiation of cell proliferation. Conversely, the decrease in this activity in plants overexpressing *ATH1* suggests a role for ATH1 in suppressing cell division by downregulating a type C cyclin-dependent kinase *cdc2cAt* within the SAM.

The effect of ATH1 appears to extend to the regulation of cyclins, which orchestrate the cell cycle together with CDKs. In plants with active nuclear ATH1, the expression of *CYC3B* and *CYCB3;1*—genes that typically peak at the initiation of bolting (Ito *et al.*, 2001; Sablowski & Dornelas, 2014; Klepikova *et al.*, 2015), is reduced. This suggests that ATH1 might suppress the transition from the G2 phase to mitosis (C4_Fig. 5a-c). From this perspective it is interesting to note that one of the genes controlled by ATH1 during the bolting process is *OBP1*. *OBP1* is a gene linked to the control of cell division, specifically influencing the regulation of certain *CYCB* genes (Skirycz *et al.*, 2008; Komaki & Sugimoto, 2012; Larrieu *et al.*, 2022). Importantly, plants overexpressing either *ATH1* or *OBP1* exhibit strikingly similar non-bolting phenotypes. Since *ATH1* overexpression leads to elevated *OBP1* expression, this suggests that ATH1 might repress inflorescence stem elongation by local upregulation of *OBP1* in the meristem, which in turn modulates cell cycle-related genes (Skirycz *et al.*, 2008). Furthermore, our study suggests impact of ATH1 on the microtubule network, crucial for cell division and elongation, by modulating α- and β-tubulin gene expression. The proper assembly of microtubules is essential for maintaining cellular integrity and facilitating mitotic spindle formation (Mathur & Hülskamp, 2002). ATH1's regulatory effect appears to dampen the expression of tubulin genes. This suggests a potential mechanism by which ATH1 inhibits bolting: it may restrain the microtubule dynamics necessary for cell division. Further investigation however is needed to determine whether ATH1 directly targets microtubule dynamics or if these effects are a downstream consequence of its influence on cell cycle progression.

In addition, the role of ATH1 in cell cycle control is further corroborated by the behavior of the *MCM3* and *MCM8* genes, whose slight upregulation in AD plants

contrasts with the downregulation observed during bolting in control plants. The MCM complex, to which these genes contribute, is critical for DNA helicase activity during the S phase, and their fine-tuned expression is essential for proper cell cycle progression and, consequently, optimal plant growth. There is evidence indicating that an overexpression of *MCM* genes could, in fact, be counterproductive to growth. For instance, an overexpression of *MCM2* has been associated with inhibited growth, leading to shorter inflorescence stems (Ni et al., 2009), an effect that mirrors the growth restraint observed in plants with an overexpression of *ATH1*.

Bolting in Arabidopsis involves not only increased cell division and elongation but also a potentially shift in their directionality along the apical-basal axis. This shift might be essential for characteristic upward stem growth. While the roles of proliferative and formative cell divisions are well-studied in Arabidopsis root development, their influence within the shoot meristem, specifically the RZ, remains unexplored (Blilou, 2024; Winter *et al.*, 2024). One could speculate that this directional shift might involve subtle changes in the balance between these division types, with perpendicular divisions likely being proliferative, expanding stem girth, and those parallel potentially reflecting formative divisions, directly driving vertical stem elongation (Sablowski & Gutierrez, 2021). Within the RZ, the regulation of cell division plays a significant role in influencing cell fate and function, with potential consequences for plant architecture and the initiation of this process. Our findings suggest a role for ATH1 in modulating cell cycle genes and potentially also in influencing cell division orientation within the RZ apex. This raises the possibility that ATH1 determines whether a cell within the RZ differentiates and contributes to vertical growth. The E2F family, particularly E2FA, plays a critical role in regulating the G1/S transition of the cell cycle, ensuring precise timing and orientation of cell division (Inzé & Veylder, 2006). These factors, along with RETINOBLASTOMA-RELATED (RBR1) proteins, maintain developmental control (Desvoyes & Gutierrez, 2020). While *E2FA* was not classified as BACA gene set, our transcriptome analysis reveals shifts in the expression of several of its target genes (e.g., MYB88, MCM8, MCM3, ORC3, ATIM, and RAD17). This could indicate an influence of ATH1 on the balance between formative and proliferative cell divisions.

**ATH1's underlying influence in RZ: swaying cell division likely through hormonal balance**

At bolting, a sharp increase in cell proliferation within the RZ apex fuels the rapid elongation allowing for the formation of the inflorescence stem. In line with this, our findings here indicate that, in the context of bolting, ATH1 plays a pivotal role in orchestrating a gene network essential for various cell cycle processes, such as cell division, DNA replication, and cytokinesis. In addition, the transcriptome analysis presented in this study suggests that ATH1 inhibits the bolting transition through local mediation of, among others, plant hormone homeostasis, including auxin, BR, and GA.

Specifically, ATH1 appears to modulate GA catabolism, potentially restraining GA levels within the SAM. This hypothesis fits with the typical surge in GA levels observed in the SAM during bolting (Eriksson *et al.*, 2006; Kinoshita *et al.*, 2020). Additionally, *ATH1* overexpression suppresses crucial BR biosynthesis genes in the meristem. Again, this aligns well with a reported critical role of both GA and BR in regulating bolting (Tong *et al.*, 2014; Unterholzner *et al.*, 2015; Ross & Quittenden, 2016), alongside the bolting-related phenotypes in BR biosynthesis mutants. Furthermore, ATH1 also appears to regulate bolting by influencing auxin homeostasis within the meristem. This is evidenced by the misregulation of several key auxin-related genes in plants with sustained ATH1 activity. Of particular interest is ATH1's potential influence on the *SHI/STY* gene family. Misexpression of these genes is known to directly affect internode elongation. Notably, plants overexpressing *SHI/STY* genes, similar to those with elevated *ATH1* levels, exhibit shorter internodes (Fridborg *et al.*, 1999; Kuusk *et al.*, 2002). Moreover, while detailed expression patterns of *SHI* family genes in the meristem remain to be fully explored, the presence of *STY1* seems inversely correlated with ATH1 levels (Kuusk *et al.*, 2006; Hajibehzad *et al.*, 2022), suggesting a potential localized ATH1 influence on this gene.

Our previous work (Chapter 3) identified ATH1 as a negative regulator of internode cell elongation during vegetative growth. This regulation is achieved, in part, by modulating auxin, BR, and GA biosynthesis and signaling pathways. During bolting, cell elongation occurs in conjunction with cell division and is responsible for the rapid elongation of the stem. Considering the effect of ATH1 on these specific hormones in the context of bolting, it is conceivable that its involvement in this developmental process extends beyond solely affecting cell division and

also includes regulation of cell elongation. This would align with its established role in regulation of internode elongation during vegetative development. Alternatively, ATH1's impact on bolting may predominantly revolve around controlling cell proliferation, stemming from hormonal regulation of the cell cycle machinery. This is because, in addition to cell elongation, plant hormones, including auxin, BR and GA, coordinate various aspects of the cell cycle, governing not just the rate of cell division, but also the length of each stage within the cycle. Furthermore, beyond their individual roles in regulating fundamental cell cycle processes, the collaborative effects and interdependence of phytohormone signaling are likely critical for regulating cell cycle advancement within a developmental context (Shimotohno *et al.*, 2021).

While a direct association between ATH1 and the regulation of cell elongation during bolting remains uncertain, there's a critical need to synchronize cell division and growth as stem cell descendants enter a transit amplifying zone, like the RZ (Willis et al., 2016). Thus, exploring whether ATH1 participates in coordinating these essential cellular processes crucial for forming an elongated inflorescence stem presents an intriguing avenue for future investigation.

## Materials and Methods

### Plant material & growth conditions

This study utilized *Arabidopsis thaliana* Col-8 accession as the wild-type background. The *ath1-3* mutant (Proveniers *et al.*, 2007), *35Spro:ATH1-HBD* (Rutjens *et al.*, 2009) and *ath1-3 ATH1:ATH1-GFP* (Ejaz *et al.*, 2021) lines, all in the Col-8 background, were previously described.

Seeds were sterilized using a 4-hour chlorine gas treatment generated from a mixture of 4 ml 37% hydrochloric acid (HCl) and 100 ml of 4.5% active chlorine commercial bleach. Sterilized seeds were planted on either soil (Primasta B.V., Asten, Netherlands) or sterile 0.8% plant agar (Duchefa Biochemie B.V., Haarlem, The Netherlands), supplemented with full-strength Murashige–Skoog medium (including MES, pH 5.8, and vitamins). Seeds were stratified for 2-3 days at 4°C before being transferred to climate-controlled growth chambers (Microclima 1000; Snijders Labs, Tilburg, The Netherlands). Plants were grown under either short-day (SD; 8 h light/16 h dark) or long-day (LD; 16 h light/8 h dark) photo-

periods with a standard light intensity of 120 µmol m−2 s−1 (Luxline Plus Cool White, Sylvania, OH, USA) and 70% relative humidity. For specific experiments, a Snijders Microclima cabinet equipped with Philips GreenPower LEDs provided controlled red, blue, and far-red light.

To investigate the dynamics of stem elongation during bolting and the influence of maintained ATH1 levels, we employed wild-type Col-8 and the *35Spro:ATH1-HBD* line. Plants were initially grown for five weeks under non-bolting inductive short-day photoperiod conditions. Following this, bolting was induced in half of the plant population from each line by transferring them to long-day conditions supplemented with far-red light (LD FR). Dexamethasone (Dex) was used to control ATH1 activity. Dex treatments were applied at various time points relative to bolting induction: 2 and 1 day prior to transfer (treatments continuing for 5 days post-transfer), on the day of transfer (treatment duration 5 days or till the end of flowering), and 2 or 5 days after transfer (treatments continuing till the end of flowering). Ethanol treatments (0.1% v/v) were used as a control. Plant growth parameters, including inflorescence stem length and internode length, were monitored at defined time points relative to bolting induction, enabling analysis of stem elongation dynamics under varying ATH1 activity levels.



**Confocal microcopy & cell height analysis**

To study cellular changes associated with bolting, plants were initially grown under non-inductive short-day (SD) conditions for 5 weeks. Subsequently, half of the plants were transferred to long-day supplemented with far-red light (LD FR) to induce bolting, while the remaining half were maintained in SD as controls. Shoot apices were collected at 0, 1, and 4 days after transfer, dissected, and stained with mPS-PI as outlined in previous studies (Truernit *et al.*, 2006; Bencivenga *et al.*, 2016). Imaging of the stained meristems was performed using a Leica SP5 confocal microscope with a 20x/0.75 long working distance objective, a resolution of 0.25 x 0.25 x 0.5 µm, excitation at 561 nm, and emission filters set to 571-700 nm. For GFP imaging, apices were cleared using the ClearSee method (Kurihara *et al.*, 2015) and imaged under identical conditions with excitation at 488 nm and detection at 502-521 nm. Image processing followed the methodology described by Bencivenga et al. (2016), utilizing custom ImageJ scripts. To analyze cell elongation changes, medial sections of the images were segmented in 2D. Using R software (www.r-project.com, the heights of cells within 15 µm

of the main axis and located either 0-45 µm or 45-90 µm from the apex summit were measured, providing insights into differential cell elongation patterns during bolting induction.

**RNA sequencing experimental setup and analysis**

Col-8 and *35Spro:ATH1-HBD* plants were grown for 35 days under non-inductive short-day (SD) conditions to prevent premature bolting and maximize sample uniformity. Plants were then transferred to LD FR conditions to initiate the bolting process. To enhance ATH1 nuclear localization, plants were treated with either 10 µM dexamethasone (DEX; Sigma-Aldrich) or a mock solution (0.1% ethanol v/v) starting immediately after germination and continuing three times per week. Shoot apices were collected at four time points (0, 2, 4, and 6 days) following the transfer to LD FR conditions (C4_Fig. 3a). Careful dissection under a binocular microscope was performed to remove rosette leaves and associated tissues until the SAM was exposed. Isolated SAM-enriched tissue was immediately snap-frozen and stored at -80°C. Three biological replicates were obtained per genotype and treatment combination, with each replicate consisting of three pooled shoot apices. RNA isolation from meristem tissue was performed using the Qiagen RNAeasy micro-kit, followed by sequencing at the Utrecht Sequencing Facility (USEQ; www.useq.nl). Raw FASTQ files underwent quality control using FastQC (v0.11.8), with subsequent trimming of low-quality reads and adapters using TrimGalore (v0.6.5). Ribosomal RNA reads were filtered using SortMeRNA (v4.3.3), and remaining reads were aligned to the reference genome using STAR (v2.7.3a). Mapped files underwent further quality checks with Sambamba (v0.7.0), RSeQC (v3.0.1), and PreSeq (v2.0.3). Read counts were generated using the Subread FeatureCounts module (v2.0.0) with Arabidopsis_thaliana.TAIR10.51.gtf as the annotation, followed by normalization using edgeR (v3.28). Differential expression analysis utilized an in-house R script with DESeq2 (v1.28), employing raw read counts as input. Genes with an average of less than 1 annotated read per sample were excluded and for remaining genes, mean read counts, log2 fold-change (log2FC), and p-values between genotypes were calculated. To isolate genes specifically influenced by bolting, differentially expressed genes (DEGs) in CE, CD, and AE were compared at each time point (2, 4, and 6 days) after bolting induction against their expression levels at time point 0. A p-value threshold of $<0.05$ was used to define significant differential expression (C4_Fig. 3b)

We developed an R-based Shiny web application (https://shokrianetalbolting.shinyapps.io/shinyapp/) to facilitate rapid exploration of individual transcripts within our RNA-seq dataset. Users can enter an Arabidopsis Gene Identifier (AGI) locus to visualize the bolting-induced log2 fold-change (log2FC) range across genotypes and treatment combinations. The application dynamically generates a plot with color-coded data points representing different treatment conditions (CE, CD, AE, AD). A loess smoother is included to depict trends in gene expression over the experimental time course.

**Gene ontology enrichment analysis**

Gene Ontology (GO) term enrichment analysis was performed on the genes depicted in C4_Fig. 2b using the clusterProfiler R package (Yu *et al.*, 2012; Wu *et al.*, 2021). We specifically analyzed biological process (BP) GO terms with a significance threshold of p-value ≤ 0.01, with false discovery rate (FDR) correction applied to account for multiple testing. Enrichment results across all time points were combined into a single data frame and subsequently filtered for significance (p-value ≤ 0.01). To visualize enrichment patterns, we constructed a heatmap where -log10 transformed p-values indicated the significance of each GO term at each time point. The heatmap was generated using the top 50 GO terms, selected based on their minimum p-values across the time series. To specifically investigate GO terms enriched within the BACA genes, we employed the ReviGO tool (Ge *et al.*, 2019). ReviGO's multidimensional scaling (MDS) algorithm semantically clustered GO terms, reducing their complex relationships into two principal components (Semantic Space X and Y). This allowed us to visualize semantic clusters of functionally related GO terms (Reijnders & Waterhouse, 2021). The initial visualization was created using the R code provided by ReviGO, representing semantic similarity along the Semantic Space X and Y axes. For enhanced clarity, final graphical refinements were made using Adobe Illustrator.

**Statistical analyses and data visualization**

All statistical analyses were conducted using R software (www.r-project.com). Specific details regarding sample size (biological replicates) and statistical tests performed are provided within the corresponding figure legends. When the assumptions of normality and homogeneity of variances were met, multi-comparison analyses were performed using multifactorial ANOVA followed by Tukey's

HSD post hoc correction. In cases where these assumptions were not satisfied, we employed Dunn's test with Benjamini-Hochberg adjustment for multiple comparisons. Data visualization was primarily performed using R packages, including pheatmap for heatmap generation and ggplot2 for other graphical representations. For optimal clarity and presentation, final adjustments and refinements to figures were made using Adobe Illustrator.

## Acknowledgements

The *ath1-3 pATH1-ATH-GFP* line was a kind gift of Robert Sablowski (John Innes Centre, UK).

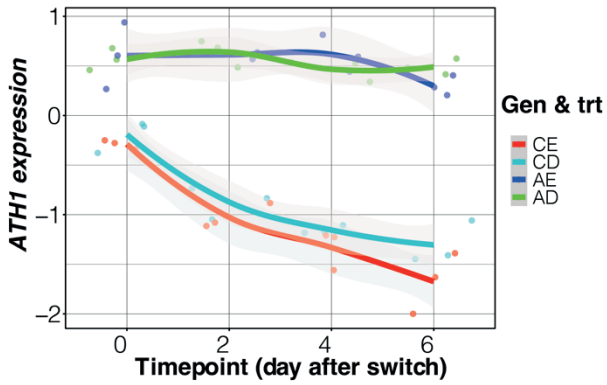


**C4_Fig. S1: *ATH1* is downregulated upon bolting induction.**

*ATH1* expression levels were obtained from RNA sequencing analysis of different genotypes (Gen) and treatments (trt) after the induction of bolting. The genotypes and treatments include AD and AE (*35Spro:ATH1-HBD* plants treated with Dex or Ethanol) and CD and CE (Col-8 plants treated with Dex or Ethanol).

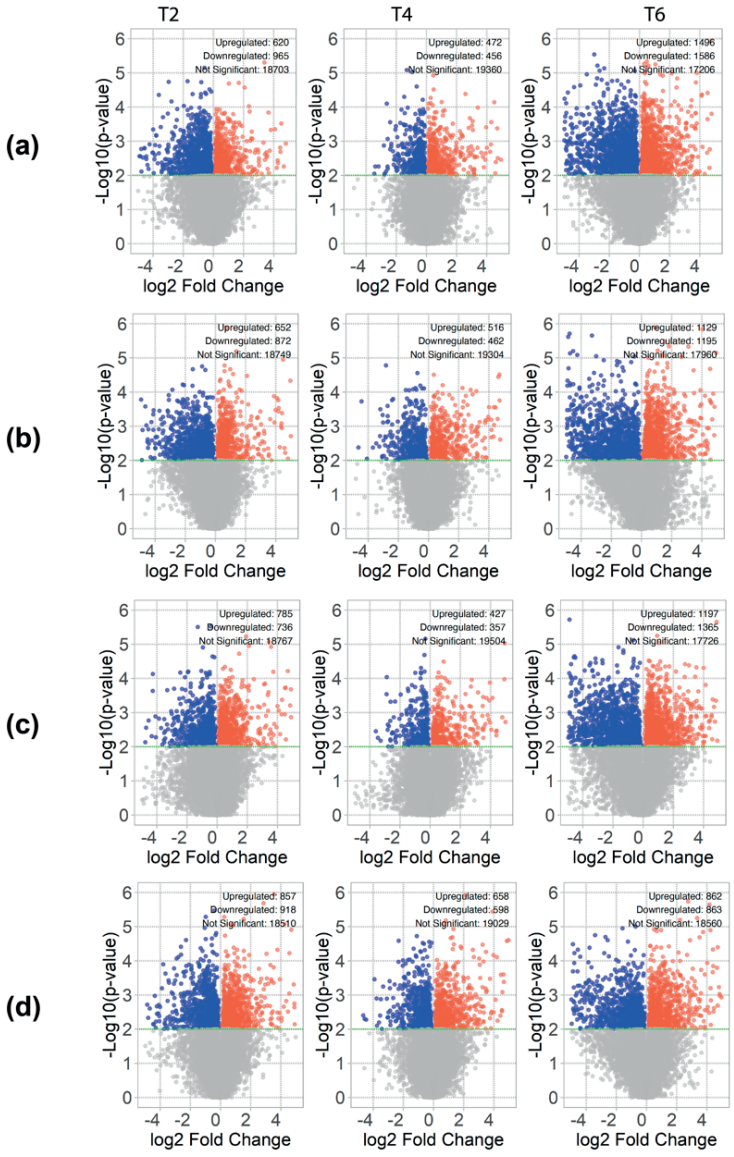


**C4_Fig. S2: Volcano plot analysis of gene expression changes after bolting induction.**

Volcano plots showing the log2 Fold Change and -Log10 (p-value) of gene expression changes in Col-8 plants treated with ethanol **(a)** or Dex **(b)**, and *35Spro:ATH1-HBD* plants treated with ethanol **(c)** or Dex **(d)** at different time points after bolting induction (T2, T4, and T6) relative to T0. The number of differentially expressed genes (DEGs) for downregulated and upregulated genes, as well as non-significant genes (gray) is indicated on the graph. The colored dots correspond to genes that meet the threshold of p-value < 0.01 for upregulated (red) or downregulated (blue) genes.

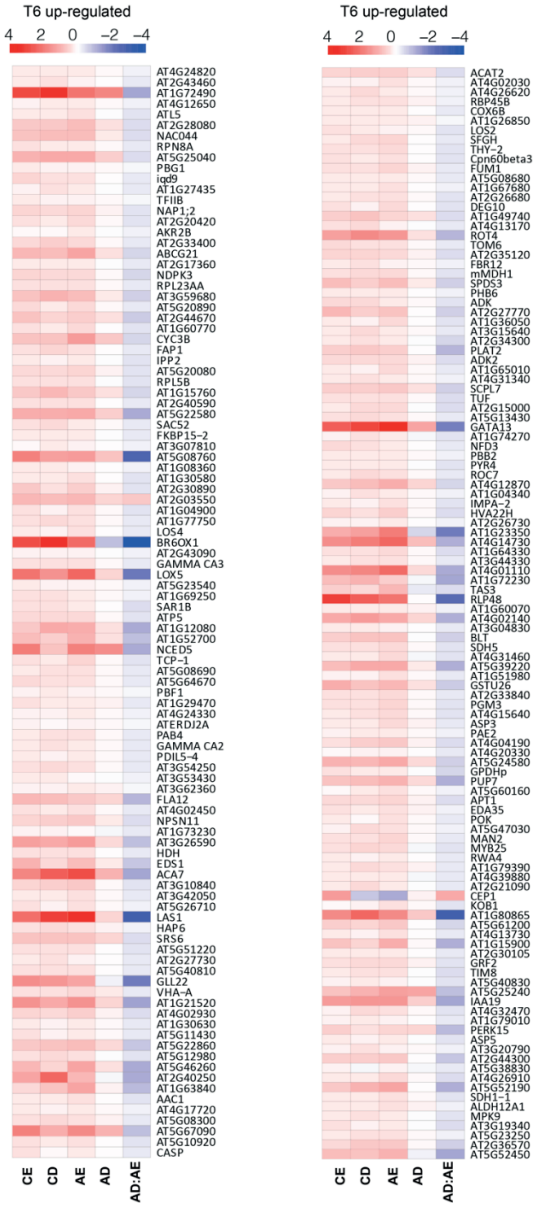


**C4_Fig. S3: Up-regulated bolting associated genes controlled by ATH1 at time point 6 after bolting induction.**

Heatmaps displaying the Log2FC values of DEGs depicted in Figure 4c, with annotated gene names included for clarity. To ensure readability of gene names, the DEGs were divided into two groups and depicted in two separate heatmaps. The color scheme reflects the Log2FC values, with upregulated DEGs indicated in red and downregulated DEGs indicated in blue.

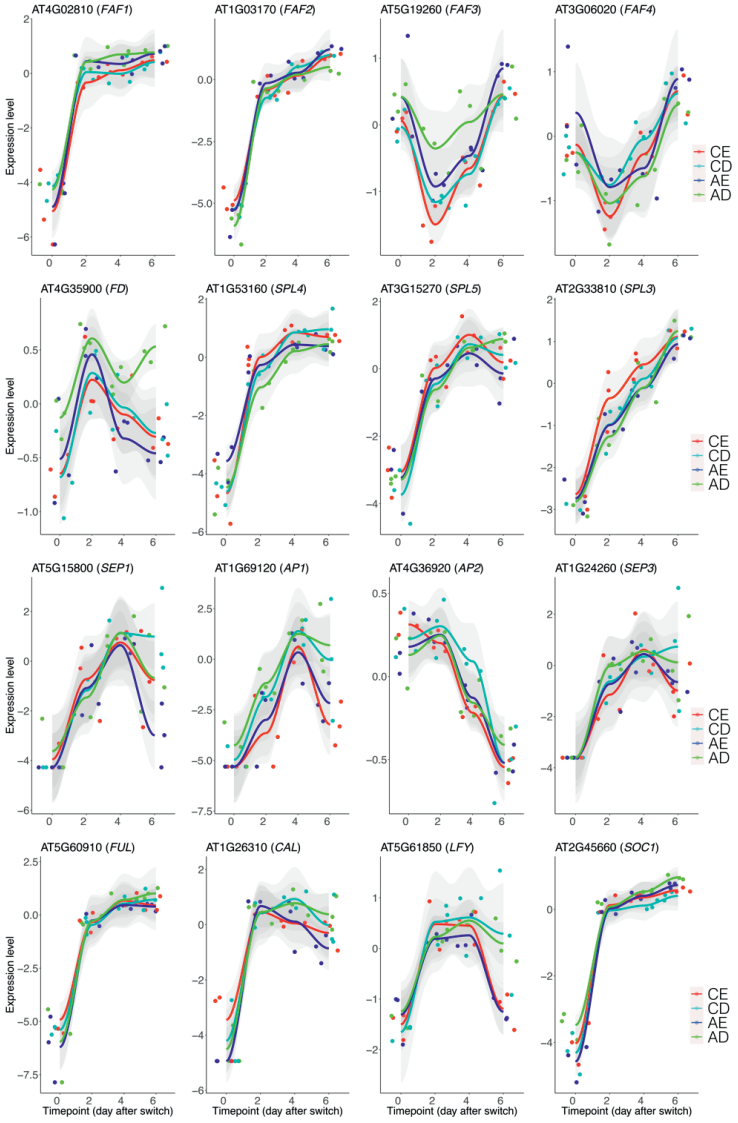


**C4_Fig. S4: Dynamics expression pattern of floral pathway integrator (FPI), floral meristem identity (FMI), flower development (FD) and other flowering-related genes during the onset of bolting.**

Set of graphs illustrates the temporal expression patterns of critical genes involved in floral pathway integration (FPI: *SOC1, FD, LFY, FUL*), specification of floral meristem identity (FMI: *LFY, AP1, FUL, CAL*), and flower development (FD: *AP1, AP2, SEP1, SEP3*) cluster across different timepoints during the bolting process in CE, CD, AE, and AD plants. Each graph presents a time series analysis from day 0 to day 6 after the bolting switch, with data points plotted to reflect gene expression levels.


Col-8
ath1-3

# Chapter 5

## Summarizing discussion

Shahram Shokrian Hajibehzad[1, 2], Sjef Smeekens[1], Marcel Proveniers[1,2]

[1] *Molecular Plant Physiology, Department of Biology, Science4Life, Utrecht University, Padualaan 8, 3584CH, Utrecht, The Netherlands*

[2] *Translational Plant Biology, Department of Biology, Science4Life, Utrecht University, Padualaan 8, 3584CH, Utrecht, The Netherlands*

Throughout its life cycle, *Arabidopsis thaliana* undergoes a series of developmental transitions mediated by a complex interaction of genetic and environmental factors. This developmental program centers upon the shoot apical meristem (SAM), a population of stem cells that give rise to the aerial structures of the plant (Bowman & Eshed, 2000; Williams & Fletcher, 2005). Upon germination and subsequent exposure to light, the SAM is activated, initiating the development of true leaves and establishing the characteristic rosette growth habit (Pfeiffer *et al.*, 2016). This compact rosette, characterized by tightly clustered leaves and minimal internode elongation, likely confers adaptive advantages such as increased stability and resistance to environmental stressors (Schaffer & Schaffer, 1979; Bello *et al.*, 2005; Larcher *et al.*, 2010; Thomson *et al.*, 2011; Fujita & Koda, 2015). Rosette formation is a widespread growth pattern among angiosperm lineages, both in monocot and dicot species, and is prevalent in several different kind of environments, including alpine, desert, temperate, and tropical areas (Givnish *et al.*, 1999; Martorell & Ezcurra, 2002; Larcher *et al.*, 2010; Cohen, 2011; Hao *et al.*, 2017).



The establishment and maintenance of the rosette habit are closely tied to photomorphogenesis, a light-dependent developmental process. Photoreceptors, such as phytochromes and cryptochromes, sense changes in light quality and intensity, triggering downstream signaling pathways that influence *ARABIDOPSIS THALIANA HOMEOBOX GENE 1* (*ATH1*) expression. The transcription factor *ATH1*, expressed within the SAM, plays a vital role in suppressing internode elongation throughout the vegetative phase, thus preserving the compact rosette architecture (Ejaz *et al.*, 2021; Hajibehzad *et al.*, 2023). *ATH1* expression, and consequently rosette formation, are influenced by both light and the availability of metabolic sugars. Sugars act as an energy source, promoting meristem activity and *ATH1* expression. The Target of Rapamycin (TOR) kinase integrates these energy and light signals, modulating *ATH1* expression and influencing rosette architecture (Hajibehzad *et al.*, 2023; Chapter 2). Our research (Chapter 3) demonstrates that ATH1 achieves this by directly targeting genes involved in cell elongation within the shoot apex, thereby ensuring the developmental robustness of the rosette habit in the face of various perturbations.

However, the rosette habit is not a permanent feature. The plant eventually transitions to the reproductive phase, a shift known as bolting. This transition, triggered by environmental cues like changes in day length and temperature,

involves significant changes in SAM dynamics. Rapid cell division and elongation within the rib zone (RZ) lead to the formation of an elongated flowering stem. The downregulation of *ATH1* within the SAM is crucial for initiating the bolting process (Gómez-Mena & Sablowski, 2008) (Chapter 4).

The development of *Arabidopsis thaliana* exemplifies the delicate balance between stability and adaptability in plant growth. This distinction is particularly evident during vegetative development, where the plant maintains a compact rosette habit across various environments. In contrast, during the bolting transition and subsequent development of the inflorescence stem, there is a considerable degree of adaptability, enabling the plant to adjust its reproductive strategy in response to environmental cues. The underlying molecular mechanisms, explored in detail in Chapters 2, 3, and 4, reveal a complex interplay between endogenous hormonal inputs, environmental cues and gene expression regulation.

**Beyond plasticity: ATH1's command over compact rosette formation in Arabidopsis**

The Arabidopsis rosette displays remarkable robustness, maintaining a consistent form across diverse environments. This contrasts with the plasticity observed in other structures, such as hypocotyls, petioles, and inflorescence stems, which readily elongate in response to environmental changes. For instance, hypocotyls rapidly elongate in low light for optimal light capture, while petioles adjust their length for photosynthetic efficiency. Similarly, the elongation of inflorescence stems during reproduction is highly responsive to cues, facilitating seed dispersal (Liscum *et al.*, 1992; Galvão *et al.*, 2019; Oh *et al.*, 2019; Favero *et al.*, 2020; Küpers *et al.*, 2023). The rosette, however, maintains its compact structure largely independent of typical environmental fluctuations ((Ejaz *et al.*, 2021; Hajibehzad *et al.*, 2023); Chapters 2 and 3).

In Chapter 3, we demonstrate that the robustness of the rosette habit depends entirely on *ATH1* expression within the SAM. ATH1 functions as a master regulator, inhibiting vegetative internode elongation through the control of the cell elongation program within the shoot apex. *ATH1* maintains an expression level that consistently enforces the compact rosette structure, even under environmental fluctuations that might otherwise significantly alter plant form. Therefore, the rosette's resilience is an actively maintained state directed by ATH1, rather than a passive consequence of growth inhibition. This robust control over

rosette architecture hints at regulatory mechanisms within the meristem that surpass the plasticity observed in other plant structures. In Chapter 2, we propose a negative regulatory feedback loop between the transcription factors ATH1 and PHYTOCHROME INTERACTING FACTOR 4 (PIF4) that likely contributes to the robustness of rosette habit. PIF4 is a known promoter of cell elongation. We demonstrate that ATH1 directly represses *PIF4* transcription within the meristem's deeper layers. This creates a regulatory feedback loop where PIF4 can, in turn, locally downregulate *ATH1*. In typical vegetative growth conditions, higher *ATH1* expression levels appear to tip this balance in favor of ATH1. This suppresses *PIF4* within the meristem's rib zone (RZ), consequently inhibiting internode elongation. The interplay between ATH1 and PIF4 potentially represents a regulatory axis within the meristem that reacts to photomorphogenic signals. While environmental factors, particularly light, can modulate PIF4 abundance (Han et al., 2019; Balcerowicz, 2020; Boccaccini et al., 2020), *ATH1* expression remains remarkably stable throughout the rosette phase, likely creating a zone within the subapical layers of the meristem where expression of multiple *PIFs*, especially *PIF4*, is suppressed. This underscores ATH1's role as a key stabilizing force, ensuring robust maintenance of the rosette habit ((Hajibehzad *et al.*, 2023), Chapter 2).



While PIFs play a significant role in rosette habit formation and maintenance, our analyses reveal that ATH1's contribution to the robustness of this architecture cannot be solely attributed to *PIF* suppression within the meristem. In chapter 3 we show that ATH1 exerts a far broader influence on the genetic network controlling cell elongation in Arabidopsis. It directly modulates hormonal levels and signaling pathways involving auxins, gibberellins, and brassinosteroids – all crucial for promoting cell elongation and integrated into the general cell elongation program by the BAP/D and HLH/bHLH modules. Beyond influencing hormonal levels within the meristem and directly repressing *PIF* expression, ATH1 targets *PACLOBUTRAZOL RESISTANCE* (*PRE*) genes within the HLH/bHLH module. *PRE* genes are key downstream promoters of cell elongation, receiving regulatory signals from the BAP/D module Bai *et al.*, 2012a,b; Hao *et al.*, 2012; Oh *et al.*, 2014, 2019). By locally suppressing *PRE* genes within the RZ, ATH1 strategically confines inhibition of internode elongation. This safeguards the rosette habit against environmental and internal signals that typically promote stem growth. Consequently, ATH1 functions as both an on/off switch and a precise modulator for a multitude of growth-promoting genes. The loss of this regulatory control in

*ath1* mutants results in phenotypic plasticity, characterized by variable internode elongation that disrupts the characteristic rosette architecture. This highlights ATH1's indispensable role in maintaining the compact vegetative stage of Arabidopsis.

**Beyond redundancy: ATH1's singular role in developmental robustness of rosette habit in Arabidopsis**

Plants, as sessile organisms, must balance robustness and plasticity to thrive in dynamic environments. Robustness ensures the maintenance of a stable phenotype despite perturbations, while plasticity allows for environmentally driven adjustments in growth and development. Examples of robustness and plasticity in plants include the consistent morphology of flowers for pollinator interactions, and the shade avoidance response where plants adapt to low-light conditions (Waddington, 1961; Holloway, 2002; Sassi *et al.*, 2014; Lachowiec *et al.*, 2016).

The Arabidopsis rosette habit is a remarkable example where a compact growth form favoring robustness relies primarily on a single regulatory gene, *ATH1*. Robustness in biological systems is typically achieved through complex gene networks offering redundancy (Hanada *et al.*, 2009, 2011). In contrast, ATH1 acts as a central control point. Its presence ensures the rosette habit, while its absence allows for flexible internode growth guided by environmental cues. This highlights ATH1's exceptional regulatory power as being both necessary and sufficient for maintaining this essential plant structure.

Our research (Chapters 2 & 3) reveals a surprising level of stability in ATH1 gene expression within the shoot apex. ATH1 mRNA levels remain constant under diverse light conditions, including monochromatic far-red light, which typically induces a suite of growth responses, collectively known as the shade-avoidance syndrome. This suggests that ATH1's transcriptional regulation is largely independent of typical environmental fluctuations. ATH1 achieves this stability through a convergence of signals: photoreceptors across the light spectrum (red, far-red, blue) and metabolic cues (like sucrose availability) all activate pathways ensuring sufficient *ATH1* expression in the SAM. Chapter 2 explores the role of TOR kinase as a central hub in this pathway, integrating light and metabolic signals that influence ATH1 expression in the meristem. This robust gene expression, where tight control and buffering protect a single gene's regulation, contributes to the overall stability of the developmental process it governs. Our findings broaden the

understanding of robustness by demonstrating how the reliable expression of a single gene can be crucial for the stability of an entire plant structure. This aligns with previous observations that essential genes exhibit lower expression variability (i.e., are more robust) than other genes, highlighting a link between robustness in gene expression and phenotypic robustness (MacNeil & Walhout, 2011).

While powerful, singular points of control carry potential risks, as disruptions to their regulation could be detrimental. However, the evolutionary advantage provided by the rosette habit's robustness likely outweighs the risks of relying on the single gene, ATH1. This emphasizes the diverse evolutionary strategies plants employ, where some situations favor tight control and simplicity, while others favor complexity and redundancy. Overall, the ATH1 gene exemplifies how a singular regulatory mechanism can provide a stable foundation for a critical developmental outcome. This contrasts with other biological systems where stability is achieved through multiple interacting pathways. The ATH1 model expands our understanding of the genetic basis of phenotypic robustness and has potential implications for engineering resilience in crop plants facing environmental challenges.



**The rosette stage: a regulated growth intermission in Arabidopsis development**

The vegetative rosette stage in Arabidopsis represents a distinct phase where vertical growth is strategically paused between the early elongation of the hypocotyl and the rapid stem elongation (bolting) associated with flowering. Our research (Chapters 2, 3, and 4) highlights the central role of the transcription factor ATH1 in maintaining this pause by suppressing internode elongation. In the absence of ATH1, the rosette stage is bypassed, revealing its role as a regulated intermission within the plant's typical vertical growth pattern.

While functionally distinct, the rosette stage exhibits intriguing similarities with both the hypocotyl and stem elongation phases. All three stages respond to similar hormonal (GA, BR, auxin) and environmental (light, temperature, photoperiod) cues (Timpte *et al.*, 1992; Kauschmann *et al.*, 1996; Jacqmard *et al.*, 2003; Nemhauser *et al.*, 2004; Fukuda *et al.*, 2009; Stavang *et al.*, 2009; Chapman *et al.*, 2012; Hornitschek *et al.*, 2012). Notably, these signals promote elongation in the hypocotyl and stem and, in the absence of ATH1, also trigger internode elongation within the rosette. Furthermore, our findings in Chapter 3 indicate

that this ATH1-suppressed internode elongation is primarily driven by cell expansion, similar to the mechanisms observed in hypocotyl growth. This implies that ATH1 temporarily restrains the hypocotyl's developmental program to pause vertical elongation growth during the rosette phase. Bolting, however, involves a more complex process that combines both cell division and elongation, unlike the primarily cell expansion-driven growth in the hypocotyl and vegetative internodes ((Sachs & Lang, 1957; Sachs *et al.*, 1959b,a; Sachs, 1965; Timpte *et al.*, 1992; Kauschmann *et al.*, 1996; Gendreau *et al.*, 1997; Gonzalez *et al.*, 2010; Bencivenga *et al.*, 2016). In Chapter 4, our findings demonstrate that ATH1 primarily suppresses bolting by inhibiting cell division. In addition, transcriptome analyses did not reveal significant overlap between ATH1-regulated genes governing compact rosette habit and those conferring inhibition of bolting (Chapters 3 and 4). Collectively, this strongly indicates that the molecular mechanism through which ATH1 enforces compact rosette growth during the vegetative growth phase is multifaceted. The Arabidopsis rosette stage, therefore, serves as a distinctive transitional phase where suppression of internode elongation by ATH1 involves countering cell elongation by terminating a developmental program primarily active during seedling development, while also preventing the induction of cell proliferation. Meanwhile, further research is needed to fully quantify the relative contributions of cell division and cell elongation to the elongation of internodes during vegetative and reproductive growth.

To grasp the transient halt in vertical growth that leads to the formation of the rosette growth habit, we must delve into the earliest stages of SAM and RZ development. Light-induced photomorphogenesis plays a dual role: it activates the SAM, initiating the production of rosette leaves, and simultaneously triggers early *ATH1* expression within the RZ. This *ATH1* expression effectively separates the activation of the SAM from that of the RZ, which is responsible for stem elongation (Quaedvlieg *et al.*, 1995; Hajibehzad *et al.*, 2023). Observations of seedling development in darkness reveal that both the meristem and *ATH1* expression remain inactive. Consequently, the RZ also exhibits minimal activity, even without ATH1's potential suppressive influence. This suggests that RZ inactivity in darkness may arise from overall SAM inactivity, where cells destined for the RZ lack sufficient production (Quaedvlieg *et al.*, 1995; Bencivenga *et al.*, 2016; Pfeiffer *et al.*, 2016). This suggests the hypothesis that the RZ inherently leans towards stem elongation, with vertical growth being the default mode. Consequently,

light-induced *ATH1* expression emerges as a crucial regulatory mechanism. It counteracts the RZ's inherent predisposition towards vertical growth, inducing a temporary pause in RZ activity. This pause facilitates the development of the compact rosette as the plant's predominant vegetative structure.

**Refining rosette crop cultivation: the ATH1 pathway to bolting resistance**

Advances in staple crop cultivation (wheat, rice, maize) have significantly improved yields. However, the potential of rosette crops (lettuce, sugar beet, onions, cabbage) remains limited by bolting – the premature elongation of the flowering stem. Bolting can dramatically reduce yield and quality. In leafy vegetables, it leads to hardened leaves and stems, decreased head formation, and increased bitterness (Guttormsen & Moe, 1985; Sessa *et al.*, 2000). In root crops like sugar beet, bolting diverts resources away from root development, reducing sugar yields by up to 29% (C'longden *et al.*, 1975). As these crops are vital for nutrition and food security, understanding and mitigating bolting is a pressing agricultural challenge.



Our research (particularly Chapter 4) investigates the genetic basis of bolting in Arabidopsis, a model for rosette plants. We have identified the transcription factor ATH1 as a pivotal regulator of cell division within SAM, regulating the bolting process. Additionally, ATH1 influences hormonal balance within the meristem, particularly auxins, gibberellins, and brassinosteroids – all crucial for plant growth and stem elongation. This suggests ATH1 may modulate hormone activity or levels within the SAM, ultimately impacting the timing and progression of bolting.

ATH1 exhibits a far-reaching regulatory influence within the RZ of the SAM, specifically targeting genes with growth-limiting potential when overexpressed. Unlike general growth inhibitors like the SHI and SRS gene families, ATH1's effect is highly localized. It targets genes crucial for stem elongation, such as *KOB1* (involved in RZ cell division and elongation), along with *SHI* and *SRS* family genes. ATH1 also influences the expression of genes involved in GA catabolism (*AT-GA2OX4* and *MYB62*) and brassinosteroid biosynthesis genes (*CYP90A1/CPD*, *DWF5*, *CYP85A1/BR6OX1*) within the RZ. While dysregulation of these genes can lead to dwarf phenotypes with reduced stem elongation, ATH1's targeted influence avoids the broader growth suppression seen in other mutants. Manipulating the ATH1 pathway offers the potential to develop more compact, robust rosette crops less prone to lodging and better adapted to high-density, nutrient-rich

cultivation. In contrast to the broad genetic changes of the Green Revolution, targeting ATH1 provides a highly localized approach, specifically suppressing unwanted stem elongation in the RZ while leaving vital structures like leaves, roots, and seed production unaffected. This research has significant implications for food security and agricultural sustainability. As global demand for nutritious vegetables increases, so does the need to improve rosette crop yields and quality. Understanding ATH1's regulatory network could pave the way for innovative breeding and biotechnological strategies to enhance these crops. By harnessing the molecular mechanisms governed by ATH1, we can work towards maximizing the yield potential of these essential plants, contributing to a more secure and nutritious global food supply.


Col-8
ath1-3

# References

**Abbas M, Berckhan S, Rooney DJ, Gibbs DJ, Conde JV, Correia CS, Bassel GW, Rosa NM la, León J, Alabadí D, *et al.* 2015**. Oxygen Sensing Coordinates Photomorphogenesis to Facilitate Seedling Survival. *Current Biology* **25**: 1483–1488.

**Abolghasemi R, Haghighi M, Etemadi N, Wang S, Soorni A. 2021**. Transcriptome architecture reveals genetic networks of bolting regulation in spinach. *BMC Plant Biology* **21**: 179.

**Achard P, Liao L, Jiang C, Desnos T, Bartlett J, Fu X, Harberd NP. 2007**. DELLAs Contribute to Plant Photomorphogenesis. *Plant Physiology* **143**: 1163–1172.

**Ahmad M, Cashmore AR. 1993**. HY4 gene of A. thaliana encodes a protein with characteristics of a blue-light photoreceptor. *Nature* **366**: 162–166.

**Alabadí D, Gallego-Bartolomé J, Orlando L, García-Cárcel L, Rubio V, Martínez C, Frigerio M, Iglesias-Pedraz JM, Espinosa A, Deng XW, *et al.* 2008**. Gibberellins modulate light signaling pathways to prevent Arabidopsis seedling de-etiolation in darkness. *The Plant Journal* **53**: 324–335.

**Alabadí D, Gil J, Blázquez MA, García-Martínez JL. 2004**. Gibberellins Repress Photomorphogenesis in Darkness. *Plant Physiology* **134**: 1050–1057.

**Andersen TG, Halkier BA. 2014**. Upon bolting the GTR1 and GTR2 transporters mediate transport of glucosinolates to the inflorescence rather than roots. *Plant Signaling & Behavior* **9**: e27740.

**Andres F, Romera-Branchat M, Martínez-Gallegos R, Patel V, Schneeberger K, Jang S, Altmüller J, Nürnberg P, Coupland G. 2015**. Floral induction in Arabidopsis thaliana by FLOWERING LOCUS T requires direct repression of BLADE-ON-PETIOLE genes by homeodomain protein PENNYWISE. *Plant Physiology*: pp.00960.2015.

**Aoi Y, Tanaka K, Cook SD, Hayashi K-I, Kasahara H. 2019**. GH3 Auxin-Amido Synthetases Alter the Ratio of Indole-3-Acetic Acid and Phenylacetic Acid in Arabidopsis. *Plant and Cell Physiology* **61**: 596–605.

**Araki T, Komeda Y. 1993**. Flowering in darkness in Arabidopsis thaliana. *The Plant Journal* **4**: 801–811.

**Argueso CT, Raines T, Kieber JJ. 2010**. Cytokinin signaling and transcriptional networks. *Current Opinion in Plant Biology* **13**: 533–539.

**Artins A, Caldana C. 2022**. The metabolic homeostaTOR: The balance of holding on or letting grow. *Current Opinion in Plant Biology* **66**: 102196.

**Arya H, Singh MB, Bhalla PL. 2021**. Overexpression of PIF4 affects plant morphology and accelerates reproductive phase transitions in soybean. *Food and Energy Security* **10**.

**Assefa AD, Choi S, Lee J-E, Sung J-S, Hur O-S, Ro N-Y, Lee H-S, Jang S-W, Rhee J-H. 2019**. Identification and quantification of selected metabolites in differently pigmented leaves of lettuce (Lactuca sativa L.) cultivars harvested at mature and bolting stages. *BMC Chemistry* **13**: 56.

**Azpiroz R, Wu Y, LoCascio JC, Feldmann KA. 1998**. An Arabidopsis Brassinosteroid-Dependent Mutant Is Blocked in Cell Elongation. *The Plant Cell* **10**: 219–230.

**Bai M-Y, Fan M, Oh E, Wang Z-Y**. **2012a**. A Triple Helix-Loop-Helix/Basic Helix-Loop-Helix Cascade Controls Cell Elongation Downstream of Multiple Hormonal and Environmental Signaling Pathways in Arabidopsis . *The Plant Cell* **24**: 4917–4929.

**Bai M-Y, Shang J-X, Oh E, Fan M, Bai Y, Zentella R, Sun T, Wang Z-Y**. **2012b**. Brassinosteroid, gibberellin, and phytochrome impinge on a common transcription module in Arabidopsis. *Nature cell biology* **14**: 810–817.

**Bainbridge K, Guyomarc'h S, Bayer E, Swarup R, Bennett M, Mandel T, Kuhlemeier C**. **2008**. Auxin influx carriers stabilize phyllotactic patterning. *Genes & Development* **22**: 810–823.

**Balanzà V, Martínez-Fernández I, Sato S, Yanofsky MF, Kaufmann K, Angenent GC, Bemer M, Ferrándiz C**. **2018**. Genetic control of meristem arrest and life span in Arabidopsis by a FRUITFULL-APETALA2 pathway. *Nature Communications* **9**: 565.

**Balkunde R, Kitagawa M, Xu XM, Wang J, Jackson D**. **2017**. SHOOT MERISTEMLESS trafficking controls axillary meristem formation, meristem size and organ boundaries in Arabidopsis. *The Plant Journal* **90**: 435–446.

**Bao S, Hua C, Shen L, Yu H**. **2020**. New insights into gibberellin signaling in regulating flowering in Arabidopsis. *Journal of Integrative Plant Biology* **62**: 118–131.

**Barton MK, Poethig RS**. **1993**. Formation of the shoot apical meristem in Arabidopsis thaliana: an analysis of development in the wild type and in the shoot meristemless mutant. *Development* **119**: 823–831.

**Baylis T, Cierlik I, Sundberg E, Mattsson J**. **2013**. SHORT INTERNODES/STYLISH genes, regulators of auxin biosynthesis, are involved in leaf vein development in Arabidopsis thaliana. *New Phytologist* **197**: 737–750.

**Bellaoui M, Pidkowich MS, Samach A, Kushalappa K, Kohalmi SE, Modrusan Z, Crosby WL, Haughn GW**. **2001**. The Arabidopsis BELL1 and KNOX TALE Homeodomain Proteins Interact through a Domain Conserved between Plants and Animals. *The Plant Cell* **13**: 2455–2470.

**Belles-Boix E, Hamant O, Witiak SM, Morin H, Traas J, Pautot V**. **2006**. KNAT6: An Arabidopsis Homeobox Gene Involved in Meristem Activity and Organ Separation. *The Plant Cell* **18**: 1900–1907.

**Bello FD, Lepš J, Sebastià M-T**. **2005**. Predictive value of plant traits to grazing along a climatic gradient in the Mediterranean. *Journal of Applied Ecology* **42**: 824–833.

**Bencivenga S, Serrano-Mislata A, Bush M, Fox S, Sablowski R**. **2016**. Control of Oriented Tissue Growth through Repression of Organ Boundary Genes Promotes Stem Morphogenesis. *Developmental Cell* **39**: 198–208.

**Bernardo-García S, Lucas M de, Martínez C, Espinosa-Ruiz A, Davière J-M, Prat S**. **2014**. BR-dependent phosphorylation modulates PIF4 transcriptional activity and shapes diurnal hypocotyl growth. *Genes & Development* **28**: 1681–1694.

**Bhatt AM, Etchells JP, Canales C, Lagodienko A, Dickinson H**. **2004**. VAAMANA—a BEL1-like homeodomain protein, interacts with KNOX proteins BP and STM and regulates inflorescence stem growth in Arabidopsis. *Gene* **328**: 103–111.

**Bishop GJ, Nomura T, Yokota T, Harrison K, Noguchi T, Fujioka S, Takatsuto S, Jones JDG, Kamiya Y. 1999**. The tomato DWARF enzyme catalyses C-6 oxidation in brassinosteroid biosynthesis. *Proceedings of the National Academy of Sciences* **96**: 1761–1766.

**Blázquez MA, Green R, Nilsson O, Sussman MR, Weigel D. 1998**. Gibberellins Promote Flowering of Arabidopsis by Activating the LEAFY Promoter. *The Plant Cell* **10**: 791–800.

**Bleecker AB, Patterson SE. 1997**. Last exit: senescence, abscission, and meristem arrest in Arabidopsis. *The Plant Cell* **9**: 1169–1179.

**Blilou I. 2024**. Unravelling how plant cells divide and differ. *Nature* **626**: 484–485.

**Booij R, Meurs EJJ. 1995**. Effect of photoperiod on flower stalk elongation in celeriac (Apium graveolens L. var. rapaceum (Mill.) DC.). *Scientia Horticulturae* **63**: 143–154.

**Boukhibar LM, Barkoulas M. 2016**. The developmental genetics of biological robustness. *Annals of Botany* **117**: 699–707.

**Bouly J, Giovani B, Djamei A, Mueller M, Zeugner A, Dudkin EA, Batschauer A, Ahmad M. 2003**. Novel ATP-binding and autophosphorylation activity associated with Arabidopsis and human cryptochrome-1. *European Journal of Biochemistry* **270**: 2921–2928.

**Bouré N, Kumar SV, Arnaud N. 2019**. The BAP Module: A Multisignal Integrator Orchestrating Growth. *Trends in Plant Science* **24**: 602–610.

**Bowman JL, Eshed Y. 2000**. Formation and maintenance of the shoot apical meristem. *Trends in Plant Science* **5**: 110–115.

**Brock MT, Maloof JN, Weinig C. 2010**. Genes underlying quantitative variation in ecologically important traits: PIF4 (PHYTOCHROME INTERACTING FACTOR 4) is associated with variation in internode length, flowering time, and fruit set in Arabidopsis thaliana. *Molecular Ecology* **19**: 1187–1199.

**Broeck LV den, Gordon M, Inzé D, Williams C, Sozzani R. 2020**. Gene Regulatory Network Inference: Connecting Plant Biology and Mathematical Modeling. *Frontiers in Genetics* **11**: 457.

**Burgie ES, Vierstra RD. 2014**. Phytochromes: An Atomic Perspective on Photoactivation and Signaling. *The Plant Cell* **26**: 4568–4583.

**Busch W, Miotk A, Ariel FD, Zhao Z, Forner J, Daum G, Suzaki T, Schuster C, Schultheiss SJ, Leibfried A, *et al.* 2010**. Transcriptional Control of a Plant Stem Cell Niche. *Developmental Cell* **18**: 841–853.

**Buti S, Pantazopoulou CK, Gelderen K van, Hoogers V, Reinen E, Pierik R. 2020**. A Gas-and-Brake Mechanism of bHLH Proteins Modulates Shade Avoidance . *Plant Physiology* **184**: 2137–2153.

**Byrne ME, Groover AT, Fontana JR, Martienssen RA. 2003**. Phyllotactic pattern and stem cell fate are determined by the Arabidopsis homeobox gene BELLRINGER. *Development* **130**: 3941–3950.

**Byrne ME, Simorowski J, Martienssen RA. 2002**. ASYMMETRIC LEAVES1 reveals knox gene redundancy in Arabidopsis. *Development* **129**: 1957–1965.

**Cai W, Li X, Liu Y, Wang Y, Zhou Y, Xu T, Xiong Y. 2017**. COP1 integrates light signals to ROP2 for cell cycle activation. *Plant Signaling & Behavior* **12**: e1363946.

**Cammarata J, Farfan CM, Scanlon MJ, Roeder AHK**. **2022**. Cytokinin–CLAVATA cross-talk is an ancient mechanism regulating shoot meristem homeostasis in land plants. *Proceedings of the National Academy of Sciences* **119**: e2116860119.

**Cao X, Wang J, Xiong Y, Yang H, Yang M, Ye P, Bencivenga S, Sablowski R, Jiao Y**. **2020**. A Self-Activation Loop Maintains Meristematic Cell Fate for Branching. *Current Biology* **30**: 1893-1904.e4.

**Capua Y, Eshed Y**. **2017**. Coordination of auxin-triggered leaf initiation by tomato LEAFLESS. *Proceedings of the National Academy of Sciences* **114**: 3246–3251.

**Castillo M-C, Coego A, Costa-Broseta Á, León J**. **2018**. Nitric oxide responses in Arabidopsis hypocotyls are mediated by diverse phytohormone pathways. *Journal of Experimental Botany* **69**: 5265–5278.

**Cazzonelli CI, Vanstraelen M, Simon S, Yin K, Carron-Arthur A, Nisar N, Tarle G, Cuttriss AJ, Searle IR, Benkova E, *et al.* 2013**. Role of the Arabidopsis PIN6 Auxin Transporter in Auxin Homeostasis and Auxin-Mediated Development. *PLoS ONE* **8**: e70069.

**Chamizo-Ampudia A, Sanz-Luque E, Llamas A, Galvan A, Fernandez E**. **2017**. Nitrate Reductase Regulates Plant Nitric Oxide Homeostasis. *Trends in Plant Science* **22**: 163–174.

**Chandler JW, Cole M, Flier A, Grewe B, Werr W**. **2007**. The AP2 transcription factors DORNRÖSCHEN and DORNRÖSCHEN-LIKE redundantly control Arabidopsis embryo patterning via interaction with PHAVOLUTA. *Development* **134**: 1653–1662.

**Chandler JW, Jacobs B, Cole M, Comelli P, Werr W**. **2011**. DORNRÖSCHEN-LIKE expression marks Arabidopsis floral organ founder cells and precedes auxin response maxima. *Plant Molecular Biology* **76**: 171–185.

**Chapman EJ, Greenham K, Castillejo C, Sartor R, Bialy A, Sun T, Estelle M**. **2012**. Hypocotyl Transcriptome Reveals Auxin Regulation of Growth-Promoting Genes through GA-Dependent and -Independent Pathways. *PLoS ONE* **7**: e36210.

**Chaves I, Pokorny R, Byrdin M, Hoang N, Ritz T, Brettel K, Essen L-O, Horst GTJ van der, Batschauer A, Ahmad M**. **2011**. The Cryptochromes: Blue Light Photoreceptors in Plants and Animals. *Plant Biology* **62**: 335–364.

**Chen M, Chory J**. **2011**. Phytochrome signaling mechanisms and the control of plant development. *Trends in Cell Biology* **21**: 664–671.

**Chen G-H, Liu M-J, Xiong Y, Sheen J, Wu S-H**. **2018**. TOR and RPS6 transmit light signals to enhance protein translation in deetiolating Arabidopsis seedlings. *Proceedings of the National Academy of Sciences* **115**: 12823–12828.

**Cheng M-C, Kathare PK, Paik I, Huq E**. **2021**. Phytochrome Signaling Networks. *Annual Review of Plant Biology* **72**: 1–28.

**Choe S, Dilkes BP, Gregory BD, Ross AS, Yuan H, Noguchi T, Fujioka S, Takatsuto S, Tanaka A, Yoshida S, *et al.* 1999**. The Arabidopsis dwarf1 Mutant Is Defective in the Conversion of 24-Methylenecholesterol to Campesterol in Brassinosteroid Biosynthesis1. *Plant Physiology* **119**: 897–908.

**Choe S, Tanaka A, Noguchi T, Fujioka S, Takatsuto S, Ross AS, Tax FE, Yoshida S, Feldmann KA**. **2000**. Lesions in the sterol Δ 7 reductase gene of Arabidopsis cause dwarfism due to a block in brassinosteroid biosynthesis. *The Plant Journal* **21**: 431–443.

**Chory J, Nagpal P, Peto CA**. **1991**. Phenotypic and Genetic Analysis of det2, a New Mutant That Affects Light-Regulated Seedling Development in Arabidopsis. *The Plant Cell* **3**: 445–459.

**Chory J, Reinecke D, Sim S, Washburn T, Brenner M**. **1994**. A Role for Cytokinins in De-Etiolation in Arabidopsis (det Mutants Have an Altered Response to Cytokinins). *Plant Physiology* **104**: 339–347.

**Chourey PS, Li Q-B, Kumar D**. **2010**. Sugar–Hormone Cross-Talk in Seed Development: Two Redundant Pathways of IAA Biosynthesis Are Regulated Differentially in the Invertase-Deficient miniature1 (mn1) Seed Mutant in Maize. *Molecular Plant* **3**: 1026–1036.

**Clark SE, Jacobsen SE, Levin JZ, Meyerowitz EM**. **1996**. The CLAVATA and SHOOT MERISTEMLESS loci competitively regulate meristem activity in Arabidopsis. *Development* **122**: 1567–1575.

**Clark SE, Williams RW, Meyerowitz EM**. **1997**. The CLAVATA1Gene Encodes a Putative Receptor Kinase That Controls Shoot and Floral Meristem Size in Arabidopsis. *Cell* **89**: 575–585.

**C'longden P, Scott RK, Tyldesley JB**. **1975**. Bolting of sugar beet grown in England. *Outlook on Agriculture* **8**: 188–193.

**Clouse SD**. **2002**. Brassinosteroids. *The Arabidopsis Book* **1**: e0009.

**Cluis CP, Mouchel CF, Hardtke CS**. **2004**. The Arabidopsis transcription factor HY5 integrates light and hormone signaling pathways. *The Plant Journal* **38**: 332–347.

**Cohen JI**. **2011**. A phylogenetic analysis of morphological and molecular characters of Lithospermum L. (Boraginaceae) and related taxa: evolutionary relationships and character evolution. *Cladistics* **27**: 559–580.

**Cole M, Nolte C, Werr W**. **2006**. Nuclear import of the transcription factor SHOOT MERISTEMLESS depends on heterodimerization with BLH proteins expressed in discrete sub-domains of the shoot apical meristem of Arabidopsis thaliana. *Nucleic Acids Research* **34**: 1281–1292.

**Collinge MA, Spillane C, Köhler C, Gheyselinck J, Grossniklaus U**. **2004**. Genetic Interaction of an Origin Recognition Complex Subunit and the Polycomb Group Gene MEDEA during Seed Development. *The Plant Cell* **16**: 1035–1046.

**Cowling RJ, Harberd NP**. **1999**. Gibberellins control Arabidopsis hypocotyl growth via regulation of cellular elongation. *Journal of Experimental Botany* **50**: 1351–1357.

**Crick J, Corrigan L, Belcram K, Khan M, Dawson JW, Adroher B, Li S, Hepworth SR, Pautot V**. **2021**. Floral organ abscission in Arabidopsis requires the combined activities of three TALE homeodomain transcription factors. *Journal of experimental botany* **73**: 6150–6169.

**Czechowski T, Stitt M, Altmann T, Udvardi MK, Scheible W-R**. **2005**. Genome-Wide Identification and Testing of Superior Reference Genes for Transcript Normalization in Arabidopsis. *Plant Physiology* **139**: 5–17.

**Dai Y, Luo L, Zhao Z**. **2023**. Genetic robustness control of auxin output in priming organ initiation. *Proceedings of the National Academy of Sciences* **120**: e2221606120.

**Dally N, Eckel M, Batschauer A, Höft N, Jung C. 2018**. Two CONSTANS-LIKE genes jointly control flowering time in beet. *Scientific Reports* **8**: 16120.

**Daum G, Medzihradszky A, Suzaki T, Lohmann JU. 2014**. A mechanistic framework for noncell autonomous stem cell induction in Arabidopsis. *Proceedings of the National Academy of Sciences* **111**: 14619–14624.

**Davière J-M, Achard P. 2013**. Gibberellin signaling in plants. *Development* **140**: 1147–1151.

**Deng X, Quail PH. 1992**. Genetic and phenotypic characterization of cop1 mutants of Arabidopsis thaliana. *The Plant Journal* **2**: 83–95.

**Deprost D, Yao L, Sormani R, Moreau M, Leterreux G, Nicolaï M, Bedu M, Robaglia C, Meyer C. 2007**. The Arabidopsis TOR kinase links plant growth, yield, stress resistance and mRNA translation. *EMBO reports* **8**: 864–870.

**Desvoyes B, Gutierrez C. 2020**. Roles of plant retinoblastoma protein: cell cycle and beyond. *The EMBO Journal* **39**: e105802.

**Devaiah BN, Madhuvanthi R, Karthikeyan AS, Raghothama KG. 2009**. Phosphate Starvation Responses and Gibberellic Acid Biosynthesis are Regulated by the MYB62 Transcription Factor in Arabidopsis. *Molecular Plant* **2**: 43–58.

**Devlin PF, Halliday KJ, Harberd NP, Whitelam GC. 1996**. The rosette habit of Arabidopsis thaliana is dependent upon phytochrome action: novel phytochromes control internode elongation and flowering time. *The Plant Journal* **10**: 1127–1134.

**Devlin PF, Patel SR, Whitelam GC. 1998**. Phytochrome E Influences Internode Elongation and Flowering Time in Arabidopsis. *The Plant Cell* **10**: 1479–1487.

**Devlin PF, Robson PRH, Patel SR, Goosey L, Sharrock RA, Whitelam GC. 1999**. Phytochrome D Acts in the Shade-Avoidance Syndrome in Arabidopsis by Controlling Elongation Growth and Flowering Time. *Plant Physiology* **119**: 909–916.

**Devlin PF, Somers DE, Quail PH, Whitelam GC. 1997**. The Brassica rapa elongated internode (EIN) gene encodes phytochrome B. *Plant Molecular Biology* **34**: 537–547.

**Devlin PF, Yanovsky MJ, Kay SA. 2003**. A Genomic Analysis of the Shade Avoidance Response in Arabidopsis . *Plant Physiology* **133**: 1617–1629.

**Diao R, Zhao M, Liu Y, Zhang Z, Zhong B. 2023**. The advantages of crosstalk during the evolution of the BZR1–ARF6–PIF4 (BAP) module. *Journal of Integrative Plant Biology*.

**Dill A, Jung H-S, Sun T. 2001**. The DELLA motif is essential for gibberellin-induced degradation of RGA. *Proceedings of the National Academy of Sciences* **98**: 14162–14167.

**Ditengou FA, Gomes D, Nziengui H, Kochersperger P, Lasok H, Medeiros V, Paponov IA, Nagy SK, Nádai TV, Mészáros T, *et al.* 2018**. Characterization of auxin transporter PIN6 plasma membrane targeting reveals a function for PIN6 in plant bolting. *New Phytologist* **217**: 1610–1624.

**Dong J, Sun N, Yang J, Deng Z, Lan J, Qin G, He H, Deng XW, Irish VF, Chen H, *et al.* 2018**. The Transcription Factors TCP4 and PIF3 Antagonistically Regulate Organ-Specific Light Induction of SAUR Genes to Modulate Cotyledon Opening during De-Etiolation in Arabidopsis. *The Plant cell* **31**: 1155–1170.

**Dong P, Xiong F, Que Y, Wang K, Yu L, Li Z, Ren M. 2015**. Expression profiling and functional analysis reveals that TOR is a key player in regulating photosynthesis and phytohormone signaling pathways in Arabidopsis. *Frontiers in Plant Science* **6**: 677.

**Ehrenreich IM, Pfennig DW. 2016**. Genetic assimilation: a review of its potential proximate causes and evolutionary consequences. *Annals of Botany* **117**: 769–779.

**Ejaz M, Bencivenga S, Tavares R, Bush M, Sablowski R. 2021**. ARABIDOPSIS THALIANA HOMEOBOX GENE 1 controls plant architecture by locally restricting environmental responses. *Proceedings of the National Academy of Sciences* **118**: e2018615118.

**Eklund DM, Ståldal V, Valsecchi I, Cierlik I, Eriksson C, Hiratsu K, Ohme-Takagi M, Sundström JF, Thelander M, Ezcurra I, *et al.* 2010**. The Arabidopsis thaliana STYLISH1 protein acts as a transcriptional activator regulating auxin biosynthesis. *The Plant cell* **22**: 349–63.

**Endrizzi K, Moussian B, Haecker A, Levin JZ, Laux T. 1996**. The SHOOT MERISTEMLESS gene is required for maintenance of undifferentiated cells in Arabidopsis shoot and floral meristems and acts at a different regulatory level than the meristem genes WUSCHEL and ZWILLE. *The Plant Journal* **10**: 967–979.

**Eriksson S, Böhlenius H, Moritz T, Nilsson O. 2006**. GA4 Is the Active Gibberellin in the Regulation of LEAFY Transcription and Arabidopsis Floral Initiation. *The Plant Cell* **18**: 2172–2181.

**Favero DS, Lambolez A, Sugimoto K. 2020**. Molecular pathways regulating elongation of aerial plant organs: a focus on light, the circadian clock, and temperature. *The Plant Journal* **105**: 392–420.

**Feng S, Martinez C, Gusmaroli G, Wang Y, Zhou J, Wang F, Chen L, Yu L, Iglesias-Pedraz JM, Kircher S, *et al.* 2008**. Coordinated regulation of Arabidopsis thaliana development by light and gibberellins. *Nature* **451**: 475–479.

**Ferrell JE. 2002**. Self-perpetuating states in signal transduction: positive feedback, double-negative feedback and bistability. *Current Opinion in Cell Biology* **14**: 140–148.

**Fleet CM, Sun T. 2005**. A DELLAcate balance: the role of gibberellin in plant morphogenesis. *Current Opinion in Plant Biology* **8**: 77–85.

**Fobert PR, Gaudin V, Lunness P, Coen ES, Doonan JH. 1996**. Distinct classes of cdc2-related genes are differentially expressed during the cell division cycle in plants. *The Plant Cell* **8**: 1465–1476.

**Folta KM, Pontin MA, Karlin-Neumann G, Bottini R, Spalding EP. 2003**. Genomic and physiological studies of early cryptochrome 1 action demonstrate roles for auxin and gibberellin in the control of hypocotyl growth by blue light. *The Plant Journal* **36**: 203–214.

**Franklin KA, Davis SJ, Stoddart WM, Vierstra RD, Whitelam GC. 2003a**. Mutant Analyses Define Multiple Roles for Phytochrome C in Arabidopsis Photomorphogenesis. *The Plant Cell* **15**: 1981–1989.

**Franklin KA, Praekelt U, Stoddart WM, Billingham OE, Halliday KJ, Whitelam GC. 2003b**. Phytochromes B, D, and E Act Redundantly to Control Multiple Physiological Responses in Arabidopsis. *Plant Physiology* **131**: 1340–1346.

**Franklin KA, Quail PH. 2010**. Phytochrome functions in Arabidopsis development. *Journal of Experimental Botany* **61**: 11–24.

**Fridborg I, Kuusk S, Moritz T, Sundberg E. 1999**. The Arabidopsis Dwarf Mutant shi Exhibits Reduced Gibberellin Responses Conferred by Overexpression of a New Putative Zinc Finger Protein. *The Plant Cell* **11**: 1019–1031.

**Frugis G, Giannino D, Mele G, Nicolodi C, Chiappetta A, Bitonti MB, Innocenti AM, Dewitte W, Onckelen HV, Mariotti D. 2001**. Overexpression of KNAT1 in Lettuce Shifts Leaf Determinate Growth to a Shoot-Like Indeterminate Growth Associated with an Accumulation of Isopentenyl-Type Cytokinins. *Plant Physiology* **126**: 1370–1380.

**Fu X, Richards DE, Ait-ali T, Hynes LW, Ougham H, Peng J, Harberd NP. 2002**. Gibberellin-Mediated Proteasome-Dependent Degradation of the Barley DELLA Protein SLN1 Repressor. *The Plant Cell* **14**: 3191–3200.

**Fujita N, Koda R. 2015**. Capitulum and rosette leaf avoidance from grazing by large herbivores in Taraxacum. *Ecological Research* **30**: 517–525.

**Fukuda M, Matsuo S, Kikuchi K, Mitsuhashi W, Toyomasu T, Honda I. 2009**. The endogenous level of GA1 is upregulated by high temperature during stem elongation in lettuce through LsGA3ox1 expression. *Journal of Plant Physiology* **166**: 2077–2084.

**Furukawa Y, Piwnica-Worms H, Ernst TJ, Kanakura Y, Griffin JD. 1990**. cdc2 Gene Expression at the G1 to S Transition in Human T Lymphocytes. *Science* **250**: 805–808.

**Gallego-Bartolomé J, Minguet EG, Grau-Enguix F, Abbas M, Locascio A, Thomas SG, Alabadí D, Blázquez MA. 2012**. Molecular mechanism for the interaction between gibberellin and brassinosteroid signaling pathways in Arabidopsis. *Proceedings of the National Academy of Sciences* **109**: 13446–13451.

**Galvão VC, Fiorucci A-S, Trevisan M, Franco-Zorilla JM, Goyal A, Schmid-Siegert E, Solano R, Fankhauser C. 2019**. PIF transcription factors link a neighbor threat cue to accelerated reproduction in Arabidopsis. *Nature Communications* **10**: 4005.

**Galvão VC, Horrer D, Küttner F, Schmid M. 2012**. Spatial control of flowering by DELLA proteins in Arabidopsis thaliana. *Development* **139**: 4072–4082.

**Gan S. 2018**. Plant Senescence, Methods and Protocols. *Methods in Molecular Biology* **1744**: 3–8.

**Ge SX, Jung D, Yao R. 2019**. ShinyGO: a graphical enrichment tool for animals and plants. *Bioinformatics* **36**: 2628–2629.

**Gendreau E, Traas J, Desnos T, Grandjean O, Caboche M, Hofte H. 1997**. Cellular Basis of Hypocotyl Growth in Arabidopsis thaliana. *Plant Physiology* **114**: 295–305.

**Gendrel A-V, Lippman Z, Martienssen R, Colot V. 2005**. Profiling histone modification patterns in plants using genomic tiling microarrays. *Nature Methods* **2**: 213–218.

**Givnish TJ, Evans TM, Pires JC, Sytsma KJ. 1999**. Polyphyly and Convergent Morphological Evolution in Commelinales and Commelinidae: Evidence from rbcL Sequence Data. *Molecular Phylogenetics and Evolution* **12**: 360–385.

**Goetz M, Rabinovich M, Smith HM. 2021**. The role of auxin and sugar signaling in dominance inhibition of inflorescence growth by fruit load. *Plant Physiology* **187**: 1189–1201.

**Goh T, Kasahara H, Mimura T, Kamiya Y, Fukaki H. 2012**. Multiple AUX/IAA–ARF modules regulate lateral root formation: the role of Arabidopsis SHY2/IAA3-mediated auxin signalling. *Philosophical Transactions of the Royal Society B: Biological Sciences* **367**: 1461–1468.

**Gómez-Mena C, Sablowski R. 2008**. ARABIDOPSIS THALIANA HOMEOBOX GENE1 Establishes the Basal Boundaries of Shoot Organs and Controls Stem Growth. *The Plant Cell* **20**: 2059–2072.

**Gonzalez N, Bodt SD, Sulpice R, Jikumaru Y, Chae E, Dhondt S, Daele TV, Milde LD, Weigel D, Kamiya Y, *et al.* 2010**. Increased Leaf Size: Different Means to an End . *Plant Physiology* **153**: 1261–1279.

**Griffiths J, Halliday K. 2011**. Plant Development: Light Exposure Directs Meristem Fate. *Current Biology* **21**: R817–R819.

**Guenot B, Bayer E, Kierzkowski D, Smith RS, Mandel T, Žádníková P, Benková E, Kuhlemeier C. 2012**. PIN1-Independent Leaf Initiation in Arabidopsis . *Plant Physiology* **159**: 1501–1510.

**Guo M, Thomas J, Collins G, Timmermans MCP. 2008**. Direct Repression of KNOX Loci by the ASYMMETRIC LEAVES1 Complex of Arabidopsis . *The Plant Cell* **20**: 48–58.

**Guttormsen G, Moe R. 1985**. Effect of plant age and temperature on bolting in Chinese cabbage. *Scientia Horticulturae* **25**: 217–224.

**Hajibehzad SS, Silva SS, Peeters N, Stouten E, Buijs G, Smeekens S, Proveniers M. 2022**. Arabidopsis thaliana rosette growth habit is a photomorphogenic trait controlled by the TALE homeodomain protein ATH1 and involves TOR kinase. *bioRxiv*: 2022.05.13.491803.

**Hajibehzad SS, Silva SS, Peeters N, Stouten E, Buijs G, Smeekens S, Proveniers M. 2023**. Arabidopsis thaliana rosette habit is controlled by combined light and energy signaling converging on transcriptional control of the TALE homeobox gene ATH1. *New Phytologist*.

**Hall H, Ellis B. 2012**. Developmentally equivalent tissue sampling based on growth kinematic profiling of Arabidopsis inflorescence stems. *New Phytologist* **194**: 287–296.

**Hamano M, Yamato Y, Yamazaki H, Miura H. 2015**. Endogenous gibberellins and their effects on flowering and stem elongation in cabbage (Brassica oleracea var. capitata). *The Journal of Horticultural Science and Biotechnology* **77**: 220–225.

**Hamasaki H, Ayano M, Nakamura A, Fujioka S, Asami T, Takatsuto S, Yoshida S, Oka Y, Matsui M, Shimada Y. 2020**. Light Activates Brassinosteroid Biosynthesis to Promote Hook Opening and Petiole Development in Arabidopsis thaliana. *Plant and Cell Physiology* **61**: 1239–1251.

**Han H, Liu X, Zhou Y. 2020**. Transcriptional circuits in control of shoot stem cell homeostasis. *Current Opinion in Plant Biology* **53**: 50–56.

**Han R, Truco MJ, Lavelle DO, Michelmore RW**. **2021**. A Composite Analysis of Flowering Time Regulation in Lettuce. *Frontiers in Plant Science* **12**: 632708.

**Hanada K, Kuromori T, Myouga F, Toyoda T, Li W-H, Shinozaki K**. **2009**. Evolutionary Persistence of Functional Compensation by Duplicate Genes in Arabidopsis. *Genome Biology and Evolution* **1**: 409–414.

**Hanada K, Sawada Y, Kuromori T, Klausnitzer R, Saito K, Toyoda T, Shinozaki K, Li W-H, Hirai MY**. **2011**. Functional Compensation of Primary and Secondary Metabolites by Duplicate Genes in Arabidopsis thaliana. *Molecular Biology and Evolution* **28**: 377–382.

**Hao G, Al-Shehbaz IA, Ahani H, Liang Q, Mao K, Wang Q, Liu J**. **2017**. An integrative study of evolutionary diversification of Eutrema (Eutremeae, Brassicaceae). *Botanical Journal of the Linnean Society* **184**: 204–223.

**Hao Y, Oh E, Choi G, Liang Z, Wang Z-Y**. **2012**. Interactions between HLH and bHLH Factors Modulate Light-Regulated Plant Development. *Molecular Plant* **5**: 688–697.

**Hao J-H, Zhang L-L, Li P-P, Sun Y-C, Li J-K, Qin X-X, Wang L, Qi Z-Y, Xiao S, Han Y-Y, *et al.* 2018**. Quantitative Proteomics Analysis of Lettuce (Lactuca sativa L.) Reveals Molecular Basis-Associated Auxin and Photosynthesis with Bolting Induced by High Temperature. *International Journal of Molecular Sciences* **19**: 2967.

**Hay A, Kaur H, Phillips A, Hedden P, Hake S, Tsiantis M**. **2002**. The Gibberellin Pathway Mediates KNOTTED1-Type Homeobox Function in Plants with Different Body Plans. *Current Biology* **12**: 1557–1565.

**He J-X, Gendron JM, Yang Y, Li J, Wang Z-Y**. **2002**. The GSK3-like kinase BIN2 phosphorylates and destabilizes BZR1, a positive regulator of the brassinosteroid signaling pathway in Arabidopsis. *Proceedings of the National Academy of Sciences* **99**: 10185–10190.

**He G, Liu J, Dong H, Sun J**. **2018**. The Blue-Light Receptor CRY1 Interacts with BZR1 and BIN2 to Modulate the Phosphorylation and Nuclear Function of BZR1 in Repressing BR Signaling in Arabidopsis. *Molecular plant* **12**: 689–703.

**Hedden P, Proebsting WM**. **1999**. Genetic Analysis of Gibberellin Biosynthesis. *Plant Physiology* **119**: 365–370.

**Heisler MG, Byrne ME**. **2020**. Progress in understanding the role of auxin in lateral organ development in plants. *Current Opinion in Plant Biology* **53**: 73–79.

**Heisler MG, Ohno C, Das P, Sieber P, Reddy GV, Long JA, Meyerowitz EM**. **2005**. Patterns of Auxin Transport and Gene Expression during Primordium Development Revealed by Live Imaging of the Arabidopsis Inflorescence Meristem. *Current Biology* **15**: 1899–1911.

**Hemerly A, Engler J de A, Bergounioux C, Montagu MV, Engler G, Inzé D, Ferreira P**. **1995**. Dominant negative mutants of the Cdc2 kinase uncouple cell division from iterative plant development. *The EMBO Journal* **14**: 3925–3936.

**Hempel FD, Feldman LJ**. **1994**. Bi-directional inflorescence development inArabidopsis thaliana: Acropetal initiation of flowers and basipetal initiation of paraclades. *Planta* **192**: 276–286.

**Hensel LL, Nelson MA, Richmond TA, Bleecker AB**. **1994**. The Fate of Inflorescence Meristems Is Controlled by Developing Fruits in Arabidopsis. *Plant Physiology* **106**: 863–876.

**Hoffmann CM, Kluge-Severin S**. **2011**. Growth analysis of autumn and spring sown sugar beet. *European Journal of Agronomy* **34**: 1–9.

**Holloway GJ**. **2002**. Phenotypic Plasticity: Beyond Nature and Nurture. *Heredity* **89**: 410–410.

**Holm M, Ma L-G, Qu L-J, Deng X-W**. **2002**. Two interacting bZIP proteins are direct targets of COP1-mediated control of light-dependent gene expression in Arabidopsis. *Genes & Development* **16**: 1247–1259.

**Hong JK, Kim JA, Kim JS, Lee SI, Koo BS, Lee Y-H**. **2012**. Overexpression of Brassica rapaSHI-RELATED SEQUENCE genes suppresses growth and development in Arabidopsis thaliana. *Biotechnology Letters* **34**: 1561–1569.

**Hornitschek P, Kohnen MV, Lorrain S, Rougemont J, Ljung K, López-Vidriero I, Franco-Zorrilla JM, Solano R, Trevisan M, Pradervand S, *et al.* 2012**. Phytochrome interacting factors 4 and 5 control seedling growth in changing light conditions by directly controlling auxin signaling. *The Plant Journal* **71**: 699–711.

**Hu W, Franklin KA, Sharrock RA, Jones MA, Harmer SL, Lagarias JC**. **2013**. Unanticipated regulatory roles for Arabidopsis phytochromes revealed by null mutant analysis. *Proceedings of the National Academy of Sciences* **110**: 1542–1547.

**Hu Q, Merchante C, Stepanova AN, Alonso JM, Heber S**. **2016**. Genome-Wide Search for Translated Upstream Open Reading Frames in Arabidopsis Thaliana. *IEEE Transactions on Nano-Bioscience* **15**: 150–159.

**Huai J, Zhang X, Li J, Ma T, Zha P, Jing Y, Lin R**. **2018**. SEUSS and PIF4 Coordinately Regulate Light and Temperature Signaling Pathways to Control Plant Growth. *Molecular Plant* **11**: 928–942.

**Ibañez C, Delker C, Martinez C, Bürstenbinder K, Janitza P, Lippmann R, Ludwig W, Sun H, James GV, Klecker M, *et al.* 2018**. Brassinosteroids Dominate Hormonal Regulation of Plant Thermomorphogenesis via BZR1. *Current Biology* **28**: 303-310.e3.

**Iino M, Haga K**. **2005**. Light Sensing in Plants. : 269–276.

**Ikeda M, Fujiwara S, Mitsuda N, Ohme-Takagi M**. **2012**. A triantagonistic basic helix-loop-helix system regulates cell elongation in Arabidopsis. *The Plant cell* **24**: 4483–97.

**Ikeda M, Mitsuda N, Ohme-Takagi M**. **2009**. Arabidopsis WUSCHEL is a bifunctional transcription factor that acts as a repressor in stem cell regulation and as an activator in floral patterning. *The Plant cell* **21**: 3493–505.

**Inzé D, Veylder LD**. **2006**. Cell Cycle Regulation in Plant Development. *Annual Review of Genetics* **40**: 77–105.

**Ito M, Araki S, Matsunaga S, Itoh T, Nishihama R, Machida Y, Doonan JH, Watanabe A**. **2001**. G2/M-Phase–Specific Transcription during the Plant Cell Cycle Is Mediated by c-Myb–Like Transcription Factors. *The Plant Cell* **13**: 1891–1905.

**Jacqmard A, Gadisseur I, Bernier G**. **2003**. Cell Division and Morphological Changes in the Shoot Apex of Arabidopsis thaliana during Floral Transition. *Annals of Botany* **91**: 571–576.

**JANICK J, LEOPOLD AC**. **1961**. A Distinction between Bolting and Flowering Effects on Senescence. *Nature* **192**: 887–888.

**Janocha D, Pfeiffer A, Dong Y, Novák O, Strnad M, Ryabova LA, Lohmann JU**. **2022**. TOR kinase controls Arabidopsis shoot development by translational repression of cytokinin catabolic enzymes. *bioRxiv*: 2021.07.29.454319.

**Jasinski S, Piazza P, Craft J, Hay A, Woolley L, Rieu I, Phillips A, Hedden P, Tsiantis M**. **2005**. KNOX Action in Arabidopsis Is Mediated by Coordinate Regulation of Cytokinin and Gibberellin Activities. *Current Biology* **15**: 1560–1565.

**Jenkins GI**. **2014**. The UV-B Photoreceptor UVR8: From Structure to Physiology. *The Plant Cell* **26**: 21–37.

**Jenkitkonchai J, Marriott P, Yang W, Sriden N, Jung J, Wigge PA, Charoensawan V**. **2021**. Exploring PIF4's contribution to early flowering in plants under daily variable temperature and its tissue-specific flowering gene network. *Plant Direct* **5**: e339.

**Jia Y, Kong X, Hu K, Cao M, Liu J, Ma C, Guo S, Yuan X, Zhao S, Robert HS, *et al.* 2020**. PIFs coordinate shade avoidance by inhibiting auxin repressor ARF18 and metabolic regulator QQS. *New Phytologist* **228**: 609–621.

**Jiao Y, Lau OS, Deng XW**. **2007**. Light-regulated transcriptional networks in higher plants. *Nature Reviews Genetics* **8**: 217–230.

**K MJ, Jindal S, Sharma M, Awasthi P, S S, Sharma M, Mannully CT, Laxmi A**. **2022**. A negative feedback loop of TOR signaling balances growth and stress-response trade-offs in plants. *Cell Reports* **39**: 110631.

**Kami C, Lorrain S, Hornitschek P, Fankhauser C**. **2010**. Chapter Two Light-Regulated Plant Growth and Development. *Current Topics in Developmental Biology* **91**: 29–66.

**Kanrar S, Onguka O, Smith HMS**. **2006**. Arabidopsis inflorescence architecture requires the activities of KNOX-BELL homeodomain heterodimers. *Planta* **224**: 1163–1173.

**Kanyuka K, Praekelt U, Franklin KA, Billingham OE, Hooley R, Whitelam GC, Halliday KJ**. **2003**. Mutations in the huge Arabidopsis gene BIG affect a range of hormone and light responses. *The Plant Journal* **35**: 57–70.

**Karimi M, Bleys A, Vanderhaeghen R, Hilson P**. **2007**. Building Blocks for Plant Gene Assembly. *Plant Physiology* **145**: 1183–1191.

**Kathare PK, Xu X, Nguyen A, Huq E**. **2020**. A COP1-PIF-HEC regulatory module fine-tunes photomorphogenesis in Arabidopsis. *The Plant Journal* **104**: 113–123.

**Kauschmann A, Jessop A, Koncz C, Szekeres M, Willmitzer L, Altmann T**. **1996**. Genetic evidence for an essential role of brassinosteroids in plant development. *The Plant Journal* **9**: 701–713.

**Kean-Galeno T, Lopez-Arredondo D, Herrera-Estrella L**. **2024**. The Shoot Apical Meristem: An Evolutionary Molding of Higher Plants. *International Journal of Molecular Sciences* **25**: 1519.

**Khan M, Ragni L, Tabb P, Salasini BC, Chatfield S, Datla R, Lock J, Kuai X, Després C, Proveniers M, *et al.* 2015**. Repression of Lateral Organ Boundary Genes by PENNYWISE and POUND-FOOLISH Is Essential for Meristem Maintenance and Flowering in Arabidopsis. *Plant physiology* **169**: 2166–86.

**Khan M, Tabb P, Hepworth SR. 2012**. BLADE-ON-PETIOLE1 and 2 regulate Arabidopsis inflorescence architecture in conjunction with homeobox genes KNAT6 and ATH1. *Plant Signaling & Behavior* **7**: 788–792.

**Kim HJ, Chiang Y-H, Kieber JJ, Schaller GE. 2013**. SCFKMD controls cytokinin signaling by regulating the degradation of type-B response regulators. *Proceedings of the National Academy of Sciences* **110**: 10028–10033.

**Kim G, Fujioka S, Kozuka T, Tax FE, Takatsuto S, Yoshida S, Tsukaya H. 2005a**. CYP90C1 and CYP90D1 are involved in different steps in the brassinosteroid biosynthesis pathway in Arabidopsis thaliana. *The Plant Journal* **41**: 710–721.

**Kim T-W, Hwang J-Y, Kim Y-S, Joo S-H, Chang SC, Lee JS, Takatsuto S, Kim S-K. 2005b**. Arabidopsis CYP85A2, a Cytochrome P450, Mediates the Baeyer-Villiger Oxidation of Castasterone to Brassinolide in Brassinosteroid Biosynthesis. *The Plant Cell* **17**: 2397–2412.

**Kim B, Jeong YJ, Corvalán C, Fujioka S, Cho S, Park T, Choe S. 2014**. Darkness and gulliver2/phyB mutation decrease the abundance of phosphorylated BZR1 to activate brassinosteroid signaling in Arabidopsis. *The Plant Journal* **77**: 737–747.

**Kim J, Yi H, Choi G, Shin B, Song P-S, Choi G. 2003a**. Functional Characterization of Phytochrome Interacting Factor 3 in Phytochrome-Mediated Light Signal Transduction. *The Plant Cell* **15**: 2399–2407.

**Kim J-Y, Yuan Z, Jackson D. 2003b**. Developmental regulation and significance of KNOX protein trafficking in Arabidopsis. *Development* **130**: 4351–4362.

**King KE, Moritz T, Harberd NP. 2001**. Gibberellins Are Not Required for Normal Stem Growth in Arabidopsis thaliana in the Absence of GAI and RGA. *Genetics* **159**: 767–776.

**Kinoshita A, Vayssières A, Richter R, Sang Q, Roggen A, Driel AD van, Smith RS, Coupland G. 2020**. Regulation of shoot meristem shape by photoperiodic signaling and phytohormones during floral induction of Arabidopsis. *eLife* **9**: e60661.

**Kitagawa M, Jackson D. 2019**. Control of Meristem Size. *Annual Review of Plant Biology* **70**: 269–291.

**Kitagawa M, Wu P, Balkunde R, Cunniff P, Jackson D. 2022**. An RNA exosome subunit mediates cell-to-cell trafficking of a homeobox mRNA via plasmodesmata. *Science* **375**: 177–182.

**Klahre U, Noguchi T, Fujioka S, Takatsuto S, Yokota T, Nomura T, Yoshida S, Chua N-H. 1998**. The Arabidopsis DIMINUTO/DWARF1 Gene Encodes a Protein Involved in Steroid Synthesis. *The Plant Cell* **10**: 1677–1690.

**Klepikova AV, Logacheva MD, Dmitriev SE, Penin AA. 2015**. RNA-seq analysis of an apical meristem time series reveals a critical point in Arabidopsis thaliana flower initiation. *BMC Genomics* **16**: 466.

**Kohnen MV, Schmid-Siegert E, Trevisan M, Petrolati LA, Sénéchal F, Müller-Moulé P, Maloof J, Xenarios I, Fankhauser C. 2016**. Neighbor Detection Induces Organ-Specific Transcriptomes, Revealing Patterns Underlying Hypocotyl-Specific Growth. *The Plant Cell* **28**: 2889–2904.

**Komaki S, Sugimoto K. 2012**. Control of the Plant Cell Cycle by Developmental and Environmental Cues. *Plant and Cell Physiology* **53**: 953–964.

**Kong D, Karve R, Willet A, Chen M-K, Oden J, Shpak ED. 2012**. Regulation of Plasmodesmatal Permeability and Stomatal Patterning by the Glycosyltransferase-Like Protein KOBITO1 . *Plant Physiology* **159**: 156–168.

**Krahmer J, Fankhauser C. 2024**. Environmental Control of Hypocotyl Elongation. *Annual Review of Plant Biology* **75**.

**Kumar SV, Lucyshyn D, Jaeger KE, Alós E, Alvey E, Harberd NP, Wigge PA. 2012**. Transcription factor PIF4 controls the thermosensory activation of flowering. *Nature* **484**: 242–245.

**Küpers JJ, Snoek BL, Oskam L, Pantazopoulou CK, Matton SEA, Reinen E, Liao C-Y, Eggermont EDC, Weekamp H, Biddanda-Devaiah M, *et al.* 2023**. Local light signaling at the leaf tip drives remote differential petiole growth through auxin-gibberellin dynamics. *Current Biology* **33**: 75-85.e5.

**Kurakawa T, Ueda N, Maekawa M, Kobayashi K, Kojima M, Nagato Y, Sakakibara H, Kyozuka J. 2007**. Direct control of shoot meristem activity by a cytokinin-activating enzyme. *Nature* **445**: 652–655.

**Kurihara D, Mizuta Y, Sato Y, Higashiyama T. 2015**. ClearSee: a rapid optical clearing reagent for whole-plant fluorescence imaging. *Development* **142**: 4168–4179.

**Kuusk S, Sohlberg JJ, Eklund DM, Sundberg E. 2006**. Functionally redundant SHI family genes regulate Arabidopsis gynoecium development in a dose-dependent manner. *The Plant Journal* **47**: 99–111.

**Kuusk S, Sohlberg JJ, Long JA, Fridborg I, Sundberg E. 2002**. STY1 and STY2 promote the formation of apical tissues during Arabidopsis gynoecium development. *Development* **129**: 4707–4717.

**Kwiatkowska D. 2008**. Flowering and apical meristem growth dynamics. *Journal of Experimental Botany* **59**: 187–201.

**Kwon C-T, Tang L, Wang X, Gentile I, Hendelman A, Robitaille G, Eck JV, Xu C, Lippman ZB. 2022**. Dynamic evolution of small signalling peptide compensation in plant stem cell control. *Nature Plants* **8**: 346–355.

**Lachowiec J, Mason GA, Schultz K, Queitsch C. 2018**. Redundancy, Feedback, and Robustness in the Arabidopsis thaliana BZR/BEH Gene Family. *Frontiers in Genetics* **9**: 523.

**Lachowiec J, Queitsch C, Kliebenstein DJ. 2016**. Molecular mechanisms governing differential robustness of development and environmental responses in plants. *Annals of Botany* **117**: 795–809.

**Landrein B, Kiss A, Sassi M, Chauvet A, Das P, Cortizo M, Laufs P, Takeda S, Aida M, Traas J, *et al.* 2015**. Mechanical stress contributes to the expression of the STM homeobox gene in Arabidopsis shoot meristems. *eLife* **4**: e07811.

**Larcher W, Kainmüller C, Wagner J. 2010**. Survival types of high mountain plants under extreme temperatures. *Flora - Morphology, Distribution, Functional Ecology of Plants* **205**: 3–18.

**Larrieu A, Brunoud G, Guérault A, Lainé S, Hennet L, Stigliani A, Gildea I, Just J, Soubigou-Taconnat L, Balzergue S, *et al.* 2022**. Transcriptional reprogramming during floral fate acquisition. *iScience* **25**: 104683.

**Laxmi A, Pan J, Morsy M, Chen R. 2008**. Light Plays an Essential Role in Intracellular Distribution of Auxin Efflux Carrier PIN2 in Arabidopsis thaliana. *PLoS ONE* **3**: e1510.

**LeClere S, Schmelz EA, Chourey PS. 2010**. Sugar Levels Regulate Tryptophan-Dependent Auxin Biosynthesis in Developing Maize Kernels . *Plant Physiology* **153**: 306–318.

**Lee S, Lee S, Yang K-Y, Kim Y-M, Park S-Y, Kim SY, Soh M-S. 2006**. Overexpression of PRE1 and its Homologous Genes Activates Gibberellin-dependent Responses in Arabidopsis thaliana. *Plant and Cell Physiology* **47**: 591–600.

**Lee MG, Norbury CJ, Spurr NK, Nurse P. 1988**. Regulated expression and phosphorylation of a possible mammalian cell-cycle control protein. *Nature* **333**: 676–679.

**Leibfried A, To JPC, Busch W, Stehling S, Kehle A, Demar M, Kieber JJ, Lohmann JU. 2005**. WUSCHEL controls meristem function by direct regulation of cytokinin-inducible response regulators. *Nature* **438**: 1172–1175.

**Leivar P, Monte E. 2014**. PIFs: Systems Integrators in Plant Development. *The Plant Cell* **26**: 56–78.

**Leivar P, Monte E, Al-Sady B, Carle C, Storer A, Alonso JM, Ecker JR, Quail PH. 2008a**. The Arabidopsis Phytochrome-Interacting Factor PIF7, Together with PIF3 and PIF4, Regulates Responses to Prolonged Red Light by Modulating phyB Levels. *The Plant Cell* **20**: 337–352.

**Leivar P, Monte E, Oka Y, Liu T, Carle C, Castillon A, Huq E, Quail PH. 2008b**. Multiple Phytochrome-Interacting bHLH Transcription Factors Repress Premature Seedling Photomorphogenesis in Darkness. *Current Biology* **18**: 1815–1823.

**Leivar P, Tepperman JM, Cohn MM, Monte E, Al-Sady B, Erickson E, Quail PH. 2012**. Dynamic Antagonism between Phytochromes and PIF Family Basic Helix-Loop-Helix Factors Induces Selective Reciprocal Responses to Light and Shade in a Rapidly Responsive Transcriptional Network in Arabidopsis. *The Plant Cell* **24**: 1398–1419.

**Leivar P, Tepperman JM, Monte E, Calderon RH, Liu TL, Quail PH. 2009**. Definition of Early Transcriptional Circuitry Involved in Light-Induced Reversal of PIF-Imposed Repression of Photomorphogenesis in Young Arabidopsis Seedlings. *The Plant Cell* **21**: 3535–3553.

**Lempe J, Lachowiec J, Sullivan AM, Queitsch C. 2012**. Molecular mechanisms of robustness in plants. *Current opinion in plant biology* **16**: 62–9.

**Lessard P, Bouly JP, Jouannic S, Kreis M, Thomas M**. **1999**. Identification of cdc2cAt: a new cyclin-dependent kinase expressed in Arabidopsis thaliana flowers. *Biochimica et biophysica acta* **1445**: 351–8.

**Leyser O**. **2017**. Auxin Signaling. *Plant Physiology* **176**: 465–479.

**Li X, Cai W, Liu Y, Li H, Fu L, Liu Z, Xu L, Liu H, Xu T, Xiong Y**. **2017**. Differential TOR activation and cell proliferation in Arabidopsis root and shoot apexes. *Proceedings of the National Academy of Sciences* **114**: 2765–2770.

**Li J, Gao K, Yang X, Guo B, Xue Y, Miao D, Huang S, An X**. **2022a**. Comprehensive Analyses of Four PtoNF-YC Genes from Populus tomentosa and Impacts on Flowering Timing. *International Journal of Molecular Sciences* **23**: 3116.

**Li Q-F, He J-X**. **2016**. BZR1 Interacts with HY5 to Mediate Brassinosteroid- and Light-Regulated Cotyledon Opening in Arabidopsis in Darkness. *Molecular Plant* **9**: 113–125.

**Li L, Ljung K, Breton G, Schmitz RJ, Pruneda-Paz J, Cowing-Zitron C, Cole BJ, Ivans LJ, Pedmale UV, Jung H-S, *et al.* 2012a**. Linking photoreceptor excitation to changes in plant architecture. *Genes & Development* **26**: 785–790.

**Li J, Nagpal P, Vitart V, McMorris TC, Chory J**. **1996**. A Role for Brassinosteroids in Light-Dependent Development of Arabidopsis. *Science* **272**: 398–401.

**Li Y, Pi L, Huang H, Xu L**. **2012b**. ATH1 and KNAT2 proteins act together in regulation of plant inflorescence architecture. *Journal of Experimental Botany* **63**: 1423–1433.

**Li L, Sheen J**. **2016**. Dynamic and diverse sugar signaling. *Current Opinion in Plant Biology* **33**: 116–125.

**Li J, Terzaghi W, Gong Y, Li C, Ling J-J, Fan Y, Qin N, Gong X, Zhu D, Deng XW**. **2020**. Modulation of BIN2 kinase activity by HY5 controls hypocotyl elongation in the light. *Nature Communications* **11**: 1592.

**Li J, Yang L, Jin D, Nezames CD, Terzaghi W, Deng XW**. **2013**. UV-B-induced photomorphogenesis in Arabidopsis. *Protein & Cell* **4**: 485–492.

**Li Y, Zhu J, Feng Y, Li Z, Ren Z, Liu N, Liu C, Hao J, Han Y**. **2022b**. LsARF3 mediates thermally induced bolting through promoting the expression of LsCO in lettuce (Lactuca sativa L.). *Frontiers in Plant Science* **13**: 958833.

**Lincoln C, Long J, Yamaguchi J, Serikawa K, Hake S**. **1994**. A knotted1-Like Homeobox Gene in Arabidopsis Is Expressed in the Vegetative Meristem and Dramatically Alters Leaf Morphology When Overexpressed in Transgenic Plants. *The Plant Cell* **6**: 1859.

**Ling J-J, Li J, Zhu D, Deng XW**. **2017**. Noncanonical role of Arabidopsis COP1/SPA complex in repressing BIN2-mediated PIF3 phosphorylation and degradation in darkness. *Proceedings of the National Academy of Sciences* **114**: 3539–3544.

**Liscum E, Young JC, Poff KL, Hangarter RP**. **1992**. Genetic separation of phototropism and blue light inhibition of stem elongation. *Plant Physiology* **100**: 267–271.

**Liu X, Cohen JD, Gardner G**. **2011**. Low-Fluence Red Light Increases the Transport and Biosynthesis of Auxin . *Plant Physiology* **157**: 891–904.

**Liu L, Li C, Song S, Teo ZWN, Shen L, Wang Y, Jackson D, Yu H**. **2018**. FTIP-Dependent STM Trafficking Regulates Shoot Meristem Development in Arabidopsis. *Cell Reports* **23**: 1879–1890.

**Livak KJ, Schmittgen TD**. **2001**. Analysis of Relative Gene Expression Data Using Real-Time Quantitative PCR and the 2−ΔΔC T Method. *Methods* **25**: 402–408.

**Lockhart JA, Gottschall V**. **1961**. Fruit-induced & apical senescence in Pisum sativum L. *Plant Physiology* **36**: 389–398.

**Long JA, Moan EI, Medford JI, Barton MK**. **1996**. A member of the KNOTTED class of homeodomain proteins encoded by the STM gene of Arabidopsis. *Nature* **379**: 66–69.

**Lopes FL, Formosa-Jordan P, Malivert A, Margalha L, Confraria A, Feil R, Lunn JE, Jönsson H, Landrein B, Baena-González E**. **2023**. Sugar signaling modulates SHOOT MERISTEMLESS expression and meristem function in Arabidopsis. *bioRxiv*: 2023.01.08.522175.

**López-Juez E, Dillon E, Magyar Z, Khan S, Hazeldine S, Jager SM de, Murray JAH, Beemster GTS, Bögre L, Shanahan H**. **2008**. Distinct Light-Initiated Gene Expression and Cell Cycle Programs in the Shoot Apex and Cotyledons of Arabidopsis . *The Plant Cell* **20**: 947–968.

**Lucas M de, Davière J-M, Rodríguez-Falcón M, Pontin M, Iglesias-Pedraz JM, Lorrain S, Fankhauser C, Blázquez MA, Titarenko E, Prat S**. **2008**. A molecular framework for light and gibberellin control of cell elongation. *Nature* **451**: 480–484.

**Ma L, Li G**. **2019**. Auxin-Dependent Cell Elongation During the Shade Avoidance Response. *Frontiers in Plant Science* **10**: 914.

**Ma D, Li X, Guo Y, Chu J, Fang S, Yan C, Noel JP, Liu H**. **2016**. Cryptochrome 1 interacts with PIF4 to regulate high temperature-mediated hypocotyl elongation in response to blue light. *Proceedings of the National Academy of Sciences* **113**: 224–229.

**Ma Y, Miotk A, Šutiković Z, Ermakova O, Wenzl C, Medzihradszky A, Gaillochet C, Forner J, Utan G, Brackmann K, *et al.* 2019**. WUSCHEL acts as an auxin response rheostat to maintain apical stem cells in Arabidopsis. *Nature Communications* **10**: 5093.

**MacNeil LT, Walhout AJM**. **2011**. Gene regulatory networks and the role of robustness and stochasticity in the control of gene expression. *Genome Research* **21**: 645–657.

**Mao Z, He S, Xu F, Wei X, Jiang L, Liu Y, Wang W, Li T, Xu P, Du S, *et al.* 2020**. Photoexcited CRY1 and phyB interact directly with ARF6 and ARF8 to regulate their DNA-binding activity and auxin-induced hypocotyl elongation in Arabidopsis. *New Phytologist* **225**: 848–865.

**Marash I, Gupta R, Leibman-Markus M, Avni A, Bar M**. **2022**. TOR mediates cytokinin-driven development and defense cues. *bioRxiv*: 2022.03.07.483332.

**Marks CE, Newbigin E, Ladiges PY**. **2011**. Comparative morphology and phylogeny of Nicotiana section Suaveolentes (Solanaceae) in Australia and the South Pacific. *Australian Systematic Botany* **24**: 61–86.

**Martínez-Fernández I, Moura SM de, Alves-Ferreira M, Ferrandiz C, Balanzà V**. **2020**. Identification of players controlling meristem arrest downstream of the FRUITFULL-APETALA2 pathway. *Plant Physiology* **184**: pp.00800.2020.

**Martorell C, Ezcurra E. 2002**. Rosette scrub occurrence and fog availability in arid mountains of Mexico. *Journal of Vegetation Science* **13**: 651–662.

**Mashiguchi K, Tanaka K, Sakai T, Sugawara S, Kawaide H, Natsume M, Hanada A, Yaeno T, Shirasu K, Yao H, *et al.* 2011**. The main auxin biosynthesis pathway in Arabidopsis. *Proceedings of the National Academy of Sciences* **108**: 18512–18517.

**Mathur J, Hülskamp M. 2002**. Microtubules and Microfilaments in Cell Morphogenesis in Higher Plants. *Current Biology* **12**: R669–R676.

**Mazzella MA, Bertero D, Casal JJ. 2000**. Temperature-dependent internode elongation in vegetative plants of Arabidopsis thaliana lacking phytochrome B and cryptochrome 1. *Planta* **210**: 497–501.

**Mazzella MA, Casal JJ. 2001**. Interactive signalling by phytochromes and cryptochromes generates de-etiolation homeostasis in Arabidopsis thaliana. *Plant, Cell & Environment* **24**: 155–161.

**McKim SM. 2019**. How plants grow up. *Journal of Integrative Plant Biology* **61**: 257–277.

**McKim SM. 2020**. Moving on up – controlling internode growth. *New Phytologist* **226**: 672–678.

**McNellis TW, Arnim AG von, Araki T, Komeda Y, Miséra S, Deng XW. 1994**. Genetic and molecular analysis of an allelic series of cop1 mutants suggests functional roles for the multiple protein domains. *The Plant Cell* **6**: 487–500.

**Mendiburu F de. 2020**. Statistical Procedures for Agricultural Research Package "agricolae" (1.3-3). The R Project for Statistical Computing. https://cran.r-project.org/package=agricolae.

**Merelo P, González-Cuadra I, Ferrándiz C. 2021**. A cellular analysis of meristem activity at the end of flowering points to cytokinin as a major regulator of proliferative arrest in Arabidopsis. *Current Biology*.

**Metzger JD, Dusbabek K. 1991**. Determination of the Cellular Mechanisms Regulating Thermo-Induced Stem Growth in Thlaspi arvense L. *Plant Physiology* **97**: 630–637.

**Mohammed B, Bilooei SF, Dóczi R, Grove E, Railo S, Palme K, Ditengou FA, Bögre L, López-Juez E. 2017**. Converging Light, Energy and Hormonal Signaling Control Meristem Activity, Leaf Initiation, and Growth . *Plant Physiology* **176**: 1365–1381.

**Montané M-H, Menand B. 2013**. ATP-competitive mTOR kinase inhibitors delay plant growth by triggering early differentiation of meristematic cells but no developmental patterning change. *Journal of Experimental Botany* **64**: 4361–4374.

**Motta MR, Zhao X, Pastuglia M, Belcram K, Roodbarkelari F, Komaki M, Harashima H, Komaki S, Bulankova P, Heese M, *et al.* 2021**. B1-type cyclins control microtubule organization during cell division in Arabidopsis. *bioRxiv*: 2021.06.29.450310.

**Moyroud E, Minguet EG, Ott F, Yant L, Posé D, Monniaux M, Blanchet S, Bastien O, Thévenon E, Weigel D, *et al.* 2011**. Prediction of Regulatory Interactions from Genome Sequences Using a Biophysical Model for the Arabidopsis LEAFY Transcription Factor . *The Plant Cell* **23**: 1293–1306.

**Müller-Xing R, Clarenz O, Pokorny L, Goodrich J, Schubert D**. **2014**. Polycomb-Group Proteins and FLOWERING LOCUS T Maintain Commitment to Flowering in Arabidopsis thaliana. *The Plant Cell* **26**: 2457–2471.

**Muramoto T, Kohchi T, Yokota A, Hwang I, Goodman HM**. **1999**. The Arabidopsis Photomorphogenic Mutant hy1 Is Deficient in Phytochrome Chromophore Biosynthesis as a Result of a Mutation in a Plastid Heme Oxygenase. *The Plant Cell* **11**: 335–347.

**Murneek AE**. **1926**. Effects Of Correlation Between Vegetative And Reproductive Functions In The Tomato (Lycopersicon Esculentum Mill.). *Plant Physiology* **1**: 3-56.7.

**Mutasa-Göttgens ES, Qi A, Zhang W, Schulze-Buxloh G, Jennings A, Hohmann U, Müller AE, Hedden P**. **2010**. Bolting and flowering control in sugar beet: relationships and effects of gibberellin, the bolting gene B and vernalization. *AoB PLANTS* **2010**: plq012.

**Nagatani A**. **2004**. Light-regulated nuclear localization of phytochromes. *Current Opinion in Plant Biology* **7**: 708–711.

**Nakamura A, Higuchi K, Goda H, Fujiwara MT, Sawa S, Koshiba T, Shimada Y, Yoshida S**. **2003**. Brassinolide Induces IAA5, IAA19, and DR5, a Synthetic Auxin Response Element in Arabidopsis, Implying a Cross Talk Point of Brassinosteroid and Auxin Signaling. *Plant Physiology* **133**: 1843–1853.

**Nemhauser JL, Mockler TC, Chory J**. **2004**. Interdependency of Brassinosteroid and Auxin Signaling in Arabidopsis. *PLoS Biology* **2**: e258.

**Ni M, Tepperman JM, Quail PH**. **1998**. PIF3, a Phytochrome-Interacting Factor Necessary for Normal Photoinduced Signal Transduction, Is a Novel Basic Helix-Loop-Helix Protein. *Cell* **95**: 657–667.

**Nomura T, Kushiro T, Yokota T, Kamiya Y, Bishop GJ, Yamaguchi S**. **2005**. The Last Reaction Producing Brassinolide Is Catalyzed by Cytochrome P-450s, CYP85A3 in Tomato and CYP85A2 in Arabidopsis *. *Journal of Biological Chemistry* **280**: 17873–17879.

**Ogawara T, Higashi K, Kamada H, Ezura H**. **2003**. Ethylene advances the transition from vegetative growth to flowering inArabidopsis thaliana. *Journal of Plant Physiology* **160**: 1335–1340.

**Oh J, Park E, Song K, Bae G, Choi G**. **2019**. PHYTOCHROME INTERACTING FACTOR8 Inhibits Phytochrome A-Mediated Far-Red Light Responses in Arabidopsis. *The Plant Cell* **32**: 186–205.

**Oh E, Zhu J-Y, Bai M-Y, Arenhart RA, Sun Y, Wang Z-Y**. **2014**. Cell elongation is regulated through a central circuit of interacting transcription factors in the Arabidopsis hypocotyl. *eLife* **3**: e03031.

**Oh E, Zhu J-Y, Wang Z-Y**. **2012**. Interaction between BZR1 and PIF4 integrates brassinosteroid and environmental responses. *Nature Cell Biology* **14**: 802–809.

**Ohnishi T, Godza B, Watanabe B, Fujioka S, Hategan L, Ide K, Shibata K, Yokota T, Szekeres M, Mizutani M**. **2012**. CYP90A1/CPD, a Brassinosteroid Biosynthetic Cytochrome P450 of Arabidopsis, Catalyzes C-3 Oxidation*. *Journal of Biological Chemistry* **287**: 31551–31560.

**Ori N, Eshed Y, Chuck G, Bowman JL, Hake S**. **2000**. Mechanisms that control knox gene expression in the Arabidopsis shoot. *Development* **127**: 5523–5532.

**Osterlund MT, Hardtke CS, Wei N, Deng XW**. **2000**. Targeted destabilization of HY5 during light-regulated development of Arabidopsis. *Nature* **405**: 462–466.

**Paciorek T, Friml J**. **2006**. Auxin signaling. *Journal of Cell Science* **119**: 1199–1202.

**Pagant S, Bichet A, Sugimoto K, Lerouxel O, Desprez T, McCann M, Lerouge P, Vernhettes S, Höfte H**. **2002**. KOBITO1 Encodes a Novel Plasma Membrane Protein Necessary for Normal Synthesis of Cellulose during Cell Expansion in Arabidopsis. *The Plant Cell* **14**: 2001–2013.

**Palmer CM, Bush SM, Maloof JN**. **2012**. Phenotypic and Developmental Plasticity in Plants. *eLS*.

**Park E, Kim Y, Choi G**. **2018**. Phytochrome B Requires PIF Degradation and Sequestration to Induce Light Responses across a Wide Range of Light Conditions. *The Plant Cell* **30**: 1277–1292.

**Park E, Park J, Kim J, Nagatani A, Lagarias JC, Choi G**. **2012**. Phytochrome B inhibits binding of phytochrome-interacting factors to their target promoters. *The Plant Journal* **72**: 537–546.

**Payá-Milans M, Poza-Viejo L, Martín-Uriz PS, Lara-Astiaso D, Wilkinson MD, Crevillén P**. **2019**. Genome-wide analysis of the H3K27me3 epigenome and transcriptome in Brassica rapa. *GigaScience* **8**: giz147.

**Pedmale UV, Huang SC, Zander M, Cole BJ, Hetzel J, Ljung K, Reis PAB, Sridevi P, Nito K, Nery JR, *et al.* 2016**. Cryptochromes Interact Directly with PIFs to Control Plant Growth in Limiting Blue Light. *Cell* **164**: 233–245.

**Pei Y, Niu L, Lu F, Liu C, Zhai J, Kong X, Cao X**. **2007**. Mutations in the Type II Protein Arginine Methyltransferase AtPRMT5 Result in Pleiotropic Developmental Defects in Arabidopsis. *Plant Physiology* **144**: 1913–1923.

**Peterson RL, Yeung EC**. **1972**. Effect of Two Gibberellins on Species of the Rosette Plant Hieracium. *Botanical Gazette* **133**: 190–198.

**Pfeiffer A, Janocha D, Dong Y, Medzihradszky A, Schöne S, Daum G, Suzaki T, Forner J, Langenecker T, Rempel E, *et al.* 2016**. Integration of light and metabolic signals for stem cell activation at the shoot apical meristem. *eLife* **5**: e17023.

**Pham VN, Kathare PK, Huq E**. **2018a**. Phytochromes and Phytochrome Interacting Factors. *Plant Physiology* **176**: 1025–1038.

**Pham VN, Kathare PK, Huq E**. **2018b**. Dynamic regulation of PIF5 by COP1–SPA complex to optimize photomorphogenesis in Arabidopsis. *The Plant Journal* **96**: 260–273.

**Pham VN, Xu X, Huq E**. **2018c**. Molecular bases for the constitutive photomorphogenic phenotypes in Arabidopsis. *Development* **145**: dev169870.

**Pierik R, Fankhauser C, Strader LC, Sinha N**. **2021**. Architecture and plasticity: optimizing plant performance in dynamic environments. *Plant physiology* **187**: 1029–1032.

**Plackett ARG, Powers SJ, Fernandez-Garcia N, Urbanova T, Takebayashi Y, Seo M, Jikumaru Y, Benlloch R, Nilsson O, Ruiz-Rivero O, *et al.* 2012**. Analysis of the Developmental Roles of the Arabidopsis Gibberellin 20-Oxidases Demonstrates That GA20ox1 , -2 , and -3 Are the Dominant Paralogs. *The Plant Cell* **24**: 941–960.

**Poethig RS**. **2003**. Phase Change and the Regulation of Developmental Timing in Plants. *Science* **301**: 334–336.

**Poethig RS**. **2013**. Vegetative phase change and shoot maturation in plants. *Current topics in developmental biology* **105**: 125–52.

**Ponnu J, Hoecker U**. **2021**. Illuminating the COP1/SPA Ubiquitin Ligase: Fresh Insights Into Its Structure and Functions During Plant Photomorphogenesis. *Frontiers in Plant Science* **12**: 662793.

**Proveniers M, Rutjens B, Brand M, Smeekens S**. **2007**. The Arabidopsis TALE homeobox gene ATH1 controls floral competency through positive regulation of FLC. *The Plant Journal* **52**: 899–913.

**Qi L, Liu S, Li C, Fu J, Jing Y, Cheng J, Li H, Zhang D, Wang X, Dong X, *et al.* 2020**. PHYTOCHROME-INTERACTING FACTORS Interact with the ABA Receptors PYL8 and PYL9 to Orchestrate ABA Signaling in Darkness. *Molecular Plant* **13**: 414–430.

**Qi X, Tang W, Li W, He Z, Xu W, Fan Z, Zhou Y, Wang C, Xu Z, Chen J, *et al.* 2021**. Arabidopsis G-Protein β Subunit AGB1 Negatively Regulates DNA Binding of MYB62, a Suppressor in the Gibberellin Pathway. *International Journal of Molecular Sciences* **22**: 8270.

**Qiu Y, Pasoreck EK, Reddy AK, Nagatani A, Ma W, Chory J, Chen M**. **2017**. Mechanism of early light signaling by the carboxy-terminal output module of Arabidopsis phytochrome B. *Nature Communications* **8**: 1905.

**Quaedvlieg N, Dockx J, Rook F, Weisbeek P, Smeekens S**. **1995**. The homeobox gene ATH1 of Arabidopsis is derepressed in the photomorphogenic mutants cop1 and det1. *The Plant Cell* **7**: 117–129.

**Quail PH**. **2007**. Phytochrome-regulated Gene Expression. *Journal of Integrative Plant Biology* **49**: 11–20.

**Rabot A, Henry C, Baaziz KB, Mortreau E, Azri W, Lothier J, Hamama L, Boummaza R, Leduc N, Pelleschi-Travier S, *et al.* 2012**. Insight into the Role of Sugars in Bud Burst Under Light in the Rose. *Plant and Cell Physiology* **53**: 1068–1082.

**Ragni L, Belles-Boix E, Günl M, Pautot V**. **2008**. Interaction of KNAT6 and KNAT2 with BREVIPEDICELLUS and PENNYWISE in Arabidopsis inflorescences. *The Plant cell* **20**: 888–900.

**Ramon M, Rolland F, Sheen J**. **2008**. Sugar Sensing and Signaling. *The Arabidopsis Book* **6**: e0117.

**Reddy GV, Meyerowitz EM**. **2005**. Stem-Cell Homeostasis and Growth Dynamics Can Be Uncoupled in the Arabidopsis Shoot Apex. *Science* **310**: 663–667.

**Reed RC, Brady SR, Muday GK**. **1998**. Inhibition of Auxin Movement from the Shoot into the Root Inhibits Lateral Root Development in Arabidopsis. *Plant Physiology* **118**: 1369–1378.

**Reed JW, Nagpal P, Poole DS, Furuya M, Chory J**. **1993**. Mutations in the gene for the red/far-red light receptor phytochrome B alter cell elongation and physiological responses throughout Arabidopsis development. *The Plant Cell* **5**: 147–157.

**Reeves PA, He Y, Schmitz RJ, Amasino RM, Panella LW, Richards CM**. **2007**. Evolutionary Conservation of the FLOWERING LOCUS C -Mediated Vernalization Response: Evidence From the Sugar Beet ( Beta vulgaris ). *Genetics* **176**: 295–307.

**Regnault T, Davière J, Heintz D, Lange T, Achard P**. **2014**. The gibberellin biosynthetic genes AtKAO1 and AtKAO2 have overlapping roles throughout Arabidopsis development. *The Plant Journal* **80**: 462–474.

**Reijnders MJMF, Waterhouse RM**. **2021**. Summary Visualizations of Gene Ontology Terms With GO-Figure! *Frontiers in Bioinformatics* **1**: 638255.

**Reinhardt D, Mandel T, Kuhlemeier C**. **2000**. Auxin Regulates the Initiation and Radial Position of Plant Lateral Organs. *The Plant Cell* **12**: 507–518.

**Reinhardt D, Pesce E-R, Stieger P, Mandel T, Baltensperger K, Bennett M, Traas J, Friml J, Kuhlemeier C**. **2003**. Regulation of phyllotaxis by polar auxin transport. *Nature* **426**: 255–260.

**Ren H, Gray WM**. **2015**. SAUR Proteins as Effectors of Hormonal and Environmental Signals in Plant Growth. *Molecular Plant* **8**: 1153–1164.

**Richard C, Lescot M, Inzé D, Veylder LD**. **2002**. Effect of auxin, cytokinin, and sucrose on cell cycle gene expression in Arabidopsis thaliana cell suspension cultures. *Plant Cell, Tissue and Organ Culture* **69**: 167–176.

**Rieu I, Eriksson S, Powers SJ, Gong F, Griffiths J, Woolley L, Benlloch R, Nilsson O, Thomas SG, Hedden P, *et al.* 2008**. Genetic Analysis Reveals That C19-GA 2-Oxidation Is a Major Gibberellin Inactivation Pathway in Arabidopsis . *The Plant Cell* **20**: 2420–2436.

**Rojo E, Sharma VK, Kovaleva V, Raikhel NV, Fletcher JC**. **2002**. CLV3 Is Localized to the Extracellular Space, Where It Activates the Arabidopsis CLAVATA Stem Cell Signaling Pathway. *The Plant Cell* **14**: 969–977.

**Roldán M, Gómez-Mena C, Ruiz-García L, Salinas J, Martínez-Zapater JM**. **1999**. Sucrose availability on the aerial part of the plant promotes morphogenesis and flowering of Arabidopsis in the dark. *The Plant Journal* **20**: 581–590.

**Rosquete MR, Barbez E, Kleine-Vehn J**. **2012**. Cellular Auxin Homeostasis: Gatekeeping Is Housekeeping. *Molecular Plant* **5**: 772–786.

**Ross JJ, Quittenden LJ**. **2016**. Interactions between Brassinosteroids and Gibberellins: Synthesis or Signaling? *The Plant Cell* **28**: 829–832.

**Ruonala R, Rinne PLH, Kangasjärvi J, Schoot C van der**. **2008**. CENL1 Expression in the Rib Meristem Affects Stem Elongation and the Transition to Dormancy in Populus. *The Plant Cell* **20**: 59–74.

**Rupp H, Frank M, Werner T, Strnad M, Schmülling T**. **1999**. Increased steady state mRNA levels of the STM and KNAT1 homeobox genes in cytokinin overproducing Arabidopsis thaliana indicate a role for cytokinins in the shoot apical meristem. *The Plant Journal* **18**: 557–563.

**Rutjens B, Bao D, Eck-Stouten EV, Brand M, Smeekens S, Proveniers M**. **2009**. Shoot apical meristem function in Arabidopsis requires the combined activities of three BEL1-like homeodomain proteins. *The Plant Journal* **58**: 641–654.

**Sablowski R**. **2007**. Flowering and determinacy in Arabidopsis. *Journal of Experimental Botany* **58**: 899–907.

**Sablowski R, Dornelas MC**. **2014**. Interplay between cell growth and cell cycle in plants. *Journal of Experimental Botany* **65**: 2703–2714.

**Sablowski R, Gutierrez C**. **2021**. Cycling in a crowd: coordination of plant cell division, growth and cell fate. *The Plant Cell* **34**: koab222-.

**Sachs RM**. **1965**. Stem Elongation. *Annual Review of Plant Physiology* **16**: 73–96.

**Sachs RM, Bretz CF, Lang A**. **1959a**. SHOOT HISTOGENESIS: THE EARLY EFFECTS OF GIBBERELLIN UPON STEM ELONGATION IN TWO ROSETTE PLANTS. *American Journal of Botany* **46**: 376–384.

**Sachs RM, Bretz C, Lang A**. **1959b**. Cell division and gibberellic acid. *Experimental Cell Research* **18**: 230–244.

**Sachs RM, Lang A**. **1957**. Effect of Gibberellin on Cell Division in Hyoscyamus. *Science* **125**: 1144–1145.

**Saijo Y, Sullivan JA, Wang H, Yang J, Shen Y, Rubio V, Ma L, Hoecker U, Deng XW**. **2003**. The COP1–SPA1 interaction defines a critical step in phytochrome A-mediated regulation of HY5 activity. *Genes & Development* **17**: 2642–2647.

**Saini S, Sharma I, Pati PK**. **2015**. Versatile roles of brassinosteroid in plants in the context of its homoeostasis, signaling and crosstalks. *Frontiers in Plant Science* **6**: 950.

**Sairanen I, Novák O, Pěnčík A, Ikeda Y, Jones B, Sandberg G, Ljung K**. **2012**. Soluble Carbohydrates Regulate Auxin Biosynthesis via PIF Proteins in Arabidopsis . *The Plant Cell* **24**: 4907–4916.

**Sarojam R, Sappl PG, Goldshmidt A, Efroni I, Floyd SK, Eshed Y, Bowman JL**. **2010**. Differentiating Arabidopsis shoots from leaves by combined YABBY activities. *The Plant cell* **22**: 2113–30.

**Sassi M, Ali O, Boudon F, Cloarec G, Abad U, Cellier C, Chen X, Gilles B, Milani P, Friml J, *et al.* 2014**. An Auxin-Mediated Shift toward Growth Isotropy Promotes Organ Formation at the Shoot Meristem in Arabidopsis. *Current Biology* **24**: 2335–2342.

**Sassi M, Lu Y, Zhang Y, Wang J, Dhonukshe P, Blilou I, Dai M, Li J, Gong X, Jaillais Y, *et al.* 2012**. COP1 mediates the coordination of root and shoot growth by light through modulation of PIN1- and PIN2-dependent auxin transport in Arabidopsis. *Development* **139**: 3402–3412.

**Sassi M, Vernoux T**. **2013**. Auxin and self-organization at the shoot apical meristem. *Journal of Experimental Botany* **64**: 2579–2592.

**Sassi M, Wang J, Ruberti I, Vernoux T, Xu J**. **2013**. Shedding light on auxin movement: Light-regulation of polar auxin transport in the photocontrol of plant development. *Plant Signaling & Behavior* **8**: e23355.

**Schaffer WM, Schaffer MV**. **1979**. The Adaptive Significance of Variations in Reproductive Habit in the Agavaceae II: Pollinator Foraging Behavior and Selection for Increased Reproductive Expenditure. *Ecology* **60**: 1051–1069.

**Schaller GE, Street IH, Kieber JJ**. **2014**. Cytokinin and the cell cycle. *Current Opinion in Plant Biology* **21**: 7–15.

**Schepetilnikov M, Dimitrova M, Mancera-Martínez E, Geldreich A, Keller M, Ryabova LA**. **2013**. TOR and S6K1 promote translation reinitiation of uORF-containing mRNAs via phosphorylation of eIF3h. *The EMBO Journal* **32**: 1087–1102.

**Schepetilnikov M, Kobayashi K, Geldreich A, Caranta C, Robaglia C, Keller M, Ryabova LA**. **2011**. Viral factor TAV recruits TOR/S6K1 signalling to activate reinitiation after long ORF translation. *The EMBO Journal* **30**: 1343–1356.

**Schepetilnikov M, Makarian J, Srour O, Geldreich A, Yang Z, Chicher J, Hammann P, Ryabova LA**. **2017**. GTPase ROP2 binds and promotes activation of target of rapamycin, TOR, in response to auxin. *The EMBO Journal* **36**: 886–903.

**Schepetilnikov M, Ryabova LA**. **2017**. Recent Discoveries on the Role of TOR (Target of Rapamycin) Signaling in Translation in Plants. *Plant Physiology* **176**: 1095–1105.

**Schlichting CarlD**. **1986**. The evolution of phenotypic plasticity in plants. *Annual Review of Ecology and Systematics* **17**: 667–693.

**Schlichting CD, Levin DA**. **1986**. Phenotypic plasticity: an evolving plant character. *Biological Journal of the Linnean Society* **29**: 37–47.

**Schneider CA, Rasband WS, Eliceiri KW**. **2012**. NIH Image to ImageJ: 25 years of image analysis. *Nature Methods* **9**: 671–675.

**Schwab DB, Casasa S, Moczek AP**. **2019**. On the Reciprocally Causal and Constructive Nature of Developmental Plasticity and Robustness. *Frontiers in Genetics* **9**: 735.

**Seeliger I, Frerichs A, Glowa D, Velo L, Comelli P, Chandler JW, Werr W**. **2016**. The AP2-type transcription factors DORNRÖSCHEN and DORNRÖSCHEN-LIKE promote G1/S transition. *Molecular Genetics and Genomics* **291**: 1835–1849.

**Seo M, Akaba S, Oritani T, Delarue M, Bellini C, Caboche M, Koshiba T**. **1998**. Higher Activity of an Aldehyde Oxidase in the Auxin-Overproducing superroot1 Mutant ofArabidopsis thaliana. *Plant Physiology* **116**: 687–693.

**Serrano-Mislata A, Bencivenga S, Bush M, Schiessl K, Boden S, Sablowski R**. **2017**. DELLA genes restrict inflorescence meristem function independently of plant height. *Nature plants* **3**: 749–754.

**Serrano-Mislata A, Sablowski R**. **2018**. The pillars of land plants: new insights into stem development. *Current Opinion in Plant Biology* **45**: 11–17.

**Sessa RA, Bennett MH, Lewis MJ, Mansfield JW, Beale MH**. **2000**. Metabolite Profiling of Sesquiterpene Lactones from Lactuca Species MAJOR LATEX COMPONENTS ARE NOVEL OXALATE AND SULFATE CONJUGATES OF LACTUCIN AND ITS DERIVATIVES*. *Journal of Biological Chemistry* **275**: 26877–26884.

**Shalitin D, Yang H, Mockler TC, Maymon M, Guo H, Whitelam GC, Lin C**. **2002**. Regulation of Arabidopsis cryptochrome 2 by blue-light-dependent phosphorylation. *Nature* **417**: 763–767.

**Shi H, Liu R, Xue C, Shen X, Wei N, Deng XW, Zhong S. 2016**. Seedlings Transduce the Depth and Mechanical Pressure of Covering Soil Using COP1 and Ethylene to Regulate EBF1/EBF2 for Soil Emergence. *Current Biology* **26**: 139–149.

**Shimotohno A, Aki SS, Takahashi N, Umeda M. 2021**. Regulation of the Plant Cell Cycle in Response to Hormones and the Environment. *Annual Review of Plant Biology* **72**: 1–24.

**Skirycz A, Radziejwoski A, Busch W, Hannah MA, Czeszejko J, Kwaśniewski M, Zanor M, Lohmann JU, Veylder LD, Witt I, *et al.* 2008**. The DOF transcription factor OBP1 is involved in cell cycle regulation in Arabidopsis thaliana. *The Plant Journal* **56**: 779–792.

**Smith HMS, Campbell BC, Hake S. 2004**. Competence to Respond to Floral Inductive Signals Requires the Homeobox Genes PENNYWISE and POUND-FOOLISH. *Current Biology* **14**: 812–817.

**Smith HMS, Hake S. 2003**. The Interaction of Two Homeobox Genes, BREVIPEDICELLUS and PENNYWISE, Regulates Internode Patterning in the Arabidopsis Inflorescence. *The Plant Cell* **15**: 1717–1727.

**Snipes SA, Rodriguez K, DeVries AE, Miyawaki KN, Perales M, Xie M, Reddy GV. 2018**. Cytokinin stabilizes WUSCHEL by acting on the protein domains required for nuclear enrichment and transcription. *PLoS Genetics* **14**: e1007351.

**Sohlberg JJ, Myrenås M, Kuusk S, Lagercrantz U, Kowalczyk M, Sandberg G, Sundberg E. 2006**. STY1 regulates auxin homeostasis and affects apical–basal patterning of the Arabidopsis gynoecium. *The Plant Journal* **47**: 112–123.

**Soons MB, Heil GW, Nathan R, Katul GG. 2004**. DETERMINANTS OF LONG-DISTANCE SEED DISPERSAL BY WIND IN GRASSLANDS. *Ecology* **85**: 3056–3068.

**Soyars CL, James SR, Nimchuk ZL. 2016**. Ready, aim, shoot: stem cell regulation of the shoot apical meristem. *Current Opinion in Plant Biology* **29**: 163–168.

**Sparks EE, Drapek C, Gaudinier A, Li S, Ansariola M, Shen N, Hennacy JH, Zhang J, Turco G, Petricka JJ, *et al.* 2016**. Establishment of Expression in the SHORTROOT-SCARECROW Transcriptional Cascade through Opposing Activities of Both Activators and Repressors. *Developmental Cell* **39**: 585–596.

**Ståldal V, Cierlik I, Chen S, Landberg K, Baylis T, Myrenås M, Sundström JF, Eklund DM, Ljung K, Sundberg E. 2012**. The Arabidopsis thaliana transcriptional activator STYLISH1 regulates genes affecting stamen development, cell expansion and timing of flowering. *Plant Molecular Biology* **78**: 545–559.

**Staswick PE, Serban B, Rowe M, Tiryaki I, Maldonado MT, Maldonado MC, Suza W. 2005**. Characterization of an Arabidopsis Enzyme Family That Conjugates Amino Acids to Indole-3-Acetic Acid. *The Plant Cell* **17**: 616–627.

**Stavang JA, Gallego-Bartolomé J, Gómez MD, Yoshida S, Asami T, Olsen JE, García-Martínez JL, Alabadí D, Blázquez MA. 2009**. Hormonal regulation of temperature-induced growth in Arabidopsis. *The Plant Journal* **60**: 589–601.

**Stortenbeker N, Bemer M. 2018**. The SAUR gene family: the plant's toolbox for adaptation of growth and development. *Journal of Experimental Botany* **70**: 17–27.

**Strasser B, Sánchez-Lamas M, Yanovsky MJ, Casal JJ, Cerdán PD**. **2010**. Arabidopsis thaliana life without phytochromes. *Proceedings of the National Academy of Sciences* **107**: 4776–4781.

**Su Y, Lagarias JC**. **2007**. Light-Independent Phytochrome Signaling Mediated by Dominant GAF Domain Tyrosine Mutants of Arabidopsis Phytochromes in Transgenic Plants. *The Plant Cell* **19**: 2124–2139.

**Su YH, Zhou C, Li YJ, Yu Y, Tang LP, Zhang WJ, Yao WJ, Huang R, Laux T, Zhang XS**. **2020**. Integration of pluripotency pathways regulates stem cell maintenance in the Arabidopsis shoot meristem. *Proceedings of the National Academy of Sciences of the United States of America* **117**: 22561–22571.

**Suetsugu N, Wada M**. **2013**. Evolution of Three LOV Blue Light Receptor Families in Green Plants and Photosynthetic Stramenopiles: Phototropin, ZTL/FKF1/LKP2 and Aureochrome. *Plant and Cell Physiology* **54**: 8–23.

**Suge H, Rappaport L**. **1968**. Role of Gibberellins in Stem Elongation and Flowering in Radish. *Plant Physiology* **43**: 1208–1214.

**Sun T**. **2011**. The Molecular Mechanism and Evolution of the GA–GID1–DELLA Signaling Module in Plants. *Current Biology* **21**: R338–R345.

**Sun J, Qi L, Li Y, Chu J, Li C**. **2012**. PIF4–Mediated Activation of YUCCA8 Expression Integrates Temperature into the Auxin Pathway in Regulating Arabidopsis Hypocotyl Growth. *PLoS Genetics* **8**: e1002594.

**Sun N, Wang J, Gao Z, Dong J, He H, Terzaghi W, Wei N, Deng XW, Chen H**. **2016**. Arabidopsis SAURs are critical for differential light regulation of the development of various organs. *Proceedings of the National Academy of Sciences* **113**: 6071–6076.

**Swarup R, Bhosale R**. **2019**. Developmental Roles of AUX1/LAX Auxin Influx Carriers in Plants. *Frontiers in Plant Science* **10**: 1306.

**Szekeres M, Németh K, Koncz-Kálmán Z, Mathur J, Kauschmann A, Altmann T, Rédei GP, Nagy F, Schell J, Koncz C**. **1996**. Brassinosteroids Rescue the Deficiency of CYP90, a Cytochrome P450, Controlling Cell Elongation and De-etiolation in Arabidopsis. *Cell* **85**: 171–182.

**Takahashi N, Lammens T, Boudolf V, Maes S, Yoshizumi T, Jaeger GD, Witters E, Inzé D, Veylder LD**. **2008**. The DNA replication checkpoint aids survival of plants deficient in the novel replisome factor ETG1. *The EMBO Journal* **27**: 1840–1851.

**Teale WD, Paponov IA, Palme K**. **2006**. Auxin in action: signalling, transport and the control of plant growth and development. *Nature Reviews Molecular Cell Biology* **7**: 847–859.

**Thomas SG, Phillips AL, Hedden P**. **1999**. Molecular cloning and functional expression of gibberellin 2- oxidases, multifunctional enzymes involved in gibberellin deactivation. *Proceedings of the National Academy of Sciences* **96**: 4698–4703.

**Thomson FJ, Moles AT, Auld TD, Kingsford RT**. **2011**. Seed dispersal distance is more strongly correlated with plant height than with seed mass. *Journal of Ecology* **99**: 1299–1307.

**Timpte CS, Wilson AK, Estelle M**. **1992**. Effects of the axr2 mutation of Arabidopsis on cell shape in hypocotyl and inflorescence. *Planta* **188**: 271–278.

**Todaka D, Nakashima K, Maruyama K, Kidokoro S, Osakabe Y, Ito Y, Matsukura S, Fujita Y, Yoshiwara K, Ohme-Takagi M, *et al.* 2012**. Rice phytochrome-interacting factor-like protein OsPIL1 functions as a key regulator of internode elongation and induces a morphological response to drought stress. *Proceedings of the National Academy of Sciences* **109**: 15947–15952.

**Tong H, Xiao Y, Liu D, Gao S, Liu L, Yin Y, Jin Y, Qian Q, Chu C. 2014**. Brassinosteroid Regulates Cell Elongation by Modulating Gibberellin Metabolism in Rice . *The Plant Cell* **26**: 4376–4393.

**Tooke F, Ordidge M, Chiurugwi T, Battey N. 2005**. Mechanisms and function of flower and inflorescence reversion. *Journal of Experimental Botany* **56**: 2587–2599.

**Tripathi S, Hoang QTN, Han Y-J, Kim J-I. 2019**. Regulation of Photomorphogenic Development by Plant Phytochromes. *International Journal of Molecular Sciences* **20**: 6165.

**Truernit E, Siemering KR, Hodge S, Grbic V, Haseloff J. 2006**. A Map of KNAT Gene Expression in the Arabidopsis Root. *Plant Molecular Biology* **60**: 1–20.

**Ueguchi-Tanaka M, Ashikari M, Nakajima M, Itoh H, Katoh E, Kobayashi M, Chow T, Hsing YC, Kitano H, Yamaguchi I, *et al.* 2005**. GIBBERELLIN INSENSITIVE DWARF1 encodes a soluble receptor for gibberellin. *Nature* **437**: 693–698.

**Ung N, Lal S, Smith HMS. 2011**. The Role of PENNYWISE and POUND-FOOLISH in the Maintenance of the Shoot Apical Meristem in Arabidopsis . *Plant Physiology* **156**: 605–614.

**Unterholzner SJ, Rozhon W, Papacek M, Ciomas J, Lange T, Kugler KG, Mayer KF, Sieberer T, Poppenberger B. 2015**. Brassinosteroids Are Master Regulators of Gibberellin Biosynthesis in Arabidopsis. *The Plant Cell* **27**: 2261–2272.

**Ursache R, Andersen TG, Marhavý P, Geldner N. 2018**. A protocol for combining fluorescent proteins with histological stains for diverse cell wall components. *The Plant Journal* **93**: 399–412.

**Vaughan JG. 1955**. The morphology and growth of the vegetative and reproductive apices of Arabidopsis thaliana (L.) Heynh., Capsella bursa-pastoris (L.) Medic. and Anagallis arvensis L. *Journal of the Linnean Society of London, Botany* **55**: 279–301.

**Venglat SP, Dumonceaux T, Rozwadowski K, Parnell L, Babic V, Keller W, Martienssen R, Selvaraj G, Datla R. 2002**. The homeobox gene BREVIPEDICELLUS is a key regulator of inflorescence architecture in Arabidopsis. *Proceedings of the National Academy of Sciences* **99**: 4730–4735.

**Visser JAGM, Hermisson J, Wagner GP, Meyers LA, Bagheri-Chaichian H, Blanchard JL, Chao L, Cheverud JM, Elena SF, Fontana W, *et al.* 2003**. PERSPECTIVE: EVOLUTION AND DETECTION OF GENETIC ROBUSTNESS. *Evolution* **57**: 1959–1972.

**Wachsman G, Modliszewski JL, Valdes M, Benfey PN. 2017**. A SIMPLE Pipeline for Mapping Point Mutations . *Plant Physiology* **174**: 1307–1313.

**Waddington CH. 1961**. Genetic Assimilation. *Advances in Genetics* **10**: 257–293.

**Wang P, Abid MA, Qanmber G, Askari M, Zhou L, Song Y, Liang C, Meng Z, Malik W, Wei Y, *et al.* 2021**. Photomorphogenesis in Plants: The Central Role of Phytochrome Interacting Factors (PIFs). *Environmental and Experimental Botany* **194**: 104704.

**Wang Z-Y, Bai M-Y, Oh E, Zhu J-Y. 2012**. Brassinosteroid Signaling Network and Regulation of Photomorphogenesis. *Annual Review of Genetics* **46**: 701–724.

**Wang G, Kong H, Sun Y, Zhang X, Zhang W, Altman N, dePamphilis CW, Ma H**. **2004**. Genome-Wide Analysis of the Cyclin Family in Arabidopsis and Comparative Phylogenetic Analysis of Plant Cyclin-Like Proteins . *Plant Physiology* **135**: 1084–1099.

**Wang W, Lu X, Li L, Lian H, Mao Z, Xu P, Guo T, Xu F, Du S, Cao X, *et al.* 2018**. Photoexcited CRYPTOCHROME1 Interacts with Dephosphorylated BES1 to Regulate Brassinosteroid Signaling and Photomorphogenesis in Arabidopsis. *The Plant Cell* **30**: 1989–2005.

**Wang X, Ma Q, Wang R, Wang P, Liu Y, Mao T**. **2019**. Submergence stress-induced hypocotyl elongation through ethylene signaling-mediated regulation of cortical microtubules in Arabidopsis. *Journal of Experimental Botany* **71**: 1067–1077.

**Wang Z-Y, Nakano T, Gendron J, He J, Chen M, Vafeados D, Yang Y, Fujioka S, Yoshida S, Asami T, *et al.* 2002**. Nuclear-Localized BZR1 Mediates Brassinosteroid-Induced Growth and Feedback Suppression of Brassinosteroid Biosynthesis. *Developmental Cell* **2**: 505–513.

**Wang Q, Qin G, Cao M, Chen R, He Y, Yang L, Zeng Z, Yu Y, Gu Y, Xing W, *et al.* 2020**. A phosphorylation-based switch controls TAA1-mediated auxin biosynthesis in plants. *Nature Communications* **11**: 679.

**Ware A, Walker CH, Šimura J, González-Suárez P, Ljung K, Bishopp A, Wilson ZA, Bennett T**. **2020**. Auxin export from proximal fruits drives arrest in temporally competent inflorescences. *Nature Plants* **6**: 699–707.

**Wei X, Wang W, Xu P, Wang W, Guo T, Kou S, Liu M, Niu Y, Yang H, Mao Z**. **2021**. Phytochrome B interacts with SWC6 and ARP6 to regulate H2A.Z deposition and photomorphogensis in Arabidopsis. *Journal of Integrative Plant Biology* **63**: 1133–1146.

**Werner T, Motyka V, Laucou V, Smets R, Onckelen HV, Schmülling T**. **2003**. Cytokinin-Deficient Transgenic Arabidopsis Plants Show Multiple Developmental Alterations Indicating Opposite Functions of Cytokinins in the Regulation of Shoot and Root Meristem Activity. *The Plant Cell* **15**: 2532–2550.

**Werner T, Schmülling T**. **2009**. Cytokinin action in plant development. *Current Opinion in Plant Biology* **12**: 527–538.

**Whitelam GC, Devlin PF**. **1997**. Roles of different phytochromes in Arabidopsis photomorphogenesis. *Plant, Cell & Enviroment* **20**: 752–758.

**Whitelam GC, Patel S, Devlin PF**. **1998**. Phytochromes and photomorphogenesis in Arabidopsis. *Philosophical Transactions of the Royal Society of London. Series B: Biological Sciences* **353**: 1445–1453.

**Williams L, Fletcher JC**. **2005**. Stem cell regulation in the Arabidopsis shoot apical meristem. *Current Opinion in Plant Biology* **8**: 582–586.

**Willige BC, Ogiso-Tanaka E, Zourelidou M, Schwechheimer C**. **2012**. WAG2 represses apical hook opening downstream from gibberellin and PHYTOCHROME INTERACTING FACTOR 5. *Development* **139**: 4020–4028.

**Willmann MR**. **2000**. CLV1 and CLV3: negative regulators of SAM stem cell accumulation. *Trends in plant science* **5**: 416.

**Winter N, Kollwig G, Zhang S, Kragler F**. **2007**. MPB2C, a microtubule-associated protein, regulates non-cell-autonomy of the homeodomain protein KNOTTED1. *The Plant cell* **19**: 3001–18.

**Winter CM, Szekely P, Popov V, Belcher H, Carter R, Jones M, Fraser SE, Truong TV, Benfey PN**. **2024**. SHR and SCR coordinate root patterning and growth early in the cell cycle. *Nature* **626**: 611–616.

**Won C, Shen X, Mashiguchi K, Zheng Z, Dai X, Cheng Y, Kasahara H, Kamiya Y, Chory J, Zhao Y**. **2011**. Conversion of tryptophan to indole-3-acetic acid by TRYPTOPHAN AMINOTRANSFERASES OF ARABIDOPSIS and YUCCAs in Arabidopsis. *Proceedings of the National Academy of Sciences* **108**: 18518–18523.

**Wood DW, Scott RK**. **1975**. Sowing sugar beet in autumn in England. *The Journal of Agricultural Science* **84**: 97–108.

**Wu S-H**. **2014**. Gene Expression Regulation in Photomorphogenesis from the Perspective of the Central Dogma. *Plant Biology* **65**: 311–333.

**Wu T, Hu E, Xu S, Chen M, Guo P, Dai Z, Feng T, Zhou L, Tang W, Zhan L, *et al.* 2021**. clusterProfiler 4.0: A universal enrichment tool for interpreting omics data. *The Innovation* **2**: 100141.

**Wu L-Y, Shang G-D, Wang F-X, Gao J, Wan M-C, Xu Z-G, Wang J-W**. **2022**. Dynamic chromatin state profiling reveals regulatory roles of auxin and cytokinin in shoot regeneration. *Developmental Cell*.

**Wu Y, Shi L, Li L, Fu L, Liu Y, Xiong Y, Sheen J**. **2019**. Integration of nutrient, energy, light, and hormone signalling via TOR in plants. *Journal of Experimental Botany* **70**: 2227–2238.

**Wu J, Wang W, Xu P, Pan J, Zhang T, Li Y, Li G, Yang H, Lian H**. **2018**. phyB Interacts with BES1 to Regulate Brassinosteroid Signaling in Arabidopsis. *Plant and Cell Physiology* **60**: 353–366.

**Wuest SE, Philipp MA, Guthörl D, Schmid B, Grossniklaus U**. **2016**. Seed Production Affects Maternal Growth and Senescence in Arabidopsis . *Plant Physiology* **171**: 392–404.

**Würschum T, Groß-Hardt R, Laux T**. **2005**. APETALA2 Regulates the Stem Cell Niche in the Arabidopsis Shoot Meristem. *The Plant Cell* **18**: 295–307.

**Wybouw B, Rybel BD**. **2018**. Cytokinin – A Developing Story. *Trends in Plant Science* **24**: 177–185.

**Xiao Y, Chu L, Zhang Y, Bian Y, Xiao J, Xu D**. **2022**. HY5: A Pivotal Regulator of Light-Dependent Development in Higher Plants. *Frontiers in Plant Science* **12**: 800989.

**Xie M, Chen H, Huang L, O'Neil RC, Shokhirev MN, Ecker JR**. **2018**. A B-ARR-mediated cytokinin transcriptional network directs hormone cross-regulation and shoot development. *Nature Communications* **9**: 1604.

**Xiong Y, McCormack M, Li L, Hall Q, Xiang C, Sheen J**. **2013**. Glucose–TOR signalling reprograms the transcriptome and activates meristems. *Nature* **496**: 181–186.

**Xu P, Chen H, Li T, Xu F, Mao Z, Cao X, Miao L, Du S, Hua J, Zhao J, *et al.* 2021**. Blue light-dependent interactions of CRY1 with GID1 and DELLA proteins regulate gibberellin signaling and photomorphogenesis in Arabidopsis. *The Plant cell* **33**: 2375–2394.

**Xu F, He S, Zhang J, Mao Z, Wang W, Li T, Hua J, Du S, Xu P, Li L, *et al*. 2018**. Photoactivated CRY1 and phyB Interact Directly with AUX/IAA Proteins to Inhibit Auxin Signaling in Arabidopsis. *Molecular Plant* **11**: 523–541.

**Xu X, Kathare PK, Pham VN, Bu Q, Nguyen A, Huq E. 2017**. Reciprocal proteasome-mediated degradation of PIFs and HFR1 underlies photomorphogenic development in Arabidopsis. *Development* **144**: 1831–1840.

**Xu X, Paik I, Zhu L, Bu Q, Huang X, Deng XW, Huq E. 2014**. PHYTOCHROME INTERACTING FACTOR1 Enhances the E3 Ligase Activity of CONSTITUTIVE PHOTOMORPHOGENIC1 to Synergistically Repress Photomorphogenesis in Arabidopsis . *The Plant Cell* **26**: 1992–2006.

**Xu X, Paik I, Zhu L, Huq E. 2015**. Illuminating Progress in Phytochrome-Mediated Light Signaling Pathways. *Trends in Plant Science* **20**: 641–650.

**Xu XM, Wang J, Xuan Z, Goldshmidt A, Borrill PGM, Hariharan N, Kim JY, Jackson D. 2011**. Chaperonins Facilitate KNOTTED1 Cell-to-Cell Trafficking and Stem Cell Function. *Science* **333**: 1141–1144.

**Yadav RK, Perales M, Gruel J, Ohno C, Heisler M, Girke T, Jönsson H, Reddy GV. 2013**. Plant stem cell maintenance involves direct transcriptional repression of differentiation program. *Molecular Systems Biology* **9**: 654–654.

**Yadav RK, Tavakkoli M, Xie M, Girke T, Reddy GV. 2014**. A high-resolution gene expression map of the Arabidopsis shoot meristem stem cell niche. *Development* **141**: 2735–2744.

**Yamaguchi S. 2008**. Gibberellin Metabolism and its Regulation. *Plant Biology* **59**: 225–251.

**Yanai O, Shani E, Dolezal K, Tarkowski P, Sablowski R, Sandberg G, Samach A, Ori N. 2005**. Arabidopsis KNOXI Proteins Activate Cytokinin Biosynthesis. *Current Biology* **15**: 1566–1571.

**Yang C, Xie F, Jiang Y, Li Z, Huang X, Li L. 2018**. Phytochrome A Negatively Regulates the Shade Avoidance Response by Increasing Auxin/Indole Acidic Acid Protein Stability. *Developmental Cell* **44**: 29-41.e4.

**Yin Y, Wang Z-Y, Mora-Garcia S, Li J, Yoshida S, Asami T, Chory J. 2002**. BES1 Accumulates in the Nucleus in Response to Brassinosteroids to Regulate Gene Expression and Promote Stem Elongation. *Cell* **109**: 181–191.

**Yoshida S, Mandel T, Kuhlemeier C. 2011**. Stem cell activation by light guides plant organogenesis. *Genes & Development* **25**: 1439–1450.

**Yoshida Y, Takada N, Koda Y. 2010**. Isolation and Identification of an Anti-Bolting Compound, Hexadecatrienoic Acid Monoglyceride, Responsible for Inhibition of Bolting and Maintenance of the Leaf Rosette in Radish Plants. *Plant and Cell Physiology* **51**: 1341–1349.

**Youn JH, Kim T-W, Joo S-H, Son S-H, Roh J, Kim S, Kim T-W, Kim S-K. 2018**. Function and molecular regulation of DWARF1 as a C-24 reductase in brassinosteroid biosynthesis in Arabidopsis. *Journal of Experimental Botany* **69**: 1873–1886.

**Yu G, Wang L-G, Han Y, He Q-Y. 2012**. clusterProfiler: an R Package for Comparing Biological Themes Among Gene Clusters. *OMICS: A Journal of Integrative Biology* **16**: 284–287.

**Zhang L-Y, Bai M-Y, Wu J, Zhu J-Y, Wang H, Zhang Z, Wang W, Sun Y, Zhao J, Sun X, *et al.* 2009**. Antagonistic HLH/bHLH Transcription Factors Mediate Brassinosteroid Regulation of Cell Elongation and Plant Development in Rice and Arabidopsis . *The Plant Cell* **21**: 3767–3780.

**Zhang T-Q, Chen Y, Wang J-W. 2021**. A single-cell analysis of the Arabidopsis vegetative shoot apex. *Developmental Cell* **56**: 1056-1074.e8.

**Zhang B, Holmlund M, Lorrain S, Norberg M, Bakó L, Fankhauser C, Nilsson O. 2017**. BLADE-ON-PETIOLE proteins act in an E3 ubiquitin ligase complex to regulate PHYTOCHROME INTERACTING FACTOR 4 abundance. *eLife* **6**: e26759.

**Zhang Y, Mayba O, Pfeiffer A, Shi H, Tepperman JM, Speed TP, Quail PH. 2013**. A Quartet of PIF bHLH Factors Provides a Transcriptionally Centered Signaling Hub That Regulates Seedling Morphogenesis through Differential Expression-Patterning of Shared Target Genes in Arabidopsis. *PLoS Genetics* **9**: e1003244.

**Zhao L, Kim Y, Dinh TT, Chen X. 2007a**. miR172 regulates stem cell fate and defines the inner boundary of APETALA3 and PISTILLATA expression domain in Arabidopsis floral meristems. *The Plant Journal* **51**: 840–849.

**Zhao J, Yang G, Jiang L, Zhang S, Miao L, Xu P, Chen H, Chen L, Mao Z, Guo T, *et al.* 2022**. Phytochromes A and B Mediate Light Stabilization of BIN2 to Regulate Brassinosteroid Signaling and Photomorphogenesis in Arabidopsis. *Frontiers in Plant Science* **13**: 865019.

**Zhao X, Yu X, Foo E, Symons GM, Lopez J, Bendehakkalu KT, Xiang J, Weller JL, Liu X, Reid JB, *et al.* 2007b**. A Study of Gibberellin Homeostasis and Cryptochrome-Mediated Blue Light Inhibition of Hypocotyl Elongation. *Plant Physiology* **145**: 106–118.

**Zhao X, Yu X, Liu X, Lin C. 2007c**. Light Regulation of Gibberellins Metabolism in Seedling Development. *Journal of Integrative Plant Biology* **49**: 21–27.

**Zheng K, Wang Y, Zhang N, Jia Q, Wang X, Hou C, Chen J-G, Wang S. 2017**. Involvement of PACLOBUTRAZOL RESISTANCE6/KIDARI, an Atypical bHLH Transcription Factor, in Auxin Responses in Arabidopsis. *Frontiers in Plant Science* **8**: 1813.

**Zhiponova MK, Morohashi K, Vanhoutte I, Machemer-Noonan K, Revalska M, Montagu MV, Grotewold E, Russinova E. 2014**. Helix–loop–helix/basic helix–loop–helix transcription factor network represses cell elongation in Arabidopsis through an apparent incoherent feed-forward loop. *Proceedings of the National Academy of Sciences* **111**: 2824–2829.

**Zhong S, Shi H, Xue C, Wang L, Xi Y, Li J, Quail PH, Deng XW, Guo H. 2012**. A Molecular Framework of Light-Controlled Phytohormone Action in Arabidopsis. *Current Biology* **22**: 1530–1535.

**Zhong M, Zeng B, Tang D, Yang J, Qu L, Yan J, Wang X, Li X, Liu X, Zhao X. 2021**. The blue light receptor CRY1 interacts with GID1 and DELLA proteins to repress GA signaling during photomorphogenesis in Arabidopsis. *Molecular Plant* **14**: 1328–1342.

**Zhou B, Luo Q, Shen Y, Wei L, Song X, Liao H, Ni L, Shen T, Du X, Han J, *et al.* 2023**. Coordinated regulation of vegetative phase change by brassinosteroids and the age pathway in Arabidopsis. *Nature Communications* **14**: 2608.


Col-8
ath1-3

# Nederlandse samenvatting

## Nederlandse samenvatting

Het proefschrift van Shahram Shokrian Hajibehzad, getiteld " Van compacte rozetten tot strekkende stengels: Het ontrafelen van de rol van ATH1 in de regulatie van internodiëngroei in *Arabidopsis thaliana*", behandelt een aantal aspecten die van belang zijn in relatie tot de verbetering van gewasopbrengst bij rozetvormende gewassen. Door zich te richten op de genetische en moleculaire mechanismen die een compacte rozetgroei en de overgang naar stengelstrekking bij bloei (doorschieten) controleren, biedt dit onderzoek handvatten om de productiviteit en kwaliteit van dit type gewassen ook in de toekomst, onder veranderende omgevingsomstandigheden, te kunnen garanderen. Hierbij staat de modelplant *Arabidopsis thaliana* (de Zandraket) centraal, terwijl het TALE-transcriptiefactoreiwit ATH1 een centrale rol speelt binnen de onderzochte regulatieprocessen.

**Hoofdstuk 1: Algemene Inleiding**

Dit hoofdstuk schetst de wereldwijde uitdagingen op het gebied van voedselzekerheid en benadrukt het belang van het optimaliseren van gewasopbrengsten in een veranderend klimaat. Het hoofdstuk beschrijft verder de verschillende ontwikkelingsstadia die een *Arabidopsis thaliana* plant tijdens de levenscyclus doorloopt, met nadruk op de sturende rol van omgevingsfactoren, met name die van licht, hierbij. Verder wordt het belang benadrukt van het begrijpen van de overgang van skotomorfogenese (groei en ontwikkeling in de afwezigheid van licht) naar fotomorfogenese (groei en ontwikkeling in de aanwezigheid van licht) en van de onderliggende regulerende routes, waarbij omgevingssignalen en planteigen signalen, zoals hormonale signalen afkomstig van gibberellinen, brassinosteroïden en auxinen, geïntegreerd worden.

**Hoofdstuk 2: Compacte rozetgroei bij *Arabidopsis thaliana* staat onder controle van licht en de energiehuishouding van de plant middels signaalroutes die samenkomen op de transcriptionele controle van het TALE homeobox-gen ATH1**

Dit hoofdstuk onderzoekt de moleculaire mechanismen die de vorming van een compacte rozet bij *Arabidopsis thaliana* bewerkstelligen. Het beschreven onderzoek laat zien dat ATH1, een TALE-homeodomein transcriptiefactoreiwit, cruciaal is voor vorming en instandhouding van een compacte rozetvorm. Aanwezigheid

van ATH1 is afhankelijk van de lichtcondities onder welke de plant wordt opgegroeid en staat onder controle van een breed scala van lichtreceptoren waarover de plant beschikt. Hiernaast is de energiestatus van de plant bepalend voor de mate van aanwezigheid van ATH1. Het hoofdstuk verkent dan ook de wisselwerking tussen licht- en energiesignalen bij ATH1 activering, waarbij het TOR kinase-eiwit als een belangrijke mediator wordt geïdentificeerd. De studie onthult verder dat lokale aanwezigheid van ATH1 essentieel is om de 'rib zone' (grondmeristeem) van het scheutmeristeem in een inactieve status te houden. Dit resulteert in het niet-strekken van nieuwgevormde internodiën, met als gevolg de vorming van een compacte rozet. ATH1 bereikt dit waarschijnlijk door, specifiek in het scheutmeristeem, de aanwezigheid van remmers van fotomorfogenese, zoals de zogenaamde PIF eiwitten, te onderdrukken. Op hun beurt onderdrukken de PIF eiwitten weer de aanwezigheid van ATH1, waardoor er een zogenaamde dubbele negatieve ATH1-PIF 'feedback loop' in het scheutmeristeem actief is. Bij aanwezigheid van ATH1 resulteert dit, lokaal, in afwezigheid van PIF eiwitten en daardoor inactiviteit van de 'rib zone' van het scheutmeristeem, met een compacte rozetgroei als resultaat. Afwezigheid van ATH1 resulteert in de activatie van de 'rib zone' en stimuleert de aanwezigheid van PIF eiwitten in dit weefsel, waardoor op deze plek celstrekking wordt geïnduceerd, met verlies van compacte rozetgroei als gevolg.

**Hoofdstuk 3: Meervoudige controle van een algemeen celstrekkingsprogramma zorgt voor robuuste compacte rozetgroei bij *Arabidopsis thaliana***

Dit hoofdstuk verdiept zich in de, op moleculair niveau, regulerende mechanismen die aan de basis liggen van compacte rozetgroei in *Arabidopsis thaliana* en aan de hand waarvan de robuustheid van dit fenotype onder wisselende omgevingscondities verklaard kan worden. Gebruikmakend van confocale microscopie, genetische analyses, RNA-sequencing en farmacologische studies wordt aangetoond dat het transcriptiefactoreiwit ATH1 in de dieper gelegen delen van het scheutmeristeem meerdere lagen van een algemeen opererend celstrekkingsprogramma remt, inclusief input en output. Dit celstrekkingsprogramma wordt vormgegeven door de zogenaamde de BAP/D- en HLH/BHLH-regulatoire modules en integreert omgevingssignalen, zoals met betrekking tot heersende licht- en temperatuurcondities, en planteigen signalen, zoals afkomstig van de plantenhormonen gibberelline, brassinosteroïde en auxine. Meervoudige controle door

ATH1 van deze modules, verschaft de kenmerkende robuustheid van het compacte rozetfenotype. Op outputniveau onderdrukt ATH1 de expressie van de zogenaamde PRE-genen, genen waarvan de afgeleide eiwitten celstrekking stimuleren. Kunstmatig verhoogde expressie van PRE-genen, lokaal in het scheutmeristeem, resulteert in het verlies van compacte rozetgroei, zelfs in aanwezigheid van ATH1.

**Hoofdstuk 4: Van compacte rozetgroei naar stengelstrekking: Onderzoek naar de door ATH1 aangestuurde moleculaire mechanismen betrokken bij het doorschieten van Arabidopsis thaliana planten**

Dit hoofdstuk brengt het genregulerende netwerk in kaart dat door ATH1 in het scheutmeristeem wordt aangestuurd voor en tijdens het proces van doorschieten. Doorschieten is het produceren van een bloemstengel bij rozetplanten. Doorschieten markeert de overgang van vegetatieve naar reproductieve groei (bloei) en is het resultaat van lengtegroei van nieuwgevormde internodiën na deze overgang. Met behulp van confocale microscopie is in kaart gebracht dat ATH1-niveaus in de 'rib zone' van het scheutmeristeem vrij snel afnemen tot niet meer waarneembaar wanneer planten tot bloei worden geïnduceerd. Het verdwijnen van ATH1 uit de scheutmeristeem valt samen met en faciliteert de strekking van de bloemstengel (doorschieten). Om het onderliggende werkingsmechanisme op te helderen zijn transgene planten gebruikt die een chemisch induceerbare vorm van ATH1 tot expressie brengen. Planten waarin deze vorm geïnduceerd wordt op het moment dat bloei wordt getriggerd schieten niet door, terwijl er wel bloemvorming plaatsvindt. Planten waarin chemische inductie achterwege blijft schieten normaal door en vormen een bloeiwijze vergelijkbaar met die van niet-transgene planten. Door de genoombrede genexpressie in scheutmeristemen van deze groepen planten met elkaar te vergelijken, is een reeks genen geïdentificeerd die betrokken zijn bij het doorschieten en waarvan de expressie onder controle staat van ATH1. Deze groep genen heeft de naam Bolting-Associated genes Controlled by ATH1 (BACA) gekregen. Op basis van bekende functies van deze genen kan worden geconcludeerd dat regulatie van de hormoonhuishouding in combinatie met het reguleren van celcyclusprogressie in het scheutmeristeem aan de basis ligt van ATH1-gemedieerde onderdrukking van doorschieten.

**Hoofdstuk 5: Samenvattende discussie**

Dit hoofdstuk vat de onderzoeksbevindingen samen en bespreekt de implicaties in de context van de huidige inzichten binnen het vakgebied. Het benadrukt het belang van ATH1 in het reguleren van de overgang van een compacte rozet naar een compacte rozet met een langgerekte bloemstengel en geeft inzicht in hoe deze mechanismen gebruikt kunnen worden om de opbrengst en kwaliteit van rozetgewassen te verbeteren. Het hoofdstuk sluit af met een reflectie op de bredere implicaties van het onderzoek met betrekking tot toepassing in landbouwgewassen en geeft suggesties voor toekomstige onderzoeksrichtingen.


Col-8
ath1-3

# About the author

## About the author

Shahram Shokrian Hajibehzad was born in Miandoab, West Azerbaijan, Iran. He completed his primary and secondary education locally before attending the University of Azerbaijan, where he earned a bachelor's degree in Plant Protection. There, he learned about plant defense mechanisms and the fundamentals of plant biology. Shahram later pursued a master's degree in Plant Biotechnology at the University of Tehran, ranking third nationwide among more than 2,500 participants in the national entrance exam for entry into the master's program. For his master's thesis, he worked on producing an antigen in plants as an oral vaccine, resulting in two published research articles and contributions to a book chapter and a review article.

After completing his master's degree, Shahram worked for a short period at Ferdowsi University of Mashhad. In March 2018, he began his PhD program at Utrecht University under the supervision of Dr. Marcel Proveniers and Prof. Dr. Sjef Smeekens. His PhD research focused on the molecular mechanisms controlling rosette habit and bolting in the model plant Arabidopsis, with findings published in the peer-reviewed journal New Phytologist and other chapters under preparation for publication. After his PhD, Shahram joined Dr. Andrés Romanowski's team as a postdoctoral researcher to study the intersection of the circadian clock and shade avoidance in Arabidopsis. During this short postdoctoral period, Shahram wrote a dispatch article published in Current Biology.

In October 2023, Shahram joined the plant breeding company Rijk Zwaan as a crop researcher, where he leads projects related to Brassica crops.